Hydroxylation of ectoine and synthetic ectoine derivatives via *E. coli*-mediated whole-cell biotransformation

Dissertation

Zur

Erlangung des Doktorgrades (Dr. rer. nat.)

der

Mathematisch-Naturwissenschaftlichen Fakultät

der

Rheinischen Friedrich-Wilhelms-Universität Bonn

vorgelegt von

Jarryd Finn Brauner

aus Bonn

Bornheim, 2021

Angefertigt mit Genehmigung der Mathematisch-Naturwissenschaftlichen Fakultät der Rheinischen Friedrich-Wilhelms-Universität Bonn.

1. Gutachter: Prof. Dr. Erwin A. Galinski
2. Gutachter: Prof. Dr. Uwe Deppenmeier

Tag der Promotion: 23.04.2021
Erscheinungsjahr: 2021

Content

Figures v

Tables vi

Abbreviations viii

1 Introduction 1

1.1 Extremophiles 1

1.2 Halophilic and halotolerant microorganisms 2

1.3 General adaptation strategies to hyperosmotic conditions 2

1.3.1 Salt-in strategy 3

1.3.2 Organic osmolyte-in strategy 3

1.4 Compatible solutes 4

1.5 Ectoines and hydroxylated derivatives 4

1.5.1 Ectoine hydroxylase EctD 6

1.5.2 Protective effects 8

1.5.3 Present and future applications 9

1.5.4 Synthetic ectoine derivatives 9

1.6 Protection mechanisms of compatible solutes 11

1.7 Whole-cell biotransformation of ectoines 13

1.7.1 Osmoadaptation of *E. coli* 13

1.7.2 *In vivo* conversion of ectoines 14

1.8 Aim of the thesis 16

2 Material & Methods 18

2.1 Chemicals, kits, enzymes and markers 18

2.2 Buffers and solutions 20

2.3 Software 21

2.4 Production of synthetic ectoine derivatives 22

2.4.1 Homoectoine as an ectoine derivative with enlarged ring size 22

2.4.2 Ectoine derivatives with different alkyl groups 23

2.5 Microbiological methods 24

2.5.1 Bacterial strains and plasmids 24

2.5.2 Culture media 24

2.5.3 Media additives 27

2.5.4 Strain preservation 27

2.5.5 Precultures / overnight cultures 28

2.5.6 Main cultures / expression cultures 28

2.5.6.1 Whole-cell biotransformation of ectoines 28
2.5.6.2 Heterologous production of EctD for Strep-tag purification 29
2.5.6.3 Solute uptake experiment 29
2.5.6.4 Reactivation of dried cells 31
2.5.6.5 Cell growth under osmotic stress 31
2.5.6.6 Preparation of chemically competent *E. coli* 32
2.6 Molecular biological methods 32
2.6.1 DNA isolation 32
2.6.2 DNA quantification 33
2.6.3 Polymerase chain reaction (PCR) 34
2.6.4 Agarose gel electrophoresis (AGE) 35
2.6.5 Restriction digestion 36
2.6.6 Ligation 36
2.6.7 Transformation 37
2.7 Protein biochemical methods 37
2.7.1 Whole-cell protein extraction 37
2.7.2 EctD enzyme purification 38
2.7.2.1 Cell disruption by ultra-sonification 38
2.7.2.2 Strep-Tactin affinity chromatography 38
2.7.3 Protein quantification 39
2.7.4 SDS-polyacrylamide gel electrophoresis (SDS-PAGE) 39
2.7.4.1 Coomassie staining 40
2.7.4.2 Silver staining 40
2.7.5 Enzyme activity assays 41
2.7.5.1 EctD activity assay 41
2.7.5.2 Lactate dehydrogenase (LDH) activity assay 42
2.8 Analytics 43
2.8.1 Bligh & Dyer (B&D) extraction 43
2.8.2 Downstream processing (DSP) 44
2.8.2.1 Cation exchange chromatography 44
2.8.2.2 Ion retardation chromatography 44
2.8.2.3 Crystallization in methanol 45
2.8.3 Transfer free energy of diketopiperazine 45
2.8.4 High performance liquid chromatography (HPLC) 46
2.8.5 Nuclear magnetic resonance spectroscopy (NMR) 47
2.8.6 Calorimetric analysis of RNase A 48
3 Results 49
3.1 Chemical synthesis of ectoine derivatives 49

3.1.1 4,5,6,7-tetrahydro-2-methyl-1H-[1,3]-diazepine-4-carboxylic acid (homoectoine) 50
3.1.2 (4S)-2-ethyl-1,4,5,6-tetrahydropyrimidine-4-carboxylic acid (2-ethylectoine) 51
3.1.3 (4S)-2-propyl-1,4,5,6-tetrahydropyrimidine-4-carboxylic acid (2-propylectoine)..... 51
3.2 *In vivo* biotransformation of ectoines by *E. coli* BL21 pET *ectDHis*..... 52
3.2.1 Use of poor nitrogen sources..... 53
3.2.2 Ammonium sulfate as N-source and different induction parameters 54
3.2.3 Hydroxylation performance at different salinities..... 56
3.2.4 Hydroxylation of ectoine derivatives 58
3.2.5 Hydroxylation in concentrated culture media 60
3.3 Conversion of ectoines by the use of different hydroxylases..... 62
3.3.1 *E. coli* BL21(DE3) as whole-cell biotransformation chassis..... 63
3.3.2 *E. coli* DH5α as whole-cell biotransformation chassis..... 64
3.3.2.1 Conversion of ectoine..... 65
3.3.2.2 Conversion of 10 mM ethylectoine and 5 mM propylectoine..... 66
3.3.2.3 Maximal uptake rates of ectoine and ectoine derivatives..... 68
3.3.2.4 EctD enzyme stability over time 69
3.3.2.5 Hydroxylation by EctD of *S. alaskensis* under the enzyme's optimal temperature .. 72
3.3.3 EctD *in vitro* analysis 73
3.4 Downstream processing of hydroxylated ectoine derivatives 75
3.5 Characterization of synthetic ectoine derivatives..... 77
3.5.1 Instability of OH-homoectoine..... 78
3.5.2 Influence of ectoines on RNase A melting temperature..... 79
3.5.3 Stabilizing properties of ectoines towards freeze-thaw stressed LDH 81
3.5.4 Impact of solute polarity on protein backbones..... 82
3.5.5 Osmoprotective properties of ectoines on whole cells 84
3.5.6 Protection from cellular desiccation by new ectoine derivatives 86
4 Discussion..... 88
4.1 Whole-cell biotransformation: An alternative for the production of hydroxylated ectoines 88
4.1.1 Optimization of whole-cell biotransformation by *E. coli* BL21 pET*ectDHis*..... 90
4.1.1.1 The use of poor N-sources..... 91
4.1.1.2 Different C/N ratios vs induction parameters..... 93
4.1.1.3 NaCl dependency..... 95
4.1.2 Hydroxylation of synthetic ectoine derivatives by *E. coli* BL21 pET*ectDHis*..... 96
4.1.3 The impact of different ectoine hydroxylases and *E. coli* strains on whole-cell biotransformation 98
4.1.3.1 *E. coli* BL21 vs. *E. coli* DH5α as *ectD* expression strains 98
4.1.3.2 Substrate ambiguity of EctD: *In vitro* vs *in vivo* studies 100
4.1.3.3 Constant whole-cell biotransformation at low temperatures..... 102

4.2 Production and purification of hydroxylated ectoine derivatives 103
4.3 Characterization of synthetic ectoine derivatives 105
4.3.1 Characterization of OH-homoectoine 106
4.3.2 Influence on the melting temperature of RNase A 107
4.3.3 Protection of LDH against freeze-thaw stress 110
4.3.4 Polar & non-polar interactions with the protein backbone 112
4.3.5 Osmostabilization of *E. coli* 114
4.3.6 Protection of *E. coli* K-12 against desiccation 116
4.3.7 Different environmental stresses determine different protection mechanisms 118
5 Summary 120
6 Appendix 123
7 References 129

Figures

Figure 1: Biosynthesis pathway of ectoine and 5-hydroxyectoine in *H. elongata*. 6
Figure 2: Hydroxylation reaction of ectoine hydroxylase EctD 7
Figure 3: EctD-Strep-tag II fusion protein crystal structure of *S. alaskensis* 8
Figure 4: Ectoine and synthetic ectoine derivatives 11
Figure 5: Whole-cell biotransformation scheme for the conversion of ectoine to 5-hydroxyectoine within a synthetic *E. coli* cell factory 15
Figure 6: Chemical synthesis of zwitterionic cyclic amino acid derivatives (Voß, 2002) 22
Figure 7: Synthesis of homoectoine. 23
Figure 8: Synthesis of ethylectoine and propylectoine. 24
Figure 9: Vacuum filtering system for the filtration of *E. coli* DH5α 30
Figure 10: Schematic Michaelis-Menten kinetics 42
Figure 11: Molecule structure of DKP 46
Figure 12: ^{13}C-NMR analysis of homoectoine 50
Figure 13: ^{13}C-NMR analysis of ethylectoine 51
Figure 14: ^{13}C-NMR analysis of propylectoine 52
Figure 15: Hydroxylation of 10 mM ectoine with *E. coli* BL21 pET *ectDHis* in MM63-1 medium by the use of poor nitrogen sources 53
Figure 16: Whole-cell biotransformation of ectoine using different ratios of glucose and $(NH_4)_2SO_4$ under different induction conditions 55
Figure 17: Optimization of ectoine hydroxylation performance at higher osmotic pressure 57
Figure 18: Hydroxylation of ectoine and synthetic ectoine derivatives homoectoine, ethylectoine and propylectoine with *E. coli* BL21 pET *ectDHis* 59
Figure 19: Hydroxylation of 30 mM ethylectoine by *E. coli* BL21 pET *ectDHis* with concentrated culture media. 61
Figure 20: Hydroxylation of 10 mM propylectoine by *E. coli* BL21 pET *ectDHis* with concentrated culture media 62
Figure 21: Whole-cell biotransformation of 20 mM ectoine by different ectoine hydroxylases, heterologously expressed by *E. coli* BL21(DE3) 64
Figure 22: Whole-cell biotransformation of ectoine by different ectoine hydroxylases, heterologously expressed by *E. coli* DH5α 66
Figure 23: Whole-cell biotransformation of ethylectoine and propylectoine by different ectoine hydroxylases, heterologously expressed by *E. coli* DH5α 67
Figure 24: Maximal uptake rates of ectoine and synthetic ectoine derivatives in *E. coli* DH5α wildtype 69

Figure 25: SDS-PAGE analysis of whole-cell proteins for visualization of heterologously overproduced EctD_Strep-tag fusion protein 70
Figure 26: SDS-PAGE analysis of heterologously overproduced and purified EctD_Strep-tag fusion protein 71
Figure 27: Ectoine hydroxylation performance of *E. coli* DH5α pASK *ectD_Sala_Strep* under optimal temperature of EctD 73
Figure 28: HPLC analysis (UV spectrum) of media supernatants (SN) and B&D extract of (NaCl-shocked) *E. coli* cells after whole-cell biotransformation of ethylectoine 76
Figure 29: HPLC chromatogram (UV spectrum) of OH-ethylectoine 77
Figure 30: ^{13}C-NMR analysis of OH-ethylectoine 77
Figure 31: pH-dependent stability of OH-homoectoine over time 78
Figure 32: Calorimetric analysis of RNase A in presence or absence of different solutes 80
Figure 33: LDH activity after freezing and thawing in presence or absence of solutes. 82
Figure 34: ΔG_{tr} change of DKP/2 in transition of pure water to solution with cosolutes in dependency of fractional polar SASA. 83
Figure 35: Impact of solutes on growth of *E. coli* under osmotic pressure 85
Figure 36: Impact of compatible solutes on growth of *E. coli* after desiccation stress 87
Figure 37: Molecule structures of ectoine (A), homoectoine (B), OH-homoetoine (C) and 3-hydroxy-Nδ-acetylornithine (D) 107
Suppl. figure 1: Uptake of ectoine in absence of OH-ectoine for *E. coli* BL21 (wildtype) 124
Suppl. figure 2: Uptake of ectoine (5 mM) in presence of OH-ectoine (5 mM) for *E. coli* BL21 (wildtype) 124
Suppl. figure 3: Uptake of ectoine (2 mM) in presence of OH-ectoine (8 mM) for *E. coli* BL21 (wildtype) 125
Suppl. figure 4: Impact of different compatible solutes on the melting point (T_m) of RNase A, measured by differential scanning calorimetry (DSC) (Voß, 2002). 125
Suppl. figure 5: Cloning scheme for pASK *ectD_Acry_Strep*, pASK *ectD_Pstu_Strep* and pASK *ectD_Sala_Strep* 126
Suppl. figure 6: Cloning scheme for pET *ectD_Pstu_His* and pET *ectD_Sala_His* 127
Suppl. figure 7: Glucose uptake rate of *E. coli* BL21 pET *ectDHis* under N-limiting conditions 128

Tables

Table 1: Applied chemicals, kits, enzymes and markers 18
Table 2: Buffers and solutions. 20
Table 3: Applied software. 21

Table 4: Applied bacterial strains and plasmids 25
Table 5: Formulation of minimal medium 63 26
Table 6: Media formulation of complex media AB medium (Antibiotic Broth Medium No. 3), LB medium (Lysogeny Broth Medium, Bertani, 1951) and 2xYT medium (Sambrook *et al*., 1989). 26
Table 7: Formulation of VA solution (Imhoff & Trüper, 1977)..... 27
Table 8: Formulation and parameters for PCR..... 34
Table 9: Primers used for PCR and DNA sequencing..... 35
Table 10: DNA restriction digestion assay..... 36
Table 11: DNA ligation assay. 36
Table 12: Composition of gels for discontinuous SDS-PAGE..... 40
Table 13: EctD enzyme activity assay..... 41
Table 14: LDH enzyme activity assay..... 43
Table 15: Benchmark data for synthesis and analysis of ectoine derivatives..... 50
Table 16: Early influx rates of ectoine or synthetic ectoine derivatives and efflux of their respective hydroxylated derivatives in *E. coli* BL21 pET *ectDHis*..... 60
Table 17: Growth rates and early ectoine influx/OH-ectoine efflux rates of *E. coli* DH5α, heterologously expressing *ectD* of different organisms, encoded on pASK-IBA3 vector DNA 65
Table 18: Growth rates and early substrate influx/product efflux rates of *E. coli* DH5α, heterologously expressing different hydroxylases for conversion of ethylectoine and propylectoine ……69
Table 19: EctD *in vitro* activity assay 74
Table 20: Molar change of transfer free energy ΔG_{tr} regarding transition of DKP/2 from pure water into solution with cosolutes. 83
Table 21: Solvent accessible surface areas (SASA) of osmolytes with partly positive, negative and neutral charge, used for calorimetric analysis of RNase A 109
Table 22: Effectivity spectrum of (hydroxylated) ectoines towards different structures and environmental stresses..... 119
Suppl. table 1: EctD protein quantification (BCA) after strep-tag purification of whole-cell proteins. 123
Suppl. table 2: Maximal ectoine uptake rate for *E. coli* BL21 in absence and presence of OH-ectoine (Brauner, 2016). 123
Suppl. table 3: Kinetic parameters of EctD enzymes under optimized conditions (Widderich *et al*., 2014)..... 123

Abbreviations

Genes are given in small italic letters, while proteins are given in standard font and with a capital first letter. Physical quantities and corresponding dimensions are abbreviated according to the International System of Units.

% (w/v)	percent weight per volume
% (v/v)	percent volume per volume
≥, ≤	larger than or equal, smaller than or equal
Acry	*Acidiphilium cryptum*
ADABA	N-γ-acetyl-L-2,4-diaminobutyric acid
ADP	adenosine diphosphate
A_{260}, A_{280}	absorption at 260 nm, absorption at 280 nm
ABC transporter	ATP binding cassette transporter
ATP	adenosine triphosphate
ADPC	5-amino-3,4-dihydro-2H-pyrrole-2-carboxylate
AHT	anhydrotetracycline
AmpR	ampicillin resistance
AP	alkaline phosphatase
APS	ammonium persulfate
Asd	aspartate-β-semialdehyd-dehydrogenase
bp	base pair(s)
BCA	bicinchoninic acid
BSA	bovine serum albumin
betaine	glycine-betaine
B&D	Bligh & Dyer
CoA	coenzyme A
CV	column volume
C-source	carbon source
DABA	L-2,4-diaminobutyric acid
DCE	decarboxyectoine, 4,5,6,7-tetrahydro-2-methyl-pyrimidine
DHMICA	4,5-dihydro-2-methylimidazole-4-carboxylate
DMSO	dimethyl sulfoxide
DNA	deoxyribonucleic acid
DNase	deoxyribonuclease
dNTP	deoxyribonucleoside triphosphate
DSC	differential scanning calorimetry
DSM	German collection of microorganisms
DTT	dithiothreitol
EctA	L-2,4-diaminobutyric acid acetyltransferase
EctB	L-2,4-diaminobutyric acid transaminase
EctC	ectoine synthase
EctD	ectoine hydroxylase
Ectoine	(4S)-2-methyl-3,4,5,6-tetrahydropyrimidine-4-carboxylic acid
EDTA	ethylenediaminetetraacetic acid
et al.	*et alii* (and others)
ethylectoine	(4S)-2-ethyl-1,4,5,6-tetrahydropyrimidine-4-carboxylic acid
fig.	figure
g	gravitational force
gDNA	genomic DNA

Glu	glutamate
guanidinoectoine	2-amino-3,4,5,6-tetrahydro-4-pyrimidinecarboxylate
H_2O_{demin}	demineralized water
H_2O_{pure}	ultrapure water
HABA	hydroxy-azophenyl-benzoic acid
Hel	*Halomonas elongata*
HPLC	high performance liquid chromatography
hydroxyectoine	(4S,5S)-5-Hydroxy-2-methyl-1,4,5,6-tetrahydropyrimidine-4- carboxylic acid
homoectoine	4,5,6,7-tetrahydro-2-methyl-1H-[1,3]-diazepine-4-carboxylic acid
His	polyhistidine-tag
IPTG	isopropyl β-D-thiogalactopyranoside
kb	kilobase(s)
K_{cat}	catalytic efficiency
kDa	kilodalton
K_m	Michaelis-Menten constant
LacI	repressor of the lac-operon
lac-promotor	promotor of the lac-operon
LB	lysogenic broth
LDH	lactate dehydrogenase
ln OD_{600}	natural logarithm of the optical density at 600 nm
LysC	L-aspartate kinase
max.	maximal
MeOH	methanol
MM63	minimal medium 63
NAD	nicotinamide adenine dinucleotide
NADP	nicotinamide adenine dinucleotide phosphate
NMR	nuclear magnetic resonance
NC	no column
NCBI	National Center for Biotechnology Information
N-source	nitrogen-source
OD_{600}	optical density at a wavelength of 600 nm
PAGE	polyacrylamide gel electrophoresis
PCR	polymerase chain reaction
PEG	polyethylene glycol
PFK	phosphofructokinase
pH	*potential hydrogenii*
ppm	parts per million
propylectoine	(4S)-2-propyl-1,4,5,6-tetrahydropyrimidine-4-carboxylic acid
Pstu	*Pseudomonas stutzeri*
RBS	ribosome binding site
RI	refractive index
RNA	ribonucleic acid
RNase A	ribonuclease A
rpm	revolutions per minute
RSB	reducing sample buffer
RT	room temperature
Sala	*Sphingopyxis alaskensis*
SASA	solvent accessible surface area
SDS	sodium dodecyl sulfate
TAE	TRIS acetic acid EDTA
TEMED	N,N,N′,N′-Tetramethylethane-1,2-diamine
TES	2-[(2-Hydroxy-1,1-bis(hydroxymethyl)ethyl)amino]ethanesulfonic acid, N-[Tris(hydroxymethyl)methyl]-2-aminoethanesulfonic acid

tet-promoter	promotor of the gene for tetracycline resistance
T_M	melting temperature
TMSP	trimethylsilyl propanoic acid
TRIS	2-Amino-2-(hydroxymethyl)propane-1,3-diol
tab.	table
U	unit
UV	ultraviolet
V_{max}	maximum rate of enzyme reaction
w/o	without

1 Introduction

1.1 Extremophiles

In the year 1974, MacElroy coined the term “extremophile”, which combines the two parts “extreme” and “-philic”, implying the preference of organisms for extreme environments. The group of extremophiles contains organisms of all three domains of life (*archaea, bacteria, eukarya*), which thrive in ecological niches like ice, hot springs, high-salt solutions as well as acidic or alkaline fluids (Rampelotto, 2013). They have been found in toxic waste, in environments with high amounts of heavy metals and depths of 6.7 km inside the Earth’s crust, thus places, which were previously considered inhospitable for life.

Extremophiles are classified into categories according to the environmental conditions in which they live. Regarding temperature, they can be classified as thermophilic and hyperthermophilic (growing at high or very high temperatures) or as psychrophilic and cryophilic (growing at low or very low temperatures). Other extremophiles are piezophilic and radiophilic organisms, growing best at high pressures or in the presence of ionizing radiation, respectively. This group of organisms can also be adapted to geochemical extremes like high osmolarity and acidic or alkaline pH values. In terms of pH, they can be classified as acidophiles and alkaliphiles (adapted to acidic or basic pH values), whereas halophiles need high NaCl concentrations. In many cases, inhabitants of extreme environments are polyextremophiles, resulting from the occurrence of two or more extreme conditions. One example would be *Thermococcus barophilus*, which as a thermophilic and piezophilic archaeon lives inside hot rocks deep under the Earth’s surface (Marteinsson *et al.*, 1999). In order to resist harsh environmental conditions, extremophiles developed a wide variety of different adaptation strategies like the production of special stabilizing macromolecules or small molecules, such as organic osmolytes (Toxopeus, Warner & MacRae, 2014). The understanding of their stabilizing effects under extreme conditions are of great interest for industry and biotechnological purposes. A well-known example for the use of biomolecules derived from extremophiles is the heat resistant *Taq* DNA polymerase, which was used for the establishment of polymerase chain reaction (PCR) and is originated from *Thermus aquaticus* (Saiki *et al*., 1988).

While extremophiles are adapted and dependent on their special ecological niche, extremotolerant organisms, which thrive under moderate conditions, are able to withstand extreme stress factors like heat or high osmolarity only to a certain extent. Such moderate

conditions are defined as temperatures between 20 - 40 °C, approximately one standard atmosphere (1 atm) and a pH near neutral, only to name a few (Satyanarayana *et al.*, 2005).

1.2 Halophilic and halotolerant microorganisms

Organisms which are salt-loving and grow in presence of high NaCl concentrations are called "halophiles". According to Ventosa *et al*. (1998), organisms can be classified as non-halophiles, (< 0.2 M NaCl), slight halophiles (0.2 M - 0.5 M NaCl), moderate halophiles (0.5 M – 2.5 M NaCl) and extreme halophiles (> 2.5 M NaCl). While strictly halophilic organisms are adapted to saline conditions and thus require high concentrations of salt for survival, halotolerant microorganisms can survive in absence as well as in presence of certain amounts of salts up to a salinity of 2.5 M NaCl, although growth rates decrease with increasing salinity. As ranges of minima, optima and maxima of salts are also dependent on other parameters like temperature and culture medium, sharp demarcations of these groups are hard to define. Therefore, Oren (2008) simplified the classification by determining halophiles as organisms which are able to grow well at salt concentrations over 10 %, while halotolerant microorganisms exhibit growth optimum under 3 % and a salt tolerance up to 10 %.

Halophiles inhabit a great variety of natural environments characterized by the presence of high salinities like sea water, saline lakes and even man-made environments like salt extraction plants (Ma *et al*., 2010). Depending on the habitat, salinities can either be constant or inconstant, causing the development of different strategies for halophilic and halotolerant organisms to overcome such fluctuations. In the following, different osmoadaptation strategies are presented.

1.3 General adaptation strategies to hyperosmotic conditions

All prokaryotes have in common, that they possess a semipermeable lipid membrane, which is not traversable for ions and organic molecules, allowing free water exchange with the environment. Hereby, microorganisms let water flow into or out of the cell, depending on the extracellular and intracellular concentration of osmolytes. A high ionic concentration leads to the binding of water molecules, causing the reduction of water activity, and with that, the amount of free water. A concentration gradient between the intracellular and extracellular milieu results in water transport from the hypotonic (lower osmotic pressure) to the hypertonic (higher osmotic pressure) region, as the chemical potential of water strives for an equilibrium. If this mechanism, called osmosis, takes place in an uncontrolled manner, there is a risk that microorganisms would lose cellular water under hypersaline conditions, resulting in collapse

of turgor pressure and thus in cell death. In order to avoid excessive water loss, halophilic and halotolerant microorganisms have evolved different effective strategies to equalize the extracellular and intracellular water activity.

1.3.1 Salt-in strategy

One possible way to avoid water loss under hypersaline conditions is the accumulation of molar concentrations of inorganic ions and counter ions, mostly K^+ and Cl^-, leading to the adjustment of cytoplasmic water activity to the extracellular milieu. Although this strategy is energetically efficient, microorganisms using this method are very inflexible regarding colonization of different habitats. That is because the possibility to take up large amounts of inorganic ions is accompanied by the adaptation of the whole enzymatic machinery to high saline conditions (Lanyi, 1974). Most proteins of halophiles using the salt-in strategy exhibit a large proportion of acidic amino acids like aspartic acid and glutamic acid. In this case, protein stabilization under high intracellular concentrations of inorganic ions is achieved by the binding of positively charged K^+ ions to negatively charged side chains of these acidic amino acids (Mevarech *et al*., 2000). The absence or reduction of K^+ ions would lead to repulsion of the negatively charged side chains, resulting in destabilization and malfunction of proteins. Several strict halophiles such as the aerobic members of halobacteriaceae, *Salinibacter ruber* and the anaerobic halanaerobiales (Bacteria) use this strategy (Oren, 2008).

1.3.2 Organic osmolyte-in strategy

Another strategy to withstand osmotic pressure is the organic osmolyte-in strategy, which is also called salt-out strategy, involving the exclusion of salt ions and simultaneous accumulation of organic compounds. These molecules, called compatible solutes, act as osmolytes which are able to shift the osmotic pressure without interfering with the cell metabolism even at high intracellular concentrations (Galinski, 1995). A more detailed characterization of these solutes is given further below (1.4). Compatible solutes are either synthesized *de novo* or imported from the surrounding medium, whereby the second option is less energy consuming and therefore often preferred by microorganisms. Since the proteome of organisms using this strategy is not adapted to high saline conditions, it allows for a higher flexibility regarding fluctuations of salt concentrations and different habitats (Ventosa *et al*., 1998).
The organic osmolyte-in strategy is a wide-spread approach and accomplished by organisms of all three life domains, including *E. coli*, which was a crucial model organism for this work.

1.4 Compatible solutes

Compatible solutes are mostly zwitterionic and highly water soluble low molecular weight molecules which have the ability to counteract negative effects of high external osmolarity. Even at high intracellular concentrations, compatible solutes do not disturb cell metabolism, which is the reason for their naming (Brown, 1976).

Next to the identification as protective components in connection with osmotic stress, compatible solutes were investigated for the last decades to reveal other important characteristics. It could be shown that compatible solutes also provide protection against other extreme conditions such as low or high temperatures, hydrostatic pressure, freezing, desiccation and the denaturation of macromolecules by ions and urea (Yancey, 2005; Hoffmann & Bremer, 2011; Caldas *et al*., 1999; Zeidler & Müller, 2019). In this context, compatible solutes are termed "extremolytes". Glycine betaine for example is one of the most widely spread compatible solutes on Earth as it can be found in all three domains of life. This compound is not only a very effective osmostress protectant but additionally exhibits shielding properties regarding heat and hydrostatic pressure, making it a so called thermolyte and piezolyte (Holtmann & Bremer, 2004; Yancey *et al*., 2002).

Due to the great variety of known compatible solutes they can be classified into different categories: 1.) amino acids (e.g. proline), 2.) amino acid derivatives (e.g. ectoine, glycine betaine), 3.) quaternary amines (e.g. Trimethylamine oxide (TMAO)), 4.) N-acetylated diamino carboxylic acids (e.g. N-δ-acetyl ornithine), 5.) sugars (e.g. trehalose), 6.) sugar derivatives (e.g. mannosylglycerate) and 7.) polyols (e.g. mannitol) (Galinski, 1995; Grant, 2004).

1.5 Ectoines and hydroxylated derivatives

Ectoine ((S)-2-methyl-1,4,5,6-tetrahydropyrimidine-4-carboxylic acid) is one of the most widespread and thoroughly studied osmolyte in the microbial world. It has been found in all three domains of life and in a broad spectrum of physiologically and taxonomically diverse microorganisms, especially in aerobic chemoheterotrophic eubacteria (Galinski & Trüper, 1994; Pastor *et al*., 2010; Widderich *et al*., 2014, 2016; Harding *et al*., 2016). This solute was identified in the year 1985 in the purple sulfur bacterium *Halorhodospira halochloris* whereas the name originates from the former name *Ectothiorhodospira halochloris* (Galinski *et al*., 1985).

A few years after the discovery of this compound, its hydroxylated derivative 5-hydroxyectoine ((S,S)-2-methyl-5-hydroxy-1,4,5,6-tetrahydropyrimidine-4-carboxylic acid) was identified in the gram-positive bacterium *Streptomyces parvulus* (Inbar & Lapidot, 1988). This solute is predominantly produced by gram-positives, but also by some gram-negative aerobic organisms like *Halomonas elongata* under simultaneous osmotic and heat stress (Schiraldi *et al*., 2006; Bursy *et al*., 2007).

Ectoine as well as 5-hydroxyectoine (OH-ectoine) are derived from L-aspartate and exhibit a heterocyclic pyrimidine ring structure. The biosynthesis pathway of these two compounds is depicted in figure 1 and has first been elucidated by Peters *et al*. (1990) in *H. halochloris* and *H. elongata*. Subsequently, Ono *et al*. (1999) made important contributions to the biochemical understanding of the enzymes involved in ectoine biosynthesis.

The first steps in ectoine synthesis are the phosphorylation and reduction of L-aspartate to aspartate-β-semialdehyde by an aspartokinase (LysC) and a dehydrogenase (Asd), respectively. On the basis of this intermediate, ectoine is formed by three enzymatic steps. Via the transaminase EctB, aspartate-β-semialdehyde is converted to L-2,4-diamino butyric acid (DABA), which subsequently is acetylated to N-acetyl-L-2,4-diamino butyric acid (ADABA) by the DABA acetyltransferase EctA. The intramolecular condensation of ADABA to ectoine is catalyzed by the ectoine synthase EctC.

Further modification of ectoine to OH-ectoine is possible via the ectoine hydroxylase EctD, catalyzing the oxidative decarboxylation of 2-oxoglutarate by which one oxygen atom is built into ectoine and the second oxygen atom is built into succinate, as a result of the cleavage of CO_2. As a result, OH-ectoine as well as succinate is formed.

So far, the industrial production of ectoine is mainly accomplished by cultivation of *H. elongata* under high salinities and high cell density (Kunte *et al*., 2014). For the production of OH-ectoine, *H. elongata* additionally needs to be cultivated at temperatures higher than 40 °C in order to achieve a total content of 50 % ectoine and OH-ectoine, respectively (Wohlfarth *et al*., 1990; Meffert, 2011). While the solute extraction was previously done by an osmotic downshock, leading to the release of ectoines out of the cells, nowadays a leaky *H. elongata* mutant with non-functional ectoine uptake and degradation systems is used by which the solutes are released continuously (Gramman *et al*., 2002; Kunte *et al*., 2014).

As described in more detail below, ectoine and OH-ectoine exhibit protective effects against osmotic pressure as well as different kinds of stresses, and even though these two solutes are distinguished by only one hydroxy group, they show partly similar but also very different stabilizing properties towards biomolecules or even whole cells. This is why the search for new

synthetic ectoine-like compatible solutes are very interesting in order to generate solutes with potentially enhanced protective abilities. Further modification of these ectoine-like solutes may be obtained by hydroxylation via EctD, as long as the enzyme recognizes them as substrates.

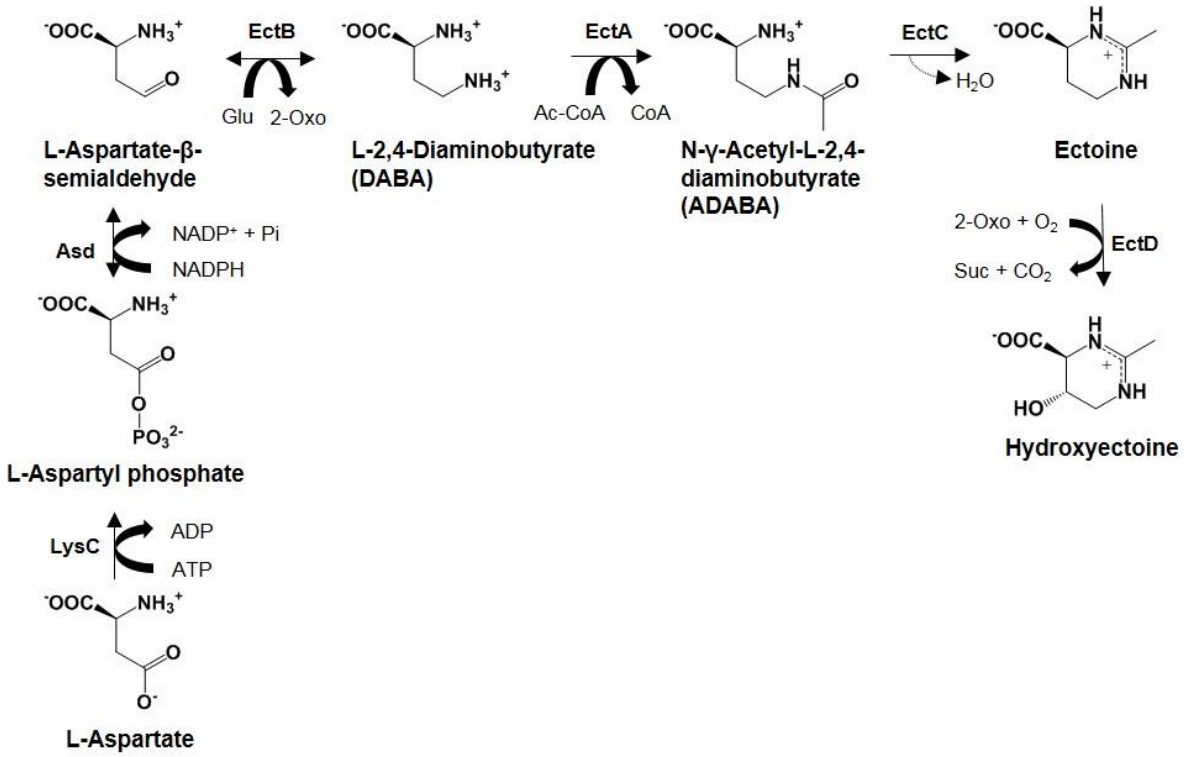

Figure 1:Biosynthesis pathway of ectoine and 5-hydroxyectoine in *H. elongata*. LysC: Aspartokinase, Asd: L-Aspartate β-semialdehyde dehydrogenase, EctB: L-2,4-Diaminobutyrate-2-oxoglutarate transaminase, Glu: glutamate, 2-Oxo: 2-Oxoglutarate, EctA: L-2,4-Diaminobutyrate acetyltransferase, Ac-CoA: Acetyl-CoA, CoA: Coenzyme A, EctC: Ectoine synthase, Suc: Succinate, EctD: Ectoine hydroxylase.

1.5.1 Ectoine hydroxylase EctD

Ectoine hydroxylase EctD is a member of the non-heme iron(II)-containing and 2-oxoglutarate dependent dioxygenases, meaning that iron, oxygen and the cofactor 2-oxoglutarate are essential for this enzyme (Ures, 2005; Bursy *et al.*, 2007). During hydroxylation, oxidative decarboxylation of 2-oxoglutarate, derived from the citrate cycle, takes place by the transfer of one oxygen atom to ectoine and another oxygen atom to 2-oxoglutarate, while iron acts as a catalyst for the activation of molecular oxygen (Widderich *et al.*, 2014). The oxygen transfer leads to the addition of a hydroxy group on ectoine and furthermore to the formation of succinate with concomitant release of CO_2 (fig. 2). For the binding of Fe^{2+} to the enzymes active site, a highly conserved 2-His-1-carboxylate facial triad motif, present in many non-heme

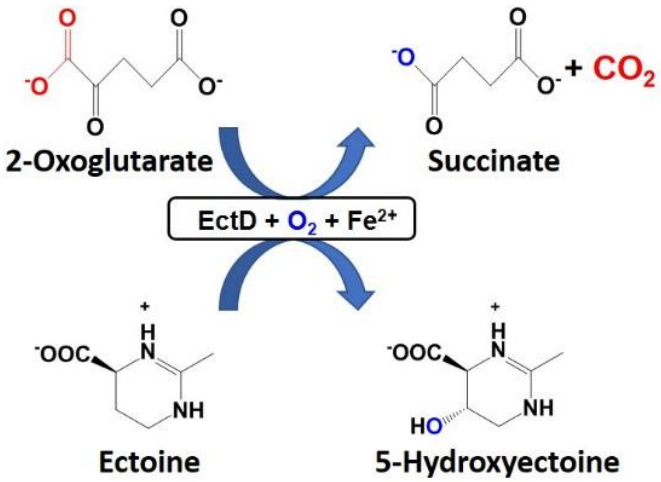

Figure 2: Hydroxylation reaction of ectoine hydroxylase EctD. The turnover of ectoine to its hydroxylated form is accomplished by decarboxylation of the cofactor 2-oxoglutarate and the simultaneous insertion of oxygen into 2-oxoglutarate and the substrate ectoine, forming succinate and 5-hydroxyectoine, respectively.

iron(II) enzymes, could be found (Bursy *et al*., 2007). This motif is part of a 17 amino acid residue region (F-x-W-H-S-D-F-E-T-W-H-x-E-D-G-M/L-P) which is strictly conserved in ectoine hydroxylases (Höppner *et al*., 2014). Next to the iron catalyst, this region exhibits five residues involved in the binding of 2-oxoglutarate and the reaction product OH-ectoine. When EctD is not active, Fe^{2+} is coordinated with the 2-His-1-carboxylate facial triad, while the other binding sites are coordinated with water molecules. After the binding of O_2 and 2-oxoglutarate, a Fe(III)-superoxide radical anion is formed, which decarboxylates 2-oxoglutarate by a nucleophilic attack. As a result, a high energy oxo-Fe(IV)-intermediate causes the cleavage of the hydrogen at the C5-atom of ectoine, which is replaced by a hydroxy group (Price *et al*., 2003; Hausinger, 2004; Bursy, 2005; Clifton *et al*., 2006).

Bioinformatic and phylogenetic studies revealed, that approximately two thirds of all ectoine producers exhibit gene sequences for *ectD*, and should be able to produce OH-ectoine directly from its precursor (Widderich *et al*., 2014). While in most OH-ectoine producers all relevant genes are organized in one operon, *ectD* of *H. elongata* is coded separately from the *ectABC* gene cluster.

To date, several bacterial ectoine hydroxylases have been biochemically investigated, including enzymes of halophilic *H. elongata*, acidophilic *Acidiphilium cryptum*, mesophilic *Pseudomonas stutzeri* and psychrophilic *Sphingopyxis alaskensis* (Widderich *et al*., 2014). Although physiologically and taxonomically very diverse, these characterized enzymes all show similar biochemical properties *in vitro*. With *Km* values ranging from 6 mM to 10 mM, they exhibit rather moderate affinities to their substrate ectoine. There is no need of salts for activity, but the presence of approximately 100 mM KCl improves the turnover rate. While the

EctD optima regarding pH (7.5 - 8) and temperature (32 °C - 40 °C) are in the same range, one exception is the temperature optimum of EctD of *S. alaskensis*, a psychrophilic organism that exhibits its enzymes optimum at 15 °C (Czech *et al*., 2019). All characterized enzymes are arranged as dimers which could be shown by crystallization of EctD, originated from *V. salexigens* and *S. alaskensis* as depicted in fig. 3 (Reuter *et al*., 2010; Höppner *et al*., 2014).

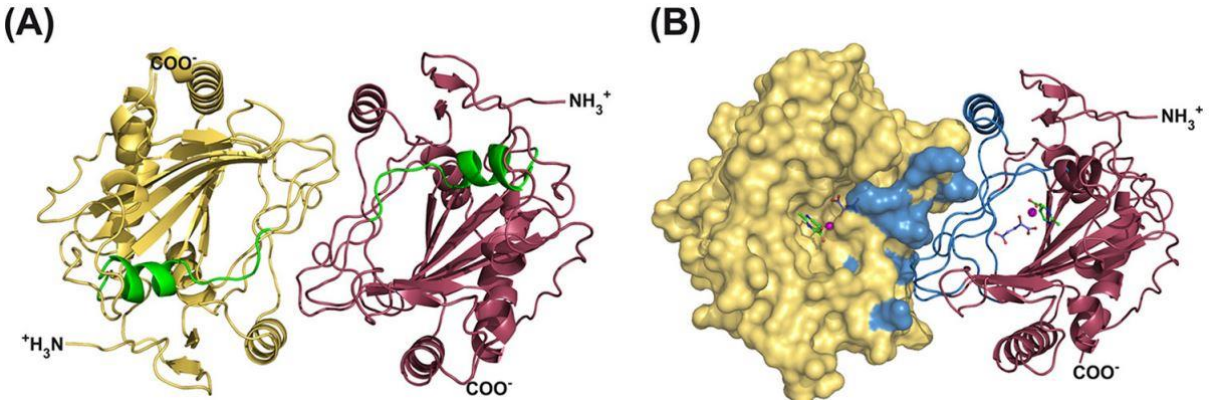

Figure 3: EctD-Strep-tag II fusion protein crystal structure of *S. alaskensis*. The enzyme is arranged as a dimer, and the two monomers are colored differently. A) Ribbon structure of EctD. The highly conserved EctD signature motif is highlighted in green. B) EctD monomers are represented on surface view (left) and ribbon structure (right). The iron catalyst is marked as a sphere in magenta, the cofactor 2-oxoglutarate and the enzyme product 5-hydroxyectoine are represented as ball and stick constructs (Höppner *et al*., 2014).

1.5.2 Protective effects

Next to the previously described osmoprotective effects of ectoine and OH-ectoine, these solutes are regarded as protecting substances towards other stress factors like air- and freeze drying of whole cells (Louis *et al*., 1994; Manzanera *et al*., 2002, 2004). Furthermore, it was shown that protein stability and functionality, as for the model enzymes lactate dehydrogenase (LDH), phosphofructokinase (PFK) and ribonuclease A (RNase A), could be maintained under heat, cold, desiccation and oxidation stress in the presence of ectoine and OH-ectoine, whereas OH-ectoine often showed superior stabilizing traits (Lippert & Galinski, 1992; Göller & Galinski, 1999; Borges *et al*., 2002; Andersson *et al*., 2000, Knapp *et al*., 1999).

Not only proteins but other biomolecules like DNA are also influenced by the presence of ectoines. While DNA is normally fragile towards UV light, ectoines are able to reduce structural damage of these molecules exposed to UVA but also to ionizing radiation (Botta *et al*., 2008; Hahn *et al*., 2017). Additionally, ectoines exhibit a notable effect on DNA melting temperature. It could be shown that ectoine decreases the melting temperature, while the opposite is the case for OH-ectoine (Kurz, 2008).

Beyond that, studies gave evidence that ectoines also show an impact on biological lipid membranes (Harishchandra *et al*., 2010). Ectoines seem to enhance the interaction of the polar head groups of membranes with surrounding water molecules, whereby membrane fluidity is increased.

1.5.3 Present and future applications

The protective effects of ectoines towards several kinds of stresses described above stirred interest for biotechnological, medical and other industrial branches. Ectoine was shown to exhibit effective stabilizing properties in methods of molecular biology, including the ability to serve as a PCR enhancer for the amplification of GC-rich DNA fragments (Schnoor *et al*., 2004) or the proper expression, folding and storage of proteins (Killian, Taylor & Castner *et al*., 2018; Barth *et al*., 2000). Due to its moisturizing property, ectoine is especially utilized in skin and medical care like creams, eye drops or nasal spray for the purpose of stabilizing and protecting epithelia and mucosa from dehydration (Graf *et al*., 2008). The application of ectoine to human skin cells reduces the release of inflammatory factors after high exposure to UVA light, and furthermore increases the formation of heat shock proteins, stimulating cell repair mechanisms (Buenger & Driller, 2004; Buommino *et al*., 2005). As it exhibits anti-inflammatory properties relevant for skin care, ectoine but also OH-ectoine were shown to have positive effects on inflammatory diseases like the chronical ulcerative colitis (Abdel-Aziz *et al.*, 2015). A recently published study revealed that ectoine is an effective drug for the treatment and prevention of chemotherapy-induced oral mucositis, caused as a side-effect by radiotherapy or chemoradiation (Rieckmann *et al.*, 2019). Moreover, ectoine and OH-ectoine improve functional nanostructures in artificial lung surfactants, giving rise to hopes that these two solutes may be favorable for a proper lung surfactant function and thus might be an effective drug for inhalation therapy during surfactant deficiency (Harishchandra *et al*., 2011). The application of ectoine or OH-ectoine against such diseases is not yet approved, but the preceding studies suggest that these solutes might be candidates for future treatment.

1.5.4 Synthetic ectoine derivatives

Besides the biosynthesis of the two natural compounds ectoine and OH-ectoine, the chemical synthesis of ectoine derivatives with potential superior protecting properties are of great interest. Over the last years, several synthetic ectoine derivatives have successfully been produced and characterized (fig. 4). These solutes exhibit either reduced or expanded sizes of

the normally six-membered ectoine ring structure or possess different functional groups. A well-known synthetic ectoine derivative is homoectoine (4,5,6,7-tetrahydro-2-methyl-1H-[1,3]-diazepine-4-carbonic acid), which does not show strong osmoprotection properties compared to glycine betaine or ectoine, but is able to significantly reduce the DNA melting temperature, thus represents a substance with PCR enhancer abilities (Nagata, 2001; Schnoor *et al*., 2004; Shi & Jarvis, 2006). This solute, consisting of a seven-membered diazepine ring, additionally exhibits protective effects against colitis in mice by preventing the downregulation of epithelial junction proteins. Although this is also true for ectoine, only homoectoine completely prevented the inflammatory reaction according to a study by Castro-Ochoa *et al*. (2019).

Downsizing of the ectoine pyrimidine ring to an imidazole leads to the formation of 4,5-dihydro-2-methylimidazole-4-carboxylate (DHMICA), which is an osmoprotective substance and additionally exhibits the ability to reduce the DNA melting temperature to a degree similar to that of ectoine. Furthermore, this solute shows superior protective traits towards RNase A stability under heat as calorimetric studies revealed (Voß, 2002).

Laurylectoine, which features a hydrophobic anchor, is able to modulate the inflammation in rat intestinal smooth muscle cells by decreasing lipopolysaccharide (LPS)-induced gene expression of corresponding cytokines (Wedeking *et al*., 2014).

Although such modifications of the primary ectoine structure were beneficial, in some cases they do not result in improved properties. The cationic substance 1,4,5,6-Tetrahydro-2-methylpyrimidine (decarboxyectoine, DCE), for instance, which lacks the carboxy group, impairs the growth of *E. coli*, making it a so-called incompatible solute. Another such incompatible solute with this effect is 2-amino-3,4,5,6-tetrahydro-4-pyrimidinecarboxylate (guanidinoectoine), that has an amino group instead of a methyl group.

Due to the fact that OH-ectoine is often accompanied with superior protective properties compared to ectoine, the possibility to eventually hydroxylate synthetic ectoine derivatives came into focus. In this context, the verified regio- and stereoselective hydroxylation of homoectoine (Vielgraf, 2008), guanidinoectoine, DHMICA (Meffert, 2011) and ADPC (Witt, 2011) by EctD of *H. elongata* suggests, that this enzyme exhibits substrate ambiguity (Jensen, 1976). That is why in this study the two new synthetic ectoine derivatives 2-ethyl-1,4,5,6-tetrahydropyrimidine-4-carboxylic acid (ethylectoine) and 2-propyl-1,4,5,6-tetrahydropyrimidine-4-carboxylic acid (propylectoine) were tested as substrates for the hydroxylation by EctD.

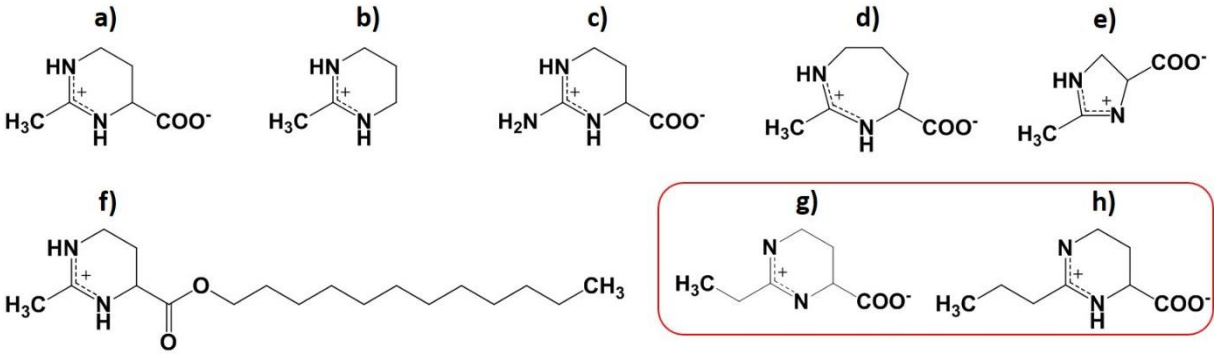

Figure 4: Ectoine and synthetic ectoine derivatives. a) ectoine, b) decarboxyectoine, c) guanidinoectoine, d) homoectoine, e) 4,5-dihydro-2-methylimidazole-4-carboxylate (DHMICA), f) laurylectoine, g) ethylectoine, h) propylectoine. Red-framed solutes were synthesized and characterized in this work.

1.6 Protection mechanisms of compatible solutes

The finding that glycerol not only decreases the surface tension of water but is additionally excluded from protein surfaces, which could also be shown for glycine betaine, led to the formulation of the "preferential interaction theory" (Gekko & Timasheff, 1981; Arakawa & Timasheff, 1983). Timasheff (1998) revised this theory later on and postulated the "preferential exclusion theory". This theory established a key understanding regarding the stabilizing effects of compatible solutes towards biomolecules like proteins in aqueous solutions.

By dissolving a protein in water, a hydration shell around this macromolecule is formed and the chemical potential of the protein solution increases under the release of free hydration energy. The chemical potential of a compound determines if a chemical reaction is accomplished with another compound. Such a reaction only takes place if the initial chemical potential is greater than after the reaction. If a protein is dissolved in water in combination with a compatible solute, the chemical potential of water is decreased (osmotic effect). Now water and solute molecules compete for the protein's surface, whereas the protein is preferentially surrounded by only one of the two types of molecules. Recently published studies confirmed the theory that compatible solutes are preferentially excluded from the proteins surface, leading to a preferential hydration of the protein (Zaccai *et al.*, 2016). In this situation, a protein that is hydrated by exclusion of solutes is apparently in the same condition as a protein dissolved in pure water. However, there is a thermodynamically difference between these two states, since a concentration gradient of the solute along the protein's surface is built up. The maintenance of this exclusion is energy consuming and by that, the unfolding of proteins is impeded.

Along with the preferential exclusion of compatible solutes goes the so-called "osmophobic effect", which is one of the thermodynamic forces for protein folding next to hydrogen bridge bonds, hydrophobic interactions as well as van der waals and electrostatic forces (Kauzmann, 1959). The unfavorable interaction between a solvent (osmolyte) and a protein's functional group, the most important of which would be the peptide backbone, is classified as solvophobic or, more specifically, osmophobic. Proteins are more stable in the presence of protecting osmolytes than in pure water, because these solutes raise the transfer free energy of the proteins denatured state, favoring the folded state. By implication, denaturing osmolytes like urea lower the energy of the unfolded state, favoring the unfolded state (Bolen & Baskakov, 2001). In this context, Street *et al*. (2006) made the key observation that the transfer free energy of a protein backbone from water to an osmolyte solution is negatively correlated with the osmolytes polar surface areas. As a consequence, the interaction between the protein backbone with polar groups of a cosolute is more favorable than with non-polar groups, meaning that proteins are more stable in presence of solutes which have a hydrophobic surface area.

In many analyses regarding cell protection or preserving functionality of biomolecules by compatible solutes, hydroxylated ones often exhibited superior effects, making them very interesting stabilizers. Especially the protection towards heat and desiccation is achieved by OH-ectoine to a higher extent compared to ectoine (Knapp *et al*., 1999; Manzanera *et al*., 2002; Manzanera *et al*., 2004). The hydroxy group is able to form stronger intermolecular hydrogen bonds, a trait that makes OH-ectoine a so-called glass-forming substance like sugars. An organic glass is a highly viscous phase with a disordered molecular and atomic pattern in contrast to the strongly ordered grid structure of crystals. It is neither a liquid nor a solid but it rather exhibits traits of both states. Since glasses preserve the random distribution of particles in a fluid and additionally prevent harmful crystal formation, the mechanic immobilization inside a glass matrix protects biomolecules from denaturation, coagulation and disintegration (Green & Angell, 1989; Sakurai *et al*., 2008; Julca *et al*., 2012). By exceeding the glass transition temperature, the solid glass-state is transformed into the liquid state. Due to the higher glass transition temperature of OH-ectoine (87 °C) compared to ectoine (47 °C), the former is an excellent desiccation protectant for biomolecules and whole cells (Tanne *et al*., 2014; Manzanera *et al*., 2002, 2004). Although ectoine is also able to form glasses, it has a strong tendency to aggregate and crystallize.

1.7 Whole-cell biotransformation of ectoines

By definition, biotransformation approaches are chemical processes for the enzymatic conversion of externally provided, defined substrates by living cells, whereby substrates and resulting products are usually unnatural for the converting organism. Involved enzymes can either be part of the organisms own enzymatic repertoire or heterologously produced. By this, biotransformation is distinguished from fermentation, which is a process for the production of defined chemical compounds based on natural metabolic pathways.

In this work, *E. coli* was used as a whole-cell biotransformation system to convert ectoines into their hydroxylated forms by heterologous production of ectoine hydroxylases of different, predominantly extremophilic organisms. Since the biotransformation process is linked to osmoadaptation mechanisms, these mechanisms will be described in detail down below.

1.7.1 Osmoadaptation of *E. coli*

E. coli is a gram-negative, facultative anaerobic and moderately halotolerant γ-proteobacterium, which is capable of tolerating salinities up to 3.8 % NaCl, whereas its growth optimum is achieved by 0.5 % NaCl at 37 °C (Larsen *et al*., 1987; Mohammed *et al*., 2009). The natural habitats of this organism are characterized by inconstant amounts of salts: the colon of warm-blooded animals, one of its natural habitats, exhibits hyperosmotic features, whereas the release of this organism out of its host may be accompanied by the absence of any osmolytes. Therefore, *E. coli* has evolved different strategies in order to allow growth under fluctuating environmental concentrations of osmotic active substances.

The first reaction of *E. coli* exposed to high osmolarity is the uptake and accumulation of inorganic K^+ ions, mediated by the secondary transporters TrkH and TrkG. The simultaneous accumulation of glutamate, induced by the higher production of glutamate dehydrogenase and glutamate synthase, is necessary for intracellular charge neutralization (Dinnbier *et al*., 1988; McLaggan *et al*., 1994). High cellular concentrations of K^+ ions impair protein stability, which is why these charged units are subsequently exchanged by highly water soluble, zwitterionic substances. This can either be carried out by the uptake of compatible solutes, or *de novo* synthesis of the very same.

The energetically favorable uptake of these compounds is enabled by the upregulation of specific transporters. Two well investigated uptake systems are the ABC transporter ProU and the secondary transporter ProP. Originally identified as an uptake system for proline, ProU and ProP accomplish the uptake of a wide spectrum of different solutes (Csonka & Epstein, 1996).

Although both transporters exhibit a similar substrate spectrum, they show fundamental differences.

ProU is an ATP-dependent transporter of the ABC superfamily, consisting of the cytoplasmic and membrane associated ATPase subunit ProV, the integral membrane protein ProW and the periplasmatic binding protein ProX. Via this complex, ProU can transport betaines, including glycine betaine and proline betaine as well as ectoine and proline. Due to ProX, the substrate affinity for glycine betaine is enhanced, which is not true for the remaining solutes (Haardt *et al*., 1995).

ProP on the other hand is a secondary transporter from the major facility superfamily. It is a symporter that transports compatible solutes together with H^+ ions into the cytoplasm (Macmillan *et al*., 1999). ProP indeed mediates the uptake of many solutes, including the aforementioned solutes and additionally pipecolic acid, but its substrate affinity is very low compared to ProU (Jebbar *et al*., 1992; Kempf & Bremer, 1998). Transport activity is enhanced with increasing osmolarity, which is why ProP is also designated as an osmosensor or regulator (Milner *et al*., 1988; Culham *et al*., 1993).

Although ProP and ProU are both involved in ectoine uptake in *E. coli*, ProP seems to be the main transport system for this compatible solute. This is based on the finding that only non-functional ProP in deletion mutants results in lower growth rates under hypersaline conditions and in presence of ectoine (Jebbar *et al*., 1992).

Besides external solute uptake, *E. coli* is capable of *de novo* synthesis of compatible solutes, including glycine betaine and trehalose. The synthesis of glycine betaine is carried out by the prior uptake of choline via the high affinity transporter BetT, and a subsequent oxidation of this molecule by the dehydrogenases BetA and BetB (Bremer & Krämer, 2000). If neither choline nor glycine betaine is available, *E. coli* is capable of synthesizing the dissaccharide trehalose. The trehalose-6-phosphate synthase OtsA, activated by K^+ ions, condensates UDP-glucose and glucose-6-phosphate to trehalose-6-phosphate, which is dephosphorylated afterwards by the Trehalose-6-phosphate phosphatase (OtsB) to trehalose (Giæver *et al*., 1988).

1.7.2 *In vivo* conversion of ectoines

Since ectoine and OH-ectoine are commercially high-value products, the development of recombinant *E. coli* cell factories for their production have been established by several authors in order to optimize production and cost efficiency compared to currently applied procedures (Meffert, 2011; Ruprecht, 2014; Brauner, 2016; Moritz, 2018; Bethlehem, 2019). *E. coli* is an excellent biocatalyst in general and especially for the production of ectoines and their

hydroxylated derivatives for several reasons. This organism is one of the best investigated prokaryotes with many different already established strains for purposes like improved heterologous protein overproduction or plasmid stability, making it a model organism in microbiology, genetics and other life sciences (Lee, 1996; Russo, 2003). Beyond that, *E. coli* as a non-halophilic is suitable for the heterologous production and conversion of ectoines, as it is able to produce ectoines under low-salt conditions, resulting in cost-effective downstream processing approaches. Moreover, *E. coli* does not catabolize ectoine or it's hydroxylated derivative (Ures, 2006; Vielgraf, 2008).

For the biotransformation of ectoine to OH-ectoine by *E. coli* (fig. 5), the substrate first must be taken up. Via the membrane associated porines OmpC and OmpF, ectoine is introduced into the periplasm and afterwards carried into the cytoplasm via the transporters ProP and ProU (Czech *et al.*, 2016). For the conversion of accumulated ectoine, a plasmid encoded ectoine

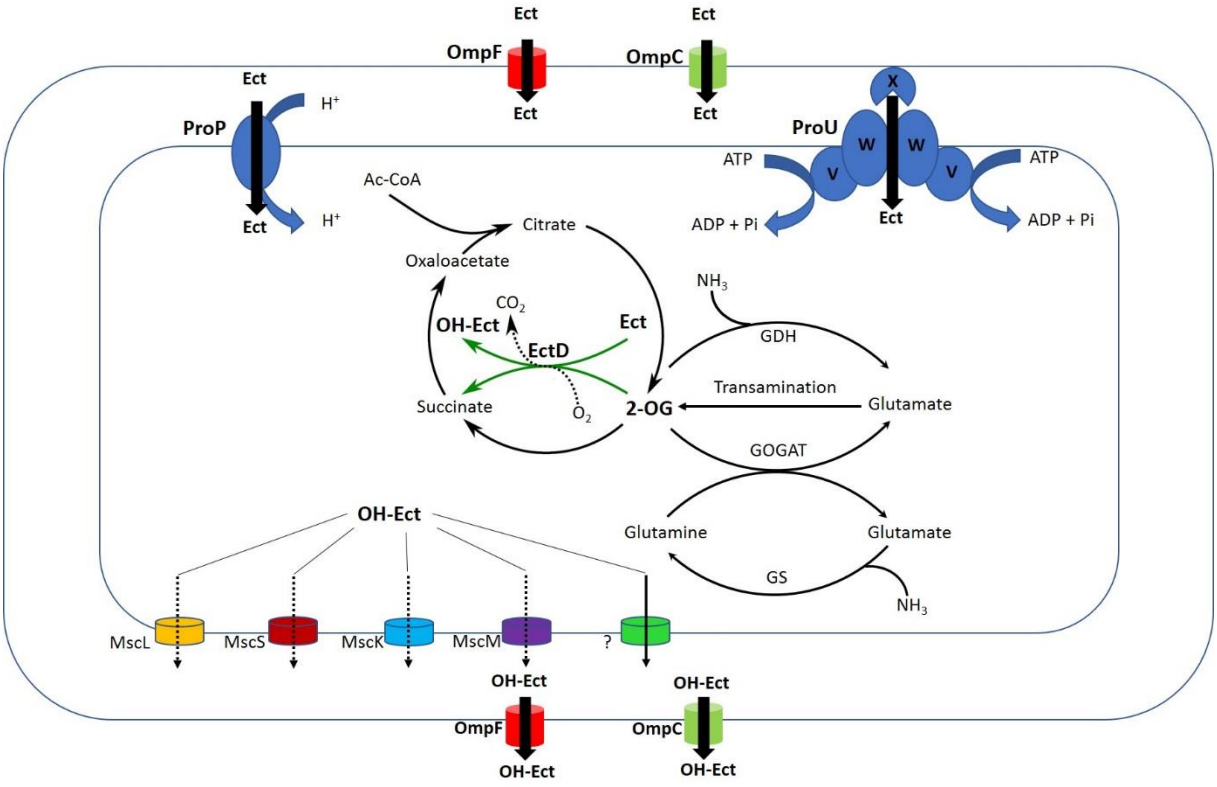

Figure 5: Whole-cell biotransformation scheme for the conversion of ectoine to 5-hydroxyectoine within a synthetic *E. coli* cell factory. Externally provided ectoine is taken up via porines OmpF/OmpC and transporters ProP/ProU into the cytoplasm. O_2-dependent hydroxylation of ectoine by heterologous EctD is coupled to oxidative decarboxylation of 2-oxoglutarate (2-OG), forming succinate and CO_2. Excretion of OH-ectoine is accomplished by a yet unknown transport mechanism independent from mechanosensitive channels (Msc). Ac-CoA = acetyl-CoA, Ect = ectoine, GDH = glutamate dehydrogenase, GOGAT = glutamate synthase, GS = glutamine synthase, OH-Ect = OH-ectoine.

hydroxylase *ectD* is heterologously expressed, since *E. coli* is not a natural OH-ectoine producer. After synthesis of EctD, the conversion of ectoine to OH-ectoine can take place inside the cytoplasm as described in 1.5.1. For the hydroxylation reaction, 2-oxoglutarate is necessary which is a central metabolite with a dual identity. This means it connects two central metabolic pathways, the central nitrogen metabolism and the tricarboxylic acid cycle (Yan *et al*., 2011).
After hydroxylation, OH-ectoine is excreted by a so far unknown mechanism, since neither a known mechanosensitive channel (MsC) nor the transporters ProP and ProU seem to be involved in this phenomenon (Edwards *et al.*, 2012; Czech *et al*., 2018). Experimental data, reported by Jebbar *et al.* (1992) suggest the existence of an unrecognized efflux system in *E. coli* which could be the cause for the MsC-independent release of OH-ectoine. However, this dynamic ectoine influx and OH-ectoine export can be exploited to convert large quantities of substrate.

1.8 Aim of the thesis

Ectoine and its hydroxylated derivative OH-ectoine are gaining more and more attention in the context of their stabilizing and protective abilities. These substances are considered as potential drugs for the treatment of several inflammatory diseases like colitis or oral mucositis. Escpecially hydroxylated ectoines are of great interest, since they show glass-forming properties and cause desiccation protection towards biomolecules or whole cells, as shown for OH-ectoine. The use of ectoines as applicable drugs for such diseases and as supplements in medical skin care causes an increased demand and calls for an improvement of the current cost-intensive production. The natural producer *H. elongata* only accumulates ectoine and hydroxyectoine simultaneously (Wohlfarth *et al*., 1990), entailing high costs due to chromatographic separation. Several *E. coli*-based synthetic cell factories for the biosynthesis of OH-ectoine (Moritz, 2018; Bethlehem, 2019) or for the conversion of ectoine to OH-ectoine (Meffert, 2011) under low salinity have already been shown to work in lab scales.
One part of this work aims for the optimization of the biotransformation process for the conversion of ectoine to its hydroxylated derivative OH-ectoine with *E. coli* as a microbial chassis. Previous studies already improved hydroxylation performance by optimizing cultivation parameters like temperature and the induction of gene expression. Furthermore, cell growth under nitrogen-limiting conditions caused high intracellular levels of the essential cofactor 2-oxoglutarate in *E. coli* (Ruprecht, 2014; Yan *et al*., 2011). However, instability of ectoine hydroxylase EctD from *H. elongata* turned out to be the critical bottleneck responsible

for constrained hydroxylation performance over time (Brauner, 2016). Besides enzyme stability, it was investigated which additional parameters determine the conversion rate of ectoine, such as substrate uptake rates, product efflux rates or the choice of the biotransformation system (different cell chassis and EctD enzymes).

EctD was already shown to exhibit a broad substrate spectrum, including several synthetic ectoine derivatives like homoectoine, guanidinoectoine or DHMICA. Therefore, another task in this work was to investigate, whether a broad substrate spectrum is unique to the hydroxylase of *H. elongata* or if homologues of other microorganisms show the same ability. Ectoine hydroxylases of four organisms (*H. elongata, A. cryptum, P. stutzeri and S. alaskensis)* were cloned and tested *in vitro* and *in vivo*. In this context, two new synthetic ectoine derivatives ethylectoine and propylectoine were tested as potential substrates for all examined hydroxylases, resulting in the formation of completely new solutes. Moreover, these new synthetic ectoines and their hydroxylated derivatives were characterized in terms of thermo- and osmostabilization as well as desiccation protection of whole cells or single biomolecules.

2 Material & Methods

2.1 Chemicals, kits, enzymes and markers

Table 1: Applied chemicals, kits, enzymes and markers. All enzymes were stored at -20 °C

Chemicals	Manufacturer
acetic acid (100 %)	Merck, Darmstadt, Germany
acetonitrile (≥ 99.9 %)	Merck
acrylamide (30 %)	Carl Roth, Karlsruhe, Germany
adenosine triphosphate (ATP) disodium salt (≥ 99 %)	Sigma-Aldrich, Steinheim, Germany
agar-agar Kobe I	Carl Roth
agarose	Carl Roth
arginine (≥ 99 %)	Merck
p-aminobenzoic acid (≥ 99 %)	Fluka, Buchs, Switzerland
ammonia solution, NH_3 (25%)	Merck
ammonium chloride, NH_4Cl (≥ 99 %)	Carl Roth
ammonium persulfate, APS (≥ 98 %)	Bio-Rad, Hercules, USA
ammonium sulfate, $(NH_4)_2SO_4$ (≥ 99.5 %)	Carl Roth
antibiotic broth medium No. 3	Oxoid Ltd., Hampshire, England
anhydrotetracycline hydrochloride	IBA, Göttingen, Germany
biotin (≥ 99%)	Sigma-Aldrich
bovine serum albumin, BSA	Sigma-Aldrich
bromophenol blue	Merck
calcium pantothenate (≥ 98 %)	Sigma-Aldrich
carbenicillin disodium salt (≥ 88 %)	Carl Roth
casein peptone (NZamin)	Carl Roth
chloroform (≥ 99.8 %)	Merck
creatine monohydrate (≥ 98 %)	Sigma-Aldrich
cyanocobalamin (≥ 97 %)	Merck
deoxyribonucleoside triphosphate mix, dNTPs (10 mM)	Thermo Fisher Scientific, Waltham, USA
desthiobiotin	IBA Life Sciences GmbH, Göttingen, Germany
deuterium oxide, D_2O (≥ 99 %)	Merck
L-2,4-diaminobutyric acid dihydrochloride, DABA (≥ 98 %)	Sigma-Aldrich
2,5-diketopiperazine, DKP (≥ 99%)	Sigma-Aldrich
dimethyl sulfoxide, DMSO (≥ 99.5 %)	Carl Roth
dipotassium hydrogen phosphate, K_2HPO_4 (≥ 99 %)	Carl Roth
dithiothreitol, DTT (≥ 99 %)	Carl Roth
ectoine (purity n/a)	Behawe Naturprodukte, Rietberg, Germany
ethanol (≥ 99.8 %)	Carl Roth
iron(II) sulfate heptahydrate, $FeSO_4$ x 7 H_2O (≥ 99 %)	Sigma-Aldrich
ethylenediaminetetraacetic acid, EDTA (≥ 99 %)	Carl Roth
formaldehyde (≥ 37 %)	Carl Roth
GelRed	Biotium, Fremont, USA
D-glucose monohydrate (≥ 99 %)	VWR, Darmstadt, Germany
glycerol (≥ 99.5 %)	Carl Roth
glycine (≥ 99 %)	Merck
glycine betaine (≥ 98 %)	Sigma-Aldrich

hydrochloric acid, HCl (37 %)	Carl Roth
hydroxyectoine (≥ 95 %)	Sigma-Aldrich
isopropanol (≥ 99.8 %)	Carl Roth
isopropyl-β-D-thiogalactopyranoside, IPTG (≥ 99 %)	Carl Roth
magnesium chloride heptahydrate, $MgCl_2$ x 7 H_2O (≥ 99 %)	Carl Roth
magnesium sulfate heptahydrate, $MgSO_4$ x 7 H_2O (≥ 99.5 %)	Merck
methanol anhydrous (max. 0.003 % H_2O)	Merck
N,N'-methylene-bis-acrylamide (2 %)	Merck
nicotinamide (≥ 99.5 %)	Fluka
nicotinamide adenine dinucleotide (NADH) disodium salt (≥ 97 %)	Fluka
silver nitrate, $AgNO_3$ (≥ 99 %)	Sigma-Aldrich
L-ornithine hydrochloride (≥ 99 %)	Merck
2-oxoglutaric acid monosodium salt (≥ 98 %)	Sigma-Aldrich
phenol/Chloroform/Isopentanol (25:24:1)	Carl Roth
potassium acetate (≥ 99 %)	Merck
potassium chloride, KCl (≥ 99.5 %)	Carl Roth
potassium dihydrogen phosphate, KH_2PO_4 (≥ 99 %)	Carl Roth
potassium hydroxide, KOH (≥ 85 %)	Carl Roth
proline (≥ 99.5 %)	Merck
pyridoxal hydrochloride (≥ 99.5 %)	Merck
pyruvate monosodium salt (≥ 99 %)	Carl Roth
Quick Coomassie stain	Generon, Slough, UK
sodium acetate trihydrate (≥ 99.5 %)	Sigma-Aldrich
sodium carbonate, Na_2CO_3 (≥ 99.5 %)	Sigma-Aldrich
sodium chloride, NaCl (≥ 99.5 %)	Carl Roth
sodium dodecyl sulfate, SDS (≥ 99 %)	Serva, Heidelberg, Germany
sodium hydroxide, NaOH (≥ 99 %)	Merck
sodium trimethylsilyl propionate, TMSP (≥ 98 %)	Merck
sodium thiosulfate heptahydrate, $Na_2S_2O_3$ x 5 H_2O (≥ 99.5 %)	Sigma-Aldrich
Strep-Tactin sepharose suspension (50 %)	IBA
N,N,N',N'-tetramethyl ethylenediamine, TEMED (≥ 99 %)	Carl Roth
2-[(2-hydroxy-1,1-bis(hydroxymethyl)ethyl)amino]ethanesulfonic acid, TES (≥ 99 %)	Carl Roth
thiamine hydrochloride (≥ 99 %)	Fluka
D-trehalose dihydrate (≥ 99.5 %)	Sigma-Aldrich
triethyl orthopropionate (97 %)	Sigma-Aldrich
trimethylamine N-oxide (TMAO) (≥ 98 %)	Sigma-Aldrich
trimethyl orthoacetate (99 %)	Sigma-Aldrich
trimethyl orthobutyrate (97 %)	Sigma-Aldrich
2-amino-2-(hydroxymethyl) propane-1,3-diol, TRIS (≥ 99.9 %)	Carl Roth
urea (≥ 99,5 %)	Carl Roth
yeast extract	Carl Roth
Enzymes	**Manufacturer**
alkaline phosphatase, FastAP (1 U/µL)	Thermo Fisher Scientific
catalase from bovine liver (2000-5000 U/mg)	Sigma-Aldrich
deoxyribonuclease I, DNase I	Sigma-Aldrich

lactate dehydrogenase (LDH) from rabbit muscle (148 U/mg)	Sigma-Aldrich
lysozyme	Carl Roth
Pfu-DNA-polymerase (2.5 U/µL)	Thermo Fisher Scientific
restriction endonucleases	Thermo Fisher Scientific
ribonuclease A, RNase A	Carl Roth
T4-DNA-ligase (5 Weiss U/µL)	Thermo Fisher Scientific
Kits	**Manufacturer**
BCA protein assay kit	VWR
Mix2Seq Kit ON	Eurofins Genomics, Ebersberg, Germany
peqGOLD gel extraction kit	Peqlab, Erlangen, Germany
Zyppy plasmid miniprep kit	Zymo Research, Irvine, USA
Markers	**Manufacturer**
GeneRuler 1 kb DNA ladder	Thermo Fisher Scientific
PageRuler prestained protein ladder	Thermo Fisher Scientific

2.2 Buffers and solutions

Unless otherwise stated, buffers and solutions were prepared in H_2O_{demin} and stored at room temperature (RT).

Table 2: Buffers and solutions.

Isolation of genomic DNA	
TES-buffer	5 mM TRIS/HCl, 5 mM NaCl, 5 mM EDTA, pH 8.0
lysozyme solution	Lysozyme (10 % w/v) in H_2O_{pure}; -20 °C
sodium acetate solution	3 M Na-acetate pH 4.8
SDS solution	SDS (10 % w/v)
Isolation of plasmid DNA (no column)	
NC buffer 1	50 mM TRIS/HCl pH 8.0, 10 mM EDTA, RNase A (10 % w/v), stored at 4 °C
NC buffer 2	200 mM NaOH, SDS (1 % w/v), pH 12.5
NC buffer 3	3 M Potassium acetate, pH 5.5, stored at 4 °C
Preparation of chemically competent cells	
TSS buffer	PEG 8000 (10 % w/v), DMSO (5 % v/v), 50 mM $MgSO_4$, resuspended in LB medium pH 6.5 (sterile filtered), stored at 4 °C
PCR	
dNTP mix	2 mM dNTPs in H_2O_{pure}, stored at -20 °C
Agarose gel electrophoresis	
1x TAE buffer	40 mM TRIS/HCl pH 8.0, 10 mM EDTA, Glacial acetic acid (0.6 % v/v)
loading dye (6x)	10 mM TRIS/HCl pH 7.6, 60 mM EDTA, Bromophenol blue (0.03% w/v), Glycerol (60% v/v), stored at 4 °C
Ligation	
ATP solution	10 mM ATP in H_2O_{pure}, stored at -20 °C
SDS PAGE	
acrylamide mix	32.7 mL Acrylamide (30 %), 10 mL Bisacrylamide (2 %), ad 50 mL (H_2O_{demin})
APS solution	APS (10 % w/v), 4 °C

stacking gel buffer	0.5 M TRIS/HCl pH 6.8
reducing sample buffer, RSB (4x)	4.5 mL conc. gel buffer, 5 mL Glycerol, SDS (5% w/v), DTT (3.86 % w/v), Bromophenol blue (tip of a spatula), ad 10 mL (H_2O_{demin}), stored at -20 °C
separating gel buffer	1.5 M TRIS/HCl pH 8.0
Laemmli buffer (1x)	0.025 M TRIS/HCl pH 8.4 - 8.9, 0.192 M Glycine, SDS (0.1 % w/v)
Silver staining	
fixing solution	500 mL Methanol, 120 mL Acetic acid (100 %), 0.5 mL Formaldehyde (37 %) ad 1000 mL H_2O_{pure}
thiosulfate solution	0.01 g $Na_2S_2O_3$ x 5 H_2O ad 50 mL H_2O_{pure}
impregnation solution	0.1 g $AgNO_3$, 0.037 mL Formaldehyde (37 %) ad 50 mL H_2O_{pure}
developing solution	3.0 g Na_2CO_3, 0.025 mL Formaldehyde (37 %), 0.004 g $Na_2S_2O_3$ x 5 H_2O ad 50 mL H_2O_{pure}
stop solution	2.5 mL Glacial acetic acid ad 50 mL H_2O_{pure}
Whole-cell protein extraction	
DNase I solution	DNase I (1 % w/v) in $H_2O_{pure,}$ stored at -20 °C
lysozyme solution	Lysozyme (10 % w/v) in $H_2O_{pure,}$ stored at -20 °C
$MgCl_2$ solution	50 mM $MgCl_2$
resuspension buffer	20 mM TRIS/HCl pH 8, 0.5 M NaCl
SDS solution	SDS (1 % w/v)
Strep-tag purification	
buffer W	100 mM TRIS/HCl, pH 8.0, 150 mM NaCl
buffer E	100 mM TRIS/HCl, pH 8.0, 150 mM NaCl, 2.5 mM Desthiobiotin
buffer R	100 mM TRIS/HCl, 150 mM NaCl, 1 mM EDTA, 1 mM HABA (hydroxy-azophenyl-benzoic acid), pH 8.0
Solute extraction	
Bligh & Dyer solution	Methanol/Chloroform/H_2O_{pure} (10:5:4 v/v)
Isocratic HPLC	
mobile phase	Acetonitrile (80 % w/v in H_2O_{pure})
^{13}C NMR	
solvent	D_2O and Na-TMSP (5 mg/mL), AcN (1 % v/v), Methanol (1 % v/v), stored at 4 °C

2.3 Software

Table 3: Applied software.

Program	Reference
ChemDraw Professional, version 18.0	PerkinElmer, Waltham, USA
ChromQuest, version 5.0	Thermo Fisher Scientific, Waltham, USA
KEGG (Kyoto Encyclopedia of Genes and Genomes)	Kyoto University, Kanehisa Laboratories, Japan
MestReNova version 8.0.1	Mestrelab Research, Santiago de Compostela, Spain
NCBI (National Center for Biotechnology Information)	U.S. National Library of Medicine, Bethesda, USA
Oligo Analyse Tool	Eurofins Genomics, Ebersberg, Germany
Pymol, version 2.2.3	DeLano Scientific LLC, USA
RBS calculator, version 2.1	Borujeni *et al*., 2014, Salis *et al*., 2009
SnapGene, version 5.0.1	GSL Biotech, Chicago, USA

Uniprot	European Bioinformatics Institute (EBI), Swiss Institute of Bioinformatics (SIB), Protein Information Resource (PIR)
VP Viewer 2000	MicroCal, Northampton, USA
WinASPECT, Version 2.2.0.0	Analytik Jena, Germany

2.4 Production of synthetic ectoine derivatives

Production of synthetic ectoines according to chemical synthesis of ectoine by Koichi *et al*. (1991) was done in order to generate ectoine derivatives with a higher fractional hydrophobic surface area. While ectoine exhibits a methyl group, the elongation of this functional group would increase its hydrophobicity. The same is true for the enlargement of the ectoine ring as it is the case for homoectoine.

For the synthesis of artificial ectoine derivatives, a diamino carboxylic acid was acetylated via an orthoester. Ring formation followed spontaneously by dehydration at 50 °C (fig. 6). By variation of different diamino carboxylic acids, the ectoine ring size could be changed, whereas different orthoesters were taken to replace the methyl group by different alkyl groups.

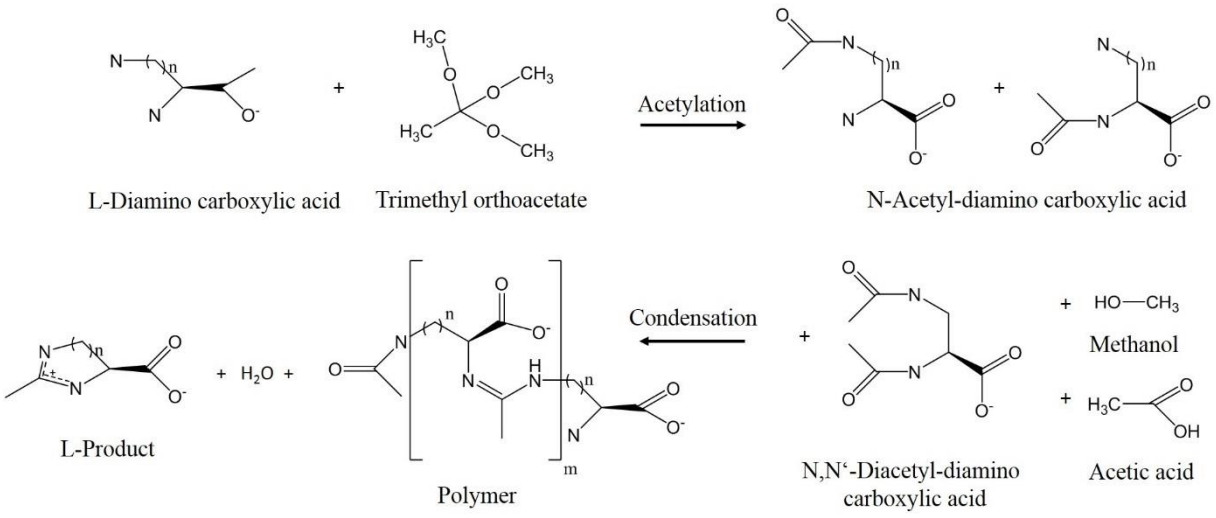

Figure 6: Chemical synthesis of zwitterionic cyclic amino acid derivatives (Voß, 2002). n = 2 corresponds to the synthesis of ectoine, n = 3 corresponds to synthesis of homoectoine. m = degree of polymerization.

2.4.1 Homoectoine as an ectoine derivative with enlarged ring size

For the synthesis of homoectoine (fig. 7), L-ornithine-HCl (e.g. 10 mmol) as diamino carboxylic acid and a 3-times excess of trimethyl orthoacetate (e.g. 30 mmol) as orthoester were mixed with anhydrous methanol (e.g. 33 mL) inside a round-bottom flask and heated at 60 °C

for 6 – 8 h. While heated, solutions were mixed by rotation with the use of a rotary evaporator (IKA, Staufen, Germany). Residual orthoester was removed by the addition of H_2O_{demin}, reacting to acetate and methanol, which were removed by vacuum drying (Vacuum System B-172, Büchi, Switzerland) under heat and rotation. The solution's pH was adjusted to 7 with NaOH and desalted by ion retardation chromatography (2.8.2.2). Desalted fractions were pooled and freeze-dried (Alpha I-6, Christ, Osterode, Germany). Solid material was dissolved in small volumes of anhydrous methanol under heating before crystallization at -20 °C. Crystals were harvested by filtering, and residual fluid was collected for another crystallization and harvest. Crystals were dried at 50 °C, grinded and analyzed by HPLC and NMR.

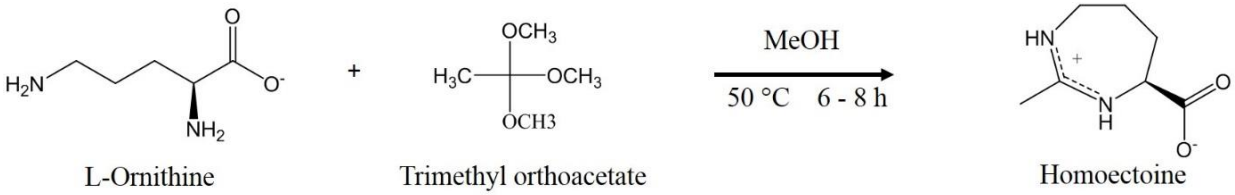

Figure 7: Synthesis of homoectoine.

2.4.2 Ectoine derivatives with different alkyl groups

Ectoine derivatives with different alkyl groups were synthesized by using L-2,4-diaminobutyric acid (DABA) and different orthoesters as educts. The synthesis of ectoines with prolonged alkyl groups was accomplished by the use of triethyl orthopropionate (ethylectoine), or trimethyl orthobutyrate (propylectoine) as orthoesters (fig. 8). Therefore, DABA x 2 HCl (e.g. 10 mmol) were mixed with a 3-times excess (30 mM) of the respective orthoester and dissolved in anhydrous methanol. Solubility of DABA in methanol was ~ 300 mM. After synthesis of ethylectoine and propylectoine, residual orthoesters were removed by the addition of H_2O_{demin}, reacting to propionate and butyrate, respectively. Synthesis and subsequent purification were carried out as previously described (2.4.1).

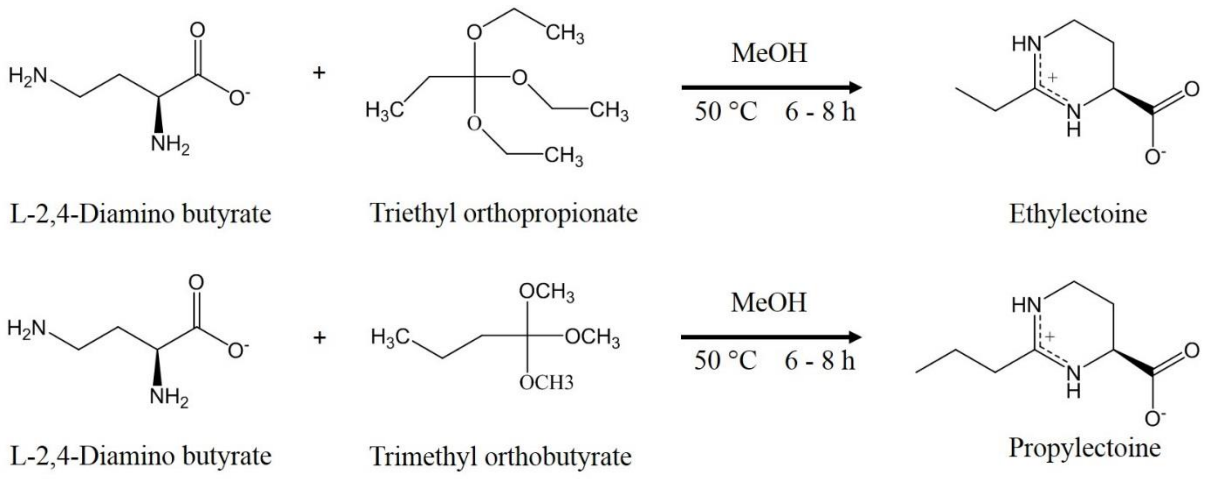

Figure 8: Synthesis of ethylectoine and propylectoine.

2.5 Microbiological methods

2.5.1 Bacterial strains and plasmids

For the heterologous expression of proteins, different *E. coli* strains were used as expression systems in combination with corresponding plasmid DNA, on which desired genes were coded. Genes, coded on pET-22b(+) vectors were under control of a strong T7-promoter, which originates from T7 phage. T7-RNA polymerase, required for transcription of desired genes was coded on the genome of *E. coli* BL21(DE3) under control of the Isopropyl-β-D-thiogalactopyranosid (IPTG) inducible lacUV5 promoter (Studier & Moffat, 1986). This vector also provides the option to add a C-terminal His_6-tag on the protein of interest.

For the use of pASK-IBA3 vector DNA, *E. coli* DH5α served as host strain. Genes of interest were coded downstream of a *tet* promoter and were induced by the supplementation of anhydrotetracycline (AHT). IBA3 vectors provided the option to add a C-terminal Strep-tag on the genes of interest.

All bacterial strains and plasmids used in this work are listed in table 4.

2.5.2 Culture media

All media were prepared in H_2O_{demin} and stored at room temperature for not more than 1 month. The percentage of NaCl is represented by a number after a dash (e.g. MM63-1 → MM63 medium + 1 % (w/v) NaCl). The pH was adjusted before adding NaCl. For the preparation of agar plates, 2 % agar (w/v) was added to the media. All media were sterilized at 121 °C for 20 min. After cooling to 60 - 70 °C, media with agar could be supplemented with sterile filtrated antibiotics. For MM63 medium (Larsen *et al*., 1987), glucose was autoclaved

separately from the rest of the media components and was added after cooling (tab. 5). $FeSO_4$ was supplemented after sterile filtration to avoid oxidation of Fe^{2+} by heat.

MM63 medium was used for EctD mediated whole-cell biotransformation experiments, cell drying experiments and osmotic stress experiments. N-limited MM63 medium contained 0.5 g/L $(NH_4)_2SO_4$ and 10 g/L glucose in order to adjust N-limiting conditions. Furthermore, it contained 0.0022 g/L $FeSO_4$ since Fe^{2+} is essential for EctD enzyme activity. AB medium agar plates (tab. 6) were used for strain preservation and cultivation of strains for isolation of genomic DNA. LB medium was used for cultivation of *E. coli* strains for plasmid isolation and for cell regeneration after transformation or drying stress. For the preparation of chemically competent *E. coli* cells, 2xYT medium was utilized.

Table 4: Applied bacterial strains and plasmids. [1] = suppl. fig 6, [2] = suppl. fig. 5

Strain	**Genotype**	**Reference**
Acidiphilium cryptum DSM 2389^T	Wildtype	Harrison, 1980
Escherichia coli BL21(DE3)	F^- *ompT gal dcm lon hsdSB*(rB^-mB^-) λ(DE3 [*lacI lacUV5-T7p07 ind1 sam7 nin5*]) [$malB^+$]$_{K-12}$(λ^S)	Studier & Moffat, 1986
Escherichia coli DH5a	F^-, *supE44*, *recA1*, *endA1*, *relA1*, *hsdR17* (rk, mk^-), *gyrA96*, λ^-, *thi*-1, Δ*lacU*169 (φ80*lacZα*M15)	Hanahan, 1983
Escherichia coli K12 DSM498^T	Wildtype	Guyer *et al*., 1981
Halomonas elongata DSM 2581^T	Wildtype	Vreeland *et al*., 1980
Pseudomonas stutzeri A1501	Wildtype	Yan *et al*., 2008
Sphingopyxis alaskensis DSM 13693^T	Wildtype	Vancanneyt *et al*., 2001
Plasmid	**Features**	**References**
pET-22b(+)	Amp^R, T7*lac*, *pelB*, $(His)_6$-tag	Novagen, Madison, USA
pET *ectDHis*	pET-22b(+) with *ectD* from *H. elongata* + His-tag	Meffert, 2011
pET *ectD_Acry_His*	pET-22b(+) with *ectD* from *A. cryptum* + His-tag	Janssen, 2015
pET *ectD_Pstu_His*[1]	pET-22b(+) with *ectD* from *P. stutzeri* + His-tag	This study
pET *ectD_Sala_His*[1]	pET-22b(+) with *ectD* from *S. alaskensis* + His-tag	This study
pASK-IBA3	AmpR, *bla*, ColE1-ori, *tet*-Repressor, *tetA*-Promotor/Operator, Strep-tag II	IBA-Lifesciences, Göttingen, Germany
pASK *ectD_Strep*[2]	pASK-IBA3 with *ectD* from *H. elongata* + Strep-tag II	Meffert, 2011
pASK *ectD_Acry_Strep*[2]	pASK-IBA3 with *ectD* from *A. cryptum* + Strep-tag II	This study
pASK *ectD_Pstu_Strep*[2]	pASK-IBA3 with *ectD* from *P. stutzeri* + Strep-tag II	This study
pASK *ectD_Sala_Strep*[2]	pASK-IBA3 with *ectD* from *S. alaskensis* + Strep-tag II	This study

Table 5: Formulation of minimal medium 63.

MM63-1 [C-limited]	Amount [g/L]	MM63-1 [N-limited]	Amount [g/L]
KH_2PO_4	13.61	KH_2PO_4	13.61
KOH	4.21	KOH	4.21
$(NH_4)_2SO_4$	1.98	$(NH_4)_2SO_4$	0.5 (C/N = 34) or 1 (C/N = 17)
$MgSO_4$ x 7 H_2O	0.25	$MgSO_4$ x 7 H_2O	0.25
$FeSO_4$ x 7 H_2O	0.0011	$FeSO_4$ x 7 H_2O	0.0022
NaCl	variable	NaCl	variable
glucose x H_2O	5	glucose x H_2O	10
pH 7.1		pH 7.1	

MM63-1 [balanced] (C/N = 8/1)	Amount [g/L]
KH_2PO_4	13.61
KOH	4.21
arginine or proline	1.41 or 3.76
$MgSO_4$ x 7 H_2O	0.25
$FeSO_4$ x 7 H_2O	0.0022
NaCl	variable
glucose x H_2O	10
pH 7.1	

Table 6: Media formulation of complex media AB medium (Antibiotic Broth Medium No. 3), LB medium (Lysogeny Broth Medium, Bertani, 1951) and 2xYT medium (Sambrook *et al.*, 1989).

AB medium components	Amount [g/L]	LB medium components	Amount [g/L]	2xYT medium components	Amount [g/L]
AB medium	17.5	casein peptone	10	casein peptone	10
NaCl	6.5	yeast extract	5	yeast extract	5
		NaCl	10	NaCl	5
pH 7.2		pH 7.2		pH 7.2	

2.5.3 Media additives

All additives were sterile filtrated before usage, unless described differently. Vitamin solution (VA solution) was stored at 4 °C, all other additives were stored at -20 °C.

Antibiotics. In order to maintain selection pressure and to avoid contamination, antibiotic stock solutions (100 mg/mL in H_2O_{demin}) were supplemented to media at RT or liquid agar below 70 °C. Carbenicillin (100 µg/mL) was used for the cultivation of *E. coli* carrying pASK and pET vectors, coding for beta lactamase.

Inductors. For the expression of genes coded downstream of the *tet* promotor in pASK vectors, AHT served as an inductor. AHT was dissolved in ethanol (2 mg/mL) and added to cultures to a final concentration of 0.2 µg/mL. The induction of genes coded after a T7 promotor on pET-22b(+) vectors was enabled by the addition of IPTG. A stock solution of 0.5 M was prepared in H_2O_{demin} and supplemented to expression cultures to a final concentration of 0.1 mM - 0.5 mM.

Substrates. Ectoine, as well as synthetic ectoine derivatives homoectoine, ethylectoine and propylectoine were used as substrates for enzymatic conversion by EctD. These substrates were dissolved in H_2O_{demin} and, depending on the experiment, supplemented at various concentrations.

Vitamin solution. The cultivation of thiamine auxotrophic *E. coli* DH5α in minimal medium was enabled by the addition of 1 mL vitamin solution (VA solution, tab. 7) per L medium. The solution was stored at 4 °C and under light exclusion.

Table 7: Formulation of VA solution (Imhoff & Trüper, 1977).

Component	Amount [mg/L]
biotin	100
cyanocobalamine	50
nicotinamide	350
p-aminobenzoic acid	200
calcium pantothenate	100
pyridoxal hydrochloride	100
thiamine hydrochloride	300

2.5.4 Strain preservation

For long-term preservation, all bacterial strains were stored in cryo cultures at -70 °C and were recultured on AB agar plates overnight before being used for inoculation of liquid cultures. Agar plates with cultivated organisms were stored no longer than two weeks at 4 °C.

2.5.5 Precultures / overnight cultures

Overnight cultures were prepared for isolation of genomic and plasmid DNA, and could also be used as precultures for main cultures or expression cultures. The preparation of overnight cultures was done by transferring 20 - 40 mL of medium into an appropriately sized Erlenmeyer flask. The cultivation of pASK-IBA3 and pET-22b(+) containing cells was carried out with the addition of carbenicillin (100 µg/mL). *E. coli* DH5α cultures in MM63 medium were supplemented with VA solution (2.5.3). Inoculation of culture medium was performed by adding fresh cell material from an agar plate. The cultures were incubated at 37 °C overnight at 180 rpm (Innova 4230, New Brunswick, Edison, USA).

2.5.6 Main cultures / expression cultures

Main culture medium was always the same as preculture medium. If precultures contained β-lactamase producing cells and carbenicillin, overnight cultures were centrifuged under sterile conditions (Avanti J-20, Beckman Coulter, rotor JA-10, 5,000 x *g*, 10 min, RT). The cell pellet was resuspended in fresh medium to remove excreted β-lactamase and was subsequently supplemented with the same additives. Afterwards, precultures were used to inoculate main culture media. Main cultures were carried out in OD-flasks, allowing a direct measurement of the optical density (OD) of undiluted culture medium via an integrated glass tube (Novaspec II, Pharmacia, Uppsala, Sweden). Up to an OD_{600} of 0.5, the relationship between cell density and OD is linear.

2.5.6.1 Whole-cell biotransformation of ectoines

The investigation of ectoine hydroxylase (EctD) substrate spectrum was realized by using plasmid coded hydroxylases of four different organisms: *H. elongata*, *A. cryptum*, *P. stutzeri* and *S. alaskensis*. The respective genes were coded on pET-22b(+)- and pASK-IBA3-vectors and subsequently integrated into *E. coli* BL21 and *E. coli* DH5α via transformation.

MM63-1 medium was supplemented with carbenicillin (100 µg/mL) and, in case of *E. coli* DH5α, with VA solution (1 mL/L). Main culture medium was then inoculated with precultures to an OD_{600} of 0.15. The working volume was either 50 mL or 100 mL. Cultures were shaken at 37 °C and 180 rpm (Innova 4230). The expression of heterologous hydroxylase genes coded on pET-22b(+) was induced by adding IPTG (0.1 or 0.5 mM) at an OD_{600} of 0.3 or 0.6. The expression of heterologous genes coded on pASK-IBA3 vectors were induced with AHT (0.2 µg/mL) at an OD_{600} of 0.5. Cultures were then supplemented with ectoine or its synthetic

derivatives at concentrations of 2 - 30 mM. Samples were taken regularly under sterile conditions and were centrifuged to obtain media supernatants for HPLC analysis and cell material for protein purification and analysis. Cultures were regularly supplemented with extra glucose to ensure a sufficient amount of carbon source.

In order to investigate the chemical instability of OH-homoectoine, culture media was centrifuged (Avanti J-20, 12,000 x *g*, 20 min, RT) and supernatants, containing OH-homoectoine were adjusted to different pH (2, 4, 6, 7, 8, 10) and filtered by a cellulose membrane (Amica Ultra-4, 3 kDa) to remove potentially excreted proteins. 20 mL of filtered supernatants were transferred into sterile flasks, sealed with parafilm and incubated at 32 °C under shaking for 120 h. Samples were taken regularly and analyzed via isocratic HPLC.

For the extraction of hydroxylated ectoine derivatives (2.8.2), cells were exposed to osmotic stress by adding NaCl (5 % w/v) when biotransformation was complete (verified via HPLC analysis). This caused an increased uptake of excreted hydroxylated solutes back into the cells. Cells were further incubated for 60 min and were harvested afterwards (Avanti J-20, 5,000 x *g*, 15 min, RT) before being stored at -20 °C. After freeze-drying of cells (Alpha I-6, Christ) at 20 °C and 0.05 mbar, solutes were extracted with B&D solution (2.8.1).

2.5.6.2 Heterologous production of EctD for Strep-tag purification

For the heterologous production of EctD in *E. coli* DH5α and subsequent Strep-tag based purification, pASK-IBA3 vectors with coded Strep-tagged *ectD* of four different organisms *H. elongata*, *A. cryptum*, *P. stutzeri* and *S. alaskensis* were used (tab. 4). 1 L of LB-1 complex medium was inoculated with preculture to an OD_{600} of 0.15 and supplemented with carbenicillin (100 µg/mL). After incubation at 37 °C to an OD_{600} of 0.5, expression of recombinant *ectD* was induced by adding AHT (0.2 µg/ml) to expression cultures. Cells were harvested 4 h after induction (Avanti J-20, 4,000 x *g*, 15 min, 4 °C) and, after removal of supernatant, pellets were stored at -20 °C.

2.5.6.3 Solute uptake experiment

These experiments were accomplished to examine whether and how fast synthetic ectoine derivatives are taken up by *E. coli* in comparison to ectoine. This data can be helpful to clarify if the uptake rate is a crucial limiting factor for the turnover rate in *E. coli*.

50 mL MM63-1 medium (C-limited) were supplemented with VA solution and inoculated with *E. coli* DH5α preculture under sterile conditions up to an OD_{600} of 0.15. Cultures were shaken

at 37 °C at 180 rpm (Innova 4230) until an OD_{600} of 0.5. At that point, ectoine or synthetic ectoine derivatives homoectoine, ethylectoine or propylectoine were added to a final concentration of 10 mM. 2 mL of culture were filtered at regular time intervals. For this purpose, the culture was transferred onto polycarbonate filters (0.2 µm pore size, Sartorius, Göttingen, Germany), which were equilibrated in MM63-1 medium without carbon source. Filtration was accomplished by applying a vacuum (fig. 9). After liquid was completely removed, the loaded filters were washed immediately by filtering 2 mL of fresh MM63-1 medium without carbon source to avoid further uptake by removing glucose as the energy source. Loaded filters were transferred to B&D solution for solute extraction (2.8.1). Via HPLC analysis, amounts of solutes were calculated and related to OD_{600}. From this, the solute uptake in nmol solute per mg whole-cell protein was determined. The amount of whole-cell proteins was estimated by multiplication of OD_{600} with the factor 0.44 (= theoretical bacterial dry mass in g/L, Bolten *et al*., 2007) and another multiplication with the factor 0.5 (= theoretical whole-cell protein amount in g/L). Maximal substrate uptake rates were given in nmol x min^{-1} x mg^{-1} and were calculated for the time period 1 - 6 min after substrate supplementation, as uptake speed was linear in this area.

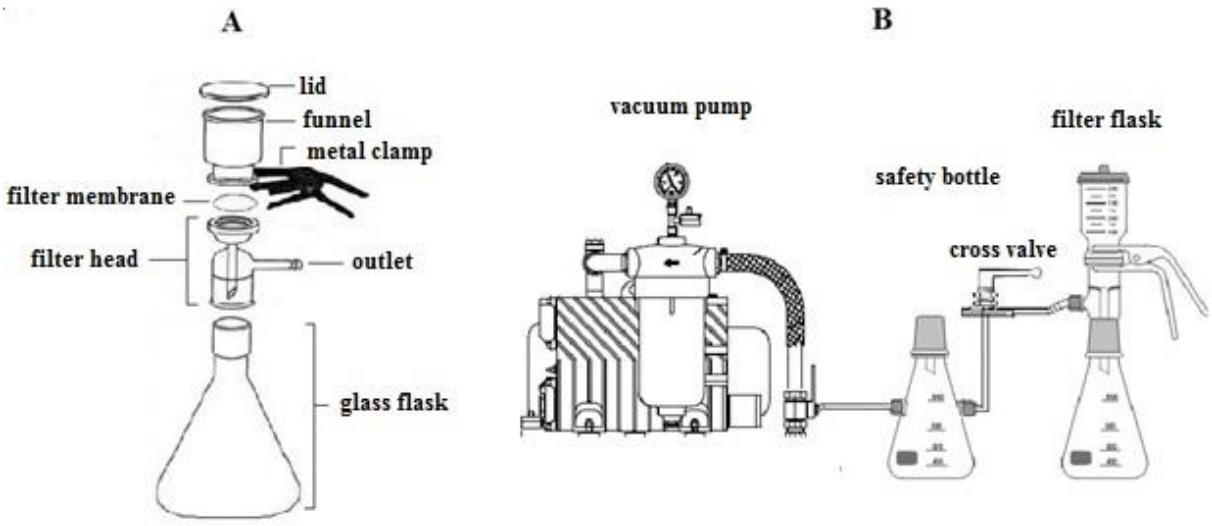

Figure 9: Vacuum filtering system for the filtration of *E. coli* DH5α. A: Filter flask components. B: System concept. Vacuum was applied by activating a connected pump and closing the system via a cross valve. A safety bottle was used to avoid contact of culture medium with the pump (modified: https://www.neubert-glas.de).

2.5.6.4 Reactivation of dried cells

Synthetic ectoine derivatives were investigated as possible protective solutes for dry stress towards whole cells. In order to prove that, *E. coli* K-12 was air dried in presence and absence of ectoine, as well as its synthetic derivatives and their hydroxylated forms. Additionally, other solutes which are known to be protective or the opposite were tested. The following solutes were examined: (OH-)ectoine, homoectoine, (OH-)ethylectoine, propylectoine, trehalose and glycine betaine.

Solutes were dissolved in MM63-1 (C-limited), sterile filtered, and mixed with preculture to a final solute concentration of 0.2 M and an OD_{600} of 0.15. Each suspension was transferred into a 96 well microtiter plate (six replicates) by pipetting 20 µL per well. As a control, preculture was mixed with MM63-1 medium without any solute. Another six wells were filled with sterile medium to rule out contamination with airborne germs. Subsequently, the microtiter plate was sealed with an acetate film (Sarstedt, Nümbrecht, Germany) and dried at 50 °C for 16 h. For the purpose of evaporation, the film was perforated with a sterile needle. After drying, each well was filled with 200 µL sterile LB-1 medium and the plate was sealed with a new acetate film. Incubation at 37 °C and OD measurement was performed automatically by a plate reader taking values every 15 min (Tecan Infinite M200, Crailsheim, Germany). The plate was shaken for 30 s every 5 min to avoid sedimentation of cells.

2.5.6.5 Cell growth under osmotic stress

Since ectoine is a well-known osmoprotectant, it is plausible to also check synthetic ectoine derivatives for this characteristic. Besides ectoines ((OH)-ectoine, homoectoine, (OH)-ethylectoine, propylectoine), also solutes which are known to be efficient (glycine betaine) or weak (creatine) osmoprotectants were tested regarding growth of *E. coli* under osmotic stress.

Overnight cultures of *E. coli* K-12 in MM63-3 medium (C-limited) were diluted with fresh medium to an OD_{600} of 0.15 and supplemented with solutes (2 mM). Each suspension was transferred into a microtiter plate by pipetting 200 µL per well (six replicates). As a control, *E. coli* K-12 suspension without any solute was transferred to the plate. To exclude contamination with airborne germs, sterile medium was also transferred to the plate. Subsequently, the plate was sealed with an acetate film and incubated at 37 °C. Incubation and OD measurement was performed in a plate reader as previously described (2.4.6.4).

2.5.6.6 Preparation of chemically competent *E. coli*

For the transformation of genetically modified plasmid DNA, *E. coli* cells were made competent using the TSS protocol of Chung *et al.* (1989). 50 mL of LB-1 medium were inoculated with *E. coli* overnight culture (1 % v/v), and incubated shaking at 37 °C up to an OD_{600} of 0.3 - 0.45. Cultures were harvested under sterile conditions (Avanti J-20, 4,000 x *g*, 15 - 20 min, 4 °C), and the cell pellet was dissolved in 2.5 mL cold TSS buffer. Aliquots of 150 µL were stored at -20 °C.

2.6 Molecular biological methods

2.6.1 DNA isolation

Genomic DNA. Isolation of genomic DNA (gDNA) was necessary for PCR as this DNA was used as a template. *S. alaskensis* gDNA was purchased from the German collection of microorganisms and cell culture GmbH (DSMZ).

Isolation of gDNA was performed by preparing overnight cultures in appropriate complex medium. Approximately 4 - 8 mL of overnight culture were centrifuged (Eppendorf 5418, Hamburg, Germany, 9,500 x *g*, 5 min, RT) and the pellet was resuspended in 1 mL TES buffer. 20 µL SDS solution (20 % w/v) were added for cell lysis, and the sample was incubated at RT for 30 min. Subsequently, 300 µL of extraction solution (phenol/chloroform/isopentanol, 25:24:1 (v/v)) were given to the lysate. After vigorous shaking and centrifugation (16,000 x *g*, 10 min, 4 °C), the upper aqueous phase was transferred into another 300 µL of extraction solution. This was repeated until no interphase with proteins was recognizable anymore. DNA was precipitated by adding 1/10 sample volume of 3 M sodium acetate (pH 4.8) and 1 sample volume icecold isopropanol. The samples were incubated at -20 °C for 30 min and centrifuged afterwards (10,000 x *g*, 10 min, 4 °C). After removing the supernatant, the DNA pellets were washed by adding 500 µL icecold ethanol (70 % w/v) and a following centrifugation (10,000 x *g*, 10 min, RT). The washing step was repeated, the supernatant removed and the DNA pellet dried at 60 °C for 10 min. 50 µL of sterile H_2O_{demin} were used to dissolve the DNA pellet, and the sample was stored at -20 °C.

Plasmid DNA. This type of DNA was used for cloning procedures and gene sequencing. For gene sequencing and insert amplification, plasmid DNA was isolated using the Zyppy plasmid-miniprep kit according to manufacturer's instructions (Zymo Research, Irvine, USA). For test digestions of vectors, the DNA was isolated via a no-column preparation. For this purpose,

approximately 1.5 - 4.5 mL overnight culture medium (LB medium) were centrifuged (Eppendorf 5418, 13,600 x *g*, 1 min, RT), the supernatant removed and the cell pellet resuspended in 200 µL NC buffer 1 by vortexing. After the addition of 200 µL NC buffer 2, the suspension was carefully inverted, causing alkaline hydrolysis of cells. The reaction was stopped by quickly adding 200 µL NC buffer 3. The samples were inverted, centrifuged (13,600 x *g*, 3 min, RT) and the supernatant mixed with 500 µL chloroform by vigorous shaking. After another centrifugation (13,600 x *g*, 3 min, RT), the supernatant was mixed with 500 µL icecold isopropanol, causing DNA precipitation. The sample was centrifuged again and the DNA pellet washed by adding 500 µL ethanol (70 % w/v) after removing the isopropanol. In a further step, the sample was centrifuged shortly, and the ethanol was removed. Finally, the DNA pellet could be dried at 60 °C for 30 min and subsequently be resuspended in 30 µL pure water. DNA was stored at -20 °C.

PCR fragments and digested DNA. For the extraction of PCR products, as well as enzymatically modified DNA, fragments were sliced out of agarose gel after electrophoresis (2.6.4) and purified by using the peqGOLD gel extraction kit (Peqlab, Erlangen, Germany) according to manufacturer's instructions.

2.6.2 DNA quantification

The concentration and purity of DNA was measured using a Nanodrop-BioSpectrometer (Eppendorf). Nucleic acids have the highest absorbance at a wavelength of 260 nm while proteins or, more specifically, aromatic amino acids show absorption maxima between 275 nm and 280 nm. By measuring samples at 260 nm and 280 nm, DNA concentration and purity could be determined by calculating the ratio of A_{260}/A_{280}. Pure DNA solution exhibits ratios of 1.7 - 1.9, whereas higher values suggest RNA contamination and lower values protein contamination. By the given DNA mass concentrations (ng/µL), the molar concentrations required for DNA ligation could be calculated:

$$DNA\ \left[\frac{mol}{\mu L}\right] = \frac{DNA\ \left[\frac{ng}{\mu L}\right]\ x\ 10^{-9}}{660\frac{g}{mol}\ x\ basepairs\ of\ fragment}$$

A semiquantitative method to calculate DNA concentration was comparing fluorescence intensity of DNA with a DNA standard of known concentration after gel electrophoresis and

staining (2.6.4). This method is a good addition to spectrophotometric DNA quantification, since one can also capture DNA contamination or incomplete DNA digestion.

2.6.3 Polymerase chain reaction (PCR)

The polymerase chain reaction (PCR) was established by Mullis *et al*. (1986) and is a method to amplify DNA fragments *in vitro*. Since this method has become a standard technique in molecular biology, detailed descriptions of its concept have been elaborated for decades (Garibyan & Avashia, 2013).

DNA amplification via PCR was carried out by using *Pfu* DNA polymerase (Thermo Fisher Scientific, Waltham, USA) according to manufacturer's instructions. This enzyme originates from the thermophilic archaeon *Pyrococcus furiosus* and exhibits 3'-5' exonuclease activity, reducing the number of amplification errors. Oligonucleotides (primers) for insert amplification and sequencing (tab. 9) were designed manually using SnapGene software (GSL Biotech, Chicago, USA) and ordered from Eurofins Genomics (Ebersberg, Germany). Primers exhibit a DNA binding part and a non-binding part, consisting of a nucleotide overhang and the restriction site sequence. In some cases, primers can also have a non-binding synthetic ribosomal binding site sequence (RBS). For the DNA binding part (Cycle A), another primer annealing temperature was chosen than for the non-binding part (Cycle B). Annealing temperatures were calculated using 'Oligo Analyse Tool' from Eurofins (tab. 8). Synthetic RBS can generate higher initiation rates during translation (Stiller *et al*., 2018) and were calculated *in silico* using RBS calculator 2.1 (Salis *et al*., 2009; Borujeni *et al*., 2014).

Table 8: Formulation and parameters for PCR. T_{MA} = primer melting temperature of DNA binding part, T_{MB} = primer melting temperature of DNA non-binding part.

Formulation		**Amplification**			
Component	Volume [µL]	Step	Cycles	Temperature [°C]	Time
Pfu-buffer (10x) + $MgSO_4$	5	initial denaturation	1	95	2 min
dNTP mix (2 mM)	5	cycle A denaturation	5	95	30 s
5' primer (10 pmol/µL)	1	cycle A annealing		T_{MA} - 5	30 s
3' primer (10 pmol/µL)	1	cycle A elongation		72	2 min/kb
DNA (10 – 500 ng/µL)	1	cycle B denaturation	30	95	30 s
glycine betaine (5 M)	10	cycle B annealing		T_{MB} - 5	30 s
Pfu polymerase (2.5 U/µL)	0.5	cycle B elongation		72	2 min/kb
H_2O_{pure}	Ad 50 µL	final elongation	1	72	10 min
		cooling	-	4	∞

Table 9: Primers used for PCR and DNA sequencing. Restriction site sequences are indicated in bold letters. RE = restriction endonuclease. The underlined sequence contains the synthetic RBS (Shine-Dalgarno sequence, AGGAGG) and its upstream area.

Name	Sequence (5'-3')	RE
for_ectD_Acry + RBS_EcoRI	TAAGCA**GAATTC**GAATAATCCTAACGAGGAAATTTAT AAGGAGGTATTTTTATGGACGATCTCTATCCG	*Eco*RI
rev_ectD_Acry_Strep_NcoI	CGG**CCATGG**GCTGCCGCGCGCTCGCGC	*Nco*I
for_ectD_Pstu + RBS_EcoRI	TAAGCA**GAATTC**CAGAGACGTAAGTCCACAATTAGAA ATTAAGGAGGTATTTTTTATGCAAGCCGACCTGTATCC	*Eco*RI
rev_ectD_Pstu_Strep_NcoI	TGCTTA**CCATGG**AGGAGATACTGTTGCGGCCGAA	*Nco*I
for_ectD_Pstu + RBS_NdeI	TAAGCA**CATATG**GGTTAGTCAACCAGAAATAATTATT AAGGAGGTATTTTTTATGCAAGCCGACCTGTAT	*Nde*I
rev_ectD_Pstu_HindIII	TGCTTA**AAGCTT**TCAGAGATACTGTTGCGG	*Hin*dIII
for_ectD_Sala + RBS_EcoRI	TAAGCA**GAATTC**AACTTTTACTTCGCACCCTCGACATAAGGC AGGATTTTTTATGCAAGACCTCTACCCCTC	*Eco*RI
rev_ectD_Sala_Strep_NcoI	TGCTTA**CCATGG**ACTGCCGGCACCGTTTCGACGA	*Nco*I
for_ectD_Sala + RBS_NdeI	TAAGCA**CATATG**AACTTTTACTTCGCACCCTCGACATA AGGCAGGATTTTTTATGCAAGACCTCTACCCCTC	*Nde*I
rev_ectD_Sala_HindIII	TGCTTA**AAGCTT**TCATGCCGGCACCGTTTC	*Hin*dIII

2.6.4 Agarose gel electrophoresis (AGE)

Agarose gel electrophoresis (AGE) is a method to separate nucleic acids by exposing these negatively charged biomolecules to an electric field in an ionic buffer solution, causing size-dependent migration to the positively charged anode.

For the evaluation and isolation of digested and non-digested DNA (PCR products and plasmids), AGE was performed. Gels were prepared by dissolving agarose in 1x TAE buffer (1 % w/v) under heat until the fluid was clear. After poured gels had hardened inside chambers (Biometra Horizon 58, Analytik Jena, Germany), gels were overlaid with 1x TAE buffer and loaded with samples and DNA ladder (1 kb GeneRuler, Thermo Fisher Scientific) in 1x loading dye. Electrophoresis was performed by applying 60 - 80 V (Power Supply 122, Consort, Turnhout, Belgium). Gel-bound DNA was stained with GelRed (Biotium, Fremont, USA) according to manufacturer's instructions and visualized in a Gel-Imager (Intas, Göttingen, Germany) under UV light excitation.

2.6.5 Restriction digestion

For cloning experiments, plasmid DNA and PCR insert DNA was hydrolyzed by restriction endonucleases, cleaving off phosphodiester bonds at specific nucleotide sequences.

Enzymatic hydrolyzation of plasmid DNA and amplicons was performed for 3 h using restriction enzymes and buffers (Thermo Fisher Scientific) according to manufacturer's instructions (tab. 10). After 2.5 h, 1 U alkaline phosphatase (AP) was added to plasmid DNA, preventing re-ligation by dephosphorylating 5' ends. Enzyme inactivation was accomplished by heating samples at 70 °C for 10 min. The following DNA purification was performed as previously described (2.6.1).

Table 10: DNA restriction digestion assay.

Component	Amount
DNA (plasmid or PCR amplicon)	5 - 10 µg
restriction enzymes	5 - 10 U
reaction buffer (10x)	2 or 4 µL
H_2O_{pure}	ad 20 µL or ad 40 µL

2.6.6 Ligation

In order to integrate insert DNA into a recipient vector after restriction digestion, ATP-dependent T4-DNA ligase (Thermo Fisher Scientific) was used, connecting adjacent 3'-hydroxy and 5'-phosphate strands. Ligation performance was increased by adjusting a plasmid:insert molar ratio of 1:3 (tab. 11). Samples were incubated at 16 °C for 16 h and enzymes were subsequently inactivated at 65 °C for 10 min. If not used immediately for transformation, samples were stored at -20 °C.

Table 11: DNA ligation assay.

Component	Amount
plasmid DNA	10 – 120 ng
insert DNA	3:1 molar ratio
ATP (10 mM)	1 µL
T4 DNA ligase buffer (10x)	2 µL
T4 DNA ligase	1 µL
H_2O_{pure}	ad 20 µL

2.6.7 Transformation

After cloning, the uptake of cloned plasmid DNA by *E. coli* was performed by using chemically competent cells. Aliquots of competent *E. coli* cells were thawed on ice and incubated with 5 - 10 µL of ligation samples for 20 min to attach DNA to cell walls. DNA uptake was achieved by a heat shock at 42 °C for 1.5 min and a subsequent cool-down on ice for 2 min. Cell suspensions were mixed with 500 µL prewarmed 2xYT medium and incubated at 37 °C for 1.5 h under shaking. Cells were plated out on AB agar plates (carbenicillin, 100 µg/mL) by applying 150 µL of the suspensions. Residual volumes were centrifuged (Eppendorf 5418, 10,000 x *g*, 1 min, RT), and the pellet was resuspended with the backflow, which was applied to another AB agar plate. Incubation was performed at 37 °C overnight.

Transformation of cloned DNA was checked by picking and plating out single colonies on AB agar plates (carbenicillin, 100 µg/mL), followed by plasmid isolation and subsequent restriction digestion and AGE as previously described (2.6.1, 2.6.5, 2.6.4).

In order to verify successful cloning, gene sequencing was performed with the Mix2seq kit from Eurofins according to manufacturer's instructions.

2.7 Protein biochemical methods

2.7.1 Whole-cell protein extraction

Soluble proteins. For the extraction method of soluble proteins established by Brünig (2005), cell pellets from 10 mL culture medium were thawed on ice and resuspended in 200 µL resuspension buffer. After adding 2 µL of lysozyme (10 % w/v), suspensions were mixed by vortexing and incubated on ice for 30 min. Subsequently, 10 µL of SDS (10 % w/v) were added to the suspensions, followed by incubation on ice for 30 min. After that, 1 µL of $MgCl_2$ (50 mM) and 2 µL DNase I (1 % w/v) were added, leading to hydrolyzation of DNA. Samples were incubated on ice for 1.5 h before freezing at -20 °C for at least 30 min. Complete cell disruption was accomplished by ultra-sonification on ice for 45 min (Sonorex TK52, Bandelin, Berlin, Germany). Samples were centrifuged (Eppendorf 5418, 16,000 x *g*, 30 min, 4 °C) and the supernatant, containing soluble proteins, stored at -20 °C in a fresh tube. Cell debris were processed further to purify insoluble proteins.

Insoluble proteins. This extraction was performed based on the method of Tetsch (2001). Cell debris from extraction of soluble cell proteins were washed twice with 750 µL resuspension buffer (16,000 x *g*, 5 min, RT), removing remaining soluble proteins. Depending on pellet size,

300 +/- 100 µL of lysozyme (1 % w/v) were used for resuspension, followed by heating at 80 °C and 800 rpm for 1.5 h (Thermomixer compact, Eppendorf).

2.7.2 EctD enzyme purification

Purification of Strep-tagged EctD was performed for enzyme activity assays with different substrates besides ectoine as its natural substrate. EctD production was conducted as previously described (2.5.6.2).

2.7.2.1 Cell disruption by ultra-sonification

Pellets of expression cultures were resuspended in 10 mL buffer W and supplemented with 5 µL protease inhibitor cocktail (Sigma-Aldrich). Subsequent ultra-sonification (Branson Sonifier Cell Disruptor & Branson Ultra Sonics Converter, Danbury, USA) was performed by using an amplitude of 50 % for 20 min at 4 °C for cell disruption (Colora Messtechnik GmbH, Lorch, Germany). Cleared lysates were gained by centrifugation (Avanti J-20, 12,000 x *g*, 20 min, 4 °C) and used for further purification.

2.7.2.2 Strep-Tactin affinity chromatography

This purification method is facilitated by a strong affinity between an immobile Strep-Tactin resin and an artificial oligopeptide (Strep-tag) which is tagged to the enzyme of interest. These Strep-tag fusion proteins are bound to the Strep-Tactin matrix, whereas the vast majority of other proteins flow through. Elution of bound enzymes is enabled by desthiobiotin, which is a biotin analogue and exhibits even higher affinity for Strep-Tactin, a streptavidin analogue.
Purification was carried out at 4 °C. Cleared lysates (2.7.2.1) were completely transferred on a Strep-Tactin-sepharose matrix (IBA GmbH, Göttingen, Germany), immobilized inside a polypropylene column (Quiagen, Hilden, Germany) with a column volume (CV) of 1 mL. Columns were washed 5 x with 1 CV buffer W (without EDTA), and elution of fusion proteins was performed by adding 6 x 0.5 CV buffer E (without EDTA). Buffers contained no EDTA in order to avoid metal complexation, which is critical for Fe^{2+} depending activity of EctD. Regeneration of the Strep-Tactin matrix was acquired by washing columns with 3 x 5 CV buffer R, containing excess amounts of azo dye 4'-hydroxyazobenzene-2-carboxylic acid (HABA), which leads to the removal of desthiobiotin. HABA was removed by washing columns again with 2 x 4 CV buffer W, and regenerated columns were stored at 4 °C in buffer W.

2.7.3 Protein quantification

To determine protein concentrations for SDS-PAGE and enzyme activity assays, a bicinchoninic acid assay (BCA), based on the biuret reaction was performed (Smith, *et al*., 1985). Here, Cu^{2+} is reduced to Cu^{+} by peptide bonds under alkaline conditions, leading to photometrically detectable BCA-copper complexes. Complexation is proportional to protein concentration which can be quantified by using protein standards (bovine serum albumin, BSA) of known concentrations. The BCA assay was performed in 96 well microtiter plates by using a BCA Protein Assay Kit (Thermo Fisher Scientific) according to manufacturer's instructions. Protein samples where diluted 1:5 - 1:50 in H_2O_{pure} and tested as triplicates. Concentrations were determined by measuring samples at 550 nm (Tecan Infinite M200), and referring the absorbance to the BSA protein standards (50 - 500 µg/mL).

2.7.4 SDS-polyacrylamide gel electrophoresis (SDS-PAGE)

SDS-PAGE is an analytical method to acquire size dependent protein separation in an electric field. The modified concept of this method, referring to Laemmli (1970) is a discontinuous electrophoresis achieved by the use of two-part gels. Proteins are concentrated inside the stacking gel with neutral pH whereas actual separation takes place in a separating gel with alkaline pH and a lower pore size. Polyacrylamide gels consist of acrylamide molecules which are polymerized linearly by ammonium persulfate (APS) and crosslinked by N,N'-methylene-bis-acrylamide, catalyzed by N,N,N‘,N‘-Tetramethyl ethylendiamin (TEMED). To eliminate the influence of protein structures and charges to the separation, SDS and DTT as denaturing and reducing agents were used (tab. 12).

Gel preparation was started by pouring separation gels which were overlaid with ethanol to obtain plain surfaces. After solidification, ethanol was removed and separation gels were overlaid with stacking gels which polymerized afterwards with a comb inside. Gels were transferred into a chamber (Mini-Protean 3, Bio-Rad) which was filled with 1x Laemmli buffer. After quantification (2.7.3), 20 µg proteins along with H_2O_{demin} and 4x RSB were mixed and incubated at 70 °C for 10 min, causing denaturation and reduction of proteins. Protein marker (PageRuler prestained, Thermo Fisher Scientific) and protein samples were applied to the gel for electrophoresis. The concentration of proteins in the stacking gel was accomplished at 60 V and separation was run at 100 V. Gels were washed with H_2O_{dest} afterwards to remove buffer solution.

Table 12: Composition of gels for discontinuous SDS-PAGE. Polymerization was achieved by adding 50 µL APS and 10 µL TEMED. T = total concentration of acrylamide and bisacrylamide

Separation gel [T = 13 %]		**Stacking gel [T = 4 %]**	
separation gel buffer	2.5 mL	stacking gel buffer	1.25 mL
acrylamide-mix	6.5 mL	acrylamide-mix	1 mL
SDS (10 % w/v)	0.1 mL	SDS (10 % w/v)	0.05 mL
H_2O_{demin}	ad 10 mL	H_2O_{demin}	ad 5 mL

2.7.4.1 Coomassie staining

Protein visualization after SDS-PAGE with Quick Coomassie Stain (Serva, Heidelberg, Germany) is suitable for amounts of at least 5 ng protein standard. This stain binds irreversible to proteins in acidic conditions, resulting in blue bands inside the gel.

After washing with H_2O_{demin}, gels were incubated in staining solution for 60 min and shaken gently (IKA Vibrax, VWR, Darmstadt, Germany). Background decolorization was obtained by washing with H_2O_{demin}. For storage and documentation, gels were dried on Whatman paper at 80 °C for 2 h by vacuum drying (Gel Dryer MGD-4534, VWR).

2.7.4.2 Silver staining

Another method for protein visualization in polyacrylamide gels is silver staining (Blum *et al*., 1987). This concept is based on the binding of silver ions to proteins with subsequent reduction to elemental silver. With a detection limit of 0.1 ng, this approach is much more sensitive compared to Coomassie staining.

Washed gels were incubated in fixing solution for 20 min for protein precipitation and subsequently overlaid with methanol (50 % w/v). Gels were washed in H_2O_{demin} for 10 min and incubated in thiosulfate solution for the enhancement of sensitivity and contrast. After washing twice with H_2O_{demin} for 1 min, gels were transferred into impregnation solution and incubated at 4 °C for 20 min under exclusion of light, leading to the attachment of silver ions to negatively charged sidechains of proteins. The subsequent application of developing solution was carried out for the reduction of silver ions to elemental silver via formaldehyde, resulting in protein visualization. For storage and documentation, the reaction was stopped by adding stop solution and gels were dried as previously described (2.7.4.1).

2.7.5 Enzyme activity assays

2.7.5.1 EctD activity assay

EctD *in vitro* studies were performed in order to determine enzyme kinetics from ectoine hydroxylases of four different organisms (*H. elongata*, *A. cryptum*, *P. stutzeri*, *S. alaskensis*), with ectoine and synthetic ectoine derivatives homoectoine and ethylectoine as substrates. All components were freshly prepared (tab. 13). KCl, 2-oxoglutarate and TES were dissolved in H_2O_{demin} and pooled to a mastermix, whereas remaining components were added separately. In case of EctD of *S. alaskensis*, catalase, dissolved in potassium phosphate-buffer (50 mM, pH 7) with a final concentration of 1300 U (Sigma-Aldrich), was necessary for activity. Final substrate concentrations of 1 - 30 mM were tested. Assays were performed in 1.5 mL reaction tubes with a final volume of 30 µL at specific temperatures and 900 rpm (Thermomixer compact, Eppendorf) for 5 min, since enzyme reactions were linear for this period. Reaction was stopped by adding 1:1 acetonitrile (100 % w/v) leading to enzyme denaturation. Samples were centrifuged and supernatants were used for HPLC analysis. Assay was performed, according to Widderich *et al*. (2014).

Table 13: EctD enzyme activity assay. Assays (V = 30 µL) were performed for 5 min at different temperatures, depending on EctD optima: *H. elongata*: 32 °C, *A. cryptum*: 32 °C, *P. stutzeri*: 35 °C, *S. alaskensis*: 15 °C.

Component	Stock solution	Final concentration
$FeSO_4$ x 7 H_2O	10 mM	1 mM
KCl	1 M	100 mM
2-oxoglutarate x Na	100 mM	10 mM
TES pH 7.5	1 M	100 mM
EctD	0.15 mg/mL	0.05 µg/mL
substrate	100 - 500 mM	variable
H_2O	-	-

For the calculation of kinetic parameters, the enzymes activities were determined and given as units (U), whereas 1 U is equivalent to the conversion of 1 µmol substrate per min. As the reaction was carried out exactly 5 min and the amounts of converted substrates were determined via HPLC, enzyme activity (U = µmol * min^{-1}) could be calculated. In order to determine specific activities for different EctD enzymes, U was divided by the amount of applied enzymes in mg (U * mg^{-1}). Maximal velocity values (V_{max}) of the enzymes reactions are equivalent to specific activities at substrate saturation. The Michaelis-Menten constant K_m (mM) determines

the substrate concentration at which the reaction velocity is half of V_{max}. Figure 10 can be consulted for the recognition of Michaelis-Menten parameters.

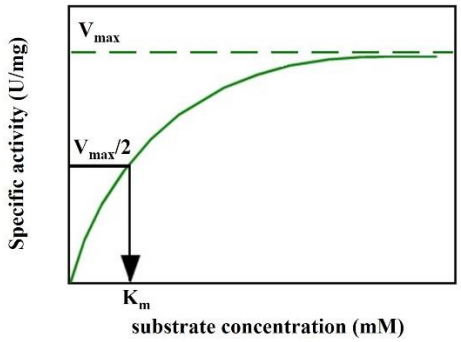

Figure 10: Schematic Michaelis-Menten kinetics. The diagram serves for the recognition of kinetic parameters in EctD *in vitro* studies.

For the calculation of turnover numbers (K_{cat}), which shows the number of converted substrate molecules per second for a single enzyme, the following calculation was applied:

$$Kcat\ (s^{-1}) = \left(\frac{spec.activity\ in\ \mu mol * \ min^{-1} * mg^{-1}}{\frac{60}{enzyme\ in\ \mu mol * mg^{-1}}}\right)$$

2.7.5.2 Lactate dehydrogenase (LDH) activity assay

The Lactate dehydrogenase (LDH) catalyzes the reduction from pyruvate to lactate which is part of the lactic acid fermentation. The use of LDH as a model enzyme for the investigation of compatible solutes as protective agents was already described by Lippert & Galinski (1992).
The following reversible reaction is catalyzed by LDH although chemical equilibrium is on the side of lactate under applied conditions:

$$\text{Pyruvate} + \text{NADH} + H^+ \longleftrightarrow \text{Lactate} + NAD^+$$

The enzyme reaction can be monitored spectrophotometrically due to the fact that NADH exhibits an absorption maximum at 340 nm.
In this study, ectoine and synthetic ectoine derivatives (homoectoine, ethylectoine, propylectoine) as well as hydroxylated ectoines (OH-ectoine, OH-ethylectoine) were tested as potential protective solutes for LDH, regarding freeze-thaw stress. Additionally, other solutes

which are known to be protective (trimethylamine N-oxide [TMAO], trehalose) or not protective (glycine betaine) were tested.

Rabbit muscle LDH (0.05 µg/mL, Fluka, Buchs, Switzerland) was dissolved in potassium phosphate-buffer (50 mM, pH 7.5) with or without solutes (1 mol/L). Samples were frozen in liquid nitrogen for 20 s and thawed at RT for 10 min. Freeze-thaw cycles were repeated up to 8 times and after each cycle, thawed LDH sample was mixed with enzyme activity assay (tab. 14) in quartz cuvettes. LDH activity was photometrically measured at 340 nm for 5 min (Specord 210, Analytik Jena). Data analysis was conducted via PC (WinASPECT, Version 2.2.0.0, Analytik Jena).

Table 14: LDH enzyme activity assay. All components were dissolved in potassium phosphate (PP) buffer.

Freeze-thaw sample	**LDH activity assay**	
Component	**Volume**	**Component**
50 mM PP buffer pH 7.5 1 mol/L test solute	890 µL	50 mM PP buffer pH 7.5
LDH (0.05 µg/mL)	50 µL	pyruvate (46 mM)
	50 µL	NADH (7 mM)
	10 µL	freeze-thaw sample

2.8 Analytics

2.8.1 Bligh & Dyer (B&D) extraction

The extraction method of Bligh & Dyer (1959, modified by Galinski & Herzog, 1990) separates cell contents into a hydrophobic chloroform phase and a hydrophilic methanol/water phase, depending on solubility of the respective substance. Macromolecular cell components like proteins are precipitated in between the immiscible layers of chloroform and methanol/water.

For extraction, 500 µL B&D solution were mixed with 30 mg freeze-dried cell material or filtered cells from 2 mL culture (2.5.6.3) for 10 min (IKA Vibrax, VWR) before adding 130 µL chloroform and 130 µL H_2O_{demin}. Samples were mixed for another 10 min and centrifuged afterwards (Eppendorf 5418, 12,000 x *g*, 5 min, RT), leading to a two-phase formation. The supernatant, containing hydrophilic substances, was collected for HPLC analysis and, in case of preparation of hydroxylated ectoine derivatives, transferred into a beaker and incubated at 50 °C for methanol evaporation before further purification via downstream processing.

2.8.2 Downstream processing (DSP)

Purification of produced hydroxylated ectoine derivatives from *E. coli* cells and from salts and other impurities (2.5.6.1) was accomplished via B&D solute extraction (2.8.1) and a subsequent DSP as described below.

2.8.2.1 Cation exchange chromatography

Ion exchangers are organic or inorganic water-insoluble polymers in which ionic groups are implemented. The counter ions of these ionic groups can be exchanged by different ions in the environment. If anionic groups are bound covalently to the matrix and the neutralizing cations are bound ionically, other cations can be exchanged depending on the affinity between the cation to the matrix.

For the purification of hydroxylated ectoine derivatives, the cation exchange resin DOWEX 50WX8 (Serva), which exhibits sulfonic acid functional groups, was filled in a column with a length of 9 cm and a diameter of 4 cm. The resin was equilibrated with 2 M ammonium chloride and washed with H_2O_{demin} until conductivity was near 0 S/m, followed by another equilibration step with H_2O_{demin} at a pH of 1.6. After B&D cell extraction, methanol free supernatants containing hydroxylated ectoine derivatives were set to a pH of 1.6 and added to the column, leading to protonation of ectoines and subsequent binding to sulfonic acid functional groups. Impurities were removed by purging with H_2O_{demin} (pH 1.6). Elution was performed gradually by adding 50 mM, 100 mM and 200 mM ammonia which competes with ectoines for the binding to sulfonic acid groups. The elution was also facilitated due to the basic pH of ammonia, leading to a deprotonation of ectoines and therefore to a decrease in affinity for the sulfonic acid groups. To keep track of the chromatographic separation, the column was connected to a conductivity detector (LF 530, WTW, Weilheim, Germany) and an UV detector (UV/VIS Filterphotometer, Knauer, Berlin, Germany) via a peristaltic pump (flow rate: 2 mL/min). The fractions containing the eluted ectoines were collected (Fraction collector 684, Büchi) and pooled before pH was adjusted to 7 with HCl to avoid hydrolysis. Samples were stored at -20 °C and freeze-dried (Alpha I-6, Christ) afterwards. To remove salts, freeze-dried samples were further purified by ion retardation chromatography (2.8.2.2).

2.8.2.2 Ion retardation chromatography

Desalting of substances was realized by preparative ion retardation chromatography with a bifunctional resin (AGII A8, Bio-Rad, Hercules, USA), exhibiting weak cation exchange

groups and strong anion exchange groups, which in unloaded state act as counterions. Loading with charged ions (e.g. Na^+, Cl^-) or molecules (e.g. glutamate) leads to temporarily binding, whereas uncharged molecules pass through the resin without deceleration.

For the desalting of ectoines and their hydroxylated forms, samples were dissolved in small amounts of H_2O_{demin} (15 - 20 mL), and pH was set to 7 in order to adjust ectoines to an uncharged state. Samples were applied to the resin (column volume = 2 L) and transported via a peristaltic pump (8 mL/min) and H_2O_{demin} as the mobile phase. The setup was the same as described in 2.8.2.1, except for a different resin and mobile phase, respectively. Fractions with UV peak and without conductivity signals were pooled, freeze-dried and further purified by crystallization in methanol.

2.8.2.3 Crystallization in methanol

In order to increase purity of isolated OH-ethylectoine, samples were further processed by methanol crystallization. Therefore, freeze-dried OH-ethylectoine samples were gradually mixed with anhydrous methanol until solid material was completely dissolved. Subsequently, the volume was gradually reduced by slow evaporation at 50 °C to achieve oversaturation until sedimentation was visible. The solution was incubated at -20 °C for 72 h, while forming product crystals which were harvested afterwards via filtration. Crystals were completely dried at 50 °C and analyzed via HPLC and NMR.

2.8.3 Transfer free energy of diketopiperazine

In order to investigate the impact of compatible solutes to transfer free energy of the peptide backbone, and therefore to protein stability, attempts of Liu and Bolen (1995) were considered. The transfer free energy ΔG_{tr} provides information regarding solubility of substances in water and in solution with other substances. If the test substance dissolves easier in pure water than in solutions with a cosolute, ΔG_{tr} reveals whether the cosolute is stabilizing ($\Delta G_{tr} > 0$) or a destabilizing ($\Delta G_{tr} < 0$) the test substance.

In this study, diketopiperazine (DKP), a cyclic dimer of glycine, was chosen as a model substance, simulating two units of a protein backbone (fig. 11). The objective of this test was to examine the influence of solutes on the solubility of DKP as compared to the solubility of DKP in pure water.

Transfer free energy can be calculated with the following formula, regarding differences of maximal solubility of DKP in pure water and in solution with a cosolute:

$\Delta G_{tr} = R \times T \times \ln (c_w/c_{os})$

R = universal gas constant, 8.314 $J \times mol^{-1} \times K^{-1}$

T = temperature, 298 K

c_w = concentration of DKP in water

c_{os} = concentration of DKP in solution with cosolute

Calculated energies were divided by 2 in order to achieve values for single protein backbone units (DKP/2). Ectoine, as well as synthetic ectoine derivatives and their hydroxylated forms were dissolved in pure water to a concentration of 1 M. Additionally, cosolutes which are known to be stabilizing (TMAO, glycine-betaine, trehalose) and destabilizing (NaCl, urea) solvents were tested. After preparation of 1 M solutions, DKP was added in excess until saturation and sedimentation. Maximal concentration of DKP in pure water was determined by dissolving DKP in excess amounts without cosolutes. All Samples were mixed at 25 °C (298.15 K) for 48 h (IKA Vibrax, VWR). After centrifugation (16,000 x *g*, 10 min, RT), supernatants were transferred into fresh tubes and analyzed via HPLC.

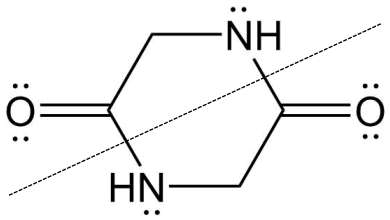

Figure 11: Molecule structure of DKP. The dashed line highlights the condensation of two glycine molecules.

2.8.4 High performance liquid chromatography (HPLC)

HPLC is an analytical method which can be used for separation, identification and quantification of substances in solution. Therefore, samples with solutes are pumped through a separation column (stationary phase) with an eluent (mobile phase) under high pressure which is needed to permeate the dense material of the separation column. Depending on the chemico-physical affinity of substances to the stationary and mobile phase, the retention of substances on the stationary phase can take longer or shorter time, leading to the detection of separate signals (e.g. UV/RI). By use of standards of known concentrations, identification and quantification of solutes can be applied.

Detection of ectoines and their hydroxylated forms, exhibiting no net charge at neutral pH, was accomplished via isocratic HPLC (constant eluent concentration). The eluent (acetonitrile, AcN 80 % - 84 % (v/v) at physiological pH) was degassed (SpectraSystem SCM1000, Thermo

Scientific), and used with a flow rate of 1 mL/min at RT (SpectraSystem P1000, Thermo Fisher Scientific). Samples were diluted appropriately in the eluent and the supernatant was applied to the sample valve (7125 injector, Rheodyne Inc.) after centrifugation (10,000 x *g*, 5 min, RT). B&D-extracts were diluted 1:2 - 1:20, whereas culture medium supernatants were diluted 1:10. For the analysis of *in vitro* enzyme assays, samples were diluted 1:7 - 1:12, and DKP containing supernatants were diluted 1:250.

As stationary phase, a reversed phase silica gel with polar amino groups attached to hydrophobic propyl chains was used (LiChospher 100 NH2, 5 µm, Merck, Darmstadt, Germany). Signals were captured by a refractive index detector (RI, Shodex RI-71, Showa Denko K.K., Tokyo, Japan) and a UV-detector (SpectraSystem UV1000, 210 nm, Thermo Fisher Scientific). Identification and quantification were carried out by measurement of 1 mM concentrated standard substances.

2.8.5 Nuclear magnetic resonance spectroscopy (NMR)

NMR is a spectroscopic method which is used for the identification and structure determination of molecules by observing local magnetic fields around atomic nuclei. The method is based on the fact that atomic nuclei with an uneven number of protons or neutrons, like ^{1}H and ^{13}C, exhibit a nuclear spin, and with that a magnetic moment.

The magnetic moment within a magnetic field shows a strict number of orientations, determined by the spin quantum number (I), and for every orientation a magnetic spin quantum number is allocated (m_I). The presence of an external magnetic field leads to energy differences and nuclear resonance phenomena are based on excitation of nuclear spin transitions between magnetic spin quantum numbers. The energy needed for transitions is contributed by resonant electromagnetic waves. Depending on the chemical environment of an atom, which is influenced by electron pulling neighboring atoms, the nucleus can either be shielded or deshielded and thus will be detected at different resonance frequencies. Adjacent atoms within a molecule with high electronegativity deshield atomic nuclei, which is why deshielded atoms are exposed to a stronger magnetic field and therefore will be found in a chromatogram at higher resonance frequencies. Resonance frequencies are given as a deviation in respect to a standard compound in parts per million (ppm).

For the validation of synthetic ectoine derivatives, a ^{13}C-NMR analysis of purified compounds was accomplished. Therefore, 30 mg of the substance to be analyzed were mixed with 5 mg sodium trimethylsilyl propionate (Na-TMSP) as a reference compound, and D_2O ad 1 mL. If desired, 10 µL AcN (100 %) and 10 µL methanol (100 %) could be added as internal standards.

NMR measurements were kindly performed by Dr. Stefan Kehraus (Institute of Pharmaceutical Biology, Bonn, Germany) using the Avance 300DPX spectrometer (Bruker, Billerica, USA) at a frequency of 75.46 MHz. Data analysis was conducted by the use of MestReNova 8.0.1 software.

2.8.6 Calorimetric analysis of RNase A

Calorimetry is a method, used to determine the amount of heat released in certain situations like phase transformation or burning of solid, fluid and gaseous substances. The amount of heat, coupled to chemical, physical or biological processes can be exothermic as well as endothermic and is detectable by calorimetric analysis.

In this study, the putative protective effect of different solutes on the stability of the enzyme ribonuclease A (RNase A) during heat stress was investigated by differential scanning calorimetric analysis (VP-DSC MicroCal, Northampton, USA). The calorimeter was used to measure the heat capacity (Cp) at a constant heating rate of a chamber containing samples with the enzyme, as well as a control sample without the enzyme. Denaturation of the enzyme, which is an endothermic reaction, leads to measurable differences of the heat capacity between both chambers, resulting into the measurement of a peak. This measuring point indicates the melting temperature T_M at which 50 % of the enzyme is in a denatured state. Higher melting temperatures of RNase A in the presence of solutes suggest protective effects, regarding heat stress.

RNase A was dissolved in sodium phosphate buffer (30 mM, pH 5.5) to a final concentration of 1 mg/mL and test solutes were added to a final concentration of 1.5 mol/L. The following solutes were tested: ectoine, OH-ectoine, ethylectoine, OH-ethylectoine, homoectoine, propylectoine, glycine-betaine, TMAO, trehalose and urea. As a control, RNase A without any solute was tested as well. Sample volumes of 600 µL were transferred air bubble-free into the reaction chamber. 600 µL of the reference solution without RNase A were transferred into the reference chamber. After loading the chambers, a pressure of 22 psi (= 1.52 bar) was adjusted. Samples and references were heated with a rate of 1 °C/min from 25 °C to 85 °C, and cooled afterwards with a rate of 1 °C/min. System control and data analysis was accomplished using VP Viewer 2000 software (MicroCal, Northampton, USA).

3 Results

The current industrial production of OH-ectoine by *H. elongata*, which is dependent on high saline conditions, is accompanied by high costs regarding desalting and chromatographic separation of OH-ectoine and ectoine. One possible way to bypass both high saline conditions and chromatographic separation is the use of *E. coli* as a whole-cell biocatalyst, converting externally provided ectoine completely into OH-ectoine. In this work, the whole-cell biotransformation process for the conversion of ectoine to OH-ectoine via heterologously produced EctD in *E. coli* was optimized by testing different strains, plasmids and cultivation conditions. Moreover, ectoine derivatives with either enlarged ring size or changed functional alkyl groups, leading to solutes with an increase of non-polar surface areas, were synthesized and characterized. As substrate ambiguity for EctD of *H. elongata* was already proven, it was also tested if synthetic ectoine derivatives were recognized not only by this enzyme, but also by EctD homologues of *A. cryptum*, *P. stutzeri* and *S. alaskensis in vivo* and *in vitro*. Newly formed synthetic ectoines and their hydroxylated derivatives were characterized for the first time.

3.1 Chemical synthesis of ectoine derivatives

As synthetic ectoine derivatives used in this work are not available for purchase, synthesis of cyclic solutes with a zwitterionic structure was carried out by a procedure modified after Koichi *et al*. (1991). As a result, enlargement of the ectoine ring (homoectoine) or replacement of the methyl group by different alkyl groups (ethylectoine, propylectoine) was achieved. Reaction conditions for the synthesis of homoectoine (Voß, 2002), ethylectoine and propylectoine (Galinski, unpublished) were developed and optimized in previous works. Acetylation of diamino carboxylic acids by corresponding orthoesters and subsequent condensation (cyclization) resulted in the desired end products. Salts, generated by neutralization of the product solutions pH, were successfully removed by ion retardation chromatography (data not shown). After cooling in anhydrous methanol at -20 °C, product crystals were harvested, dried and analyzed by HPLC and ^{13}C-NMR, where they showed to be in their purest form. Analytic benchmark data are summarized in table 15.

Table 15: Benchmark data for synthesis and analysis of ectoine derivatives. The yield is related to the respective amount of diamino components. T_{ret} = retention time in the applied isocratic HPLC system.

Solute	Chemical formula	Molar mass	Yield	T_{ret}
homoectoine	$C_7H_{12}N_2O_2$	156.19 g/mol	30 %	6.1 min
ethylectoine	$C_7H_{12}N_2O_2$	156.19 g/mol	60 %	6.4 min
propylectoine	$C_8H_{14}N_2O_2$	170.21 g/mol	65 %	4.8 min

3.1.1 4,5,6,7-tetrahydro-2-methyl-1H-[1,3]-diazepine-4-carboxylic acid (homoectoine)

For the synthesis of homoectoine, which possesses an expanded seven-membered diazepine ring structure, L-ornithine as a diamino carboxylic acid and trimethyl orthoacetate as an orthoester were dissolved in methanol. After one hour at 50 °C and under rotation, all compounds were dissolved completely, but synthesis was performed at constant conditions for another 4 h. The end product's yield was ~ 30 % on average in relation to the educt L-ornithin. This relatively low yield probably resulted from a high degree of by-product polymerization, suggested by a strong yellowish coloring of the product solution. Residual orthoesters were hydrolyzed with water to methanol and acetic acid and were removed by evaporation under heat and vacuum. All by-products (N-α-acetyl ornithine, N-δ-acetyl ornithine and N,N'-diacetyl ornithine) were identified in a previous study (Voß, 2002). After purification, the successful synthesis of homoectoine was verified by ^{13}C-NMR analysis (fig. 12).

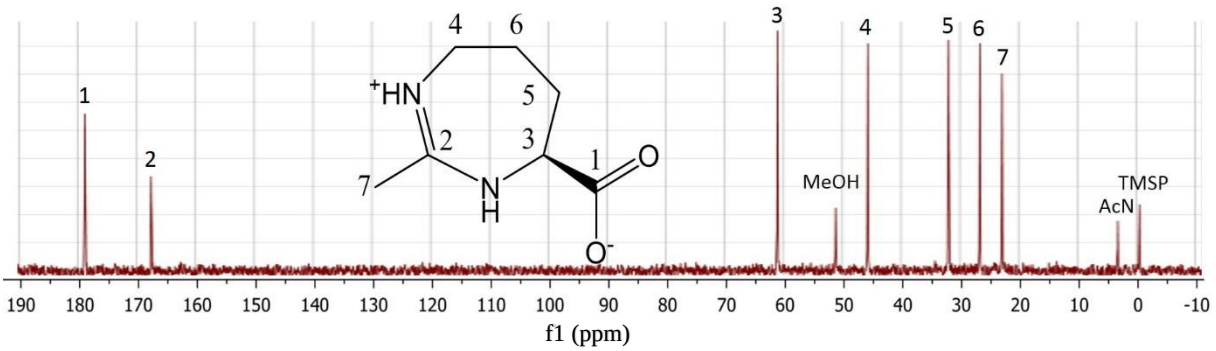

Figure 12: ^{13}C-NMR analysis of homoectoine. The spectrum reveals the carbon detection pattern at specific resonance frequencies (ppm) for the synthetic ectoine derivative homoectoine. Besides the peaks dedicated to homoectoine, additional signals for the internal standards methanol (MeOH), acetonitrile (AcN) and the reference compound sodium trimethylsilyl propionate (TMSP) were detected.

3.1.2 (4S)-2-ethyl-1,4,5,6-tetrahydropyrimidine-4-carboxylic acid (2-ethylectoine)

Besides the change of the ring size, another option to produce an ectoine analogue was to change its functional groups in position 2. In this case, the methyl group of ectoine was replaced by an ethyl group, resulting in an increase of the nonpolar surface area of the molecule.

For the synthesis of ethylectoine, L-2,4-diamino butyrate and triethyl orthopropionate were used as a diamino carboxylic acid and orthoester, respectively. Complete dissolving of all compounds in methanol took 3 h at 50 °C, which is about 2 h longer compared to the synthesis step of homoectoine. Furthermore, the product solution showed only low viscosity and weak yellow coloring. Residual orthoesters were removed from the product solution by the addition of water, forming ethanol and propionic acid, which evaporated under heat and vacuum. A final yield of 60 % was achieved after purification of ethylectoine. ^{13}C-NMR analysis of the product revealed high purity, since no unspecific peak could be detected. Besides the reference compound TMSP, the residual seven peaks of the NMR spectrum could be assigned to the carbon structure of ethylectoine (fig. 13).

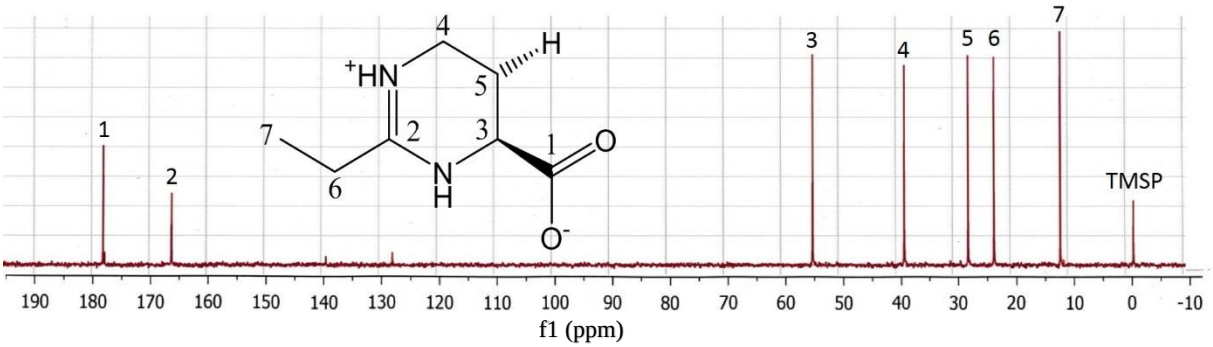

Figure 13: ^{13}C-NMR analysis of ethylectoine. The spectrum reveals the carbon detection pattern at specific resonance frequencies (ppm) for the synthetic ectoine derivative ethylectoine. Besides the peaks dedicated to homoectoine, an additional signal for the reference compound sodium trimethylsilyl propionate (TMSP) was detected.

3.1.3 (4S)-2-propyl-1,4,5,6-tetrahydropyrimidine-4-carboxylic acid (2-propylectoine)

In order to generate an ectoine analogue with even more hydrophobic properties than ethylectoine, yet another derivative with a prolonged alkyl group was synthesized. By the exchange of the methyl group with a propyl group, the synthetic ectoine derivative propylectoine was produced. The synthesis of this compound was performed almost exactly like ethylectoine, except for the use of L-2,4-diaminobutyrate and trimethyl orthobutyrate as diamino carboxylic acid and orthoester, respectively. The complete dissolving of all

components in methanol took ~ 3 h, and the same intensity of yellow coloration and viscosity was observed compared to the synthesis of ethylectoine. A total yield of 65 % of the desired product was achieved. A ^{13}C-NMR analysis verified the substance's detection pattern and revealed no contamination (fig. 14).

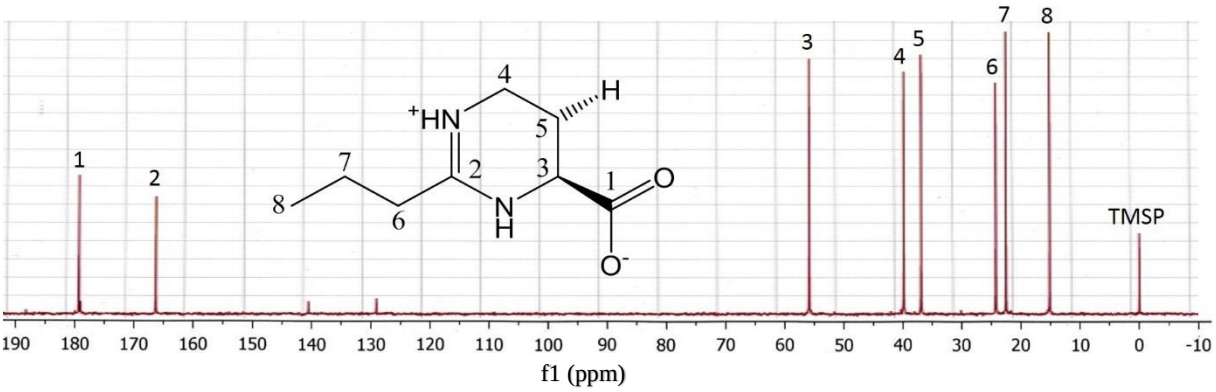

Figure 14: ^{13}C-NMR analysis of propylectoine. The spectrum reveals the carbon detection pattern at specific resonance frequencies (ppm) for the synthetic ectoine derivative propylectoine. Besides the peaks dedicated to propylectoine, an additional signal for the reference compound TMSP was detected.

3.2 *In vivo* biotransformation of ectoines by *E. coli* BL21 pET *ectDHis*

The attempt to convert ectoine to its hydroxylated form OH-ectoine with the aid of *E. coli*, heterologously expressing ectoine hydroxylase *ectD* of *H. elongata*, has already been accomplished in previous works (Meffert, 2011; Ruprecht, 2014; Brauner, 2016). *E. coli* is not only able to take up ectoine but also continuously excretes converted OH-ectoine by a so far unknown mechanism and without metabolizing any of these solutes. Therefore, this organism represents an appropriate biotransformation system for the production of OH-ectoine. Beyond that, it was shown that EctD of *H. elongata* is able to hydroxylate substrates with structural similarity to ectoine as well, which is why this biotransformation system could be used to generate completely new substances.

Although several optimization efforts were pursued, including the choice of media, different cultivation parameters or appropriate strains, the turnover was limited to a concentration of ~ 10 mM ectoine. The strain *E. coli* BL21 pET *ectDHis*, expressing *ectD* of *H. elongata* encoded on the pET-22b(+) vector turned out to be the hitherto most effective biotransformation system. The key points for achieving an efficient production were cultivation at the enzyme's optimal temperature of 32 °C under nitrogen-limited conditions, leading to high intracellular levels of 2-oxoglutarate (Yan *et al*., 2011). However, enzyme instability over time and the

reduced glucose uptake in the stationary growth phase turned out to be the processes main bottleneck (Brauner, 2016). In the following experiments, hydroxylation performance in *E. coli* BL21 pET *ectDHis* was further optimized. All results were achieved in shaking flask experiments.

3.2.1 Use of poor nitrogen sources

Since the stability of EctD over time is a crucial limiting factor in the applied biotransformation system, one attempt to overcome this bottleneck was to continuously produce the corresponding enzyme over an extended period. Bren *et al*. (2016) showed that glucose as carbon source (C-source), in combination with a poor nitrogen source (N-source) like arginine or glutamate, leads to the decrease of growth rates for *E. coli* and furthermore to higher intracellular levels of TCA intermediates, including 2-oxoglutarate. The idea of using poor N-sources and glucose as C-source was to provide the essential cofactor 2-oxoglutarate to EctD in increased quantities. A reduced growth rate also usually leads to more soluble recombinant proteins during heterologous production (De Groot & Ventura, 2006). Lowered growth rates additionally are accompanied with the delayed reach of the stationary growth phase. Therefore, the production time for EctD and thus the hydroxylation process can be extended until C- and N-sources are depleted.

A balanced MM63-1 medium, containing glucose as the C-source and arginine or glutamate as

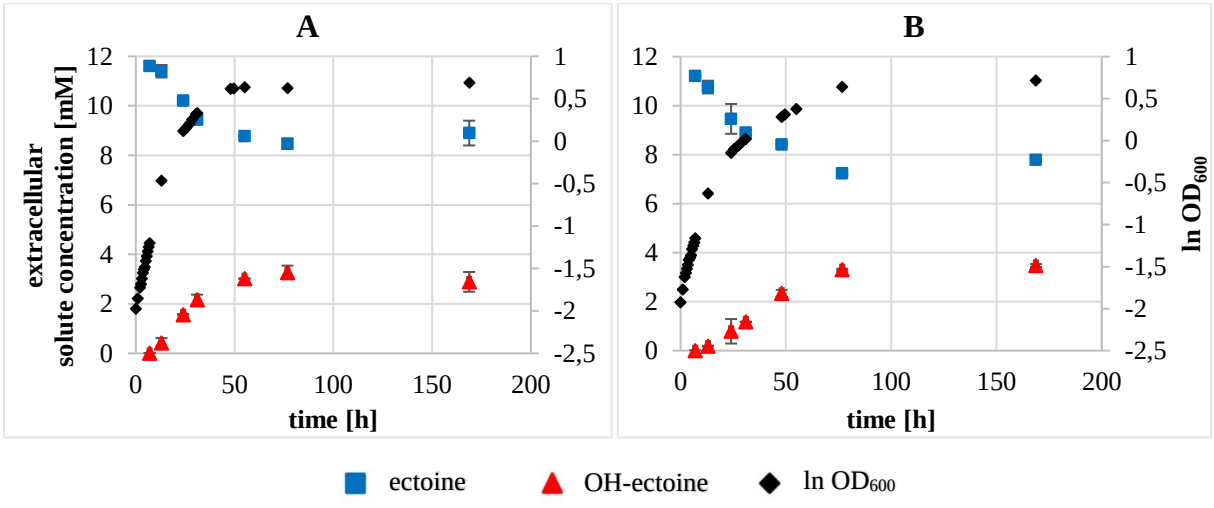

Figure 15: Hydroxylation of 10 mM ectoine with *E. coli* BL21 pET *ectDHis* in MM63-1 medium by the use of poor nitrogen sources. A) arginine as N-source, B) glutamate as N-source. C/N ratios were 8/1. Glucose was used as C-source (10 g/L). Cultures were induced at OD_{600} = 0.3 with IPTG (0.1 mM) and subsequently supplemented with ectoine. Temperature was reduced from 37 °C to 32 °C after induction. Indicated concentrations are arithmetic means of triplicates corresponding to media supernatants and were determined via HPLC.

N-sources was used for the conversion of 10 mM ectoine in a shaking flask experiment (fig. 15, tab. 5). Induction was performed by the addition of IPTG (0.1 mM) at OD_{600} = 0.3 and 32 °C. In case of arginine as the applied N-source, stationary phase was reached at ~ 50 h, whereas the use of glutamate as N-source almost doubled this time. Growth rates were calculated in the exponential growth phase after induction with IPTG and were $\mu = 0.031\ h^{-1}$ (arginine) and $\mu = 0.024\ h^{-1}$ (glutamate). Ectoine conversion was incomplete as both attempts showed high residual concentrations in the media supernatants. When both cultures reached stationary phase, no further ectoine turnover was observed. Therefore, the use of poor N-sources turned out to be unsuitable for the whole-cell biotransformation of ectoine.

3.2.2 Ammonium sulfate as N-source and different induction parameters

Even though glutamate or arginine as N-sources lead to lowered growth rates and 2-oxoglutarate should have been available in excess, hydroxylation performance was not sufficient to completely convert 10 mM ectoine. In the following experiment, ammonium sulfate was used as N-source in combination with glucose as C-source, which turned out to be more efficient in previous experiments (Ruprecht, 2014; Brauner, 2016). These studies showed that the reduction from 2 g/L to 0.5 g/L $(NH_4)_2SO_4$ and the simultaneous increase of glucose from 5 g/L to 10 g/L (compared to MM63 formula) improved hydroxylation performance. Even though the performance was improved under these conditions, the biomass formation and thus probably the total mass of EctD was low, compared to the use of C-limited MM63 medium. This is why in the following experiment the amount of N-source was increased to 1 g/L $(NH_4)_2SO_4$ while 10 g/L glucose as C-source was used (C/N = 17/1), which still remains a N-limited medium. Furthermore, induction conditions like IPTG concentration (0.1 mM or 0.5 mM) and the time of induction (OD_{600} = 0.3 or OD_{600} = 0.6) were varied. As a control, optimized conditions used in a previous work (Ruprecht, 2014) were tested as well (C/N = 34/1, application of 0.1 mM IPTG at OD_{600} = 0.3).

Figure 16 illustrates that the most efficient hydroxylation performance was obtained at a C/N ratio of 17/1 and induction with 0.1 mM IPTG at OD_{600} = 0.6 (grey line), as this attempt showed the fastest and a complete conversion of ectoine to OH-ectoine. An IPTG concentration of 0.5 mM tended to decrease hydroxylation efficiency since all induction attempts with 0.5 mM IPTG exhibited incomplete ectoine conversion. Cultures induced with 0.1 mM IPTG at OD_{600} = 0.3 with a C/N ratio of 34/1 showed a lower conversion rate compared to cultures

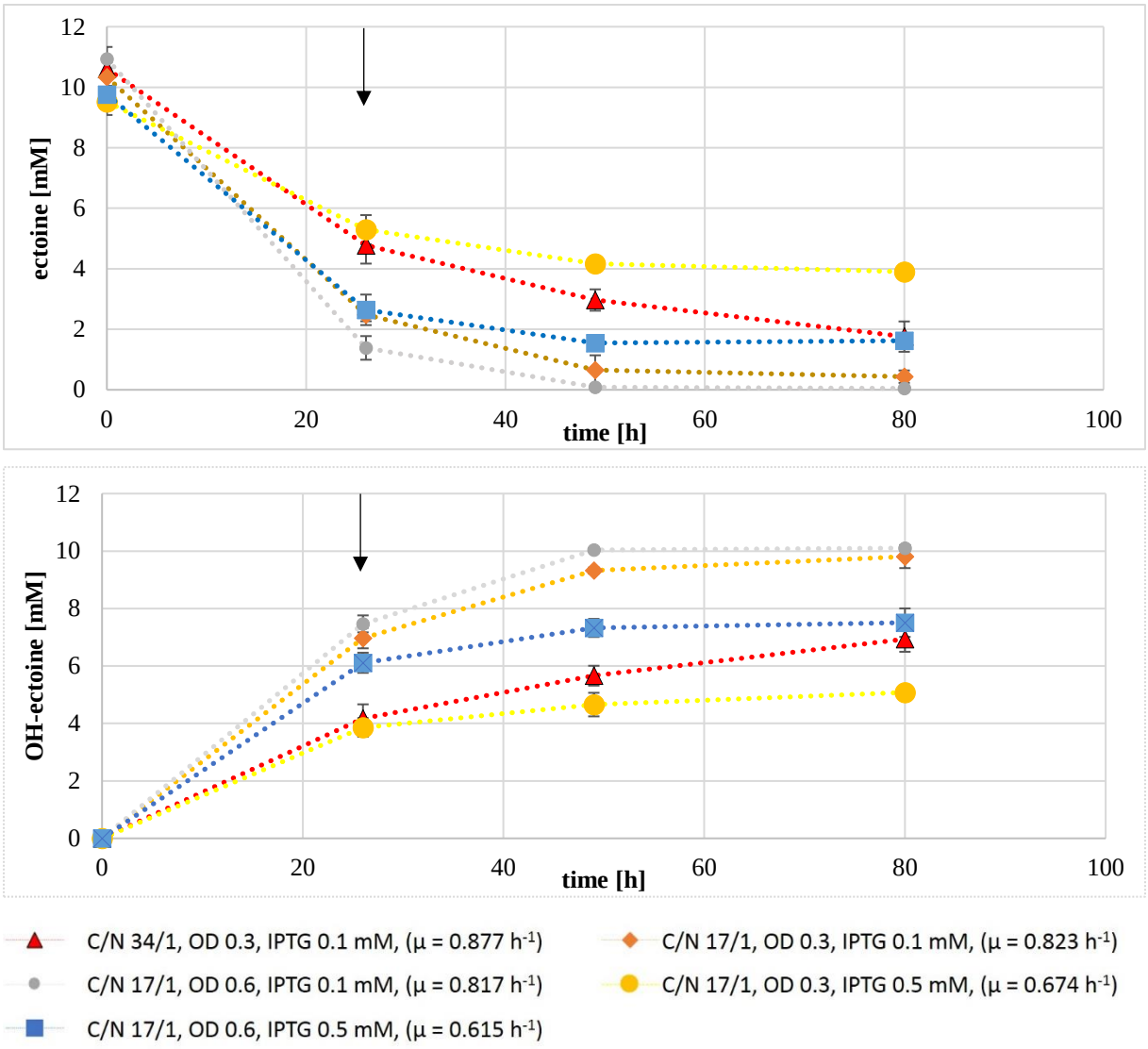

Figure 16: Whole-cell biotransformation of ectoine using different ratios of glucose and $(NH_4)_2SO_4$ under different induction conditions. *E. coli* BL21 pET *ectDHis* was cultivated in N-limited MM63-1 medium with glucose as C-source and $(NH_4)_2SO_4$ as N-source. C/N ratios were either 34/1 (0.5 g/L $(NH_4)_2SO_4$) or 17/1 (1 g/L $(NH_4)_2SO_4$) with 10 g/L glucose each. Induction was performed at OD_{600} = 0.3 or 0.6 with final concentrations of 0.1 mM or 0.5 mM IPTG. The temperature was reduced from 37 °C to 32 °C after induction. Indicated concentrations are arithmetic means of triplicates corresponding to media supernatants and were determined via HPLC. Growth rates (h^{-1}), given in the legend, were calculated in exponential growth phase after induction with IPTG at 32 °C. Additional glucose (5 g/L, black arrow) was applied to guarantee sufficient energy for ectoine uptake and 2-oxoglutarate regeneration.

incubated under the same conditions but with a C/N ratio of 17/1. Furthermore, cultures incubated in medium with a C/N ratio of 17/1 showed a higher OD_{600} at the stationary growth phase compared to cultures with a C/N ratio of 34/1. The calculation of growth rates indicates that cultures induced with the higher IPTG concentration exhibited slower growth. As already shown in previous works (Ruprecht, 2014; Molitor, 2015), ectoine conversion took place in the

exponential growth phase but also in resting cells after reaching stationary phase under N-limiting conditions up to ~ 50 h after induction. In summary, it can be stated that most effective hydroxylation performances were achieved by a late induction with low concentrations of IPTG in combination with a C/N ratio of 17/1.

3.2.3 Hydroxylation performance at different salinities

In the previous experiments, the choice of N-sources as well as the C/N ratios and induction parameters were optimized for improved hydroxylation performance. For these experiments, *E. coli* cultures grew in presence of only 1 % NaCl. In the following it was tested whether increased NaCl contents in the media optimize ectoine hydroxylation performance in *E. coli*, since this organism is able to accumulate compatible solutes to a higher degree under osmotic stress (Kempf & Bremer, 1998). Therefore, *E. coli* BL21 pET *ectDHis* was cultivated in MM63 medium under optimized and N-limited conditions (3.2.2) but with 3 % NaCl. As a control, cultures with 1 % NaCl were tested as well. All cultures were supplemented with either 10 mM, 15 mM or 20 mM ectoine (fig. 17).

Cultures supplemented with 10 mM ectoine accomplished a complete conversion with both 1 % and 3 % NaCl, whereas substrate uptake and conversion were finished sooner by cultures growing at 3 % NaCl. An initial ectoine concentration of 15 mM lead to an incomplete conversion, but again cultures with a higher NaCl content showed a slightly increased turnover speed. It should be noted that 120 h after induction, culture media were concentrated due to evaporation, which is why these samples exhibit increased values for solute concentrations compared to the sample before.

The application of 20 mM ectoine also lead to an incomplete turnover, and the hydroxylation performance can approximately be compared to cultures supplemented with 15 mM ectoine.

Altogether, figure 17 indicates that an increased NaCl concentration only had a slight beneficial effect for the improvement of ectoine conversion. Additionally, the increase of initial ectoine concentrations slightly increased the final amount of converted ectoine, although it was not possible to completely convert 15 mM or more substrate.

Since elevated NaCl concentrations had no significant improving effect, this approach was not further investigated.

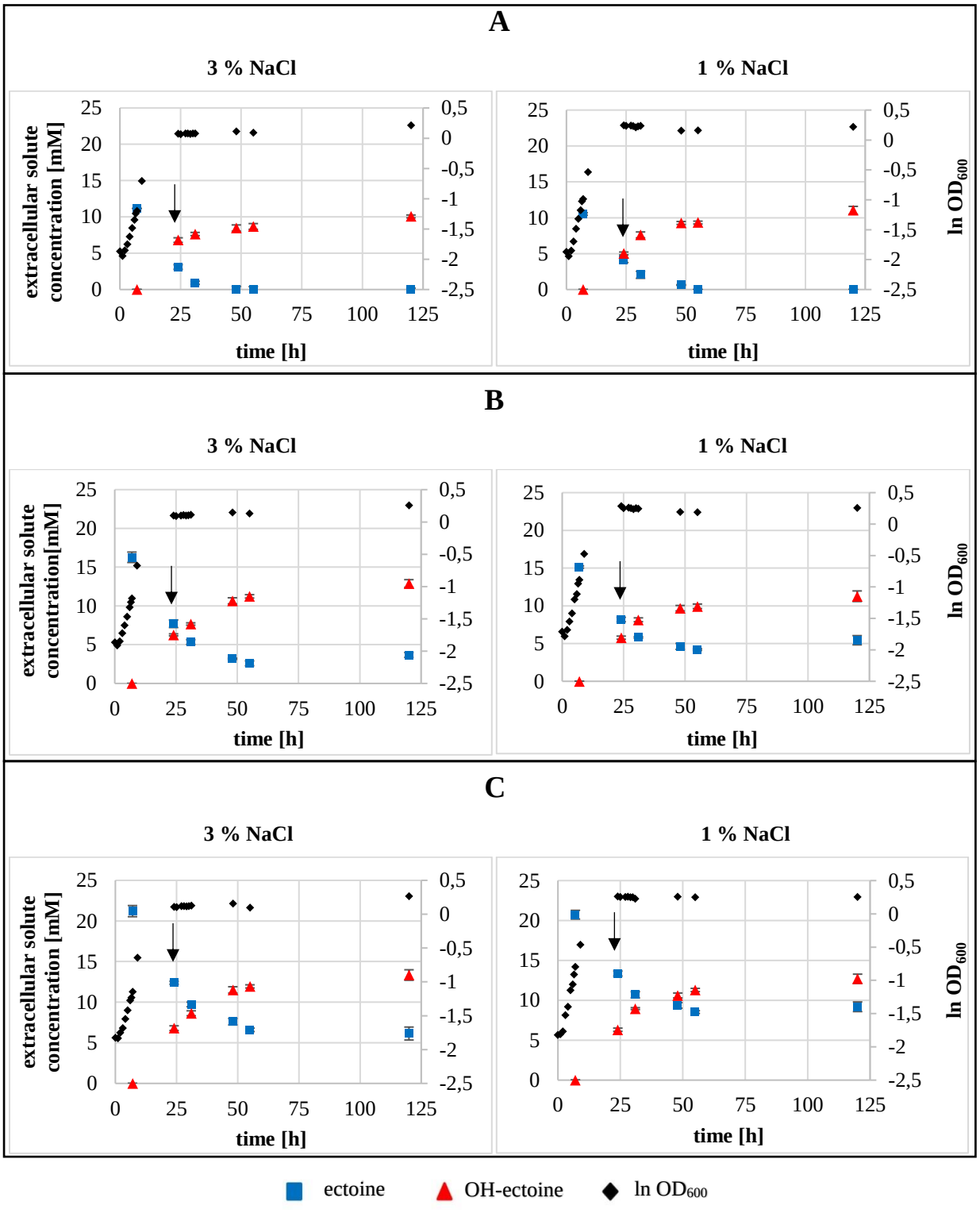

Figure 17: Optimization of ectoine hydroxylation performance at higher osmotic pressure. *E. coli* BL21 pET *ectDHis* was cultivated in MM63 medium (N-limited, C/N = 17/1) with 1 % or 3 % NaCl, and supplemented with 10 mM (A), 15 mM (B) or 20 mM (C) ectoine, temperature was set from 37 °C to 32 °C after IPTG induction (0.1 mM, OD_{600} = 0.6). Indicated concentrations are arithmetic means of triplicates corresponding to media supernatants and were determined via HPLC. Additional glucose (5 g/L, black arrow) was applied to guarantee sufficient energy for ectoine uptake and 2-oxoglutarate regeneration.

3.2.4 Hydroxylation of ectoine derivatives

As the hydroxylation of several ectoine analogues like homoectoine has already been shown (Vielgraf, 2008), it was reviewed whether the new synthesized analogues ethylectoine and propylectoine can also be converted by EctD of *H. elongata*. Therefore, *E. coli* BL21 pET *ectDHis* was cultivated in MM63-1 medium with 0.5 g/L $(NH_4)_2SO_4$ and 10 g/L glucose and supplemented with 10 mM of ethylectoine or propylectoine after induction with IPTG (0.1 mM) at OD_{600} = 0.3. For the purpose of comparability, ectoine and homoectoine were tested as well. This experiment was carried out before optimization of hydroxylation conditions (3.2.2).

As shown in figure 18, *E. coli* is able to take up all ectoine derivatives indicated by the gradual decrease of measured substrate concentration over time. HPLC analysis of media supernatants revealed a decrease of substrates and an increase of a second substance that was assumed to be the substrate's hydroxylated derivative. After the hydroxylation process ended, the sum of residual substrate and product concentrations approximately corresponded to the initial substrate concentrations minus the amount of intracellular accumulated solutes. The only exceptions were cultures, supplemented with homoectoine. These cultures exhibited a discrepancy of 4 mM at the end of the biotransformation, resulting from a decline of the product concentration after 45 h.

It is noteworthy that growth rates for *E. coli* ranged from 0.30 - 0.32 h^{-1} for all cultures except for those supplemented with propylectoine which was decreased by half (0.14 h^{-1}). Growth rates were calculated in the exponential growth phase after supplementation of IPTG and substrates to be hydroxylated.

Data analysis revealed that the highest hydroxylation performance took place within the first hours after substrate supplementation, which is why early substrate influx and product efflux rates were calculated between 2 h and 4 h post induction. The time period between 0 h and 2 h post induction was neglected, since cells initially accumulate the substrates until saturation, which would distort actual uptake and efflux rates after saturation. Concentration changes per time (nmol/min) were correlated to the amount of whole-cell proteins per mg. Total protein amount (g) was approximately determined by multiplication of directly measured OD_{600} with the factor 0.44 (equals bacterial dry mass in g/L) and another multiplication with 0.5 (Bolten *et al*., 2007).

In order to determine substrate conversion rates , early substrate uptake and product efflux rates 3 h after substrate supplementation were calculated (tab. 16). Note: The **early substrate** uptake rates should not be confused with the **maximal substrate** uptake rate, which represents the

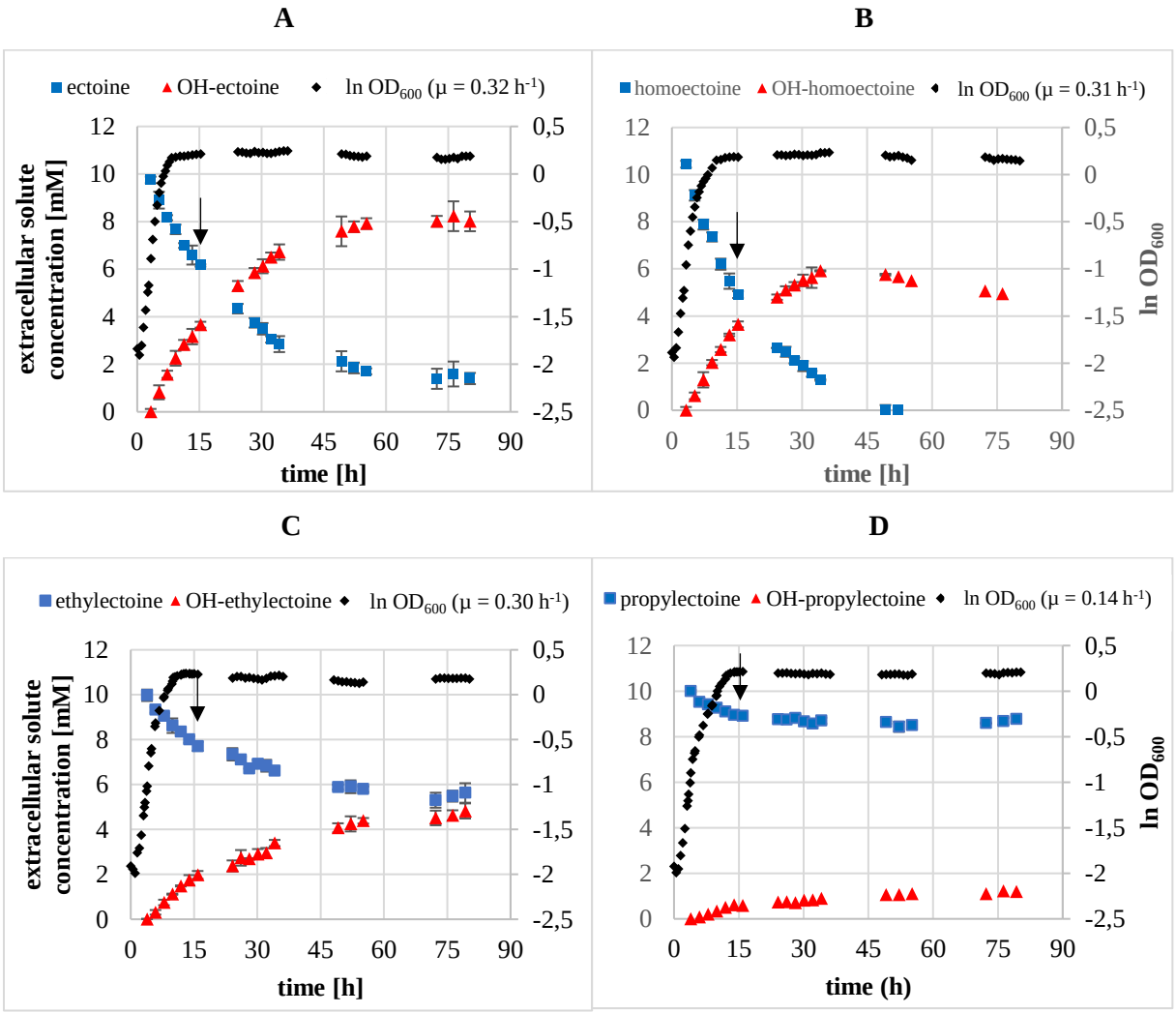

Figure 18: Hydroxylation of ectoine and synthetic ectoine derivatives homoectoine, ethylectoine and propylectoine with *E. coli* BL21 pET *ectDHis*. Cultivation was carried out in MM63-1 medium with 0.5 g/L $(NH_4)_2SO_4$ and 10 g/L glucose. Cultures were supplemented with 10 mM ectoine (A), homoectoine (B), ethylectoine (C) or propylectoine (D) after induction with IPTG (0.1 mM) at OD_{600} = 0.3. Indicated concentrations are arithmetic means of triplicates corresponding to media supernatants and were determined via HPLC. Growth rates (h^{-1}) given in the legend were calculated in the exponential growth phase after gene induction with IPTG at 32 °C. Additional glucose (5 g/L, black arrow) was applied to guarantee sufficient energy for ectoine uptake and 2-oxoglutarate regeneration.

actual substrate uptake rate without the distortion of values by EctD-mediated substrate conversion (3.3.2.3).

Data indicate that substrate influx rates generally were similar to product efflux rates in each case except for cultures supplemented with homoectoine, which showed an influx rate twice as high as the efflux rate (39.1 nmol x min^{-1} x mg^{-1} compared to 21.5 nmol x min^{-1} x mg^{-1}). Moreover, OH-homoectoine concentration in the media supernatants decreased after homoectoine was completely converted. This was due to the instability of OH-homoectoine as previously described (Ruprecht, 2014; Brauner, 2016). It may therefore be assumed that the

real substrate uptake rate of homoectoine was distorted as the intracellular decay of OH-homoectoine facilitates the uptake of homoectoine.

By comparing all rates, it turned out that the total substrate conversion was higher when the early uptake und efflux rates were high. Thus, ectoine with early influx/efflux rates of ~ 28 nmol x min^{-1} x mg^{-1} showed a higher proportion of converted substrate (83 %), compared to ethylectoine (45 %) and propylectoine (14 %), which showed influx/efflux rates of ~ 12 and 6 nmol x min^{-1} x mg^{-1}, respectively (tab. 16).

Table 16: Early influx rates of ectoine or synthetic ectoine derivatives and efflux of their respective hydroxylated derivatives in *E. coli* BL21 pET *ectDHis*. Rates were calculated for the time period of 2 h - 4 h post induction and correlated with whole-cell proteins, derived from directly measured OD_{600} 3 h post induction. The Total turnover represents the ratio of final and initial substrate concentration during biotransformation. Data refer to fig. 18.

Substrate	Early substrate influx rate ($\frac{nmol}{min*mg}$)	Early product efflux rate ($\frac{nmol}{min*mg}$)	Total turnover (%)
ectoine	28.6 ± 3.2	28.3 ± 2.6	83.8 ± 2.6
homoectoine	39.1 ± 5.2	21.5 ± 3.7	100.0 ± 0
ethylectoine	12.5 ± 2.6	11.9 ± 2.1	45.1 ± 5.2
propylectoine	6.2 ± 1.2	6.1 ± 1.6	14.1 ± 1.5

3.2.5 Hydroxylation in concentrated culture media

Hydroxylation performance of ethylectoine and propylectoine in *E. coli* BL21 pET *ectDHis* was poor, compared to ectoine. In order to obtain a better conversion rate, it is necessary to increase the turnover rate. Optimization attempts, regarding media composition and induction conditions were already carried out (3.2.1, 3.2.2.). One possibility to further increase turnover rates would be a concentration of induced cells in a smaller media volume, leading to a concentration of EctD enzymes as well. Thus, it was examined whether and to what extant the concentration of cells improves the hydroxylation performance by cultivating cells in MM63-1 medium (1 g/L $(NH_4)_2SO_4$ and 10 g/L glucose) and harvesting cells 4 h after induction with IPTG (0.1 mM, OD_{600} = 0.6). Cells were subsequently resuspended in 1/10 of the initial volume of MM63-1 medium without N-source in order to achieve high intracellular 2-oxoglutarate levels as described above. Afterwards, cultures were supplemented with 30 mM ethylectoine (fig. 19 A) or 10 mM propylectoine (fig. 20 A). As a control, hydroxylation attempts as usual were carried out by adding 30 mM ethylectoine (fig. 19 B) or 10 mM propylectoine (fig. 20 B)

30 min after IPTG induction (0.1 mM, OD_{600} = 0.6) without previous concentration of culture media.

Looking at ethylectoine and OH-ethylectoine in concentrated culture media, it is noteworthy that the conversion speed was significantly increased compared to non-concentrated cultures. The final concentration of ethylectoine/OH-ethylectoine 60 h after induction was approximately decreased/increased fourfold compared to non-concentrated cells. It is also worthy of note that hydroxylation occured until ~ 25 h after induction and subsequently conversion was strongly reduced.

The situation for the conversion of propylectoine was similar, as the concentration of culture medium also lead to an approximate fourfold decrease/increase of substrate/product amounts 60 h after induction compared to non-concentrated culture media. However, in this case the hydroxylation process seemed to stop already 15 h after induction and supplementation with propylectoine. To avoid a deficiency of carbon source during hydroxylation, additional glucose was fed in regular intervals.

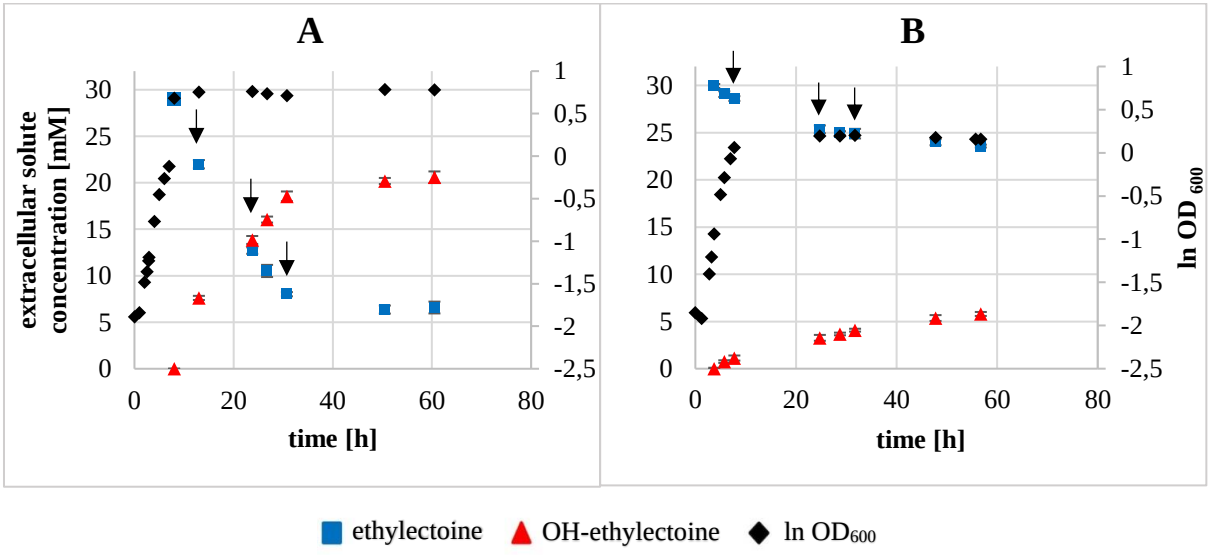

Figure 19: Hydroxylation of 30 mM ethylectoine by *E. coli* BL21 pET *ectDHis* with concentrated culture media. Cells were cultivated in MM63-1 medium with 10 g/L glucose and 1 g/L $(NH_4)_2SO_4$ and induced with IPTG (0.1 mM) at OD_{600} = 0.6 before decreasing temperature from 37 °C to 32 °C. Cells were cultivated for 4 h after induction and concentrated in 1/10 volume of the initial MM63-1 medium (without N-source) and supplemented with 30 mM ethylectoine (A) or cells were supplemented with 30 mM ethylectoine 30 min after induction without cell concentration (B). Additional glucose (2.5 g/L) was fed to provide sufficient energy source (black arrows). Indicated concentrations are arithmetic means of triplicates corresponding to media supernatants and were determined via HPLC.

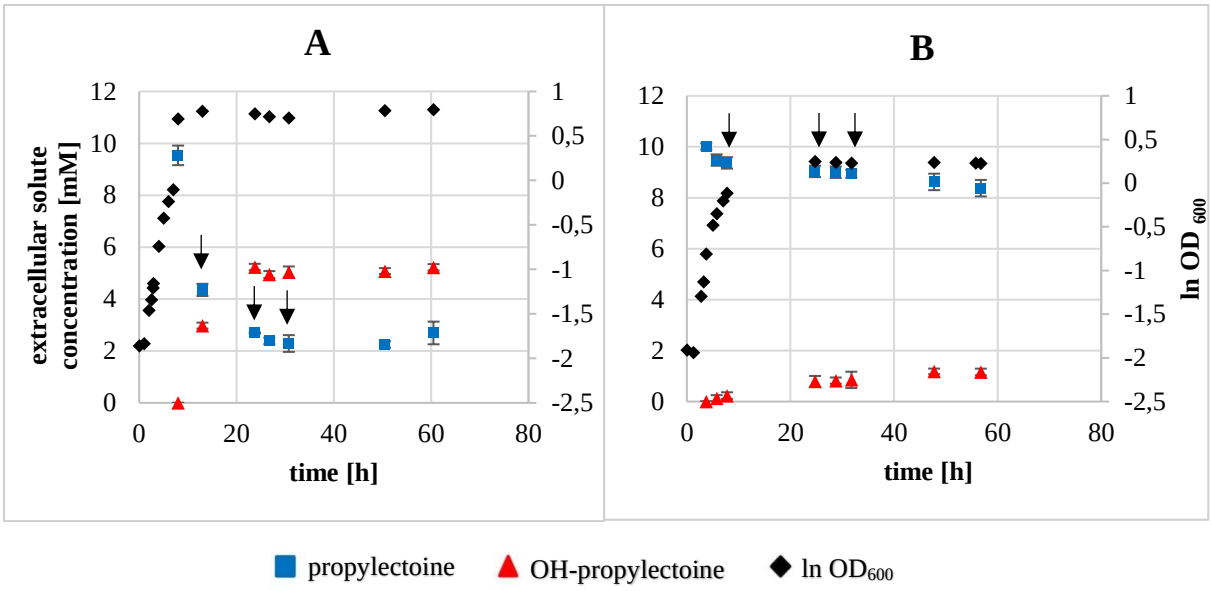

Figure 20: Hydroxylation of 10 mM propylectoine by *E. coli* BL21 pET *ectDHis* with concentrated culture media. Cells were cultivated in MM63-1 medium with 10 g/L glucose and 1 g/L $(NH_4)_2SO_4$ and induced with IPTG (0.1 mM) at OD_{600} = 0.6 before decreasing temperature from 37 °C to 32 °C. Cells were cultivated for 4 h after induction and concentrated in 1/10 volume of the initial MM63-1 medium (without N-source) and supplemented with 10 mM propylectoine (A) or cells were supplemented with 10 mM propylectoine 30 min after induction without cell concentration (B). Additional glucose (2.5 g/L) was fed to provide sufficient energy source (black arrows). Indicated concentrations are arithmetic means of triplicates corresponding to media supernatants and were determined via HPLC.

Although concentration of culture media improved the hydroxylation speed of both, ethylectoine and propylectoine, resuspension of cells in 1/10 of the initial volume should have led to a 10-fold increase of enzyme concentration and therefore an approximate 10-fold increase of hydroxylation performance. Discrepancies between the initial and final solute concentrations resulted from the intracellular solute accumulation of highly concentrated cells.

3.3 Conversion of ectoines by the use of different hydroxylases

In the following it was examined whether EctD homologues of other extremophilic organisms beside moderate halophilic *H. elongata* are able to convert not only ectoine but also synthetic ectoine derivatives. Furthermore, hydroxylation performances of these enzymes were compared with one another for ectoine and, if possible, for ectoine derivatives. Therefore, EctD of psychrophilic *S. alaskensis* and acidophilic *A. cryptum* were tested *in vivo* via biotransformation in *E. coli* and *in vitro* after Strep-tag purification. Also, EctD of non-extremophilic, ubiquitous

P. stutzeri was tested, since this enzyme was shown to exhibit high V_{max} values for the turnover of ectoine *in vitro* (Widderich *et al*., 2014).

3.3.1 *E. coli* BL21(DE3) as whole-cell biotransformation chassis

All previously shown results regarding hydroxylation of ectoines were generated by the use of EctD of the moderate halophilic bacterium *H. elongata*, encoded on a pET-22b(+) vector and heterologously produced by *E. coli* BL21(DE3) as part of a biotranformation machinery. In a further experiment it was tested whether hydroxylases of other organisms exhibit similar or even an enhanced hydroxylation performance. Therefore, *ectD* homologues of *A. cryptum*, *P. stutzeri* and *S. alaskensis* were cloned into pET-22b(+) vector DNA. For reasons of comparability with formerly used *E. coli* BL21 pET *ectDHis*, all hydroxylase enzymes were overproduced in *E. coli* BL21(DE3) as a His_6-tag fusion protein attached to the C-terminus. The corresponding recombinant strains were used as whole-cell biotransformation systems for the *in vivo* conversion of ectoine. Therefore, cells were cultivated and induced under optimized conditions in N-limited MM63-1 medium with 1 g/L $(NH_4)_2SO_4$ and 10 g/L glucose (3.2.2). As all examined EctD enzymes exhibit a similar optimal temperature *in vitro* (*H. elongata* = 32 °C, *A. cryptum* = 32 °C, *P. stutzeri* = 35 °C) except for *S. alaskensis* (15 °C) (Widderich *et al*., 2014; Czech *et al*., 2019), all cultures were induced at 32 °C with IPTG (0.1 mM, OD_{600} = 0.6) and subsequently supplemented with 20 mM ectoine. In order to ensure a sufficient supply of C-source for the regeneration of 2-oxoglutarate and energy for ectoine uptake, glucose was fed in regular intervals.

Figure 21 shows the ectoine hydroxylation process of all four recombinant *E. coli* strains for ~ 50 h. All strains showed a similar growth rate of ~ 0.46 h^{-1}. Although none of the tested strains accomplished a total conversion of 20 mM ectoine, there were differences in hydroxylation performances. While only a little more than 10 mM ectoine was converted by EctD of *H. elongata* as previously shown, all other tested biotransformation systems were able to convert greater amounts of ectoine. A slight improvement was achieved by EctD of *P. stutzeri*, which was able to convert ~ 13 mM ectoine. The hydroxylation process stopped ~ 45 h after induction of both *E. coli* overexpressing *ectD* of *H. elongata* and *P. stutzeri*. Best results were achieved by *E. coli*, producing EctD of *A. cryptum* or *S. alaskensis*, as they were able to convert ectoine over the entire considered time, even though the incubation temperature was much higher than the postulated *S. alaskensis* EctD optimum of 15 °C. There was no or little decrease in hydroxylation performance for these two approaches except for the time between the first two samples, which was caused by the initial cell saturation with ectoine. Early substrate influx

and product efflux rates could not be calculated due to insufficient sampling at the beginning of the biotransformation.

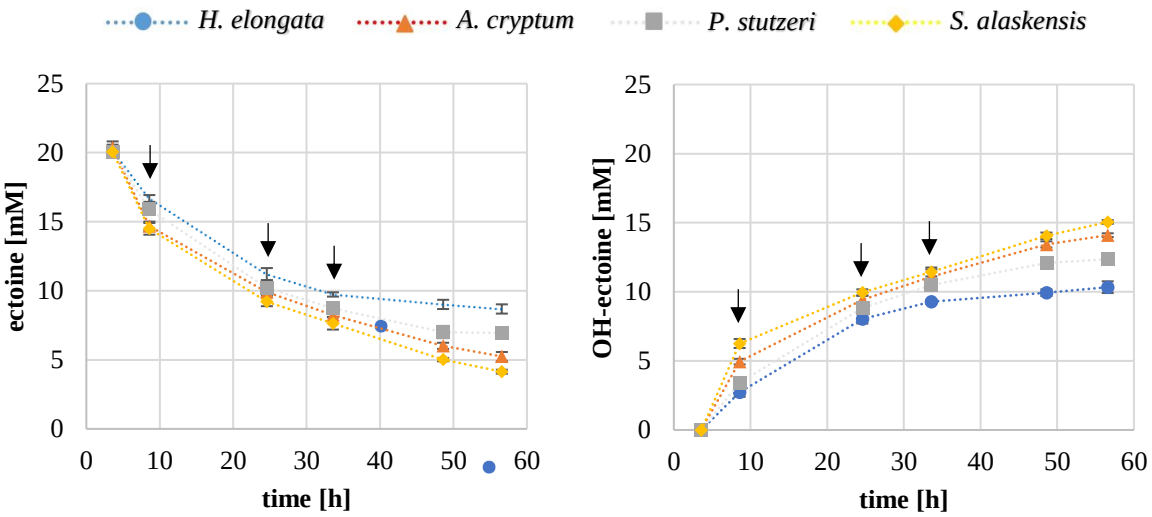

Figure 21: Whole-cell biotransformation of 20 mM ectoine by different ectoine hydroxylases, heterologously expressed by *E. coli* BL21(DE3). *ectD* genes of *H. elongata*, *A. cryptum*, *P. stutzeri* and *S. alaskensis* were encoded on pET-22b(+) vector DNA. Cells were cultivated in MM63-1 medium (1 g/L $(NH4)_2SO_4$, 10 g/L glucose) and supplemented with ectoine after induction with IPTG (0.1 mM, OD_{600} = 0.6), followed by temperature reduction from 37 °C to 32 °C. Additional glucose (2.5 g/L) was fed to provide sufficient energy source (black arrows). Indicated concentrations are arithmetic means of triplicates corresponding to media supernatants and were determined via HPLC.

3.3.2 *E. coli* DH5α as whole-cell biotransformation chassis

As shown in 3.3.1, biotransformation of ectoine was carried out in *E. coli* BL21(DE3) heterologously expressing *ectD* of different organisms, encoded on pET-22b(+) vectors. Over the course of different strain testing, these hydroxylases were also expressed in *E. coli* strain DH5α. Therefore, *ectD* genes were cloned into pASK-IBA3 vector DNA, and overproduced as C-terminal Strep-tag fusion proteins whereas gene expression was induced by the supplementation of AHT. The use of pASK instead of pET vector DNA was necessary because in pET systems the gene of interest's transcription is accomplished by T7 RNA polymerase, which is not encoded in the genome of *E. coli* DH5α.

Beside the hydroxylation of ectoine, it was investigated whether all tested hydroxylases were able to also convert synthetic ectoine derivatives as already shown for EctD of *H. elongata*. Therefore, *E. coli* DH5α strains carrying pASK-IBA3 with *ectD* of either *H. elongata*, *A. cryptum*, *P. stutzeri* or *S. alaskensis* were cultivated in N-limited MM63-1 medium with

10 g/L glucose and 1 g/L $(NH_4)_2SO_4$. Gene expression was induced with AHT at OD_{600} = 0.5. Subsequently, 20 mM ectoine, 10 mM ethylectoine or 5 mM propylectoine were supplemented.

3.3.2.1 Conversion of ectoine

Figure 22 shows the hydroxylation process for ectoine with an initial concentration of 20 mM. As depicted, hydroxylation performance of *E. coli* DH5α overproducing EctD of *H. elongata* and *P. stutzeri* was very similar. Both showed a steep decrease/increase of ectoine/OH-ectoine within the first 4 h post induction with early ectoine influx rates of ~ 37 nmol x min^{-1} x mg^{-1} and OH-ectoine efflux rates of ~ 29 nmol x min^{-1} x mg^{-1} (tab. 17). After ~ 19 h, the ectoine conversion rate decreased, and after ~ 45 h no further hydroxylation was detectable. Since the last sample was taken 96 h post induction, the evaporation of culture media caused a higher and therefore inaccurate residual concentration of solutes in the media supernatants.

By the use of EctD of *A. cryptum*, an almost complete turnover of 20 mM ectoine was realized, and the conversion occured during the whole considered time (fig. 22, orange line). However, it could not be clearified if EctD activity was present through the whole period between 45 h and 96 h post induction. With 68 nmol x min^{-1} x mg^{-1}, this approach showed the highest early ectoine influx rate, which correlates with the OH-ectoine efflux rate of 66 nmol x min^{-1} x mg^{-1}. About 45 h after induction, the conversion rate significantly decreased, leading to 1.6 mM residual ectoine at the end of the hydroxylation process.

Table 17: Growth rates and early ectoine influx/OH-ectoine efflux rates of *E. coli* DH5α, heterologously expressing *ectD* of different organisms, encoded on pASK-IBA3 vector DNA. Cells were cultivated in MM63-1 medium with 10 g/L glucose and 1 g/L $(NH_4)_2SO_4$. Growth rates were calculated in exponential growth phase after gene induction with AHT at 35 °C. Ectoine influx/OH-ectoine efflux rates were calculated for the time period 2 h - 4 h post induction and correlated with whole-cell proteins, derived from directly measured OD_{600} 3 h post induction.

Expression system	*E. coli* DH5α pASK *ectD_Hel_Strep*	*E. coli* DH5α pASK *ectD_Acry_Strep*	*E. coli* DH5α pASK *ectD_Pstu_Strep*	*E. coli* DH5α pASK *ectD_Sala_Strep*
growth rate μ (h^{-1})	0.19 ± 0.02	0.11 ± 0.02	0.20 ± 0.03	0.17 ± 0.03
early ectoine influx ($\frac{nmol}{min*mg}$)	36.5 ± 6.3	68.1 ± 3.7	38.1 ± 2.6	61.9 ± 3.1
early OH-ectoine efflux ($\frac{nmol}{min*mg}$)	31.9 ± 3.5	66.2 ± 4.4	29.2 ± 5.1	58.6 ± 2.9

A complete turnover of 20 mM ectoine was achieved by the use of EctD of *S. alaskensis*. Although the early ectoine influx/OH-ectoine efflux rates of 62 $\frac{nmol}{min*mg}$ / 59 $\frac{nmol}{min*mg}$ were slightly lower compared to EctD of *A. cryptum*, conversion of the entire substrate was observed.

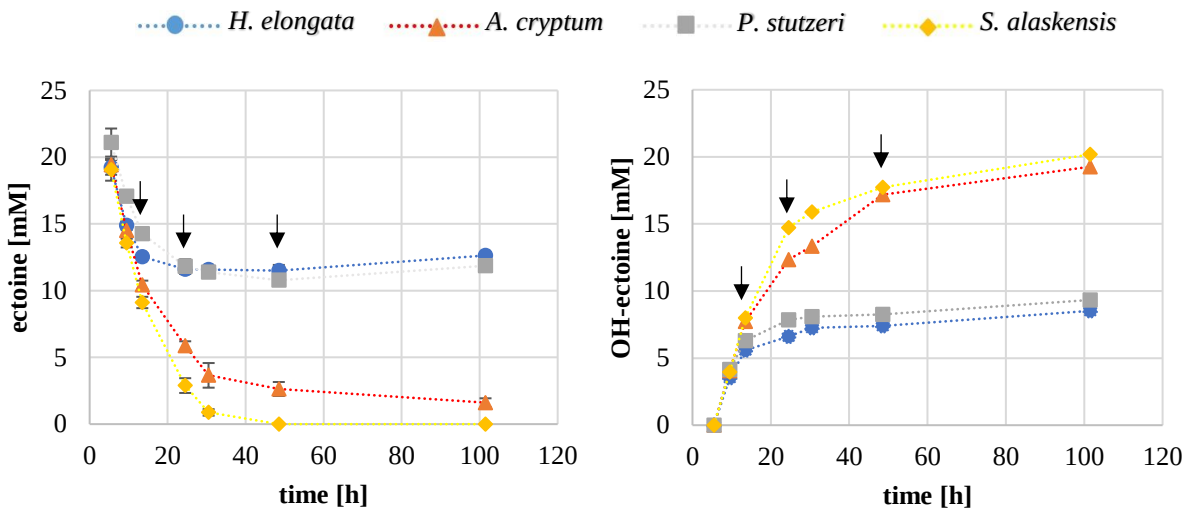

Figure 22: Whole-cell biotransformation of ectoine by different ectoine hydroxylases, heterologously expressed by *E. coli* DH5α. *ectD* genes of *H. elongata*, *A. cryptum*, *P. stutzeri* and *S. alaskensis* were encoded on pASK-IBA3 vector DNA. Cells were cultivated in MM63-1 medium (1 g/L $(NH_4)_2SO_4$, 10 g/L glucose) and supplemented with 20 mM ectoine after induction with AHT (0.2 µg/mL, OD_{600} = 0.5), followed by a temperature reduction from 37 °C to 35 °C. Additional glucose (2.5 g/L) was fed to provide sufficient energy source (black arrows). Indicated concentrations are arithmetic means of triplicates corresponding to media supernatants and were determined via HPLC.

3.3.2.2 Conversion of 10 mM ethylectoine and 5 mM propylectoine

It was already shown, that EctD of *H. elongata* recognizes both ethylectoine and propylectoine as substrates for hydroxylation. In further experiments it was tested whether hydroxylases of *A. cryptum*, *P. stutzeri* and *S. alaskensis* share this promiscuity. As shown in figure 23, all four overproduced hydroxylases were capable of converting these ectoine derivatives. By the use of EctD of *H. elongata* and *P. stutzeri*, ~ 6 mM of the initial 10 mM ethylectoine were converted and substrate conversion stopped 24 h post induction. Both EctD of *A. cryptum* and *S. alaskensis* on the other hand showed actitvity over the whole considered time. Here, only traces of the substrates were detected 50 h post induction and the product quantities were comparable to the initial substrate concentrations. It is noticeable that early substrate influx/product efflux rates of *E. coli* overexpressing *ectD* of *P. stutzeri* were similar compared to the system overexpressing *ectD* of *S. alaskensis*. However, an almost complete turnover was

only accomplished by the latter biotransformation system, suggesting differences in enzyme stability (tab. 18).

Hydroxylation of propylectoine proceeded much slower and ended earlier compared with ethylectoine. None of the four biotransformation systems was capable of converting 5 mM substrate. With the exception of the *P. stutzeri* enzyme which was even less efficient, they all showed a similar hydroxylation performance by converting a maximum of 1 - 1.5 mM.

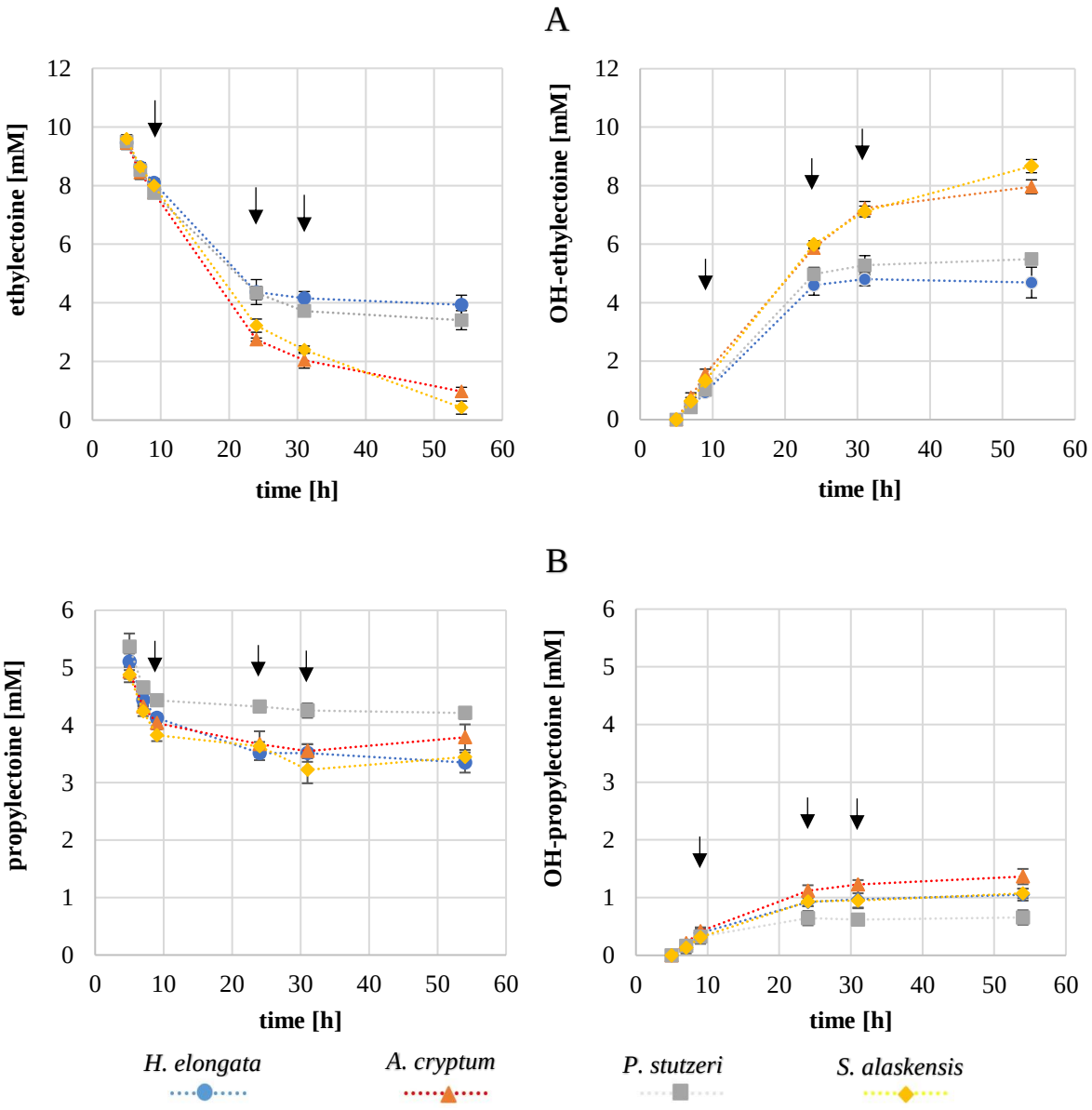

Figure 23: Whole-cell biotransformation of ethylectoine and propylectoine by different ectoine hydroxylases, heterologously expressed by *E. coli* DH5α. *ectD* genes of *H. elongata*, *A. cryptum*, *P. stutzeri* and *S. alaskensis* were encoded on pASK-IBA3 vector DNA. Cells were cultivated in MM63-1 medium (1 g/L $(NH_4)_2SO_4$, 10 g/L glucose) and supplemented with 10 mM ethylectoine (A) or 5 mM propylectoine (B) after induction with AHT (0.2 µg/mL, OD_{600} = 0.5), followed by temperature reduction from 37 °C to 35 °C. Additional glucose (2.5 g/L) was fed to provide sufficient energy source (black arrows). Indicated concentrations are arithmetic means of triplicates corresponding to media supernatants and were determined via HPLC.

Table 18: Growth rates and early substrate influx/product efflux rates of *E. coli* DH5α, heterologously expressing different hydroxylases for conversion of ethylectoine and propylectoine. Growth rates were calculated for the exponential growth phase after substrate supplementation. Influx/efflux rates were calculated for the time period of 2 h – 4 h post induction and correlated with whole-cell proteins, derived from directly measured OD_{600} 3 h post induction. Data refer to fig. 23.

Expression system	*E. coli* DH5α pASK *ectD_Hel_Strep*	*E. coli* DH5α pASK *ectD_Acry_Strep*	*E. coli* DH5α pASK *ectD_Pstu_Strep*	*E. coli* DH5α pASK *ectD_Sala_Strep*
growth rate μ (h^{-1}) with ethylectoine	0.23 ± 0.02	0.14 ± 0.02	0.20 ± 0.02	0.17 ± 0.01
growth rate μ (h^{-1}) with propylectoine	0.16 ± 0.02	0.11 ± 0.01	0.16 ± 0.01	0.14 ± 0.02
early ethylectoine influx ($\frac{nmol}{min*mg}$)	19.24 ± 3.4	28.78 ± 4.2	25.12 ± 2.2	22.21 ± 1.0
early OH-ethylectoine efflux ($\frac{nmol}{min*mg}$)	18.35 ± 2.3	33.8 ± 3.0	21.58 ± 2.9	24.20 ± 1.9
early propyelectoine influx ($\frac{nmol}{min*mg}$)	11.78 ± 1.1	12.10 ± 1.9	8.60 ± 1.4	9.17 ± 1.5
early OH-propylectoine efflux ($\frac{nmol}{min*mg}$)	9.60 ± 1.2	8.78 ± 1.8	6.18 ± 1.8	8.12 ± 1.1

3.3.2.3 Maximal uptake rates of ectoine and ectoine derivatives

In previous experiments it was shown that the conversion of ectoine is carried out explicitly faster compared to ethylectoine and propylectoine via whole-cell biotransformation (tab. 17, 18). We wanted to test whether differential hydroxylation speed of synthetical ectoine derivatives is caused due to different substrate uptake rates. Indeed, these rates were already calculated, but the calculation was determined after cellular saturation with the substrates. However, after saturation, solute uptake is also dependent on substrate conversion by EctD and product efflux, by what real solute uptake rates are not reflected. Hence, maximal uptake rates for ectoine, ethylectoine and propylectoine were determined for *E. coli* DH5α wildtype immediately after substrate supplementation and without the expression of *ectD*.

Therefore, cells were cultivated in MM63-1 medium and supplemented with 10 mM of the respective solute in the exponential growth phase. Immediately after the supplementation with the solute, defined volumes of culture medium were filtered in short time intervals and intracellular solutes were extracted by the B&D extraction method. Via HPLC analysis of the extracts and the estimated theoretical amount of whole-cell protein (derived from measured OD_{600}), solute uptake in nmol solute per mg protein could be calculated and was plotted against time (fig. 24). A linear uptake was observed for all substrates for ~ 6 min, followed by a

decrease upon cellular saturation. A noticeable finding was that ethylectoine was accumulated to a greater extent (~ 800 nmol/mg) compared to the other solutes (~ 600 nmol/mg).

To verify if certain solutes are taken up at different speed, affecting hydroxylation performances *in vivo*, maximal solute uptake rates (nmol x min^{-1} x mg^{-1}) were calculated within the range of linear solute uptake immediately after substrate supplementation.

Maximal substrate uptake rates of all examined solutes were ranged between 65 - 75 nmol x min^{-1} x mg^{-1} and thus were quite similar. As maximal uptake rates show no significant distinction, it is unlikely that solute uptake is a crucial reason for differential hydroxylation performance of the examined solutes.

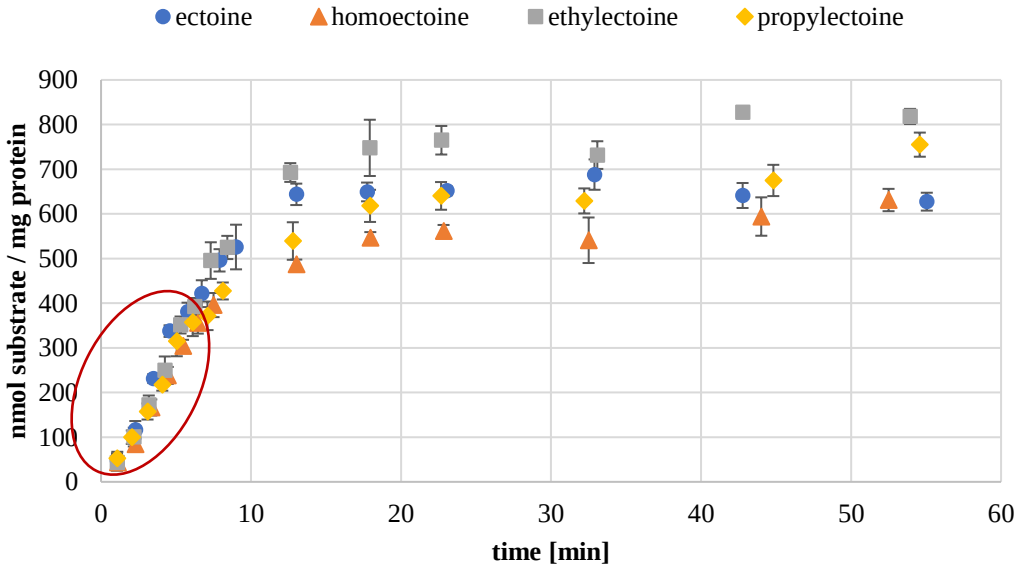

Solute	Ectoine	Homoectoine	Ethylectoine	Propylectoine
max. uptake rate	73.49 $\frac{nmol}{min*mg}$	65.63 $\frac{nmol}{min*mg}$	75.50 $\frac{nmol}{min*mg}$	65.87 $\frac{nmol}{min*mg}$

Figure 24: Maximal uptake rates of ectoine and synthetic ectoine derivatives in *E. coli* DH5α wildtype. Cells were cultivated at 37 °C in MM63-1 medium with 10 g/L glucose and 1 g/L $(NH_4)_2SO_4$ and supplemented with 10 mM ectoine, homoectoine, ethylectoine or propylectoine at OD_{600} = 0.5. Intracellular amounts of solutes were calculated in regular intervals by cell filtration, B&D extraction and HPLC analysis (triplicates). Amounts of solutes (nmol) per whole-cell protein (mg) were plotted against time (min) in order to calculate max. solute uptake rates. Max. uptake rates were calculated for the linear increase within the first 6 min after supplementation (red box).

3.3.2.4 EctD enzyme stability over time

Although max. substrate influx rates in *E. coli* DH5α wildtype were similar for all considered solutes (fig. 24), hydroxylation performances of *E. coli* DH5α pASK-IBA3 strains

overproducing four different hydroxylases were different. Hydroxylation by *E. coli* DH5α, overproducing EctD of *H. elongata* and *P. stutzeri* stopped ~ 24 h post induction, whereas the two other strains, overproducing EctD of *A. cryptum* and *S. alaskensis* showed an extended hydroxylation period (fig. 22, 23). In this context, it was investigated if enzyme degradation over time could be the cause of these differences. For this purpose, whole-cell protein samples were taken from *E. coli* DH5α pASK-IBA3, overproducing EctD_Strep-tag fusion proteins of *H. elongata*, *A. cryptum*, *P. stutzeri* and *S. alaskensis* before induction and at different times after induction. For visualization, proteins were analyzed by SDS-PAGE and gels were stained with Coomassie (fig. 25). Except for proteins samples containing EctD of *H. elongata*, it was shown that clearly visible protein bands formed at the expected spots in the SDS gel after induction. The proteins of interest exhibit a size between 35 and 39 kDa. Furthermore, putative EctD protein bands of *P. stutzeri* significantly became weaker over the period of time until it was barely visible after 66 h. On the contrary, putative EctD protein bands of *A. cryptum* and *S. alaskensis* were clearly visible until 66 h post induction and showed no loss of intensity over the period of time.

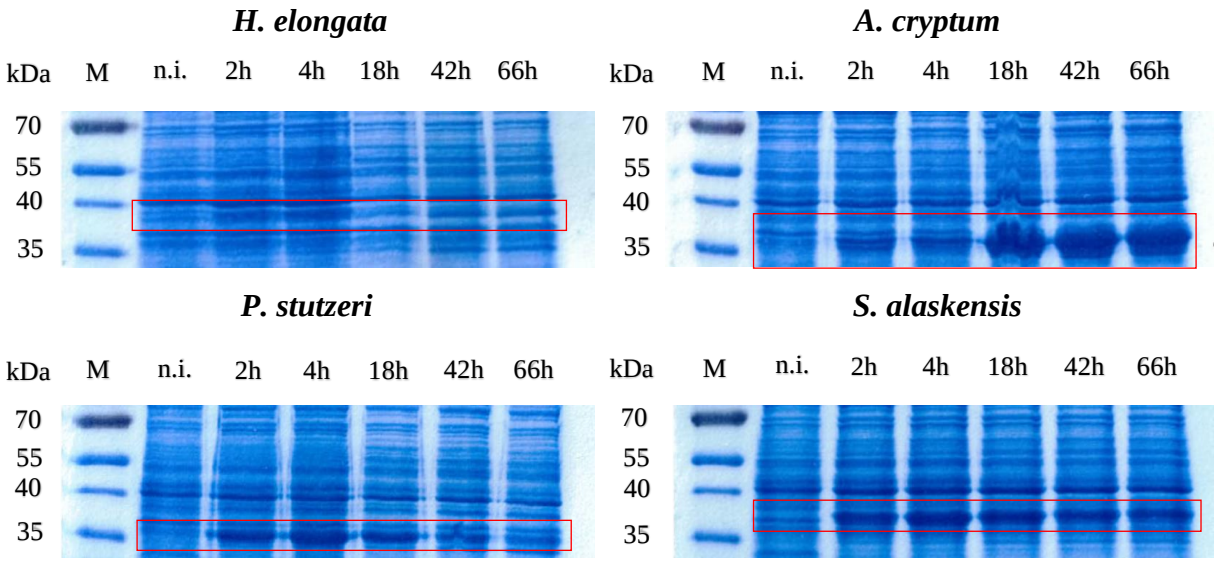

Figure 25: SDS-PAGE analysis of whole-cell proteins for visualization of heterologously overproduced EctD_Strep-tag fusion protein. Soluble proteins (20 µg/lane) were extracted from *E. coli* DH5α pASK-IBA3, overproducing EctD of *H. elongata* (38.4 kDa), *A. cryptum* (35.1 kDa), *P. stutzeri* (35.2 kDa) and *S. alaskensis* (35.1 kDa) with a C-terminal Strep-tag. Cells were cultivated in MM63-1 medium with 10 g/L glucose and 1 g/L $(NH_4)_2SO_4$. Protein samples before induction (n.i.) up to 66 h post induction with AHT (0.2 µg/mL) were examined and gels were stained with Coomassie. M = PageRuler prestained protein ladder.

In order to exclude overlapping proteins with the proteins of interest, 100 mg of whole-cell protein samples were purified via Strep-Tactin affinity chromatography. Purified proteins were subsequently analyzed via SDS-PAGE once more (fig. 26). Gels were stained with silver, since protein proportions in these purified samples were significantly lower compared to whole-cell protein samples and silver staining is more sensitive than Coomassie. Silver stained SDS-PAGE gels showed (if any) only single protein bands between 35 and 40 kDa. Purified samples of not induced cells never showed any band formation. Protein bands for samples with purified EctD of *H. elongata* were not visible since no detectable proteins were available after Strep-tag purification (suppl. tab. 1). Very intensive protein bands were visible for samples with purified EctD of *A. cryptum*, whereas the greatest amounts were available 18 h - 66 h post induction, and intensity stayed constant after 18 h. In case of purified EctD of *P. stutzeri* the highest protein proportion was available 4 h post induction and the band intensity significantly decreased over the period of time. Protein bands for samples of purified EctD of *S. alaskensis* were already clearly visible 2 h post induction and intensity stayed constant over the entire period of time. It can be concluded that EctD enzymes of *A. cryptum* and *S. alaskensis* were more stable compared to EctD of *P. stutzeri* and *H. elongata*.

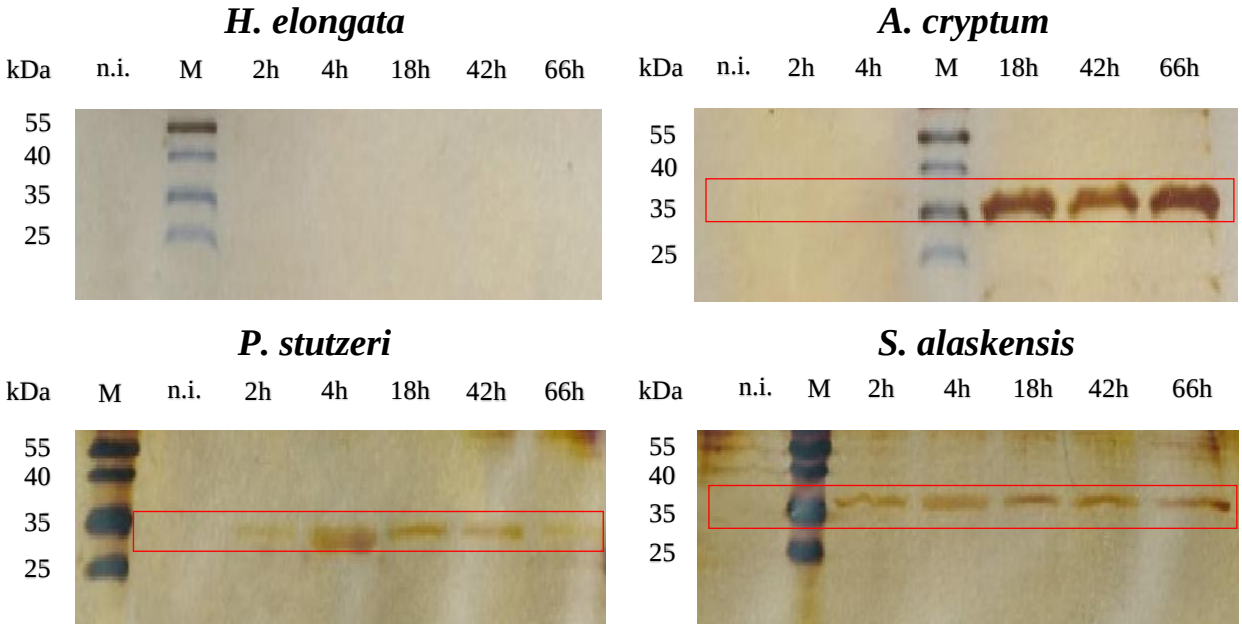

Figure 26: SDS-PAGE analysis of heterologously overproduced and purified EctD_Strep-tag fusion protein. 100 mg of whole-cell protein fractions containing EctD_Strep-tag fusion proteins of *H. elongata* (38.4 kDa), *A. cryptum* (35.1 kDa), *P. stutzeri* (35.2 kDa) and *S. alaskensis* (35.1 kDa) were purified by Strep-Tactin XT Spin columns. Same volumes of purified protein fractions were applied on each lane. Proteins were derived from cells cultivated in MM63-1 medium with 10 g/L glucose and 1 g/L $(NH_4)_2SO_4$. Protein samples of not induced cells (n.i.) and samples up to 66 h after induction with AHT (0.2 µg/mL) were examined and gels were stained with silver. M = PageRuler prestained protein ladder.

3.3.2.5 Hydroxylation by EctD of *S. alaskensis* under the enzyme's optimal temperature

The best results regarding hydroxylation performance by the use of *E. coli* DH5α as a biotransformation system were achieved by heterologously overproduced EctD of *A. cryptum* and *S. alaskensis*. In a further step it was investigated if hydroxylation performance can be optimized by applying cultivation temperatures which correspond to the optimal EctD temperatures. EctD of *A. cryptum* exhibits a temperature optimum of 32 °C *in vitro* (Widderich *et al*., 2014) and hydroxylation attempts were already performed at 35 °C, which is why significant improvement by temperature adjustment was not presumed. Hence, the focus had been put on EctD of *S. alaskensis*, which shows an optimum at 15 °C (Czech *et al*., 2019). Therefore, *E. coli* was cultivated in MM63-1 medium with 10 g/L glucose and 1 g/L $(NH_4)_2SO_4$ and induced with AHT before decreasing the cultivation temperature from 37 °C to 35 °C. Cells were cultivated until reaching stationary phase to produce sufficient amounts of EctD under advantageous conditions for *E. coli*. After reaching stationary phase, temperature was set to the optimal EctD temperature of 15 °C. As a control, another culture was further incubated at 35 °C. Since 20 mM ectoine were completely converted by *E. coli* DH5α pASK_*ectD_Strep* in a previous experiment (3.3.2.1), the initial ectoine concentration was set to 30 mM.

As shown in figure 27, a complete turnover of 30 mM ectoine was achieved by cultivation at 35 °C, although here a decrease in hydroxylation performance over time could be observed, indicated by declining ectoine uptake and OH-ectoine efflux (fig. 27 A). Cultures incubated at 15 °C after reaching stationary phase (fig. 27 B) were able to take up ectoine and excrete OH-ectoine at constant speed over the whole considered time, although substrate uptake and product efflux was significantly reduced compared to cells incubated at 35 °C. Presumably due to a relatively low hydroxylation performance, cultures incubated at 15 °C were not able to completely convert 30 mM ectoine within the considered time period, as a residual concentration of 5 mM substrate was found after 120 h. In contrast to cultures incubated at 35 °C, both ectoine influx and OH-ectoine efflux showed a linear course at 15 °C for the whole time. Furthermore, it was noticeable that cultures incubated at 35 °C showed a slight decrease in OD_{600} after reaching stationary phase, suggesting an upcoming death phase. Elevated values for OD_{600} and OH-ectoine were determined 120 h post induction, as culture medium was concentrated due to evaporation. On the contrary, the OD_{600} of cultures incubated at 15 °C, as well as the corresponding culture volume was constant over the whole considered time, indicating no emerging death phase. In summary, it can be assumed that enzyme instability and the upcoming death phase of *E. coli* limitates the hydroxylation process, which is accelerated at the higher cultivation temperature of 35 °C.

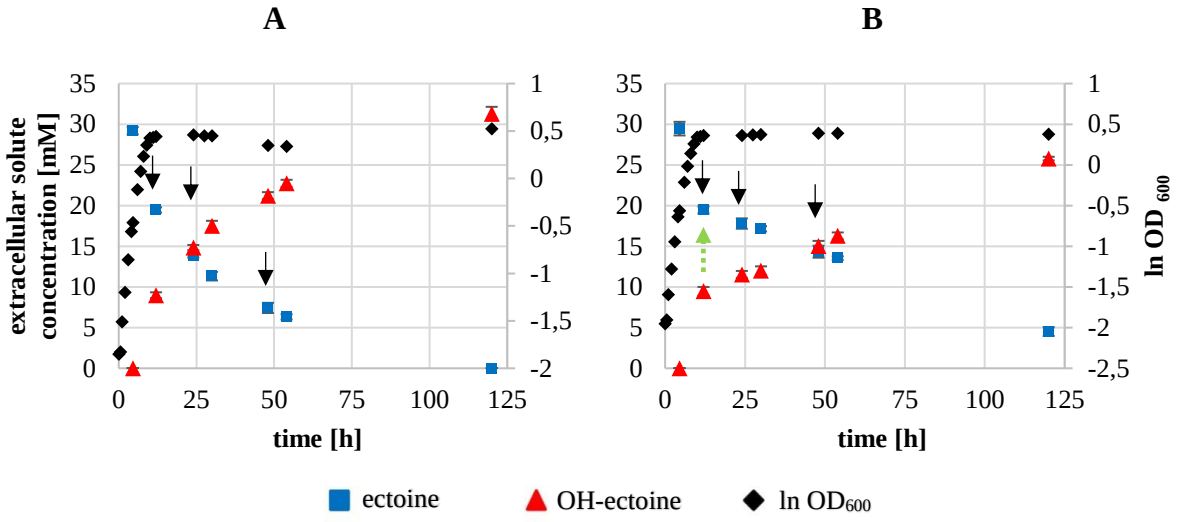

Figure 27: Ectoine hydroxylation performance of *E. coli* DH5α pASK *ectD_Sala_Strep* under optimal temperature of EctD Cells were cultivated in MM63-1 medium (1 g/L $(NH_4)_2SO_4$, 10 g/L glucose) and supplemented with 30 mM ectoine after induction with AHT (0.2 µg/mL, OD_{600} = 0.5), followed by temperature reduction from 37 °C to 35 °C. When cultures entered stationary phase, cells were further cultivated at 35 °C (**A**) or at an EctD (Sala) optimal temperature of 15 °C (**B**, dashed green arrow). Additional glucose (5.0 g/L) was fed to provide sufficient energy source (black arrows). Indicated concentrations are arithmetic means of triplicates corresponding to media supernatants and were determined via HPLC.

3.3.3 EctD *in vitro* analysis

Previous experiments suggested that ectoine hydroxylation performance in *E. coli* DH5α is highly dependent on the choice of the respective hydroxylase, as different EctD enzymes showed different stability over time in consequence of degradation (fig. 25, 26). Beyond that, different hydroxylation performances could also be caused by different EctD activities. In order to check this hypothesis, *in vitro* assays were carried out with all four investigated EctDs, generating V_{max} and K_{cat} values, according to Michaelis-Menten kinetics. Besides ectoine, also ethylectoine and homoectoine were used as substrates, as differences in whole-cell biotransformation performances regarding these synthetic ectoine derivatives could not be explained by different solute uptake rates *in vivo* (fig. 24).

Varying amounts of ectoine, ethylectoine and homoectoine (1 - 30 mM) together with a constant amount of EctD enzymes (0.05 µg/mL) were dissolved in a reaction mix, containing cofactors 2-oxoglutarate and Fe(II) sulfate as well as KCl and TES under optimized conditions (Widderich *et al.*, 2014). EctD *in vitro* assays were carried out at the enzyme's optimal temperatures under shaking, as the reaction is highly O_2-dependent (tab. 19). Propylectoine was

not tested since *in vivo* hydroxylation performance was very poor compared to the other tested solutes.

V_{max} is the maximal reaction rate of an enzyme while the active site is saturated with substrate. K_{cat} is defined as the enzyme's turnover number and equals the number of substrate molecule conversions per second by a single enzyme. Here, K_{cat} values were determined during substrate saturation. The higher V_{max} and K_{cat}, the faster the substrate conversion.

Table 19 shows V_{max} and K_{cat} values for ectoine, ethylectoine and homoectoine, corresponding to EctD of *H. elongata*, *P. stutzeri*, *A. cryptum* and *S. alaskensis*. All studied enzymes generally exhibited similar kinetic parameters for ectoine with V_{max} values of ~ 4.3 - 5.6 U/mg, whereas EctD of *A. cryptum* stood out with a comparatively low value of 1.8 U/mg. In regards to K_{cat} it can be noted, that ~ 5 - 6 molecules ectoine per second were converted by one EctD enzyme except for EctD of *A. cryptum* which was capable of converting only ~ 2 molecules.

Synthetic ectoine derivatives ethylectoine and homoectoine were converted slower compared to ectoine, as V_{max} and K_{cat} values for these substances were always lower. V_{max} values for ethylectoine ranged from ~ 1 - 2 U/mg for all considered enzymes, while EctD of *A. cryptum* stood out again with a relatively low value of 0.8 U/mg. Comparatively low conversion rates of ethylectoine can also be deduced by the turnover numbers, which ranged from ~ 0.9 - 2.5 molecules ethylectoine per second.

Regardless of the enzyme, homoectoine was converted faster compared to ethylectoine. V_{max} values and K_{cat} values ranged from ~ 2 - 3 U/mg and ~ 2 - 4 molecules homoectoine per second,

Table 19: EctD *in vitro* activity assay. Kinetic parameters V_{max} and K_{cat} for ectoine, ethylectoine and homoectoine were determined for recombinantly produced EctD_Strep fusion proteins of *H. elongata*, *A. cryptum*, *P. stutzeri* and *S. alaskensis*. Turnover numbers (K_{cat}) were derived from maximal enzyme velocity values (V_{max}) at substrate saturation.

	Ectoine		**Ethylectoine**		**Homoectoine**	
	V_{max} [U/mg]	**K_{cat} [s^{-1}]**	**V_{max} [U/mg]**	**K_{cat} [s^{-1}]**	**V_{max} [U/mg]**	**K_{cat} [s^{-1}]**
***H. elongata* (T = 32 °C)**	4.61 ± 0.23	5.90 ± 0.29	1.27 ± 0.06	1.62 ± 0.08	3.13 ± 0.09	4.01 ± 0.11
***A. cryptum* (T = 32 °C)**	1.81 ± 0.03	2.13 ± 0.03	0.76 ± 0.02	0.89 ± 0.02	1.19 ± 0.08	1.39 ± 0.10
***P. stutzeri* (T = 35 °C)**	5.56 ± 0.11	6.52 ± 0.13	2.15 ± 0.09	2.52 ± 0.11	2.31 ± 0.15	2.71 ± 0.18
***S. alaskensis* (T = 15 °C)**	4.29 ± 0.04	5.02 ± 0.05	0.92 ± 0.03	1.08 ± 0.03	1.84 ± 0.11	2.15 ± 0.13

respectively. Also in case of homoectoine, V_{max} and K_{cat} values, regarding EctD of *A. cryptum*, showed the smallest values.

3.4 Downstream processing of hydroxylated ectoine derivatives

Hydroxylated ectoine derivatives were purified after whole-cell biotransformation in *E. coli* BL21 pET *ectDHis*, which heterologously produced EctD of *H. elongata*. Because OH-homoectoine showed significant instability over time (fig. 18) and OH-propylectoine production was very low, the focus was on the production and purification of OH-ethylectoine. Therefore, cells were cultivated in 20 x 100 mL MM63-1 medium with 10 g/L glucose and 1 g/L $(NH_4)_2SO_4$, and supplemented with 3 mM ethylectoine after IPTG induction (0.1 mM, OD_{600} = 0.6, 32 °C). This relatively low concentration of substrate was chosen to ensure a complete hydroxylation and because *E. coli* is only capable of accumulating solutes to a certain extent. After a biotransformation process of 24 h, cultures were "shocked" with NaCl (5 % w/v), which should cause enhanced uptake of the hydroxylated product from the media supernatant (Kempf & Bremer, 1998). After 60 min, cells were harvested, freeze dried and the solute was extracted via the B&D method.

HPLC analysis revealed, that no residual ethylectoine (retention time ~ 7.5 min) was detectable in media supernatants after 24 h, as pooled supernatants showed no signal at the retention time according to 1 mM ethylectoine standard (fig. 28). Instead, only a signal for OH-ethylectoine emerged ~ 3 min later (retention time ~ 10.5 min). Media supernatants of NaCl-shocked cultures exhibited only traces of residual OH-ethylectoine, as the rest was intracellularly accumulated, shown by HPLC analysis of the B&D extract. Furthermore, HPLC analysis of B&D extracts showed no signal for residual ethylectoine.

Because no standard substance for OH-ethylectoine was available at that time, OH-ethylectoine concentrations were calculated using 1 mM ethylectoine as a reference substance. The B&D extract analysis of NaCl-schocked cells revealed a yield of 196 mg OH-ethylectoine per g bacterial dry mass (~ 20 % solute/bacterial dry mass), and the total bacterial dry mass in 2 L culture media was 4.48 g. This means that 878.1 mg OH-ethylectoine were accumulated intracellularly. Culture media supernatants after NaCl shock showed a residual OH-ethylectoine concentration of 0.18 mM, which equals 61.9 mg OH-ethylectoine in 2 L. In total, ~ 940 mg OH-ethylectoine were accounted for.

Since an initial solute concentration of 3 mM ethylectoine was defined in culture media, a total conversion would result in a final amount of 1.03 g OH-ethylectoine. Thus, an experimental discrepancy of less than 7 % to the theoretical value was observed.

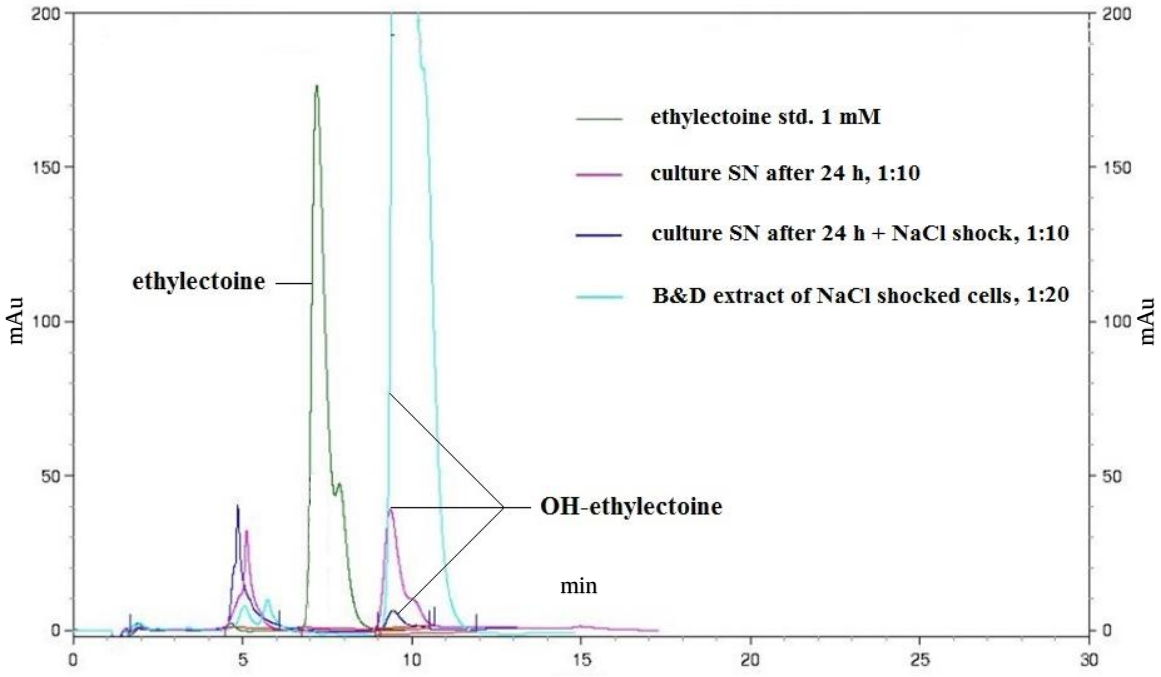

Figure 28: HPLC analysis (UV spectrum) of media supernatants (SN) and B&D extract of (NaCl-shocked) *E. coli* cells after whole-cell biotransformation of ethylectoine. Conversion of 3 mM ethylectoine was carried out by *E. coli* BL21 pET *ectDHis* in MM63-1 medium with 10 g/L glucose and 1 g/L $(NH_4)_2SO_4$. 24 h after induction and substrate supplementation, a NaCl shock (5 % w/v) was performed for 60 min before cells were harvested and solutes were extracted via B&D solution. Samples were analyzed via isocratic HPLC with 80 % AcN as the eluent and a reversed amino phase silica gel (LiChospher 100 NH2) as the stationary phase. mAu = milli-absorbance unit.

For further purification, B&D extracts that contained OH-ethylectoine were incubated at 50 °C for methanol evaporation. Product solutions were subsequently purified via cation exchange chromatography and desalted by ion retardation chromatography as previously described (2.8.2.1 - 2.8.2.2, data not shown). Purified samples were freeze-dried, and showed a crystal formation with a white-yellowish coloration. After this purification step, the weight of the solid product was 690 mg. In order to remove residual impurities, the product was incubated in a supersaturated methanol solution at -20 °C, by which pure white crystals were formed over time. After complete drying at 50 °C, the product was analyzed via HPLC analysis (fig. 29) and ^{13}C-NMR analysis (fig. 30), confirming the generation of OH-ethylectoine with no detectable impurities. The final dry weight of purified OH-ethylectoine was 467 mg.

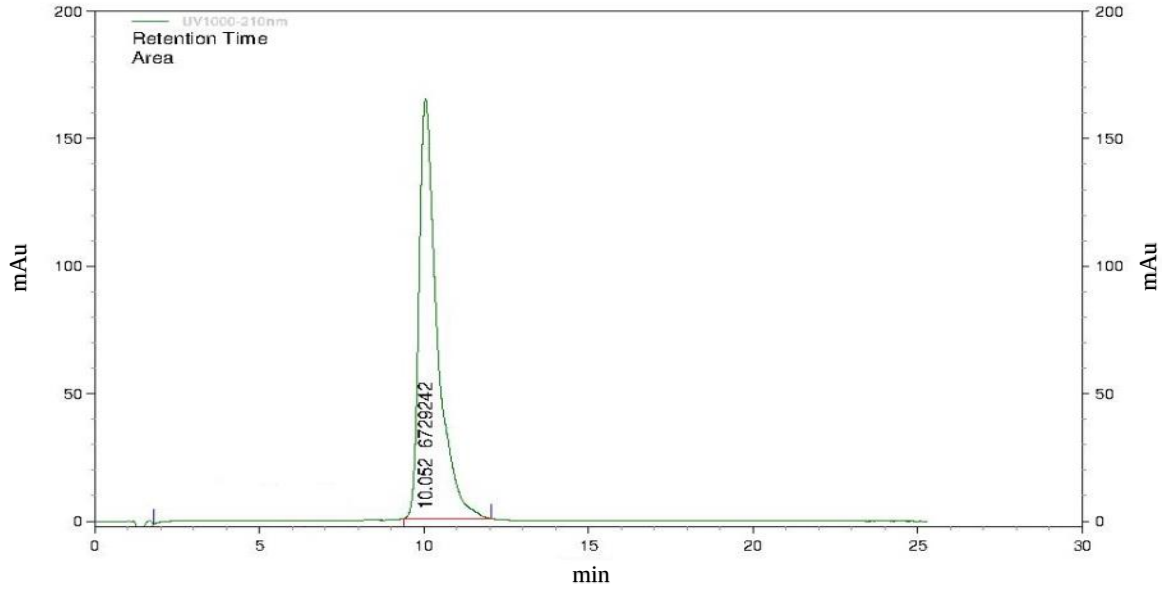

Figure 29: HPLC chromatogram (UV spectrum) of OH-ethylectoine. The sample with a final concentration of 1 mM was analyzed via isocratic HPLC with 80 % AcN as eluent and a reversed amino phase silica gel (LiChospher 100 NH2) as stationary phase. mAU = milli-absorbance unit.

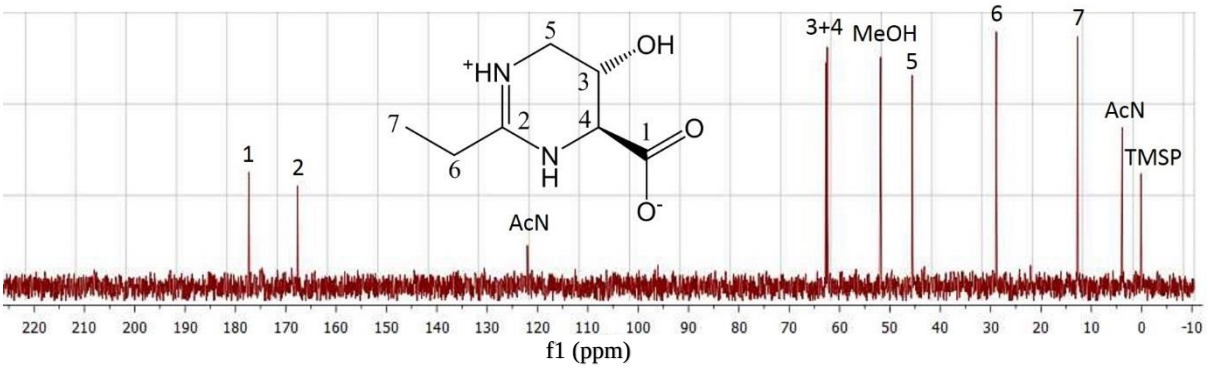

Figure 30: ^{13}C-NMR analysis of OH-ethylectoine. The spectrum shows the carbon detection pattern at specific resonance frequencies (ppm) for the hydroxylated synthetic ectoine derivative OH-ethylectoine. Next to the peaks dedicated to ethylectoine, additional signals for TMSP, MeOH and AcN were detected.

3.5 Characterization of synthetic ectoine derivatives

Previous experiments predominantly dealt with the hydroxylation of ectoine and synthetic ectoine derivatives. In the following, synthetic ectoine derivatives (OH)-ethylectoine, propylectoine and homoectoine were characterized. These characterization studies include potential thermo-, osmo- and desiccation protection abilities towards biomolecules or whole cells. As it was not possible to prepare pure OH-homoectoine in this work, due to instability of the substance, this phenomenon was investigated, as well.

3.5.1 Instability of OH-homoectoine

As previously shown for the whole-cell biotransformation of homoectoine, the hydroxylated product OH-homoectoine in media supernatants showed a successive decrease in concentration over time (fig. 18). In the work of Ruprecht (2014), NMR analysis of purified OH-homoectoine samples already revealed a mixture of OH-homoectoine and its open chain variant 3-Hydroxy-Nδ-acetylornithine (fig. 37).

It is not yet clear why hydroxylated homoectoine is converted to its open ring form. This is why in the following it was tested, whether instability is based on a specific pH or if it is caused due to proteins, possibly excreted into the media supernatant by *E. coli* during biotransformation. Therefore, media supernatants, containing OH-homoectoine, were adjusted to pH values between 2 and 10. Afterwards, supernatants were filtered using cellulose membrane filters for the removal of proteins up to 3 kDa in size. The samples were subsequently sealed with parafilm to avoid evaporation during incubation at 32 °C. Samples were regularly analyzed via HPLC.

As can be seen in figure 31 A, OH-homoectoine concentration stayed constant over the considered time of 120 h under acidic condition of pH 2 - 4. A pH of 6 or higher led to a successive decrease of OH-homoectoine over the time. However, OH-homoectoine concentrations decreased more rapidly at pH 7 and pH 10. Interestingly, there appears to be two maxima of degradation, one at neutral pH and the other at very alkaline pH's. The same results were generated for samples which were not filtered by cellulose membrane and thus possibly contained excreted proteins (fig. 31 B). While alkaline hydrolysis at very alkaline pH had to be expected, the instability at neutral pH was surprising.

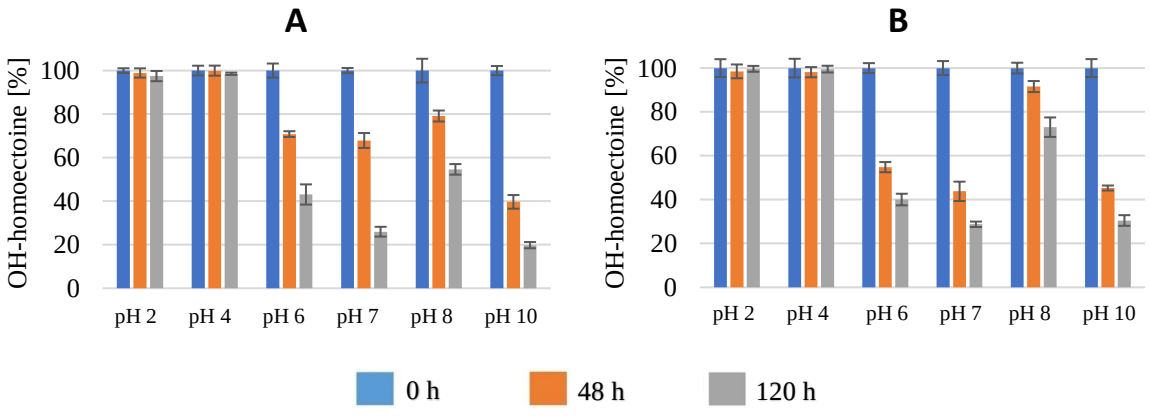

Figure 31: pH-dependent stability of OH-homoectoine over time. Media supernatants, containing OH-homoectoine after whole-cell biotransformation of 10 mM homoectoine were set to different pHs. Subsequently, supernatants were filtered using cellulose membranes with a pore size of 3 kDa (A). In order to investigate the influence of possibly excreted proteins, additional parts of supernatants were not filtered after pH adjustment (B). Percentages of OH-homoectoine refer to maximal OH-homoectoine concentrations in the beginning of the experiment (0 h) and are arithmetic means of triplicates.

3.5.2 Influence of ectoines on RNase A melting temperature

As previously described, compatible solutes exhibit a great variety of stabilizing abilities towards different kinds of stresses. RNase A is a model enzyme for the investigation of thermostabilizing properties of solutes, since denaturation of the enzyme's secondary and tertiary structures is highly reversible, which can be observed by differential scanning calorimetric analysis (Stelea *et al*., 2001). Here, the melting point T_M is determined by a temperature gradient and gives the temperature at which 50 % of the enzyme is denatured. The T_M can be visualized as a peak in heat capacity (Cp) because protein denaturation is an energy consuming process. This well-established setup was used to investigate if synthetic ectoine derivatives homoectoine, ethylectoine and propylectoine show stabilizing properties against heat stress compared to the natural compound ectoine. As a control, other solutes which are known to be stabilizing (TMAO, glycine betaine) or destabilizing (urea) were also tested (Voß, 2002). Furthermore, solutes with one (OH-ectoine, OH-ethylectoine) or more hydroxyl groups (trehalose) were studied as well. A thermostabilizing effect is indicated by increased T_M values of RNase A in the presence of a solute compared to T_M of RNase A in absence of any solute. Figure 32 shows the differential scanning calorimetric analysis of RNase A under the influence of different solutes, all at a final concentration of 1.5 M. T_M of RNase A in pure buffer was 64.90 °C. In the presence of synthetic ectoine derivatives ethylectoine (63.30 °C), homoectoine (61.19 °C) and propylectoine (60.89 °C) the T_M is decreased compared to the T_M of RNase without any solute, meaning that the enzyme was transferred to the denatured state at lower temperatures. However, the use of ectoine (64.79 °C) led to no noticeable shift of T_M. It was observed that T_M values were lower for ectoines with higher hydrophobicity. Propylectoine and homoectoine as the most hydrophobic considered ectoine derivatives showed nearly the same T_M like urea, which is known as a protein denaturing solute.

On the contrary, the use of hydroxylated ectoine derivatives OH-ethylectoine (66.74 °C) and OH-ectoine (68.45 °C) resulted in T_M values which exceeded that of RNase A in pure buffer. The same applies to polyhydroxylated trehalose, showing the highest T_M of 73.67 °C. As expected, glycine betaine and TMAO serving as control solutes showed elevated T_M values of 67.77 °C and 69.72 °C, respectively.

In total, a T_M range of 13.5 °C (from destabilizing to stabilizing solutes) was recorded, considering all solutes. It can be concluded that hydroxylated substances led to thermostabilization of RNAse A, while hydrophobic synthetic ectoines showed destabilizing abilities.

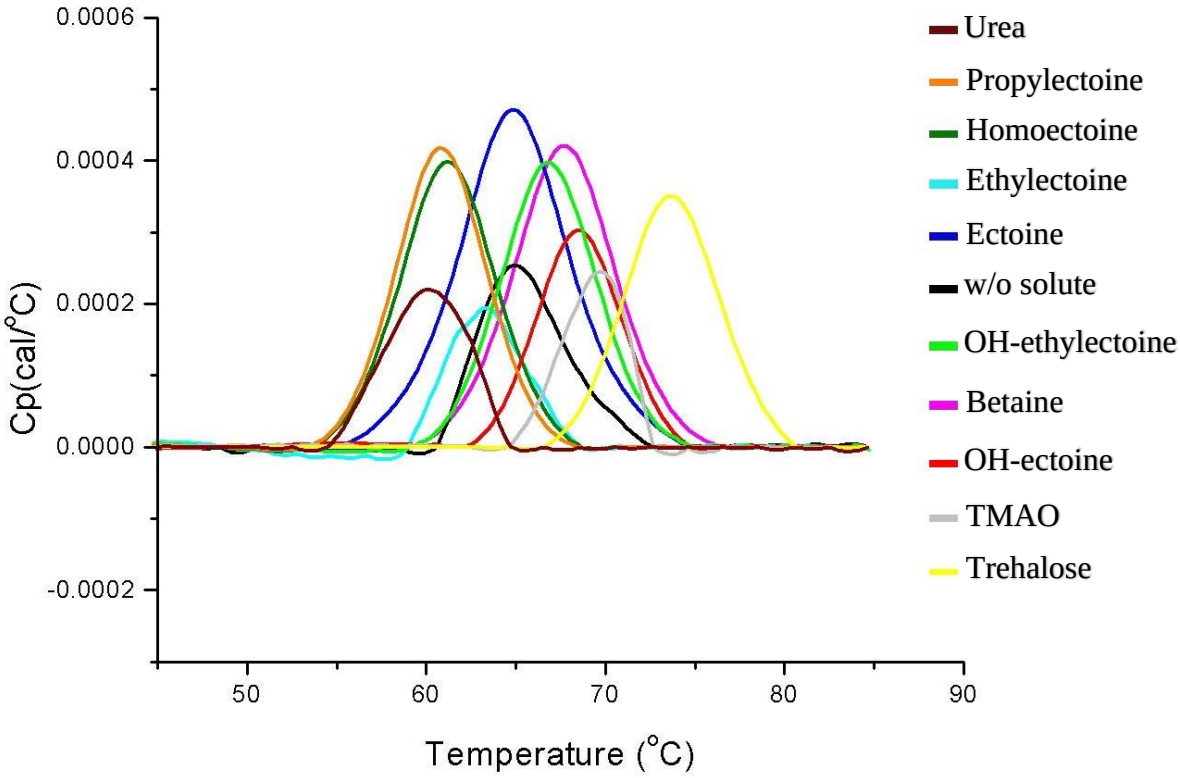

Solute [1,5 M]	T_M [°C]	ΔT_M [°C]
urea	60.03	-4.87
propylectoine	60.89	-4.01
homoectoine	61.19	-3.71
ethylectoine	63.30	-1.6
ectoine	64.79	-0.11
w/o solute	64.90	0
OH-ethylectoine	66.74	+1.84
glycine betaine	67.77	+2.87
OH-ectoine	68.45	+3.55
TMAO	69.72	+4.82
trehalose	73.67	+8.77

Figure 32: Calorimetric analysis of RNase A in presence or absence of different solutes. Melting temperatures (T_M) correspond to peaks during differential scanning calorimetric analysis. Melting temperature changes (ΔT_M) are differences between T_M of RNase A w/o solutes and T_M of RNase A with a specific solute (1.5 M).

3.5.3 Stabilizing properties of ectoines towards freeze-thaw stressed LDH

Another option to investigate protective properties of new synthetic ectoine derivatives is a freeze-thaw stress experiment with the enzyme lactate dehydrogenase (LDH). This enzyme catalyzes the reduction from pyruvate to lactate and simultaneously the oxidation of the cofactor NADH to NAD^+. By performing a photometrical analysis at 340 nm, the decrease of NADH can be monitored during the reaction. For every enzyme known to date, activity decreases over time, especially after exposing to alternating warm and cold temperatures.

In order to verify if the solutes indeed have an impact on LDH activity under freeze-thaw conditions, the enzyme (either in absence of presence of a solute) was frozen in liquid nitrogen and thawed at RT up to eight times. After each freeze-thaw cycle, samples were taken and mixed with an LDH activity assay, in order to calculate residual LDH activity by measuring the decrease of NADH during the enzyme reaction.

Figure 33 shows the residual LDH activity plotted against the number of freeze-thaw cycles. Tested solutes (1 M) were synthetic ectoine derivatives ethylectoine, homoectoine and propylectoine, next to naturally occurring ectoine. Hydroxylated substances OH-ectoine, OH-ethylectoine and trehalose were tested likewise. Glycine betaine and TMAO, known to be stabilizing and non-stabilizing solutes, respectively, were tested as well. As a control, LDH activity was tested in absence of solutes.

The decrease of LDH activity tended to be linear in the course of freezing and thawing. After 7 freeze/thaw cycles, no residual LDH activity could be detected in samples without any solute. Furthermore, the absence of solutes led to an early loss of LDH activity compared to samples with solutes. However, there were significant differences in the ability to maintain LDH activity between the applied solutes. Glycine betaine, known as a poor stabilizer regarding heat/thaw stress (Göller & Galinski, 1999), showed a final residual LDH activity of 16 % which is clearly low compared to the other solutes. A significant increase of LDH stability was achieved by ectoine and its non-hydroxylated derivatives which may be correlated to their enhanced hydrophobicity. There seems to be a tendency for increased stabilization in the order ectoine, ethylectoine, propylectoine and homoectoine. By the use of homoectoine and propylectoine, a residual LDH activity of 56 % and 50 % was calculated after 8 cycles. The less hydrophobic derivatives ethylectoine and ectoine only showed a final residual activity of 45 % and 37 %, respectively. Highly polar hydroxylated or polyhydroxylated solutes most significantly stood out. Especially OH-ectoine (81 %) and OH-ethylectoine (77 %), closely followed by trehalose (75 %) caused the highest residual activity of LDH. This is probably due to their glass-forming abilities, as discussed later on. TMAO, which is known to exhibit protective properties towards

freeze-thaw stress, showed a stabilizing effect similar to the investigated hydroxylated solutes, as the final residual LDH activity in presence of this solute was 74 %.

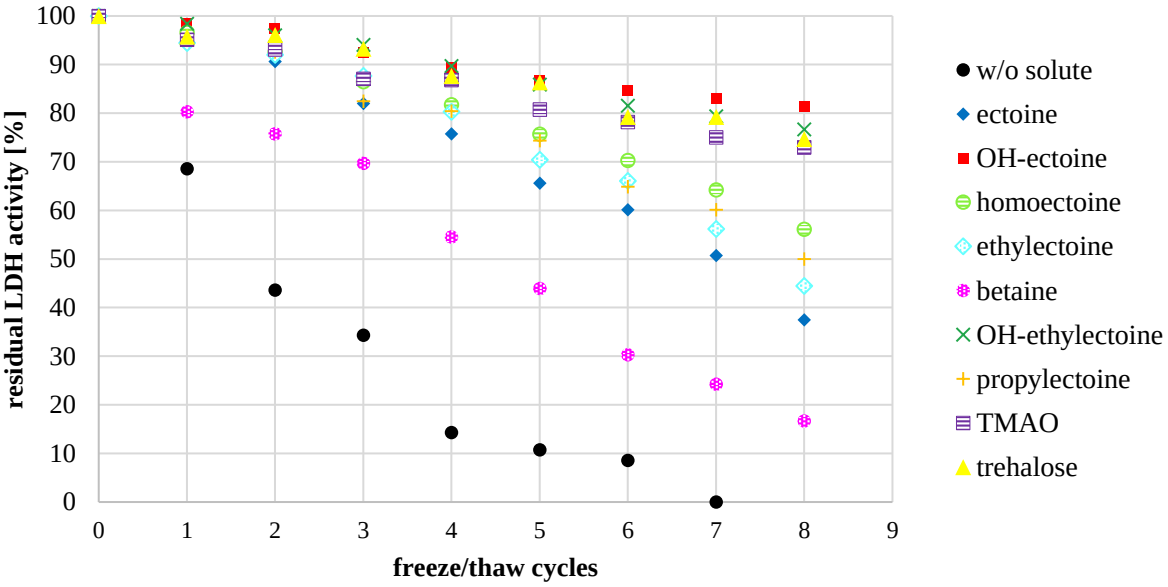

Figure 33: LDH activity after freezing and thawing in presence or absence of solutes. LDH containing samples with or without solutes (1 M) were frozen in liquid nitrogen and thawed at RT. After each cycle, LDH activity was calculated by photometric measurement of NADH decrease at 340 nm.

3.5.4 Impact of solute polarity on protein backbones

The protective effects of compatible solutes on several biomolecules like proteins is very likely resulting from the fact that they are preferentially excluded from the biomolecules surface, leading to a preferential hydration and therefore to stabilization of the molecule. Along with this preferential exclusion theory goes the osmophobic effect, which establishes a relationship between the osmolytes hydrophobicity and the ability to solvate a protein backbone. According to that theory, protecting osmolytes show a minor solvent accessible polar surface area and are therefore preferentially excluded from the protein backbone (1.6).

In order to prove that, transfer energies (ΔG_{tr}) of a protein backbone from water to water/osmolyte solutions were calculated (2.8.3). Diketopiperazine (DKP), which is a cyclodipeptide of two glycines, acted as a protein backbone model and was dissolved either in pure water or in a solution with cosolutes (1 M) until saturation of DKP was reached. If the DKP concentration in solution with a cosolute was higher compared to the DKP concentration in pure water, ΔG_{tr} showed a negative value, meaning that the respective cosolute had a denaturing effect (tab. 20). ΔG_{tr} was plotted against the examined solute's fractional polar

solvent accessible surface areas (SASA), calculated by Pymol software. This relationship was proposed by Street *et al.*, 2006.

As shown in figure 34, TMAO which exhibits very small proportions of polar solvent accessible surface areas showed the highest change of ΔG_{tr} (+92 cal/mol), followed by glycine betaine (+68 cal/mol). It is striking that ΔG_{tr} values decreased with increasing proportions of the examined molecules polar surface areas.

Table 20: Molar change of transfer free energy ΔG_{tr} regarding transition of DKP/2 from pure water into solution with cosolutes. a) Street *et al.*, 2006, b) Voß, 2002.

Solute	Change of ΔG_{tr} (cal/mol)	Reference
TMAO	+92 ± 3	+89 ± 2 [a]; +96 ± 1 [b]
glycine betaine	+68 ± 2	+65 ± 3 [a]; +66 ± 3 [b]
propylectoine	+66 ± 2	
ethylectoine	+62 ± 3	
OH-ethylectoine	+60 ± 3	
ectoine	+58 ± 2	+61 ± 3 [b]
OH-ectoine	+54 ± 3	+55 ± 2 [b]
trehalose	+45 ± 2	+54 ± 8 [a]
homoectoine	+41 ± 2	+42 ± 2 [b]
urea	-36 ± 2	-41 ± 2 [a]; -37 ± 3 [b]

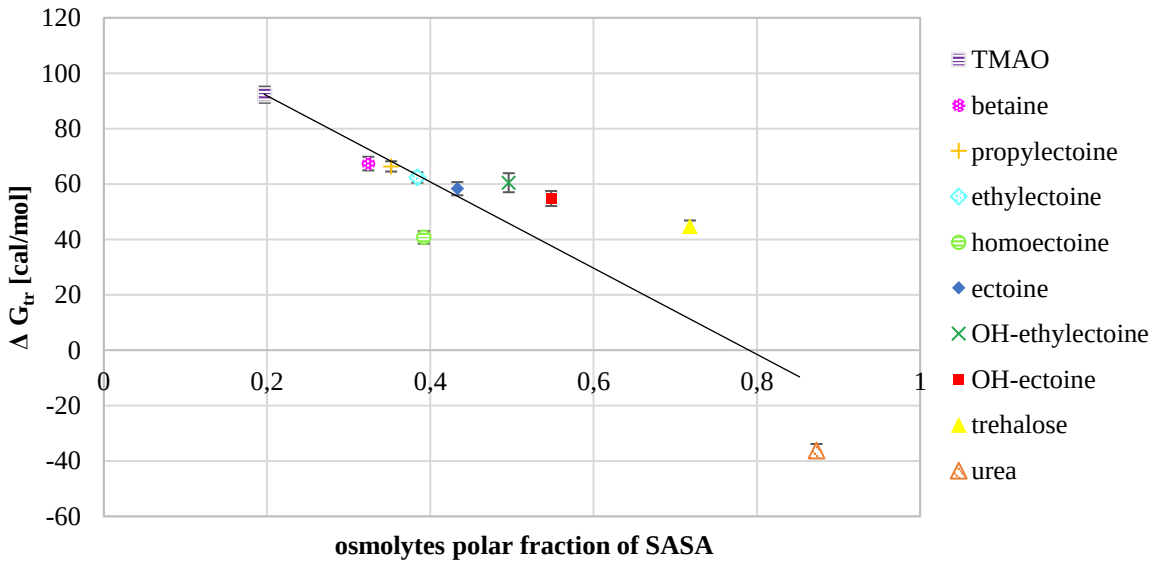

Figure 34: ΔG_{tr} change of DKP/2 in transition of pure water to solution with cosolutes in dependency of fractional polar SASA. ΔG_{tr} values (cal/mol) from table 20 were plotted against the quotient of the solutes polar fractions of SASA and total SASA. The linear regression line shows a coefficient of determination (R^2) of 0.77. Indicated values are arithmetic means and standard deviations were derived from three parallel experiments.

Accordingly, propylectoine (+66 cal/mol) showed a higher ΔG_{tr} compared to ethylectoine (+62 cal/mol) and ectoine (+58 cal/mol). However, homoectoine which has a fractional polar SASA as ethylectoine deviates from a linear relationship. Hydroxylated ectoine derivatives OH-ethylectoine (+60 cal/mol) and OH-ectoine (+54 cal/mol) exhibited lower but rather similar ΔG_{tr} compared to their non-hydroxylated derivatives, although their fractional polar SASA were significantly higher. Urea, which exhibited the highest proportion of fractional polar SASAs was the only considered solvent that led to an increased solubility of DKP compared to pure water, resulting in a negative ΔG_{tr} value of -36 cal/mol.
In conclusion, all solutes except for urea led to a decreased solubility of DKP, and calculated changes of ΔG_{tr} were higher for solutes with small fractional polar SASAs.

3.5.5 Osmoprotective properties of ectoines on whole cells

In order to withstand high osmotic pressure, microorganisms accumulate osmolytes which adjust the intracellular water activity to that of the extracellular milieu. Among the best studied osmolytes are ectoine, OH-ectoine and glycine betaine (Czech *et al*., 2018). In the following it was tested if chemically similar ectoine derivatives show the same or even enhanced osmoprotective abilities on the growth of *E. coli* compared to naturally occurring ectoine. Therefore, *E. coli* K-12 was cultivated in MM63 medium (C-limited) with 3 % and 5 % (w/v) NaCl and supplemented with 2 mM of solutes (fig. 35). Besides ectoine and OH-ectoine, synthetic ectoine derivatives ethylectoine, OH-ethylectoine, homoectoine and propylectoine were investigated. Glycine betaine as a well-known osmostabilizing solute and creatine, known to be an incompatible solute, were tested likewise (Waßmann, 2013).
At 3 % NaCl, *E. coli* was able to grow in the presence of all tested solutes, but there were notable differences in growth. The use of homoectoine and propylectoine showed no improvement compared to cells without any solute. All three cultures showed a lag phase of ~ 4 h, followed by a poor exponential growth phase which ended after ~ 25 h post inoculation. The final OD_{600} of those cultures at stationary phase was ~ 0.35. The use of creatine even impaired growth, since those cultures lacked an exponential and stationary growth phase entirely. With ectoine and ethylectoine, *E. coli* showed improved growth indicated by a clearly noticeable exponential phase ~ 3 h post inoculation. Furthermore, both cultures entered stationary phase earlier than the aforementioned cultures at ~ 20 h and showed a higher final OD_{600} of ~ 0.41. The best results were generated by the use of OH-ectoine, OH-ethylectoine and glycine betaine. Even though these cultures entered exponential phase simultaneously with

cultures supplemented with ectoine and ethylectoine, they showed higher final OD values after entering stationary phase.

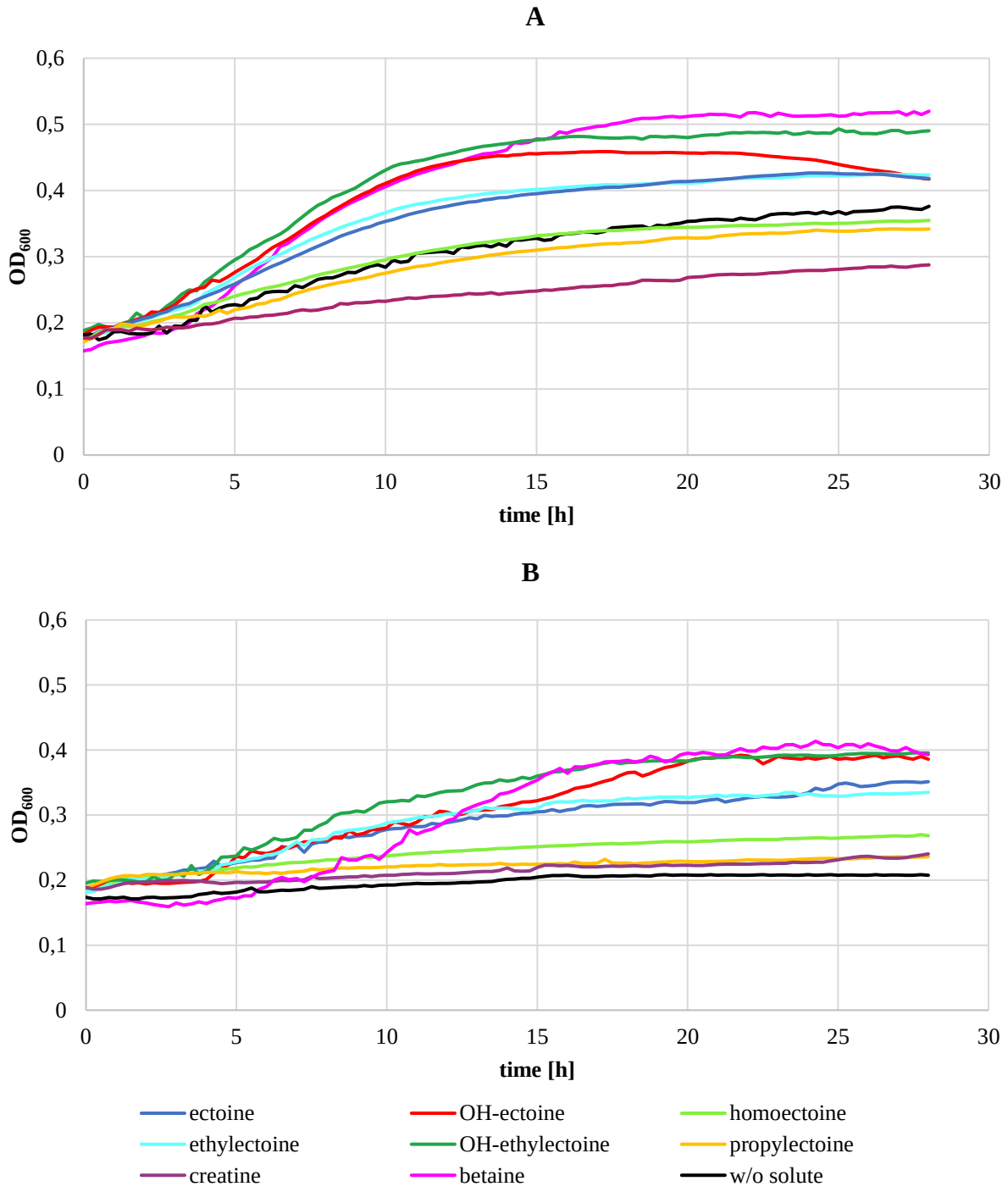

Figure 35: Impact of solutes on growth of *E. coli* under osmotic pressure. *E. coli* K-12 was cultivated in the presence or absence of solutes (2 mM) in MM63 medium (C-limited) with 3 % (A) or 5 % (B) NaCl (w/v) at 37 °C under shaking. Given values are arithmetic means, derived by six parallel attempts. Standard deviations are not shown to provide a clear overview.

In the presence of higher osmotic pressure with 5 % NaCl, no growth occurred in *E. coli* cultures supplemented with propylectoine, creatine or in the absence of any solute. A slight improvement was achieved by the addition of homoectoine, although growth was slow and linear with no distinguishable growth phases. Ectoine and ethylectoine showed improvement regarding growth, since a clear transition to exponential (~ 5 h) and stationary (~ 15 h) phase was noted. The use of glycine betaine, OH-ethylectoine and OH-ectoine showed the most significant improvement again.

Altogether, it can be stated that growth under higher osmotic pressure at 5 % NaCl was impaired in comparison to growth at 3 %. Hydroxylated compounds and glycine betaine most successfully restored growth under these inhibiting conditions.

3.5.6 Protection from cellular desiccation by new ectoine derivatives

Another possibility to characterize new formed ectoine derivatives was to check their potential to protect cells against desiccation stress. Desiccation features a further option to decrease water activity and thus the availability of free water molecules, leading to severe damage of cells and macromolecules like proteins or nucleic acids. In order to examine the effect of compatible solutes towards desiccation of whole cells, *E. coli* K-12 in MM63-1 medium was air-dried in the absence or presence of ectoine and synthetic ectoine derivatives homoectoine, ethylectoine or propylectoine as putative stabilizing solutes. OH-ectoine, OH-ethylectoine and trehalose were also tested in order to investigate whether hydroxylated compounds show a greater stabilizing impact compared to the other tested solutes. Glycine betaine, known to be an effective osmostabilizer, was tested as well. After complete evaporation of culture media at 50 °C, cells were rehydrated with fresh medium, and OD_{600} was measured periodically during shaking cultivation at 37 °C.

Figure 36 represents growth data of rehydrated *E. coli* K-12, after drying in absence and presence of compatible solutes (200 mM). Although *E. coli* showed growth after ~ 16 h in the absence of any externally provided solute, the application of trehalose (~ 5.5 h), OH-ectoine (~ 5 h) and OH-ethylectoine (~ 7 h) led to an earlier entering of the exponential growth phase. Cultures supplemented with the other non-hydroxylated solutes, however, did not show a shortened lag phase. In fact, these solutes were detrimental as no growth was observed within the considered time period of 40 h.

In summary, it can be said that (poly)-hydroxylated solutes protected *E. coli* cells from desiccation, while the tested non-hydroxylated solutes gave no protection.

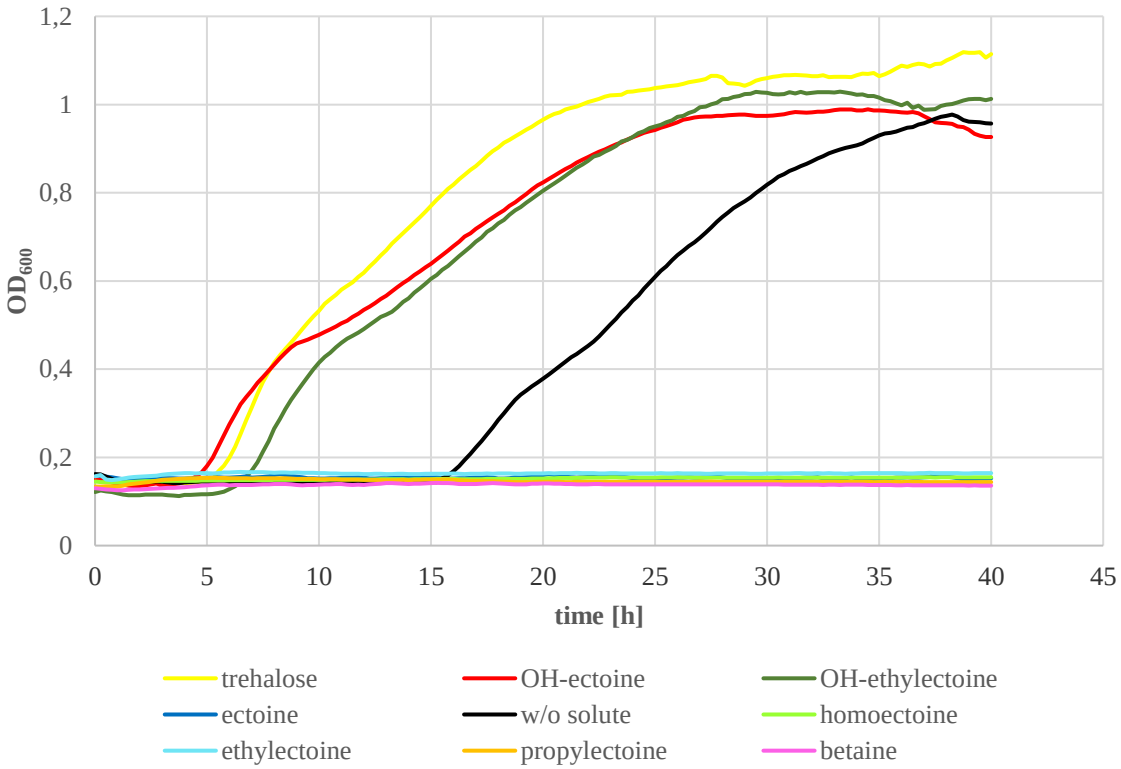

Figure 36: Impact of compatible solutes on growth of *E. coli* after desiccation stress. *E. coli* K-12 cultures in MM63-1 medium (C-limited) were completely air-dried at 50 °C in the presence or absence of compatible solutes (200 mM) and growth was measured after rehydration with fresh medium. Given OD_{600} values are arithmetic means derived by six parallel attempts. Standard deviations are not shown to provide a clear overview.

4 Discussion

4.1 Whole-cell biotransformation: An alternative for the production of hydroxylated ectoines

In recent years, it was shown that OH-ectoine is an effective solute for the stabilization of biomolecules against several stress factors like heat, desiccation or freeze-drying (Knapp *et al*., 1999; Louis *et al*., 1994; Manzanera *et al*., 2002, 2004). OH-ectoin often shows even superior stabilizing abilities compared to ectoine, leading to a growing demand for this compound by industrial branches like the medical, biotechnological or cosmetic industry.

The large-scale production of OH-ectoine is currently carried out by the natural producer *H. elongata* at high saline conditions and elevated cultivation temperatures. The cultivation of this organism at 11 % NaCl (w/v) and 43 °C leads to the accumulation of ~ 50/50 % ectoine/OH-ectoine (Meffert, 2011). These accumulated ectoines can be extracted by an osmotic down shift [2 % (w/v) NaCl], that triggers the transient opening of mechanosensitive channels (Booth & Blount, 2012). The subsequent release of the accumulated solutes into the medium supernatant is known as “bacterial milking” (Sauer & Galinski, 1998). However, the large-scale production of ectoines is now accomplished by a mutant *H. elongata* strain that exhibits deletions in ectoine/OH-ectoine uptake and degradation systems, leading to continuous excretion of these solutes into the medium (Grammann *et al*., 2002; Kunte *et al*., 2014). Even though the NaCl concentration could be lowered and the product titer is no longer depending on intracellular accumulation by using this strain, the production still suffers high purification costs, including chromatographic separation of ectoine and OH-ectoine.

Therefore, the need of alternatives for a cost-effective production of OH-ectoine is evident. At present, it is not possible to chemically produce OH-ectoine due to the unavailability of OH-DABA. There are two alternative biotechnological options for the production of OH-ectoine under low-salt conditions: 1.) The heterologous production of OH-ectoine in non-halophilic organisms (Moritz, 2018, Bethlehem, 2019) and 2.) the conversion of ectoine via a whole-cell biotransformation approach. In this work, the biotransformation approach was investigated by utilizing *E. coli* strains, heterologously producing ectoine hydroxylases. *E. coli* is not only able to take up ectoines naturally via the transporters ProP and ProU, but also intracellularly converts ectoines by heterologously produced EctD proteins and subsequently excretes these products by a so far unknown mechanism, independent of mechanosensitive channels (Jebbar *et al*., 1992; Czech *et al.*, 2016). This in combination with the fact that *E. coli*

is not able to metabolize ectoine or OH-ectoine makes this organism a suitable biotransformation chassis and it already has been used as such in previous studies (Meffert, 2011; Ruprecht, 2014; Brauner, 2016).

An early attempt for the biotransformation of ectoine was the use of *E. coli* DH5α VIBO, heterologously expressing *ectD* of *H. elongata* using the salt-inducible ectoine promotor (*promA*) of *Marinococcus halophilus* (Vielgraf, 2008). The addition of 2 - 4 % NaCl (w/v) induced *ectD* expression and simultaneously enhanced the uptake of ectoine. Meffert (2011) showed, that the use of this *E. coli* strain led to an incomplete conversion of 10 mM ectoine in a C-limited MM63 medium. Since no complete turnover was achieved, it was assumed that *promA* of *M. halophilus* is a relatively weak promotor, resulting in insufficient *ectD* expression. Subsequently, another biotransformation system was constructed by using *E. coli* BL21, a strain that is suitable for overproduction of recombinant proteins, as it is deficient for the major protease Lon and the outer membrane protease OmpT (Marisch *et al*., 2013). By the use of pET-22b(+) plasmid DNA, *ectD* of *H. elongata* was put under control of a strong T7 promoter, whereas production of a genome-coded T7 DNA polymerase was induced by supplementation of IPTG. With this strain, called *E. coli* BL21 pET*ectDHis*, a nearly complete turnover of 10 mM ectoine was achieved, although a relatively high amount of NaCl [3 % (w/v)] was necessary, as well (Meffert, 2011).

While the use of different C-sources, like glycerol or proline, did not improve hydroxylation performance, the study by Ruprecht (2014) showed that 2-oxoglutarate was identified as a bottleneck for the biotransformation in *E. coli*. Therefore, it was a crucial optimization approach to cultivate *E. coli* under N-limiting conditions in order to supply EctD enzymes with the cofactor 2-oxoglutarate over an extended time span. Yan *et al*. (2011) showed that nitrogen limitation with a simultaneous excess of the carbon source is known to increase 2-oxoglutarate levels in *E. coli*. Intracellular 2-oxoglutarate concentrations increase from ~ 0.5 mM in the exponential phase to ~ 4 mM in the stationary phase under N-limiting conditions (Chubukov & Sauer, 2014). The use of customized N-limited MM63 medium by decreasing the N-source (ammonium sulfate) and increasing the C-source (glucose) led to a prolonged hydroxylation process in the stationary growth phase in previous works (Ruprecht, 2014; Brauner, 2016). By this optimization attempt, almost a complete turnover of 10 mM ectoine was achieved, without the need of high NaCl concentrations.

4.1.1 Optimization of whole-cell biotransformation by *E. coli* BL21 pET*ectDHis*

In this work, the focus was initially on hydroxylation optimization of ectoines with *E. coli* BL21 pET*ectDHis*, since this strain was hitherto one of the best performing organisms in recent past. The biotransformation process was carried out under N-limiting conditions, because by that the intracellular concentrations of 2-oxoglutarate are increased and it is possible to analyze the durability of hydroxylases, as no further enzymes are produced in the stationary phase. Also, the hydroxylation reaction was hereby not bound to the formation of biomass, and the excess amount of glucose was now used for the regeneration of 2-oxoglutarate in the stationary phase. On the other hand, growth under N-limiting conditions has the disadvantage that the glucose uptake is significantly reduced. By that, the regeneration of 2-oxoglutarate is limited to the reduced uptake of glucose (Doucette *et al*. 2011).

In a previous study (Brauner, 2016) it was questioned, which factors probably limit the biotransformation process under N-limiting conditions. These factors were: 1.) a reduced glucose uptake rate under N-depletion which limits the regeneration of 2-oxoglutarate, 2.) a competition between ectoines and their hydroxylated derivatives for the uptake system of *E. coli* and 3.) the loss of enzyme activity and/or degradation. Another idea was that the product efflux limits the educt influx and therefore the educt conversion. This can be excluded as a main limiting factor since the hydroxylation with same *E. coli* strains and different hydroxylases result in different product efflux rates (tab. 17).

In this earlier study it turned out that indeed there was a significant decrease of glucose uptake over time (97.9 nmol x min^{-1} x mg^{-1} in the exponential phase and 15.3 nmol x min^{-1} x mg^{-1} in the stationary phase, suppl. fig. 7). In a study of Chubukov & Sauer (2014) a similar glucose uptake rate of 0.46 mmol x h^{-1} x g^{-1} (~ 8 nmol x min^{-1} x mg^{-1}) was calculated. Such discrepancies can be explained by the fact, that in this work the calculation was done with amounts of whole-cell proteins which were derived from directly measured OD_{600} of the culture medium. Based on a glucose uptake rate of 15 nmol x min^{-1} x mg^{-1}, this limits the generation of pyruvate to ~ 30 nmol x min^{-1} x mg^{-1} via glycolysis, and pyruvate is inserted to the TCA cycle by acetyl-CoA formation. The pyruvate conversion rate equals the maximum 2-oxoglutarate conversion rate and therefore limits the maximal ectoine hydroxylation rate when the N-source is depleted. Although the actual ectoine conversion rate (~ 10 nmol x min^{-1} x mg^{-1}) is lower than the pyruvate conversion rate in the stationary phase, a limiting influence cannot be excluded for the biotransformation process.

Furthermore, it was observed that there is a competition between ectoine and OH-ectoine for the uptake in *E. coli*, but ectoine is clearly preferred compared to OH-ectoine. Only if OH-

ectoine concentrations are at least 5 times higher than ectoine, there is a noticeable uptake of OH-ectoine (suppl. fig. 1-3). Nevertheless, the conversion rate of ectoine is still significantly lower than the reduced ectoine uptake under these conditions. Therefore, it is verly likely that the hydroxylase enzyme itself limits the biotransformation process. This is supported by the fact that the ectoine conversion rate is a logarithmical first order process, meaning that the reaction speed is dependent from the stability of the enzyme. If enzymes decay, the reaction speed is not linear but exponentially decreasing. Generally, it can be postulated that the whole-cell biotransformation of ectoines by *E. coli* is limited by the substrate uptake and product efflux rate in the exponential growth phase. In the stationary growth phase, reduced glucose uptake and decreasing EctD enzyme stability over time most probably limit the process.

As a consequence, a possible way to improve the process is to either increase the amount of heterologously produced hydroxylases and/or to produce hydroxylases with a higher durability.

4.1.1.1 The use of poor N-sources

Yet another option to increase intracellular levels of the important cofactor 2-oxoglutarate was the use of different poor nitrogen sources in combination with glucose as the C-source. These N-sources are called “poor” because they cannot directly be assimilated in the nitrogen metabolism. The opposite is true for ammonium, which is directly used for the enzyme reaction of glutamine synthase and glutamate dehydrogenase - essential enzymes in the central nitrogen metabolism (fig. 5; Yan *et al*., 2011). Bren *et al.* (2016) showed that the use of single amino acids like arginine, glutamate or proline as N-sources in combination with glucose as C-source leads to a decreased formation of amino acids/biomass and high intracellular levels of TCA intermediates, especially 2-oxoglutarate, due to nitrogen shortage. On the contrary, fast growth rates of *E. coli* under aerobic conditions are achieved by the use of glucose and ammonium as the C- and N-source, respectively (Reitzer, 2003). Here, concentrations of TCA intermediates (including 2-oxoglutarate) are low because they are rapidly consumed for amino acid biosynthesis, as long as ammonium is available.

In this study, a balanced MM63 medium with poor nitrogen sources in combination with glucose as the C-source was used in order to take advantage of two consequences: 1.) Rapid growth of *E. coli* often is accompanied by incorrect folding of recombinant overproduced proteins. By the use of poor N-sources, the slowed growth could possibly enhance correct folding of heterologously produced EctD. 2.) Although here, the hydroxylation process is limited to C/N depletion, it takes a significantly long time to enter stationary phase. In theory,

E. coli would be able to produce EctD over an extended time compared to the situation when ammonium sulfate is used as N-source.

As seen in figure 15, the growth of *E. coli* BL21 pET*ectDHis* indeed was impaired by the use of arginine ($\mu = 0.031\ h^{-1}$) and glutamate ($\mu = 0.024\ h^{-1}$) as nitrogen sources, compared to the growth with ammonium sulfate ($\mu = 0.87\ h^{-1}$, fig. 16). Although the hydroxylation process was prolonged due to late entering of stationary phase, only 1/3 of the applied 10 mM ectoine was converted. The diminished hydroxylation performance could be the result of several reasons: Compared to the use of ammonia as the N-source, the proportion of correctly folded enzymes was probably increased, while the total amount of enzymes was comparatively low. This might be caused by too high initial concentrations of N-sources or by a non-optimal ratio of C/N-sources. In a work of Bhattacharya & Dubey (2008), the heterologous expression of *mspI* (DNA methyltransferase) in *E. coli* was strongly dependent not only on the choice of the N-source and its initial concentration but also on the C/N ratio.

In my work, a C/N ratio of 8/1 was applied, because this ratio is necessary for a balanced medium, but according to the results of Bhattacharya & Dubey, this ratio is unfavorable for heterologous gene expression compared to a ratio of 15/1. Since no SDS-PAGE of whole cell proteins was performed in this work, a reduced amount of EctD can only be assumed, but it would be interesting to repeat this experiment and to test different C/N ratios with a subsequent SDS-PAGE analysis.

It is conceivable that glucose uptake was impaired by the use of poor N-sources. 2-oxoglutarate, which is available in high amounts when poor nitrogen sources are used, is capable of blocking glucose uptake by inhibiting the PtsI protein, which is the first involved enzyme of the phosphotransferase system (Bren *et al.*, 2016; Doucette *et al*., 2011). PtsI catalyzes the dephosphorylation of phosphoenolpyruvate (PEP) to pyruvate, initiating a cascade of phosphate group transfer that ultimately leads to the phosphorylation and uptake of glucose. If this cascade is impaired by 2-oxoglutarate which competes with PEP for the PEP binding site of PtsI, glucose uptake will also be impaired. It is true that high intracellular 2-oxoglutarate concentrations are also available by using N-limited MM63 medium with ammonia as N-source, but 2-oxoglutarate levels only rise when the N-source is depleted (Yan *et al*, 2011).

Therefore, it is likely that the key for an effective hydroxylation process is not the availability of excessive amounts of the cofactor 2-oxoglutarate, but the general availability of this substrate over an extended time period. This is only given under N-limiting conditions, as the regeneration of 2-oxoglutarate depends on the availability of glucose. By the use of a C-limited MM63 medium, the hydroxylation of 10 mM ectoine is terminated prematurely and incomplete,

as the glucose is consumed significantly earlier (~ 8 h) compared to the loss of EctD enzyme activity over time (Meffert, 2011; Ruprecht, 2014).

Furthermore, a reduced glucose uptake results in perturbations of global metabolic networks, as transcriptome analyses of *E. coli* showed (Jung *et al*., 2019). Such perturbations also negatively affect ATP generation, which probably also affects the ATP-dependent uptake of ectoine via ProP. Therefore, the potentially reduced ectoine uptake in the stationary phase may also be a possible limiting factor for this hydroxylation process.

Another important result was, that the final OD_{600} of *E. coli* growing on poor N-sources was comparatively high. High cell densities implicate reduced O_2 contents in media of shake flask cultures. Since EctD-mediated hydroxylation is an O_2 dependent process, this might be another bottleneck for that attempt. In this experiment, the final measured OD_{600} values were ~ 2 for cultures supplemented with both arginine or glutamate. Since the OD was determined by direct measurement of undiluted culture media, real OD values were probably even higher. Vasala *et al*. (2006) showed that an OD_{600} of 2 for *E. coli* in a 1 L shaking flask with 200 ml medium, which approximately corresponds to the applied ratio of culture media to the vessels volume in this work, already results in a significant drop of O_2 over time.

In order to identify these possible bottlenecks, further experiments like an SDS-PAGE analysis of whole cell proteins at different times, the determination of glucose/ectoine uptake rates (2.5.6.3) and the measurement of the mediums O_2 partial pressure would be appropriate.

4.1.1.2 Different C/N ratios vs induction parameters

Even though the use of poor N-sources was a promising attempt for an improved hydroxylation performance, ammonium sulfate turned out to be more effective under the given conditions. In order to further improve hydroxylation of ectoines in *E. coli* BL21 pET*ectDHis*, $(NH_4)_2SO_4$ was used as N-source, but different ratios of C-source (glucose) and N-source were tested. Furthermore, it was aspired to improve the induction of *ectD* by the application of varying concentrations of the inductor IPTG at different growth phases. As the sufficient amount of the essential cofactor 2-oxoglutarate turned out to be a key aspect, different ratios of glucose and ammonium sulfate were chosen in a way that a N-limitation was available in every approach. Therefore, C/N ratios of 34/1 and 17/1 (with 10 g/L glucose as reference) were tested, whereas induction was performed either at an OD_{600} of 0.3 or 0.6 with 0.1 mM or 0.5 mM IPTG. Results clearly showed that an application of 0.5 mM IPTG did not improve hydroxylation, but that the most efficient transformation could be achieved with 0.1 mM IPTG and a C/N ratio of 17/1 (fig. 16). In contrast to that, the combination of 0.1 mM IPTG and a C/N ratio of 34/1 resulted

only in a moderate hydroxylation performance. Induction at OD 0.3 or 0.6 approximately resulted in the same hydroxylation course, indicating that at least these two tested OD values have no great impact on *ectD* expression.

As discussed earlier (4.1.1.1), the initial concentration of the C- and the N-source as well as the C/N ratio is essential for a high-level expression of a heterologous gene in *E. coli*. The working group of Bhattacharya *et al*. (2008) showed that too high or low concentrations of the C- and N-source, as well as too high or low C/N ratios result in a decreased rate of target gene expression, a loss of plasmid copy number, and thus a loss of the desired recombinant proteins. They showed that glucose as the C-source and $(NH_4)_2SO_4$ or glycine as the N-source in M9 minimal medium were most efficient for heterologous gene expression. More interestingly, they showed that 10 g/l glucose and a C/N ratio of 15 was optimal which are remarkably similar values compared to those generated in this work (fig. 16).

Concerning induction, too high concentrations of IPTG can result in the formation of inclusion bodies due to protein misfolding (Donovan *et al*., 1996), whereas the application of too low IPTG concentrations probably entails a weak gene expression. Figure 16 shows that *E. coli*, induced with 0.5 mM IPTG, showed a reduced growth rate (~ 0.6 h^{-1}) compared to those induced with 0.1 mM IPTG (~ 0.8 h^{-1}). This suggests that an enhanced EctD production was indeed triggered by the induction with the higher amount of IPTG. As, however, induction with 0.5 mM IPTG tended to result in weaker hydroxylation, it can be assumed that a major proportion of EctD aggregated. Donovan *et al*. (1996) showed that a reduced IPTG induction can lead to an increase in proper folding of proteins due to a lower transcription rate. *E. coli* BL21, like many B-strains, is known for its fast growth (Luli & Strohl, 1990) which is accompanied with high transcription and translation rates. The use of this *E. coli* strain in combination with a strong T7 promoter of the applied pET-22b(+) vector probably lead to an uncontrolled and incorrect EctD formation at high concentrations of IPTG. A common method to avoid this is to reduce the incubation temperature after induction, leading to decreased growth rates and therefore to an improved performance of recombinant gene expression (Farewell & Neidhardt, 1998). In a previous work, the induction temperature already was reduced to 32 °C, the optimum of EctD of *H. elongata*, which indeed was shown to be beneficial compared to 37 °C, the temperature optimum of *E. coli* (Ruprecht, 2014). Even lower temperatures were tested as well, but 32 °C turned out to be most beneficial.

4.1.1.3 NaCl dependency

E. coli as a halotolerant organism shows optimal growth at low salt conditions (0 – 1 %, w/v, depending on the media composition). Nevertheless, *E. coli* is capable of taking up ectoine even at 1 % NaCl (w/v), which was surprising (Ruprecht, 2014). Therefore, the biotransformation process can be carried out at low salt concentrations, which reduces costs for the purification of hydroxylated ectoines from the medium. Hydroxylation via whole-cell biotransformation requires certain NaCl concentrations because ectoine uptake is linked to osmotic pressure. In a previous study, Meffert (2011) showed an increased hydroxylation performance in *E. coli* BL21 pET *ectDHis* at relatively high NaCl concentrations (3 %, w/v). This work should again elucidate the impact of osmotic pressure on the ectoine biotransformation system, taking optimization of C/N sources and induction conditions into account. Thus, hydroxylation performance was tested in the presence of 1 % or 3 % NaCl (w/v) and 10 mM - 30 mM ectoine. As shown in figure 17, hydroxylation speed and total conversion was slightly improved in presence of 3 % NaCl (~ 500 mM) compared to cultures supplemented with 1 % NaCl (~ 117 mM). This finding can be explained by the enhanced ectoine uptake at high osmotic pressure (Jebbar *et al*., 1992), and a probably higher intracellular concentration of NaCl that favours EctD activity (Widderich *et al*., 2014). Generally, increasing external concentrations of NaCl are accompanied by a rise of intracellular concentrations of this salt, as flux analyses performed by Shabala *et al*. (2009) indicated. According to their study, external NaCl concentrations of ~ 100 mM and 350 mM resulted in the accumulation of ~ 8 mM and 100 mM NaCl, respectively, if no external compatible solute is provided. Intracellular concentrations of 50 - 100 mM NaCl would be beneficial for the hydroxylation process, as *in vitro* studies revealed highest activity for EctD of *H. elongata* under this condition (Widderich *et al*., 2014). Therefore, it is possible that the whole-cell biotransformation of ectoine is improved at 3 % NaCl due to higher intracellular amounts of NaCl. However, it is unclear how the NaCl influx is changed in presence of ectoine. The results of Jebbar *et al*. (1992) indicate, that the growth of *E. coli* is impaired at 3 % NaCl even in the presence of ectoine. It can be assumed that ectoine is not sufficient to generate an osmotic equilibrium, causing elevated intracellular NaCl concentrations.

In an earlier work it was shown that with both substances available, *E. coli* prefers the uptake of ectoine over OH-ectoine (Brauner, 2016; suppl. fig. 1-3; suppl. tab. 2). Only in the late phase of the hydroxylation process, when most of the ectoine is converted to hydroxyectoine and excreted into the medium, a competition between the substrate and the product for uptake becomes relevant. Therefore, it is conceivable that an elevated osmotic pressure favors the

uptake of ectoine in a late biotransformation phase compared to cultivation at lower NaCl concentrations. Nevertheless, the impact of higher NaCl concentrations were comparatively low, which is why following experiments in this work were carried out using 1 % NaCl (w/v). The use of low salt concentrations is advantageous for the large-scale production of OH-ectoine, as high salinity increases reactor corrosion and complicates downstream processing (Schubert *et al*., 2007).

4.1.2 Hydroxylation of synthetic ectoine derivatives by *E. coli* BL21 pET*ectDHis*

In previous studies it was shown, that EctD of *H. elongata* exhibits substrate ambiguity, meaning that ectoine but also other substrates with structural similarity are recognized by this enzyme (Witt, 2011; Meffert, 2011). As ethylectoine and propylectoine only show minor structural differences to ectoine in length of the alkyl groups, hydroxylation of these substances was tested by whole cell biotransformation with *E. coli* BL21 pET*ectDHis* in this work. The successful whole-cell biotransformation of homoectoine, exhibiting an enlarged ring size, was already shown in previous studies (Vielgraf, 2008; Meffert, 2011; Ruprecht, 2014).

Figure 18 shows that all tested solutes were taken up by *E. coli*, as substrate concentration in the supernatant continuously decreased over time. The identification of intracellular accumulated solutes via B&D extraction and HPLC analysis was later carried out in another experiment using *E. coli* DH5α (fig. 24). Although all tested solutes were taken up by *E. coli* BL21 pET*ectDHis*, hydroxylation performances differed significantly. To evaluate this in more detail, substrate influxes and product effluxes in the early biotransformation process were estimated. Looking at the efflux rates of OH-ectoine and OH-homoectoine, it seems that ectoine was converted a little more effectively than homoectoine. On the other side, looking at the influx rates, homoectoine was taken up much faster compared to ectoine. These results may appear contradictory but can be explained by the structural instability of OH-homoectoine. In previous works, the disintegration of OH-homoectoine into the open chain molecule 3-Hydroxy-Nδ-acetylornithine was observed during whole-cell biotransformation of homoectoine (Ruprecht, 2014; Molitor, 2015). It is unknown if this open ring form acts as an osmolyte or if it is metabolized by the cells over time. If the latter is the case, the efflux of OH-homoectoine and the simultaneous intracellular decay of this molecule probably leads to an increased influx of the substrate homoectoine until cellular saturation is reached again. It is also conceivable, that the lower product concentration in the medium simultaneously favours the export of the product and the import of the substrate.

The conversion of ethylectoine and propylectoine was significantly reduced, compared to ectoine. The impaired hydroxylation of these synthetic ectoine derivatives might be explained by two reasons: 1.) substrate influx or product efflux or both might be reduced or 2.) the enzymatic conversion rate is diminished for these solutes. This work showed that a reduced influx of these solutes cannot be the reason for the impaired hydroxylation performance of ethylectoine and propylectoine, as the analysis of maximal substrate uptake rates revealed the approximate same uptake speed for all tested solutes (fig. 24). Instead, *in vitro* studies showed that hydroxylation of ethylectoine indeed is diminished due to reduced enzymatic turnover, as V_{max} and K_{cat} values were significantly lower for this solute compared to ectoine (tab. 19). V_{max} and K_{cat} values could not be generated for propylectoine as the turnover could only marginally be detected by the applied assay conditions (data not shown). *In silico* modelling and docking analysis, which were carried out with EctD of *S. alaskensis*, showed that propylectoine only barely fits into the active site of EctD (Czech, personal communication). *In vitro* studies also showed that homoectoine indeed is not converted quicker than ectoine by EctD of *H. elongata*, even though early homoectoine influx rates during whole-cell biotransformation were higher compared to those of ectoine (fig. 18, tab. 16). These findings support the hypothesized accelerated uptake of homoectoine due to the decay of OH-homoectoine over time.

Since the whole-cell biotransformation of ethylectoine and propylectoine was comparatively low, the amount of EctD must be increased in order to raise the conversion of these solutes. One option to raise the concentration of EctD was to concentrate cells. This was done by resuspending cells 4 h after induction into 1/10 of the initial culture volume. By doing so, cells as well as heterologously produced EctD enzymes were concentrated 10-fold, and ethylectoine/propylectoine was added afterwards. Although an approximate 10-fold increase was expected, the actual improvement was only a 4-5-fold increase of converted substrates compared to not concentrated cultures (fig. 19 + 20). This may be the resulted from two reasons: First, it is possible that the concentration of culture media 4 h after induction was too early to exploit the complete potential of EctD production, whereby the number of enzymes was not 10-fold the number of non-concentrated media. *E. coli* was unable to produce more EctD after the concentration step, because this medium did not contain N-source in order to achieve high intracellular 2-oxoglutarate levels. Secondly, the concentration of culture media could have led to an insufficient O_2 partial pressure due to high cell density. EctD as a dioxygenase is dependent on O_2, and a lack of it would impair the hydroxylation process as previously described (Vasala *et al*., 2006; 4.1.1.1). Since no O_2 probe was used, a repetition of this experiment in a bioreactor with controlled conditions regarding O_2 partial pressure would

clarify this hypothesis. Nevertheless, by the approach of a media concentration the conversion of 20 mM ethylectoine and 5 mM propylectoine was achieved which is a significant improvement.

4.1.3 The impact of different ectoine hydroxylases and *E. coli* strains on whole-cell biotransformation

Although hydroxylation is not limited to the exponential growth phase due to N-limiting cultivation conditions, the exponential decrease of the hydroxylation reaction over time (first order enzyme reaction) suggests enzyme instability of EctD of *H. elongata* (fig. 18). For this reason, different hydroxylases including those of *A. cryptum*, *P. stutzeri* and *S. alaskensis* were tested in whole-cell biotransformation experiments by heterologous expression in *E. coli* BL21(DE3) as well as in *E. coli* DH5α.

4.1.3.1 *E. coli* BL21 vs. *E. coli* DH5α as *ectD* expression strains

Initially, the whole-cell biotransformation of ectoine was accomplished by heterologously expressing the four hydroxylases each in *E. coli* BL21(DE3). Best results were attained with strains expressing *ectD* of *S. alaskensis* and *A. cryptum*, as the conversion of ectoine was faster and showed only a minor decrease over cultivation time. With these two strains, the conversion of ~ 15 mM ectoine was achieved, which is a moderate improvement considering that here no elevated NaCl concentrations were applied in order to increase the turnover as previously described (fig. 21). Strains, expressing *ectD* of *P. stutzeri* and *H. elongata* were less effective since ectoine conversion rates were lower and decreased earlier to a greater extent, compared to the other two strains.

By the use of *E. coli* DH5α, the whole-cell biotransformation process was further improved, and again the use of EctD of *S. alaskensis* and *A. cryptum* led to outstanding performance results (fig. 22, tab. 18). Although no optimization attempts regarding induction parameters or the choice of media were carried out in the first place, a complete conversion of the applied 20 mM ectoine was achieved by these two strains through cultivation at 35 °C. This indicates, that the hydroxylation efficiency is highly dependent on the choice of *ectD* and the expression host.

The results raise two questions: 1.) What are possible causes for different hydroxylation efficiencies when different EctD enzymes are used? 2.) Why was the use of *E. coli* DH5α preferable compared to *E. coli* BL21(DE3)?

In previous studies, Czech *et al*. (2016) also showed substantial differences in the efficiency of the whole-cell biotransformation of ectoine in *E. coli* when different EctD enzymes were used. It can be hypothesized that such discrepancies are related to the ion pool of the *E. coli* cytoplasm, since small but noticeable variations in response to salts (KCl, NaCl) have been reported for different EctD enzymes in the course of EctD *in vitro* analyses (Widderich *et al*., 2014, 2016). Although this might be a contributing factor, the primary reason for the differential hydroxylation performance is likely based on enzyme stability. Widderich *et al*. (2014) showed that the four enzymes used in this work exhibit different stabilities towards high temperature, giving hints of general stability. According to that study, EctD of *H. elongata* was the most labile enzyme, whereas EctD of *S. alaskensis* showed to be one of the most stable ones. Indeed, whole-cell biotransformation was most ineffective/effective by the use of EctD of *H. elongata* and *S. alaskensis*, respectively. In order to verify if the decrease of substrate conversion is caused by decreasing enzyme activity or enzyme degradation, an SDS-PAGE analysis was carried out. It was shown that the different hydroxylation performance by the use of different hydroxylases was indeed caused by enzyme degradation over time in *E. coli* DH5α (fig. 25, 26).

However, it is still questionable why hydroxylation performance was beneficial in *E. coli* DH5α. By looking at the time course of different hydroxylation processes of the *E. coli* DH5α and BL21 expression strains, it is striking that EctD enzymes produced in BL21 seemed to be active for a longer period of time, whereas conversion rates at the beginning of the process was faster in DH5α (fig. 21, 22). Thus, it is possible that DH5α strains were able to produce more correctly folded EctD, with a decreased stability compared to those produced in BL21. This would explain the initially higher conversion rates and the early decrease of ectoine conversion in DH5α compared to BL21. An additional SDS-PAGE analysis of samples from *E. coli* BL21 would be interesting to prove if EctD degradation is delayed in this strain compared to *E. coli* DH5α. Basically, *E. coli* BL21 is a strain that is suitable for the stable production of recombinant proteins, due to its deficiency for the major protease Lon and the outer membrane protease OmpT (Marisch *et al*., 2013). *E. coli* DH5α, on the contrary, is rarely utilized in production processes as its genome exhibits several mutations affecting metabolism and cell growth. This strain is typically used for DNA preservation because of its deficiency for the recombinase RecA and the endonuclease EndA1, preventing plasmid DNA recombination and increasing plasmid stability (Casali, 2003).

It cannot be predicted whether a recombinant protein will be properly folded and functional or nonfunctional as an inclusion body. Although *E. coli* BL21 is engineered for protein expression

purposes, the combination with a high copy vector (pET-22b) and a strong promoter (T7) often leads to excessive metabolic stress of the host cells and consequently to a loss of effective protein production or protein folding (Hoffmann & Rinas, 2004). Furthermore, the T7 RNA polymerase exhibits an average elongation rate of 200 – 400 nucleotides per second which is ~ five times the activity of the *E. coli* host RNA polymerase (Golomb & Chamberlin, 1974; Vogel & Jensen, 1994). The resulting high transcription rates are often negatively correlated with the solubility and proper protein folding (Donovan, 1996).

On the contrary, *E. coli* DH5α is a comparatively slowly growing strain which generally does not exceed growth rates over 0.3 h^{-1} in MM63 medium (Bethlehem, 2019). At slow growth conditions, all cell processes, including transcription and translation are also slowed down and proteins have more time to fold properly (Sorensen & Mortensen, 2005). Transcription rates of *ectD* were probably relatively low in *E. coli* DH5α as the genes were under control of a weak *tet* promoter, which contributes to a proper protein folding. It seems that these conditions were generally beneficial for the whole-cell biotransformation process.

4.1.3.2 Substrate ambiguity of EctD: *In vitro* vs *in vivo* studies

Whole-cell biotransformation studies in this work revealed that substrate ambiguity is not a unique feature of EctD of *H. elongata*, as all four tested recombinant hydroxylases were also able to recognize and convert ethylectoine, propylectoine and homoectoine (fig. 23, tab. 19). In a recently published study by Czech *et al*. (2019) it was shown that homoectoine is converted *in vitro* and *in vivo* by EctD of *P. stutzeri* and *S. alaskensis*. Therefore, it was reasonable that substances with structural similarity to ectoine were recognized by these enzymes, as well. The biotransformation efficiency of ethylectoine and propylectoine was reduced compared to ectoine irrespective of the specific overproduced EctD enzyme or the *E. coli* host strain (fig. 18, 23, tab. 16 - 18). In order to evaluate if differential hydroxylation performances of ectoine and synthetic ectoine derivatives are based on the activity of the different enzymes, *in vitro* studies were carried out for the considered hydroxylases and substrates (tab. 19). It is difficult to directly compare *in vitro* activities of these enzymes due to required optimization for every enzyme. Some optimization attempts were already accomplished, including the temperature, pH, the choice and concentration of a salt (e.g. NaCl, KCl) and the amount of the cofactors Fe^{2+} and 2-oxoglutarate (Widderich *et al*., 2014). Nevertheless, the effectivity of EctD is probably dependent on several further components which are intracellularly regulated. Catalase, for example, can reduce damaging effects of reactive oxygen species which are produced during the reaction of non-heme iron(II) containing oxoglutarate-dependent dioxygenases like EctD

(Herr & Hausinger, 2018). In case of EctD activity of *S. alaskensis*, the presence of catalase is even essential for *in vitro* activity (Czech *et al*., 2019). Thus, *in vitro* studies only give hints to EctD-mediated substrate conversion *in vivo*, since the applied assay conditions do not necessarily correspond to intracellular conditions of *E. coli*. In this work, the same assay conditions were applied for each enzyme except for the incubation temperatures, which corresponded to the postulated optimal temperatures (Widderich *et al*., 2014). As a consequence, it was still possible to directly compare the conversion effectivities of the different substrates for the respective enzymes.

Comparing the V_{max} and K_{cat} values, it can be stated that the conversion of the respective substrates was similar for all investigated enzymes (tab. 19). In the work of Widderich *et al*., the considered hydroxylases showed V_{max} (1 – 6 U/mg) and K_{cat} (1.2 – 8.9 s^{-1}) values for ectoine within the same range as it was shown in this work (suppl. tab. 3). Czech *et al*., 2019, on the other hand, showed that V_{max} of ectoine and homoectoine for EctD of *P. stutzeri* was 23.5 U/mg and 67.2 which is significantly higher than the values, generated in this work. It is unlikely that synthetical homoectoine is converted more rapidly than the natural substrate ectoine, which makes the results of Czech *et al*. questionable. In order to verify the results, it is necessary to repeat this *in vitro* experiment.

In this work, the highest V_{max} and K_{cat} values were generated by the use of ectoine, the natural substrate of EctD, for all considered enzymes (tab. 19). V_{max} and K_{cat} values were significantly lower for the synthetical ectoine derivatives because these substrates do not fit well into the enzymes active site as *in silico* modelling and docking analysis showed (Czech, personal communication). The only exception was EctD of *A. cryptum* which showed comparatively low V_{max} and K_{cat} values for all considered substrates. These results were unexpected, since this enzyme was one of the most efficient ones during whole-cell biotransformation (fig. 21-23). It was hypothesized that the whole-cell biotransformation by *E. coli* DH5α pASK *ectD_Acry_Strep* was so effective because the total amounts of this recombinant enzyme were relatively high (suppl. tab. 1). Thus, its low enzyme activity would have been compensated. This was already suggested by SDS-PAGE analyses of the whole-cell proteins (fig. 25). In order to prove that, 100 mg of purified whole-cell proteins from all four *E. coli* DH5α biotransformation strains were further purified via Strep-tag affinity chromatography, and again analyzed via SDS-PAGE (fig. 26). The results indicate that EctD of *A. cryptum* was available to a much higher extent compared to EctD of the other three organisms. Additionally, it was shown again that EctD of *A. cryptum* and *S. alaskensis* was more stable over time than EctD of

P. stutzeri. Unfortunately, it was not possible to detect EctD of *H. elongata* after Strep-tag purification, probably because of a failed purification approach.

The differences in heterologous enzyme production could be explained by different translation rates due to different ribosome binding site sequences (Salis *et al*., 2009; Borujeni *et al*., 2014). This computer-based calculation of translation initiation rates is a useful method to estimate heterologous protein production efficiency. The translation initiation rate is a rate-limiting step in protein production from mRNA. Indeed, predicted translation initiation rates were highest for EctD of *A. cryptum* (~ 520,000) compared to EctD of *H. elongata* (~ 140,000), *P. stutzeri* (~ 180,000) *S. alaskensis* (~ 150,000).

Regarding this information, it can be concluded that the most efficient whole-cell biotransformation performances were achieved with *E. coli* strains that produced durable enzymes in high amounts, which was true for *E. coli* DH5α pASK *ectD_Acry_Strep* and *E. coli* DH5α pASK *ectD_Sala_Strep*.

4.1.3.3 Constant whole-cell biotransformation at low temperatures

In a last attempt to further optimize whole-cell biotransformation, hydroxylation experiments were performed different cultivation temperatures. Optimal temperatures for all considered EctD enzymes ranged between 30 °C and 35 °C, except for EctD of *S. alaskensis*, exhibiting an optimum at 15 °C *in vitro* (Widderich *et al*., 2014; Czech *et al*., 2019). EctD of *S. alaskensis* heterologously produced in *E. coli* DH5α was outstanding due to high stability over time, although cultivation at 35 °C exceeded the enzyme's optimum by far. Another whole-cell biotransformation approach testing both temperatures was carried out with this strain. As a result, it could be shown if lower temperatures are potentially beneficial for the biotransformation process using this psychrophilic enzyme. *E. coli* shows a high content of non-translating ribosomes at 15 °C, leading to a decrease in cell growth and to a defect in the translation initiation phase (Farewell & Neidhardt, 1998). Therefore, cells were incubated at 35 °C until stationary phase was reached before lowering the temperature to 15 °C. As shown in figure 27, control cultures constantly incubated at 35 °C were able to completely convert the applied 30 mM ectoine, which is a 3-fold increase compared to the starting situation of this work. Despite this increase on hydroxylation performance, a decrease of hydroxylation performance over time was recognized. In contrast, the conversion of ectoine by cultures incubated at 15 °C exhibited a constant hydroxylation rate after reaching the stationary phase for the whole considered time of ~ 120 h. This shows that enzyme stability could indeed be further enhanced at this lower, optimal temperature, enabling an extension of the

biotransformation process. Even higher concentrations than 30 mM of substrate could possibly be converted by this approach, which needs to be verified in future experiments. Nevertheless, figure 27 also shows that hydroxylation speed is significantly slower at 15 °C compared to 35 °C. This could be caused by a potential lower uptake of C-source (glucose) or ectoine. In a study by Nedwell (1999) it was shown that temperatures below growth optimum decreases the efficiency of transport proteins embedded in the membrane of microorganisms. This effect is probably caused due to stiffening membranes lipids at low temperatures. Thus, it is conceivable that the affinity of ProP/ProU for ectoines is decreased at low temperatures, leading to an impaired uptake of these solutes. The group of Gadgil *et al*. (2008) furthermore showed that a temperature shift from the growth optimum of *E. coli* to lower temperatures results in the down-regulation of genes involved in glycolysis and the phosphotransferase system that mediates glucose uptake. The reduced uptake of glucose can further affect the regeneration of 2-oxoglutarate which is essential for EctD activity. In order to verify these potential bottlenecks, it would be necessary to determine uptake rates of glucose and ectoine at low temperatures.

Further approaches to optimize the biotransformation process at low temperatures could include the use of a different *E. coli* strain, called "ArcticExpress", which co-expresses cold-adapted chaperonins Cpn10 and Cpn60 from *Oleispira Antarctica*. These chaperonins exhibit high protein refolding activity at low temperatures and therefore contribute to improved protein processing at lower temperatures. This strain in combination with *ectD* of *S. alaskensis* coded on a pCold expression vector could probably further improve whole-cell biotransformation at low temperatures, as these vectors contain a cold-shock protein A (*cspA*) promoter. By a cold-shock at 15 °C, target protein synthesis can be induced and the expression of host proteins as well as protease activity is simultaneously decreased, resulting in high yields of active recombinant proteins (Hartinger *et al*., 2010).

4.2 Production and purification of hydroxylated ectoine derivatives

Since it was shown that ethylectoine is taken up and converted by EctD to OH-ethylectoine (fig. 18, 23, tab. 19) this solute was produced and purified in large amounts in order to identify and characterize its putative stabilizing traits. There were two options to purify this solute: As *E. coli* was not only able to take up ethylectoine but also to excrete OH-ethylectoine, one option was to purify it from the media supernatant. A second option would be the extraction of the solute from the cells. Both options have advantages and disadvantages.

During purification from the media supernatant, the number of different contaminants is usually relatively small, as the main contaminants are media components (salts). These relatively high

salinities are simultaneously a disadvantage in the course of purification and require a desalination by ion retardation chromatography. Nevertheless, only small sample volumes (~ 30 ml) are properly separable on a lab scale column volume of 2 L, and every approach takes approximately 3 – 4 h, making this a very time-consuming process for the purification. An alternative to reduce the duration of desalination would be the concentration of the media supernatant by evaporation. However, this strategy is limited to the volume, at which media components and solutes precipitate. The reduction of MM63-1 media supernatant by evaporation was tested in this work, but only a small proportion of the initial volume could be removed until sedimentation of salts and media components was observed (data not shown).
This is why the second option, the extraction of intracellular accumulated OH-ethylectoine, was chosen. While here the problem of high amounts of salts during downstream processing can be bypassed, the number of contaminants is higher. Using the B&D-extraction from cells, not only the solute of interest, but also all polar cellular components are isolated as well. Nevertheless, this approach was promising, as it was already successfully applied for the purification of other solutes (Korsten, 2011). Therefore, a whole-cell biotransformation of 3 mM ethylectoine was carried out by *E. coli* BL21 pET *ectDHis* in N-limited MM63-1 medium. After the complete substrate conversion, most of the product (~ 2 mM) was located in the media, whereas the rest was intracellularly accumulated (fig. 28). In order to increase intracellular concentrations of the product, the cultures were supplemented with high amounts of NaCl (5 % w/v), forcing the cells to increase the solute uptake for the compensation of the osmotic pressure (Kempf & Bremer, 1998). After that, only a small concentration of OH-ethylectoine (0.18 mM) was left in the media supernatant, meaning that the majority of the solute was now inside the cells. It was important, that cells were harvested not less than 45 min and not more than 60 min after supplementation with NaCl. When harvested earlier, cells only partly took up OH-ethylectoine, while exceeding 60 min also lead to reduced intracellular concentrations (data not shown). After a certain time, *E. coli* produces trehalose which is the only compatible solute that this organism forms as an osmostress protectant (Giæver *et al*., 1988), and this sugar probably partly replaces OH-ethylectoine due to better osmostabilizing abilities. At NaCl concentrations of 0.2 M (~ 1.2 % NaCl w/v), *E. coli* is already triggered to synthesize small amounts of this sugar to compensate the relatively slight osmotic pressure. By the exposure of even higher NaCl concentrations (0.3 – 0.5 M), trehalose synthesis is significantly increased to 0.1 – 0.4 µmol / mg whole-cell protein (~ 68 – 273 mg trehalose per g bacterial dry mass) after 4 h of incubation at 37 °C (Welsh *et al*., 1991).

B&D extraction of OH-ethylectoine was followed by cation exchange chromatography for further purification. After elution from the resin with ammonia, fractions containing this solute were subsequently adjusted to neutral pH and purified by ion retardation chromatography. This was done because NH_4Cl most probably has been formed during elution (NH_3 + HCl → NH_4Cl). Besides NH_4Cl, also other contaminants like glutamate, which are charged at neutral pH could be separated by ion retardation chromatography. It is possible that glutamate may have been accumulated by *E. coli* after NaCl shock, as this amino acid is one of the major organic osmolyte for cells grown under osmotic stress (Dinnbier *et al*., 1988). Additional FMOC-ADAM-HPLC (9-fluorenylmethyl chloroformate-1-amino-adamantane-HPLC) analyses would be appropriate in future works for the verification of glutamate. This method is suitable for the detection of substances, exhibiting reactive primary or secondary amino groups like amino acids (Kunte *et al*., 1993).

In the last purification step, OH-ethylectoine was crystallized in methanol, according to Schuh *et al*. (1985). The application of product crystallization is a common method to purify compatible solutes like glycine betaine or trehalose (Zhang, 2006; Peng *et al*., 1999). Nevertheless, it is still questionable if this step is really necessary for the purification of OH-ethylectoine, as this method is accompanied by product loss. After purification by crystallization, HPLC and NMR analysis showed no detectable contamination in the product (fig. 29, 30). Since product purity was not examined before crystallization, additional NMR and HPLC analyses should be accomplished after each purification step in future experiments.

4.3 Characterization of synthetic ectoine derivatives

After the successful chemical production of ethylectoine and propylectoine (fig. 13, 14), these solutes were characterized regarding stabilizing abilities towards heat, desiccation, osmotic pressure and freeze-thaw stress of either enzymes or whole cells. Hydroxylated ectoines were tested as well, since many studies already highlighted the superior protective traits of hydroxylated substances.

In order to prove the model of Street *et al*. (2006), that postulates a negative correlation between the fractional polar SASA with the transfer free energy of peptide backbones from water to a water/osmolyte solution, synthetic ectoine derivatives with different proportions of fractional polar SASAs were tested.

Since it was not possible to purify OH-homoectoine due to instability, the pH-dependent disintegration of this compound was investigated as well.

4.3.1 Characterization of OH-homoectoine

In previous studies (Ruprecht, 2014; Molitor, 2015), it was shown that during whole-cell biotransformation of homoectoine two different substances were generated: OH-homoectoine, and its open ring form 3-hydroxy-Nδ-acetylornithine. It is known, that the pyrimidine ring of ectoine is unstable under alkaline conditions, leading to the formation of either Nα-acetyl-L-2,4-diaminobutyric acid (α-ADABA) or Nγ-acetyl-L-2,4-diaminobutyric acid (γ-ADABA). The same is true for alkaline hydrolysis of OH-ectoine, forming hydroxylated ADABA derivatives (Kunte *et al*., 1993). Due to the resonance structure of ectoine, a partial positive charge is located on the C5-atom between the two N-atoms (fig. 37). Under alkaline conditions, OH-ions perform a nucleophilic attack preferably on this C-atom, leading to hydrolysis at elevated temperatures of ~ 50 °C. If an additional OH-group is attached to this molecule, as it is the case for OH-ectoine, the electron pulling effect is enhanced, leading to an increased positive charge at the C5-atom. At room temperature, OH-ectoine still remains stable under alkaline conditions. This stability is a result of the half-chair conformation with the COO^- group in axial position (Inbar *et al*., 1993).

In contrast to that, homoectoine as a seven membered diazepine does not show this type of conformation and is a more unstable molecule compared to ectoine. The addition of another CH_2-group inside the ring leads to a higher ring tension, which is energetically unfavorable.

An additional OH-group in homoectoine also leads to an enhanced electron pulling effect on the C6-atom between the two N-atoms, leading to hydrolysis even at room temperature. Therefore, it is plausible, that the purification of OH-homoectoine was not successful by alkaline elution during cation exchange chromatography, as the major part most likely hydrolyzed in ammonia solution (pK_s = 9.25), used as the eluent (2.8.2.1).

A continuous decrease of OH-homoectoine was also observed during whole-cell biotransformation (fig. 18), although cells were cultivated at pH 7 and 32 °C. This is why OH-homoectoine containing supernatants were kept and adjusted to different final pH values ranging from 2 - 10. In order to exclude a further modification of OH-homoectoine by unknown cellular or protein activities, supernatants were sterile filtered and subsequently filtered by a cellulose membrane, removing residual cells and putative excreted proteins. As seen in figure 31, stability of OH-homoectoine was maintained over time at acidic pH values between 2 and 4. At a pH of 6 and higher, a decrease of OH-homoectoine over time was noticed, indicating that the stability of this solute is strongly pH-dependent. Although the trend is going towards instability of OH-homoectoine with increasing pH, it is remarkable, that at a pH of 8

this solute is more stable compared to pH 10 or pH 7. This anomaly could be reproduced for several times and, so far, lacks a reasonable explanation.

Due to the instability of OH-homoectoine, this solute's possible stabilizing traits are largely unknown. To date, there is only one characterization study which showed that both homoectoine and OH-homoectoine are moderately effective osmostress protectants for *E. coli* MG1655 (Czech *et al.*, 2019). The study also revealed that the effectiveness of OH-homoectoine was even weaker than that of homoectoine, possibly due to reduced uptake and stability in the used pH neutral growth medium.

Regarding these results, it is questionable if the purification of this solute is worthwhile at all, because it will not be applicable under pH neutral or alkaline conditions. Possible applications of OH-homoectoine are solutions for the stabilization of biomolecules. Such extremolyte-based solutions are already available for the stabilization of enzymes and antibodies (bitop, Dortmund). In case of OH-homoectoine, these solutions would be suitable for the storage of enzymes with an acidic pH optimum only. An example would be the gastric proteinase pepsin, which exhibits a pH optimum of ~ 2 and is irreversibly inactivated at an pH of over 7 (Campos & Sancho, 2003).

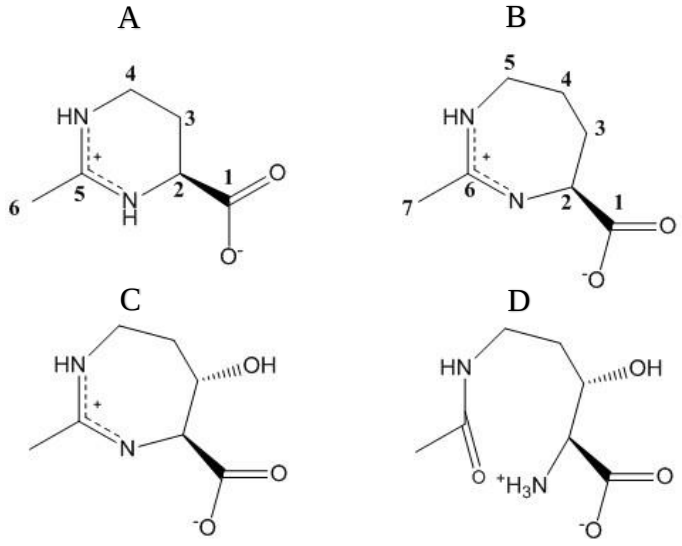

Figure 37: Molecule structures of ectoine (A), homoectoine (B), OH-homoetoine (C) and 3-hydroxy-Nδ-acetylornithine (D).

4.3.2 Influence on the melting temperature of RNase A

In order to withstand heat stress, many organisms have been shown to accumulate high concentrations of specific thermostabilizing compatible solutes. Some organisms like the extreme thermophilic *Methanothermus fervidus* accumulate cyclic diphosphoglycerate (Hensel

& König, 1987), while *Saccharomyces cerevisiae* is able to accumulate trehalose in a heat-shock response (Hottiger *et al*., 1994). *In vitro* studies revealed that these solutes were able to increase temperature stability of the cells own enzymes like glyceraldehyde-3-phosphate dehydrogenase and glucose-6P-dehydrogenase, but also of heterologous enzymes like bovine glutamic dehydrogenase. An accumulation of thermostabilizing solutes was also shown for aerobic heterotrophic bacteria like *Streptomyces* strains, that formed OH-ectoine from ectoine at elevated growth temperatures, suggesting that especially hydroxylated compatible solutes show increased thermotolerance towards cells and biomolecules (Malin & Lapidot, 1996).

The differential scanning calorimetry analyses of thermal-induced unfolding of bovine RNase A used in this work is an established method in order to estimate potential thermostabilizing abilities of compatible solutes. This enzyme is a model molecule for the investigation of thermal denaturation, as it is capable of denaturing and renaturing without losing considerable enzymatic activity. The presence of certain solutes causes a shift of the RNase A melting temperature, measurable by the change in heat capacity during heating. Using this method, different authors could already identify solutes with thermostabilizing abilities, which were partly confirmed in this study. Especially the use of hydroxyectoine exhibited a significant stabilizing impact, as the T_M of RNase A was increased (Knapp *et al*, 1999). In the work of Voß (2002, suppl. fig. 4), it could be shown that the stabilizing effects of different ectoines were quite distinct: While ectoine showed a moderate stabilizing effect, the synthetic ectoine derivative DHMICA was superior. On the contrary, decarboxyectoine showed an extreme destabilizing effect while homoectoine was only slightly destabilizing. These findings suggest, that even marginal differences in the molecular structure of ectoine can cause essential changes in the solutes stabilizing traits.

In this work, ectoine and synthetic derivatives homoectoine, ethylectoine and propylectoine as well as hydroxylated solutes (trehalose, OH-ectoine, OH-ethylectoine) were tested with regards to their putative thermostabilizing effect on RNase A. Furthermore, solutes that are already known to be effective thermostabilizers (glycine betaine, TMAO) were tested and compared to the denaturing compound urea.

It could be shown that all tested non-hydroxylated synthetic ectoines did not increase but even decrease T_M of RNase A, and the destabilizing effect correlated with increasing hydrophobicity of the tested ectoines (fig. 32). Trehalose and hydroxylated ectoines turned out to be effective thermostabilizers. The same was also true for glycine betaine and TMAO as already shown in previous works (Voß, 2002; Misra & Kishore, 2012). In order to prove if the solutes hydrophobicity is correlated with their thermostabilizing abilities, SASA calculations were

performed. Figure 32 and table 21 indeed show, that ectoines with extended alkyl chains (and therefore increasing hydrophobicity) are correlated with decreasing T_M values. It can be assumed that hydrophobic solutes exhibit an enhanced affinity to hydrophobic areas during protein unfolding, since more hydrophobic groups are exposed to the solvent by denatured proteins (Arakawa & Timasheff, 1985). Thus, the preferential exclusion of the solute is reduced, causing a decreased enzyme stability.

Hydroxylated solutes like OH-ectoine, OH-ethylectoine and trehalose, revealing to be most effective towards thermostabilization of RNase A, exhibit relatively high proportions of fractional polar SASAs. Nevertheless, the ratio of polar to nonpolar fractions does not seem to be the only factor for being an effective thermostabilizer: Both TMAO and trehalose turned out to be effective thermostabilizers, although TMAO exhibits very low polar fractions in contrast to trehalose. Like trehalose, urea shows very high polar fractions as well, but is characterized as a destabilizing solute (Yancey *et al*., 2002).

Table 21: Solvent accessible surface areas (SASA) of osmolytes with partly positive, negative and neutral charge, used for calorimetric analysis of RNase A. Partial positive/negative/neutral charge was determined by SASA of nitrogen/oxygen/carbon atoms via PyMol. Polar SASA equals the sum of SASA with partial positive and negative charge, while total SASA equals the sum of charged and uncharged SASA. Solutes are sorted in descendent order in accordance to their heat stabilization of RNase A. Solutes marked with a star were not used for calorimetric analysis in this study.

Solute	SASA pos. charge [Å^2]	SASA neg. charge [Å^2]	SASA neutr. charge [Å^2]	SASA polar / SASA total [Å^2/Å^2]
trehalose	0	349.670	136.741	0.718
TMAO	0	42.658	171.221	0.197
OH-ectoine	38.244	126.168	134.941	0.548
glycine betaine	0	88.419	182.805	0.324
OH-ethylectoine	28.634	133.525	164.233	0.496
ectoine	33.276	90.734	163.131	0.432
ethylectoine	29.457	90.607	192.607	0.384
homoectoine	32.988	88.805	186.378	0.392
propylectoine	29.474	90.630	220.007	0.352
urea	105.147	50.683	22.431	0.874
DHMICA*	46.294	89.269	132.817	0.504
decarboxyectoine*	43.145	0	188.021	0.186
acetamin*	108.259	0	76.271	0.587

Therefore, it is also important to evaluate the proportion of partially positively and negatively charged areas. Thermostabilizing solutes tend to exhibit major proportions of negatively charged SASAs, and the most effective tested solutes even exhibited no positively charged SASAs. Urea, on the other hand, exhibits a vast majority of positively charged SASA. Decarboxyectoine and acetamidine, which are cationic structures, were shown to be most destabilizing towards RNase A under heat stress, suggesting that positively charged molecules are disadvantageous in this regard (Voß, 2002; suppl. fig 4). Thus, it is conceivable that besides hydrophobicity, also partial charge of the solute's SASA plays an important role for thermostabilization towards RNase A. Further experiments could focus on how solutes affect other enzymes in differential scanning calorimetry like LDH (which in this work was investigated regarding heat-thaw stress). It would also be insightful to investigate microbial growth at elevated temperatures in presence of the examined synthetic ectoine derivatives, especially OH-ethylectoine. It is known that many organisms like *H. elongata* accumulate OH-ectoine rather than ectoine in order to survive heat-stress due to its thermostabilizing abilities like the increase of DNA melting temperature (Bursy *et al*., 2007; Kurz, 2008).

4.3.3 Protection of LDH against freeze-thaw stress

With respect to manufacturing, transport and storage of enzymes, the pharmaceutical and chemical industry is interested in additives to protect these proteins from several stresses. Stress can be induced by freezing and thawing enzyme solutions, occurring in the daily routine in scientific work. The early loss of enzyme activity due to repeated freezing and thawing entails the regular purchase of fresh enzymes. Therefore, it is desirable to increase enzyme durability, especially that of labile ones. LDH and PFK are such labile enzymes, as they are sensitive towards freeze-thawing and heat stress (Lippert & Galinski, 1992; Galinski, 1993).

In this work, LDH was used as a model enzyme for the investigation of freeze-thaw stress compensating solutes, especially new synthetic ectoines. Besides ectoines [(OH)-ectoine, (OH)-ethylectoine, homoectoine, propylectoine], also a polyhydroxylated sugar (trehalose) and two quaternary amines (glycine-betaine, TMAO) were tested. In the presence or absence of tested solutes, LDH was frozen in liquid nitrogen and slowly thawed at RT before residual dehydrogenase activity was measured spectrophotometrically.

All tested solutes showed a stabilizing effect towards freeze-thaw stress, as residual enzyme activity after 8 freeze-thaw cycles was higher compared to enzymes treated with no solute (fig. 33). While glycine betaine was the least effective of the tested solutes, ectoines maintained LDH activity to a significantly greater extent. Most effective solutes were hydroxylated (OH-

ectoine, OH-ethylectoine) and polyhydroxylated (trehalose) compounds as well as TMAO, which were able to stabilize LDH approximately to the same degree.

Freezing and thawing is not only a thermal stress factor for LDH. In fact, it is a process, leading to the recurring formation of harmful ice crystals. During the process of freezing, a major liquid part forms ice, while biomolecules like enzymes contain residual water which is not freezable (Yang & Rupley, 1979). This non-freezable water only amounts ~ 20 – 40 % of the biomolecules dry weight. While ice is formed during freezing, all dissolved buffer salts and solutes are concentrated in the non-freezable water. LDH is thus exposed to changing concentrations of salts and fluctuating pH after each freeze-thaw cycle. Therefore, it might be possible, that the applied solutes exhibit different buffer capacities, leading to different maintenance of pH during freezing and thawing. Göller *et al*. (1999) also evaluated the meaning of buffer capacity of compatible solutes regarding LDH preservation during freeze-thaw stress. It was shown that stabilizing solutes indeed tend to exhibit pK_a values near the buffer's pH, suggesting higher buffer capacities and therefore an avoidance of fluctuating pH. However, other authors could show a rather similar ranking of stabilizing solutes by the use of a Tris-HCl buffer, known to maintain pH during freezing and thawing, which indicates that buffer capacity is not the only considerable factor (Lippert & Galinski, 1992).

In this work, the tested hydroxylated compounds showed most preserving traits towards freezing and thawing, probably due to their glass-forming abilities. For OH-ectoine and trehalose, the transition into such amorphous glass-states (vitrification) was already verified (Tanne, 2013; Crowe *et al*., 1998). It is likely that the same applies to OH-ethylectoine, as these substances exhibit OH-groups which are postulated to be the reason for glass-formation during water deficiency. Fourier transform infrared and spin label electron spin resonance studies indicated that the superior glass-forming properties of hydroxylated compounds result from strong intermolecular H-bonds with the compound's OH-group (Tanne *et al*., 2014). Vitrification takes place in solutions of highly concentrated glass-forming agents, resulting in a solidification and avoidance of ice crystal formation by preserving the disordered molecular and atomic pattern. Thus, it is conceivable that the distribution of buffer salts stayed constant during the process of freezing and thawing of LDH, and as a consequence avoided a change of pH. Furthermore, by the avoidance of harmful ice-crystals, LDH was probably preserved to a greater extent, compared to non-glass-forming compounds.

Previous studies revealed, that stabilizing effects of compatible solutes against freeze-thaw stress are apparently dependent on the enzyme to be stabilized: LDH was most efficiently stabilized by ectoines and hydroxylated compounds like OH-ectoine and trehalose, while

glycine betaine showed almost no effect, as confirmed in this work. In case of the enzyme PFK, on the contrary, glycine betaine turned out to be a very effective stabilizer (Lippert & Galinski, 1992; Galinski, 1993). For both enzymes, polyhydroxylated sugars were beneficial as demonstrated in that work. These controversial findings point out, that the protective trait of a compatible solute regarding freeze-thaw stress is probably caused by two effects: 1.) preferential exclusion of the solute from the enzymes surfaces in the non-freezable water and 2.) vitrification of the solution.

4.3.4 Polar & non-polar interactions with the protein backbone

As already mentioned earlier, the preferential exclusion model, postulated by Timasheff (1998) and confirmed by Zaccai *et al*. (2016), is a commonly accepted molecular mechanism, explaining the osmolyte-induced protein stability in aqueous solution. The work of Street *et al*. (2006) gives further insight into the question which and why solutes are preferentially excluded from a protein surface. It is based on the findings of previous studies, which showed that the protein backbone makes the dominant contribution to the free-energy change between the enzyme's native and denatured state (Auton & Bolen, 2004, 2005; Liu & Bolen, 1995). According to the theory of Street *et al*., the free energy of a protein backbone, transferred from water in a water-osmolyte solution, negatively correlates with the osmolyte's fractional polar SASA. As a consequence, such a connection would mean that the degree of an osmolyte's stabilizing ability for the peptide backbone can directly be estimated by deriving the transfer free energy from the calculated fractional polar SASA.

In order to prove this mechanism, the cyclic glycine dimer DKP was used as a protein backbone model in this work, and the transfer free energy was calculated by measuring DKP concentrations in pure water and in osmolyte-solutions. An impeded solvation of DKP in an osmolyte solution results in positive values for the transfer free energy, meaning that it is an unfavorable and therefore stabilizing process.

The results suggest, that solutes with high proportions of polar regions like urea were predominantly most destabilizing (fig. 34). On the contrary, TMAO and glycine betaine which exhibit high proportions of non-polar regions reduced the solubility of DKP, thus showed stabilizing traits. Especially the direct comparison of solutes with the same basic structure (ectoine) but changing functional groups like elongated alkyl groups (ethylectoine, propylectoine) or the attachment of an hydroxy group (OH-ectoine) or a mixture of both (OH-ethylectoine) were interesting: while ectoine approximately exhibits equal proportions of polar and non-polar regions, the non-polar fraction increases with extended alkyl-groups attached to

the C5-atom. Thus, ethylectoine and propylectoine are solutes with a more hydrophobic character, compared to its natural analogue. As seen in figure 34, these solutes also slightly increased the transfer free energy, compared to ectoine.

While the elongation of alkyl-groups increases the solutes non-polar fractions, the attachment of a hydroxy-group leads to an increase of the solute's polar fraction. Although the tendency was observed, that polar hydroxylated ectoine derivatives were more destabilizing towards DKP compared to their non-hydroxylated analoga, there were only marginal differences. It is also striking that trehalose reduced solubility of DKP, although it exhibits a high proportion of polar areas due to a high number of oxygen atoms. The same was shown for sucrose and the sugar alcohol sorbitol (Street *et al*., 2006). Urea is also a highly polar compound but this solute favored the dissolving of DKP. The difference between destabilizing urea and the stabilizing solutes with high polar areas are the different proportions of negatively and positively charged parts. Furthermore, urea is not excluded from the hydration shell (Hua *et al*., 2008). Polarity of urea is caused due to high proportions of solvent accessible surface areas of positively charged nitrogen atoms. These positively charged surfaces apparently interact preferably with the peptide backbone which leads to a destabilization of a protein. The stabilizing solutes in this experiment exhibited either solely negatively charged areas or at least very small proportions of positively charged regions in combination with high proportions of non-polar regions. The destabilization of DKP may be explained by interactions with the peptide backbones polar groups, bearing a partial positive (amide nitrogen) and a negative (carbonyl oxygen) charge. Considering, that favorable/unfavorable interactions occur between polar groups with unlike/like charges, it appears that the solutes partial charge also plays a significant role for their DKP stabilizing trait (Zhou & Pang, 2018). While the backbone amide nitrogen of DKP exhibits only one lone electron pair, the carbonyl oxygen with its two lone electron pairs has two interaction sites (fig. 11). If DKP is exposed to solutes with high partial positive charges, the interaction possibly predominates over a repulsion due to a higher number of interaction sites of the carbonyl oxygen compared to the amide nitrogen.

Altogether, it can be stated, that preferential exclusion from DKP was achieved by solutes that caused neutral or no interactions, which is true for solutes with high proportions of non-polar regions and partial negative charge.

The described osmolyte/protein backbone interaction mechanisms represent a comparatively simplified model as other types of interactions such as solvent/side chain interactions are neglected. All nitrogen or oxygen atoms were treated as equally polar for the calculation of SASA, while hydrogen atoms were completely ignored due to simplification. Nevertheless, it

is a groundwork for the establishment of a further universal molecular theory that can be consulted for the evaluation of solutes as potential stabilizing compounds. In order to additionally include the effect of compatible solutes towards the transfer free energy of amino acids, Voß (2002) investigated the maximal solubility of all 20 proteinogenic amino acids in pure water and calculated ΔG_{tr} for the transfer in a water/osmolyte solution. Considering that the transfer free energies for amino acids were rather low, it can be concluded, that a major part of osmolyte-induced stability indeed depends on the solubility of the protein backbone as postulated Liu & Bolen (1995). Nevertheless, the impact of amino acid residues must not be ignored, as ectoine and ectoine analogues with their partly aromatic structure favorably interact with aromatic amino acids phenylalanine, tryptophan and tyrosine (Voß, 2002). Thus, proteins or enzymes that exhibit higher proportions of these amino acids like α-lactalbumin would theoretically be destabilized by ectoines to a certain extent (Friedman, 2018). It is difficult to predict to what extent a protein will be stabilized by a solute by just considering transfer free energies since not only the number of amino acids but also their arrangement within the protein is crucial (Lins & Brasseur, 1995).

4.3.5 Osmostabilization of *E. coli*

As previously described, fluctuations in environmental osmolarity triggers water fluxes across the semi-permeable membranes. Under hyperosmotic/hypoosmotic conditions, many microorganisms avoid excessive water loss/influx by adjusting external and internal water activities via the accumulation/exclusion of compatible solutes.

The accumulation of compatible solutes under high-saline conditions has beneficial effects on cellular hydration, necessary for biochemical processes. Furthermore, the functionality of biomolecules like proteins, DNA and membranes can be promoted due to thermodynamic driving forces, generated by preferential exclusion of the osmolytes from these macromolecules surfaces.

In this work it was tested, whether certain compatible solutes, especially new synthetic ectoine derivatives, can mediate osmoprotection like its natural analogue ectoine. Therefore, *E. coli* was cultivated at NaCl-concentrations which were either barely tolerable (3 % w/v) or non-tolerable (5 % w/v) in the presence or absence of externally supplied compatible solutes (fig. 35). It could be shown that osmoprotection was achieved by ectoine, OH-ectoine and glycine betaine, as expected (Pastor *et al*., 2010; Roeßler & Müller, 2001), but also by some of the tested synthetic ectoine derivatives (ethylectoine, OH-ethylectoine). These solutes shortened the lag phase and facilitated growth even at 5 % NaCl. Homoectoine had a minor

osmostabilizing effect, as it only bearly affected growth at 3 % NaCl and led to a very slow but steady growth at 5 % NaCl without an apparent exponential growth phase. Homoectoine was already reported to provide only moderate osmostress resistance for several *E. coli* strains, which could be confirmed in this work (Nagata, 2001; Voß, 2002; Czech, 2019). Propylectoine did not affect growth of *E. coli* at all, and creatine even impaired growth.

These distinctive results raise the question if the tested solutes are taken up by *E. coli* at all. In this and previous works it could be demonstrated that all considered solutes indeed can be taken up by *E. coli* (fig. 24; Brauner, 2016; Czech *et al*., 2019; Sell, 2009). According to these studies, the solute uptake is ProP/ProU mediated, as uptake experiments with ProP/ProU deletion strains suggest. In this study, maximal uptake rates for all considered ectoines was between 65 – 75 nmol x min^{-1} x mg^{-1} in *E. coli* DH5α. Jebbar *et al*. (1992) showed a maximal ectoine uptake rate of only 16 nmol x min^{-1} x mg^{-1}. However, these values are hard to compare since the group of Jebbar used radioactively marked ectoine, and the uptaken substrate was determined via scintillation spectrometry. They also used another *E. coli* strain MC4100 which makes it more difficult to compare these different rates.

Nevertheless, since all considered ectoines can be accumulated by *E. coli*, it seems reasonable to suppose that the differences in osmostabilization arise from the solutes physico-chemical attributes. In the past, effective compatible solutes were characterized as such with neutrality of net charge and high solubility. Furthermore, a combination of polar and relatively hydrophobic moieties was identified to be beneficial (Galinski, 1993). An effective compatible solute must be able to stabilize macromolecules like enzymes via preferential exclusion when it is intracellularly accumulated under hyperosmotic conditions. It is likely that the investigated solutes are excluded from protein surfaces to a different degree. For creatine it was shown that this solutes guanidino-group is responsible for the disruption of ion homeostasis and destabilization of ribosomal complexes in *E. coli* (Waßmann, 2013). As cell metabolism is hereby impaired, this compound is called an incompatible solute which excludes a stabilizing effect for *E. coli*.

To a certain degree, every stabilizing solute also partly interacts with macromolecules, which contributes to destabilization. An effective osmostabilizing solute is able to overcompensate those destabilizing effects. Glycine betaine, for example, is an excellent osmoprotective compatible solute (Oren, 2008). Nevertheless, if glycine betaine is available in too high concentrations, direct interactions between this solute and protein side chains outweighs its indirect protective abilities by preferential exclusion, leading to a decrease of protein protection (Voß, 2002). In case of propylectoine, it can be assumed that it was not able to overcompensate

destabilizing interactions with protein side chains, leading to an impaired preferential exclusion. Since the highly hydrophobic propylectoine showed no protective traits towards osmostress compared to less hydrophobic homoectoine, ethylectoine and ectoine, it can be concluded that ectoines with increasing hydrophobicity are counterproductive for the osmostabilization of *E. coli*.

Although osmostabilizing and destabilizing properties of the investigated solutes could be identified, it would be reasonable to use trehalose deficient *E. coli* strains for future works. Precultures of *E. coli* K-12 were already adapted to 3 % NaCl in this work, which most probably caused trehalose formation (Welsh *et al*., 1991). Therefore, a mixture of trehalose and externally provided solute was probably intracellularly accumulated, that subsequently distorted the stabilizing or destabilizing effects of the investigated solutes.

4.3.6 Protection of *E. coli* K-12 against desiccation

In this work it was tested, whether synthetic ectoines, especially new formed hydroxylated OH-ethylectoine, are capable of maintaining viability of *E. coli* K-12 after air drying and rehydration. It is well-known that solutes with attached hydroxy-groups like OH-ectoine and trehalose are beneficial for the stabilization of whole cells, exposed to desiccation (Louis *et al*., 1994; Manzanera *et al*., 2002; Korsten, 2011).

The results indicate that cells supplemented with hydroxylated solutes (trehalose, OH-ectoine, OH-ethylectoine) showed viability after de-/rehydration (fig. 36). Cultures, supplemented with ectoine, ethylectoine, propylectoine, homoectoine and glycine betaine, by contrast, showed no growth. Another interesting result was that non-supplemented *E. coli* also showed viability, although a delayed growth was detected. This rises two questions: 1.) Why were also non-supplemented *E. coli* cultures viable after dehydration? 2.) Which stabilizing mechanism is involved against desiccation of whole cells?

The first question may be answered by the fact, that *E. coli* was slowly dehydrated over several hours and over that time, osmotic pressure was gradually elevated by the dissolved salts. The successive increase of osmotic pressure probably triggered slow trehalose formation to a certain extent (Giæver *et al*., 1988). By that, only a reduced number of cells which produced sufficient amounts of this solute may have been able to survive desiccation. This would explain the delayed entrance of exponential growth phase compared to cultures supplemented with OH-ectoine or OH-ethylectoine, which were already available at the beginning of the dehydration process. In order to prove that, it would be helpful to repeat this experiment by using an *E. coli* strain which is deficient in trehalose formation.

Furthermore, the accumulation of solutes which did not provide desiccation protection probably impaired the formation of trehalose. One possible explanation is that there exists a feedback regulation between the active uptake systems for compatible solutes and trehalose synthesis. Previous works verified that the presence of betaines and ectoine dramatically reduce or completely prevent the synthesis of trehalose (Larsen *et* al., 1987; Rod *et al*., 1988; Waßmann, 2013).

The second question concerns the mode of action of a desiccation protectant. In order to understand the involved mechanisms, it is important to know that drying is a different kind of stress compared to freezing or osmotic pressure. It is true that freezing removes bulk water from a system, leading to a decrease of water activity like it is the case at hypersaline conditions. The specificity of a stabilizing solute towards biomolecules during freezing is relatively low. Any solute which is dissolved in the non-freezable water and which is preferentially excluded from the molecule's hydration shell serves as a protectant. The difference to dehydration is that here not only bulk water but, also the non-freezable water is removed, which causes changes in the physical properties of all biomolecules like enzymes or phospholipids (Crowe *et al*., 1990).

However, to date it is not clear which biochemical or molecular mechanisms are involved in compatible solute-mediated desiccation protection, but several hypotheses have been put forward. In the following, three famous theories will shortly be described: The "water replacement hypothesis" states that during desiccation, water molecules are surrogated by specific compatible solutes, which adopt the structure giving function of water and directly interact with macromolecules (Clegg, 1982). These structure giving substitutes must show similar chemical characteristics like water, especially in regards to polarity. Hydroxylated or polyhydroxylated solutes would be preferred in this matter. Sugars like trehalose or sucrose, but also OH-ectoine are such hydroxylated solutes which additionally are able to develop highly viscous amorphous cytoplasmatic matrices (Tanne, 2013). The formation of these glasses is part of the so-called "vitrification hypothesis" (Green & Angell, 1989). The transition from a fluid into a glass is achieved in the presence of highly concentrated glass-forming substances, which are interconnected via hydrogen bonds. As a result, an extreme increase of viscosity and a subsequent solidification of the fluid is attained. In this reversible state, molecular dynamics of all biomolecules are highly restricted, leading to metabolic stasis (Bellavia *et al*., 2011). The immobilization of biomolecules inside such a glass matrix preserves them from denaturation, since the random distribution of particles inside a fluid is being kept by the amorphous character of a glass. Moreover, glass-formation implies the prevention of excessive harmful crystal-formation, by which integrity of membranes, organelles and other biomolecules is stabilized

(Sun & Leopold, 1997). This theory supports the finding, that externally provided trehalose favored desiccation survival of *E. coli* K-12 (fig. 36). Although this strain is not capable of taking up trehalose (Louis *et al*., 1994), whole cells are probably included inside preserving glasses if this solute is available in high concentrations.

A third theory, called "water entrapment hypothesis", is derived from the preferential exclusion theory and postulates that over the course of dehydration, compatible solutes are likewise excluded from a biomolecules surface with a simultaneous inclusion of residual water molecules between the solute and the biomolecule (Belton & Gil, 1994). Hereby, a thin water film can accomplish hydration of proteins, membranes and other macromolecules which are sensitive towards desiccation.

All these theories comprise plausible thoughts and are not necessarily mutually exclusive, but can rather be combined in order to understand the stabilizing effects of compatible solutes under desiccation.

4.3.7 Different environmental stresses determine different protection mechanisms

To sum up the results achieved for solute mediated stabilization studies, it can be pointed out that there is no single solute which can universally cope with every kind of environmental stress towards every biomolecule or whole cells.

While enzymes with a high proportion of polar residues may favorably be stabilized by non-polar solutes, the opposite effect will be achieved by polar solutes. This at least will theoretically be the case in aqueous solutions, where preferential exclusion of the solute from the biomolecule's hydration shell takes place. Furthermore, the arrangement and accessibility of polar/non-polar residues in a biomolecule is essential. Depending on the behavior of a denaturing enzyme, it can either be arranged in "loose bundles" (upper limit model), allowing favored contact with the solute, or in "tight chunks" (lower limit model), preventing increased contact with the solute (Creamer *et al*., 1997). The absence of any water, which is the situation for (freeze-)dried biomolecules or cells, usually prevents a preferential exclusion which is why direct interactions between a solute and a biomolecule are the consequence. This interaction can either be favorable (destabilizing) or unfavorable (stabilizing). In this regard, hydroxylated compounds are a special exception, as they are able to either form structure-preserving glasses or to stabilize biomolecules by direct interaction due to their similar chemical characteristics like water. There is also a big difference between the stabilization of single enzymes or whole cells, since it cannot exactly be predicted, which and how solutes interact with the microorganism's diverse biomolecules. To get a general overview regarding the efficiency of

the investigated solutes towards different stresses and targets, a summary table is given below (tab. 22). Nevertheless, studies like the preferential exclusion model (Timasheff, 1998) in combination with the model of Street *et al*. (2006) give important reference points in order to evaluate the stabilizing trait of a solute.

Table 22: Effectivity spectrum of (hydroxylated) ectoines towards different structures and environmental stresses. Very effective (++), effective (+), no/moderate effect (0), negative effect (-).

Stress	Ectoine	OH-ectoine	Ethylectoine	OH-ethylectoine	Propylectoine	Homoectoine
Heat stress (RNase A)	0	+	-	+	-	-
Freeze-thaw-stress (LDH)	+	++	+	++	+	+
Osmostress (*E. coli* cells)	+	+	+	+	0	0
Dessication (*E. coli* cells)	0	+	0	+	0	0

5 Summary

In this work, whole-cell biotransformation systems for the conversion of ectoines were established, which significantly surpass the performance of other such systems (Meffert, 2011; Ruprecht, 2014; Czech *et al*., 2016). Furthermore, the chemical syntheses of ectoine derivatives, that were also shown to be convertible by different ectoine hydroxylases, were successfully accomplished. For the first time, (hydroxylated) ectoine derivatives were purified and characterized. All milestones achieved in this work are summarized below:

- For whole-cell biotransformation, the choice of the N-source and C-source is essential. The most effective combination is achieved by $(NH_4)_2SO_4$ and glucose.
- Working under N-limiting conditions is a key element for increasing the hydroxylation performance of ectoines. Although glucose uptake (and therefore 2-oxoglutarate regeneration) is decreased under N-depletion, total conversion of ectoines is increased compared to C-limited conditions. This is likely because the supply of 2-oxoglutarate is ensured over an extended time period when glucose is still available. The availability of excessive amounts of this cofactor seems not to be crucial.
- During exponential growth of *E. coli*, hydroxylation performance is probably dependent on the uptake/efflux rate of (OH)-ectoines and the EctD conversion rate, while the reduced glucose uptake rate in combination with decreasing enzyme activity/stability over time seem to be the limiting factors during stationary phase under N-limiting conditions.
- Biotransformation efficiency also depends on the choice of the *E. coli* strain and recombinant EctD. From the investigated *E. coli* strains, DH5α is most effective. Furthermore, the four different tested hydroxylases exhibit differential stability, with EctD of *A. cryptum* and *S. alaskensis* being the most stable ones. Therefore, the combinations of *E. coli* DH5α heterologously expressing *ectD* of *A. cryptum* or *S. alaskensis* turned out to be very effective biotransformation systems. The complete conversion of 30 mM ectoine was accomplished by the use of these strains, which is a threefold improvement compared to the starting situation of this study.
- At elevated NaCl concentrations (3 % w/v), whole-cell biotransformation is only slightly improved. Therefore, high salt conditions are unnecessary which simplifies purification of hydroxylation products from the media supernatant.
- New synthetic ectoine derivatives with prolonged alkyl chains (ethylectoine, propylectoine) were successfully synthesized. These solutes, as well as homoectoine can be taken up by *E. coli* and converted by ectoine hydroxylases. Hydroxylation products are excreted into the media

supernatant during whole-cell biotransformation. The identification of OH-ethylectoine (this work) and OH-homoectoine (Ruprecht, 2014) was successfully performed via ^{13}C-NMR. The identification of OH-propylectoine still needs to be confirmed.

- Substrate ambiguity is not limited to EctD of *H. elongata*, since all other tested EctD enzymes originating from *A. cryptum*, *P. stutzeri* and *S. alaskensis* recognize ethylectoine, propylectoine and homoectoine as convertible substrates.
- While whole-cell biotransformation approaches at 32 °C – 35 °C result in a gradual loss of enzyme activity and hydroxylation performance over time (first order enzyme reaction), a stable hydroxylation process is obtained by EctD of psychrophilic *S. alaskensis* at 15 °C, which is the optimal temperature of this enzyme. Although conversion rates are diminished at lower temperatures, the constant conversion may be advantageous in order to extent the hydroxylation process, and by that, to convert even higher amounts of substrates.
- OH-homoectoine is highly instable and stability is dependent on acidic conditions. Hydrolysis of this compound is probably induced by an unfavorable conformation in combination with an electron pulling effect of the hydroxy group that favors a nucleophilic attack of OH^- ions under alkaline conditions.
- Since OH-homoectoine is an unstable compound, a stable hydroxylated synthetical derivative of ectoine with increased hydrophobicity (OH-ethylectoine) was successfully produced.
- The purification of OH-ethylectoine was successfully accomplished by cation exchange chromatography and ion retardation chromatography, followed by methanol crystallization. While this solute was extracted from cells, it is generally possible to purify even higher amounts from media supernatants, since *E. coli* is able to excrete this hydroxylation product. Due to instability of OH-homoectoine and low amounts of putative OH-propylectoine during biotransformation, purification of these solutes was not performed.
- New (hydroxylated) synthetic ectoine derivatives were characterized for the first time regarding their stabilizing traits towards enzymes or whole cells at different environmental stresses. Hydroxylated compounds (OH-ethylectoine, OH-ectoine) are predominantly effective against denaturing effects of high temperatures (RNase A), freeze-thaw stress (LDH), desiccation (*E. coli*) and osmotic pressure (*E. coli*). Non-hydroxylated synthetic ectoines show similar properties like ectoine as they are able to preserve LDH from freeze-thaw stress (ethylectoine, propylectoine, homoectoine) and whole cells of *E. coli* from osmotic pressure (ethylectoine). They do not show protection against desiccation of cells or against heating stress towards RNase A.
- The model of Street *et al.* (2006), postulating a negative correlation between the fractional polar SASA of the solute with the transfer free energy of peptide backbones (diketopiperazine) from

water to a water/osmolyte solution was widely validated by the use of synthetic ectoines with different levels of hydrophobicity.

- There is no single solute that is capable of compensating every environmental stress. Stress preserving features depend on the traits of the structure to be preserved (polar/non-polar portions of enzymes/membranes/whole cells) and on the environmental conditions. While preferential exclusion of a solute can be achieved in aqueous solutions, other function-preserving mechanisms like glass-formation or favorable direct interactions with biomolecules will be involved under waterless conditions.

6 Appendix

Suppl. table 1: EctD protein quantification (BCA) after strep-tag purification of whole-cell proteins. The samples were regularly taken from *E. coli* DH5α, heterologously expressing *ectD* of *H. elongata* (Hel), *A. cryptum* (Acry), *P. stutzeri* (Pstu) or *S. alaskensis* (Sala).

	0 h [µg/ml]	2 h [µg/ml]	4 h [µg/ml]	18 h [µg/ml]	42 h [µg/ml]	66 h [µg/ml]
Hel	9.85	0	0	0	0	0
Acry	9.34	40.44	56.32	389.56	365.51	363.82
Pstu	46.48	81.41	277.73	50.08	38.83	36.56
Sala	46.33	97.66	176.02	148.71	131.41	134.69

Suppl. table 2: Maximal ectoine uptake rate for *E. coli* BL21 in absence and presence of OH-ectoine (Brauner, 2016).

	10 mM ectoine/ 0 mM OH-ectoine	5 mM ectoine/ 5 mM OH-ectoine	2 mM ectoine/ 8 mM OH-ectoine
Maximal ectoine uptake rate [nmol x min^{-1} x mg^{-1}]	111.48	101.40	63.15
Maximal OH-ectoine uptake rate [nmol x min^{-1} x mg^{-1}]	-	7.73	19.61

Suppl. table 3: Kinetic parameters of EctD enzymes under optimized conditions (Widderich *et al.*, 2014).

EctD from	K_m [mM ectoine]	v_{max} [U/mg]	k_{cat} [s^{-1}]	k_{cat}/K_m [mM^{-1} s^{-1}]	K_m [mM 2-oxoglutarate]
V. salexigens	5.9±0.3	6.4±0.2	7.7	1.31	4.9±0.3
S. alaskensis	9.8±0.5	1.0±0.2	1.2	0.12	2.7±0.3
H. elongata	5.7±0.6	2.5±0.2	2.8	0.49	4.8±0.4
P. stutzeri	6.2±0.4	6.7±0.2	8.9	1.44	4.6±0.5
P. lautus	9.5±0.7	1.3±0.1	1.6	0.17	3.9±0.2
A. ehrlichii	9.0±0.3	1.0±0.1	1.2	0.13	5.0±0.3
A. cryptum	10.0±0.6	2.8±0.3	3.4	0.34	4.1±0.4

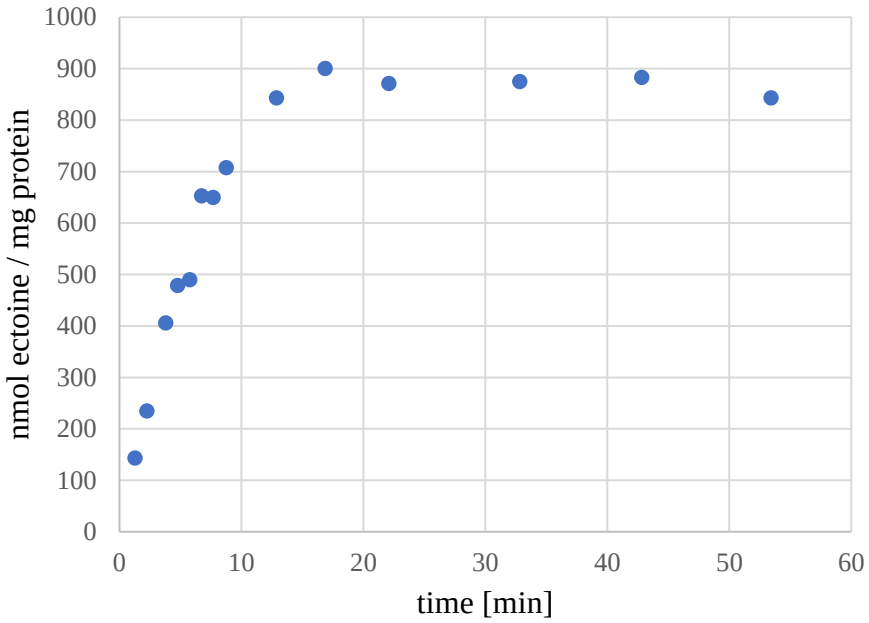

Suppl. figure 1: Uptake of ectoine in absence of OH-ectoine for *E. coli* BL21 (wildtype). Cultivation was carried out at 32 °C in MM63-1 medium with 10 g/L glucose and 0.5 g/L $(NH_4)_2SO_4$ and supplemented with 10 mM ectoine at OD_{600} = 0.5. Intracellular amounts of solutes were calculated in regular intervals by cell filtration, B&D extraction and HPLC analysis. Amounts of solutes (nmol) per whole-cell protein (mg) were plotted against time (min) in order to calculate max. solute uptake rates (suppl. tab. 2). Max. uptake rates were calculated for the linear increase within the first 6 min after supplementation (Brauner, 2016).

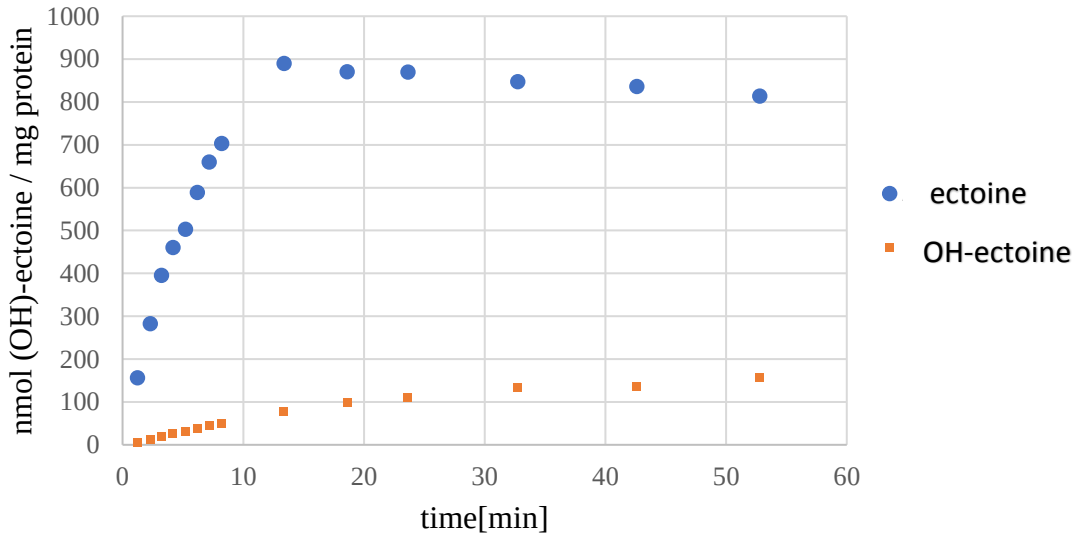

Suppl. figure 2: Uptake of ectoine (5 mM) in presence of OH-ectoine (5 mM) for *E. coli* BL21 (wildtype). Cultivation was carried out at 32 °C in MM63-1 medium with 10 g/L glucose and 0.5 g/L $(NH_4)_2SO_4$ and supplemented with ectoine (5 mM) and OH-ectoine (5 mM) at OD_{600} = 0.5. Intracellular amounts of solutes were calculated in regular intervals by cell filtration, B&D extraction and HPLC analysis. Amounts of solutes (nmol) per whole-cell protein (mg) were plotted against time (min) in order to calculate max. solute uptake rates (suppl. tab. 2). Max. uptake rates were calculated for the linear increase within the first 6 min after supplementation (Brauner, 2016).

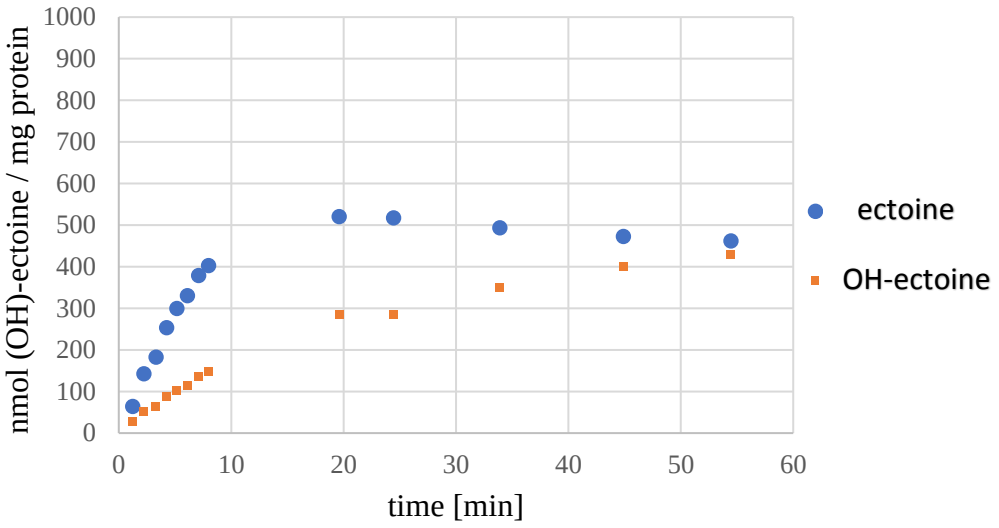

Suppl. figure 3: Uptake of ectoine (2 mM) in presence of OH-ectoine (8 mM) for *E. coli* BL21 (wildtype). Cultivation was carried out at 32 °C in MM63-1 medium with 10 g/L glucose and 0.5 g/L $(NH_4)_2SO_4$ and supplemented with ectoine (2 mM) and OH-ectoine (8 mM) at OD_{600} = 0.5. Intracellular amounts of solutes were calculated in regular intervals by cell filtration, B&D extraction and HPLC analysis. Amounts of solutes (nmol) per whole-cell protein (mg) were plotted against time (min) in order to calculate max. solute uptake rates (suppl. tab. 2). Max. uptake rates were calculated for the linear increase within the first 6 min after supplementation (Brauner, 2016).

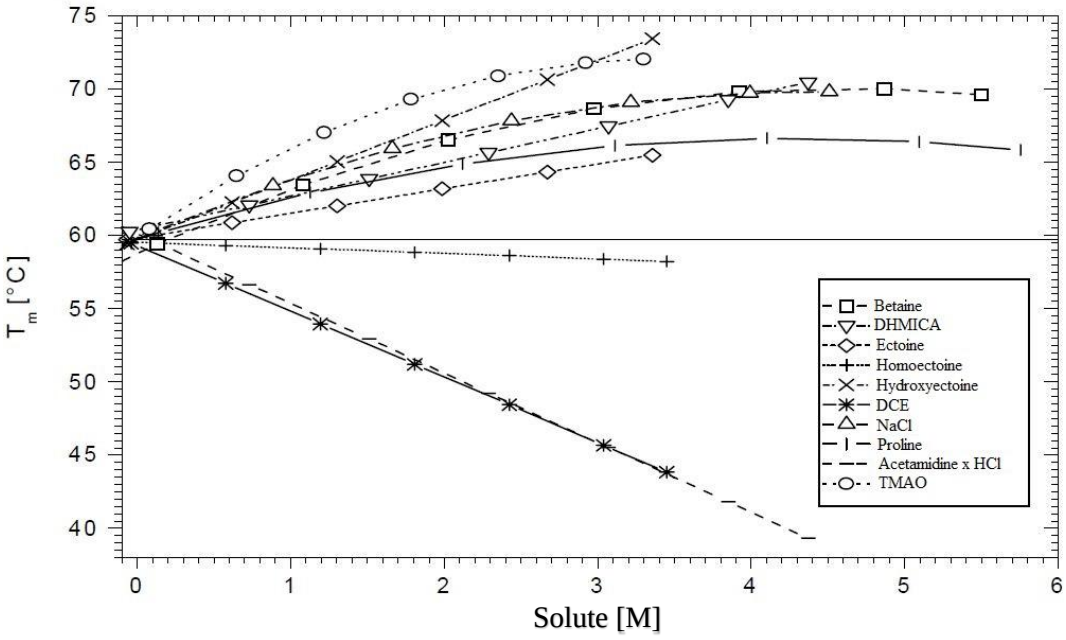

Suppl. figure 4: Impact of different compatible solutes on the melting point (T_m) of RNase A, measured by differential scanning calorimetry (DSC) (Voß, 2002).

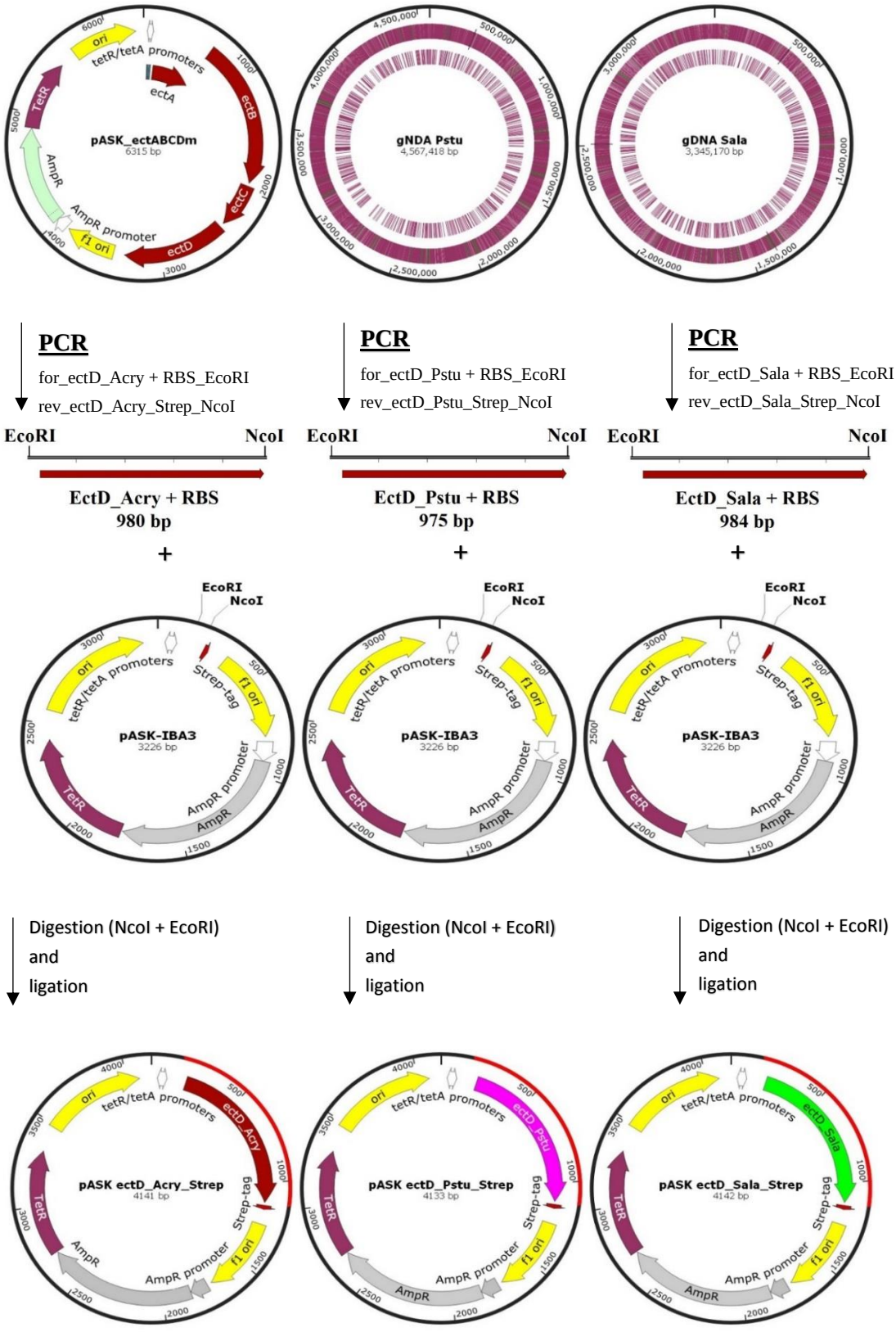

Suppl. figure 5: Cloning scheme for pASK *ectD_Acry_Strep*, pASK *ectD_Pstu_Strep* and pASK *ectD_Sala_Strep*. Plasmid or gDNA based ectD amplification was followed by the enzymatic hydrolyzation of PCR products and pASK IBA-3 plasmid backbones with *Eco*RI and *Nco*I. Cloning was finished by ligation of digested plasmid DNA and PCR products. AmpR = ampicillin resistance, f1 ori = phage origin or replication, ori = ColE1 origin of replication, tetR = tetracycline operon repressor, tetA = tet-operator.

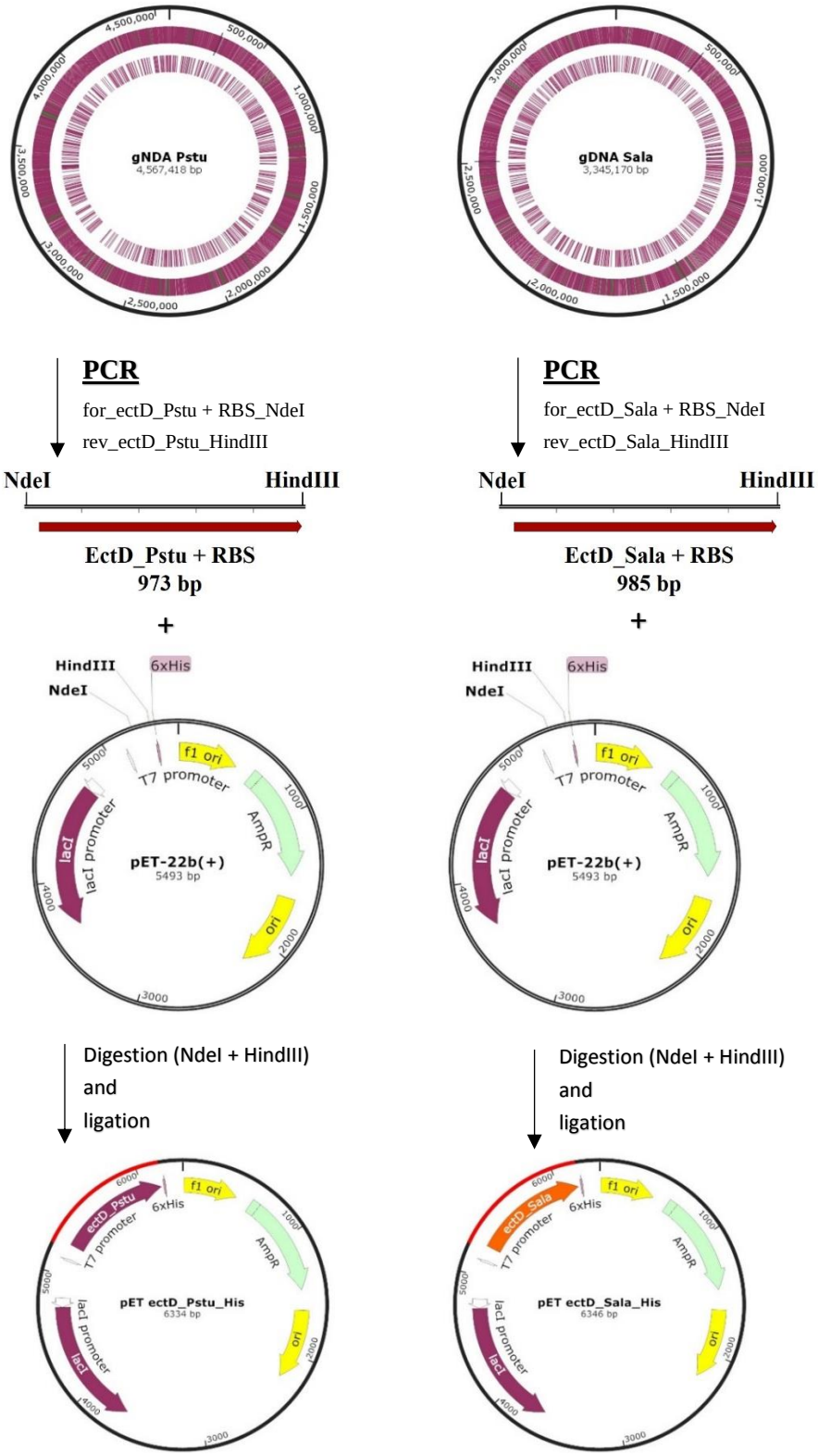

Suppl. figure 6: Cloning scheme for pET *ectD_Pstu_His* and pET *ectD_Sala_His*. gDNA based *ectD* amplification was followed by the enzymatic hydrolyzation of PCR products and pET-22b(+) plasmid backbones with *Nde*I and *Hind*III. Cloning was finished by ligation of digested plasmid DNA and PCR products. AmpR = ampicillin resistance, f1 ori = phage origin or replication, lacI =lactose repressor, ori = ColE1 origin of replication, T7 = phage T7, 6xhis = His-Tag

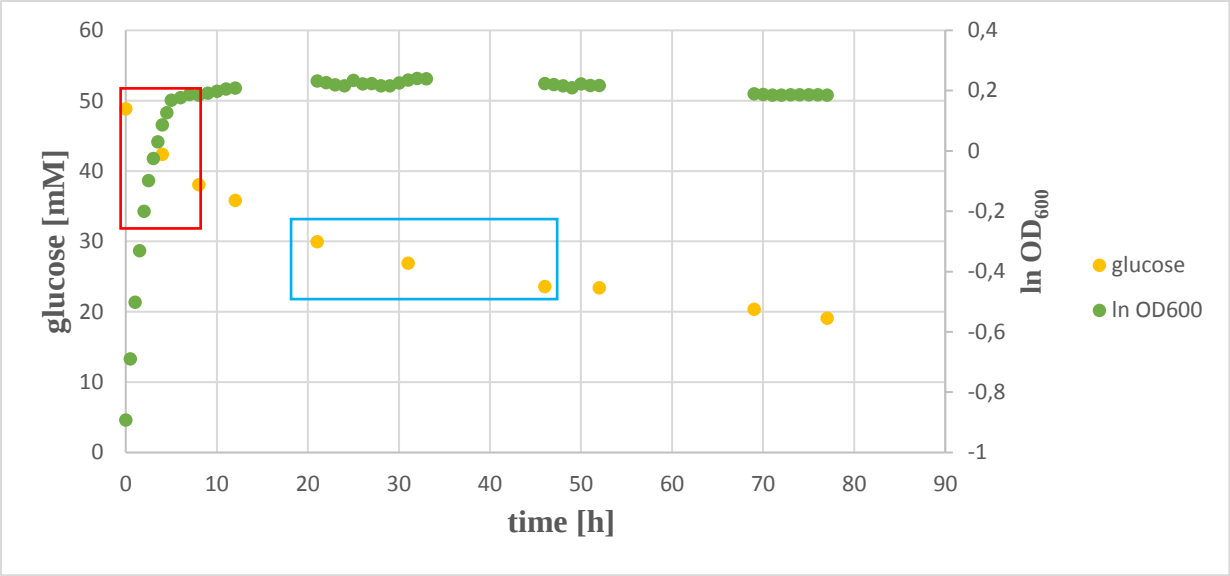

glucose uptake rate at exponential growth phase	97.9 nmol x min^{-1} x mg^{-1}
glucose uptake rate at stationary growth phase	15.3 nmol x min^{-1} x mg^{-1}

Suppl. figure 7: Glucose uptake rate of *E. coli* BL21 pET *ectDHis* under N-limiting conditions. Cells were cultivated in N-limited MM63-1 medium. Glucose uptake rates were determined for the exponential (red frame) and stationary (blue frame) growth phase (Brauner, 2016).

7 References

Abdel-Aziz, H. *et al.* (2015) 'Bacteria-Derived Compatible Solutes Ectoine and Hydroxyectoine act as Intestinal Barrier Stabilizers to Ameliorate Experimental Inflammatory Bowel Disease', *Journal of Natural Products*, 78(6), pp. 1309-1315.

Andersson, M. M., Breccia, J. D. & Hatti-Kaul, R. (2000) 'Stabilizing effect of chemical additives against oxidation of lactate dehydrogenase', *Biotechnology and Applied Biochemistry*, 32(3), pp. 145-153.

Arakawa, T. & Timasheff, S. N. (1983) 'Preferential interactions of proteins with solvent components in aqueous amino acid solutions', *Archives of Biochemistry and Biophys*ics, 224(1), pp. 169-177.

Arakawa, T. & Timasheff, S. N. (1985) 'The stabilization of proteins by osmolytes' *Biophysical Journal*, 47(3), pp. 411–414.

Auton, M. & Bolen, D. W. (2004) 'Additive Transfer Free Energies of the Peptide Backbone Unit That Are Independent of the Model Compound and the Choice of Concentration Scale', *Biochemistry*, 43(5), pp. 1329–1342.

Auton, M. & Bolen, D. W. (2005) 'Predicting the energetics of osmolyte-induced protein folding/unfolding', *Proceedings of the National Academy of Sciences of the United States of America*, 102(42), pp. 15065-15068.

Barth S. *et al.* (2000) 'Compatible-solute-supported periplasmic expression of functional recombinant proteins under stress conditions', *Applied and Environmental Microbiology*, 66(4), pp. 1572–1579.

Bellavia, G. *et al.* (2011) 'Protein Thermal Denaturation and Matrix Glass Transition in Different Protein−Trehalose−Water Systems', *The Journal of Physical Chemistry B*, 115(19), pp. 6340–6346.

Belton, P. S. & Gil, A. M. (1994) 'IR and Raman spectroscopic studies of the interaction of trehalose with hen egg white lysozyme', *Biopolymers*, 34(7), pp. 957–961.

Bertani, G. (1951) 'Studies on lysogenesis. I. The mode of phage liberation by lysogenic *Escherichia coli*', *Journal of Bacteriology*, 62(3), pp. 293–300.

Bethlehem, L. (2019) 'Design and generation of an efficient *E. coli* cell-factory', Dissertation, Rheinische Friedrich-Wilhelms-Universtität Bonn.

Bhattacharya, S. K. & Dubey, A. K. (2008) 'High-Level Expression of a Heterologous Gene in *Escherichia coli* in Response to Carbon-Nitrogen Source and C/N Ratio in a Batch Bioreactor', *Biotechnology Progress*, 13(2), pp. 151-155.

Bligh, E. G. & Dyer, W. J. (1959) 'A rapid method of total lipid extraction and purification', *Canadian Journal of Biochemistry and Physiology*, 37(8), pp. 911–917.

Blum, H., Beier, H. & Gross, H. J. (1987) 'Improved silver staining of plant proteins, RNA and DNA in polyacrylamide gels', *Electrophoresis*, 8(2), pp. 93–99.

Bolen, D. W. & Baskakov, I. V. (2001) 'The osmophobic effect: natural selection of a thermodynamic force in protein folding', *Journal of Molecular Biol*ogy, 310(5), pp. 955–963.

Bolten, C. J. *et al.* (2007) 'Sampling for metabolome analysis of microorganisms', *Analytical Chemistry*, 79(10), pp. 3843-3849.

Booth, I. R. & Blount, P. (2012) 'The MscS and MscL families of mechanosensitive channels act as microbial emergency release valves', *Journal of Bacteriol*ogy, 194(18), pp. 4802–4809.

Borges, N. *et al.* (2002) 'Comparative study of the thermostabilizing properties of mannosylglycerate and other compatible solutes on model enzymes', *Extremophiles*, 6(3), pp. 209–216.

Botta, C. *et al.* (2008) 'Genotoxicity of visible light (400 – 800 nm) and photoprotection assessment of ectoine, L-ergothioneine and mannitol and four sunscreens', *Journal of Photochemistry and Photobiology B: Biology*, 91(1), pp. 24–34.

Brauner, J. F. (2016) 'Kinetik der Hydroxylierung von Ectoin und Homoectoin im Zuge einer Ganzzellbiotransformation durch *E. coli* BL21 pET*ectDHis*', Master thesis, Rheinische Friedrich-Wilhelms-Universität Bonn.

Bremer, E. & Krämer, R. (2000) 'Coping with osmotic challenges: osmoregulation through accumulation and release of compatible solutes in *B. subtilis*', *Comparative Biochemistry and Physiology - Part A Molecular & Integrative Physiology*, 126(1), pp. 79-97.

Bren, A. *et al*. (2016) 'Glucose becomes one of the worst carbon sources for *E. coli* on poor nitrogen sources due to suboptimal levels of cAMP', *Scientific Reports*, 6, p. 24834.

Brown, A. (1976) 'Microbial water stress. *Microbiology and Molecular Biology* Reviews, 40(4), pp. 803-846.

Brünig, A. (2005) ‚Molekulargenetische und physiologische Studien zur Entwicklung eines Expressionssystems in *Halomonas elongata* DSMZ 2581T', Diploma thesis, Rheinische Friedrich-Wilhelms-Universität Bonn.

Buenger, J. & Driller, H. (2004) 'Ectoine: an effective natural substance to prevent UVA-induced premature photoaging' *Skin Pharmacology and Physiology*, 17(5), pp. 232–237.

Buommino, E. *et al*. (2005) 'Ectoine from halophilic microorganisms induces the expression of hsp70 and hsp70B' in human keratinocytes modulating the proinflammatory response', *Cell Stress Chaperones*,10(3), pp. 197-203.

Bursy, J. (2005) 'Osmotisch regulierte Biosynthese der kompatiblen Solute Ectoin und Hydroxyectoin in *Salibacillus salexigens*: Biochemische Charakterisierung der Ectoin-Hydroxylase EctD und Identifizierung ihres Strukturgenes' Dissertation, Universität Marburg.

Bursy, J. *et al*. (2007) 'Osmotically induced synthesis of the compatible solute hydroxyectoine is mediated by an evolutionarily conserved ectoine hydroxylase', *Journal of Biological Chemistry*, 282(43), pp. 31147-31155.

Caldas, T. *et al*. (1999) 'Thermoprotection by glycine betaine and choline', *Microbiology*, 145(9), pp. 2543–2548.

Campos, L. A., Sancho, J. (2003) 'The active site of pepsin is formed in the intermediate conformation dominant at mildly acidic pH', *FEBS Letters*, 538(1-3), pp. 89-95.

Casali, N. (2003) '*Escherichia coli* host strains', *Methods in molecular biology*, 235(4), pp. 27–48.

Castro-Ochoa, K. F. *et al*. (2019) 'Homoectoine protects against colitis by preventing a claudin switch in epithelial tight junctions', *Digestive Diseases and Sciences*, 64(2), pp. 409–420.

Chubukov, V. & Sauer, U. (2014) 'Environmental Dependence of Stationary-Phase Metabolism in *Bacillus subtilis* and *Escherichia coli*', *Applied and Environmental Microbiology*, 80(9), pp. 2901-2909.

Chung, C. T., Niemela, S. L. & Miller, R. H. (1989) 'One-step preparation of competent *Escherichia coli*: transformation and storage of bacterial cells in the same solution', *Proceedings of the National Academy of Sciences of the United States of America*, 86(7), pp. 2172–2175.

Clegg, J. S. *et al*. (1982) 'Cellular responses to extreme water loss: The water-replacement hypothesis', *Cryobiology*, 19(3), pp. 306–316.

Clifton, I. J. *et al*. (2006) 'Structural studies on 2-oxoglutarate oxygenases and related double-stranded beta-helix fold proteins', *Journal of Inorganic Biochemistry*, 100(4), pp. 644-669.

Creamer, T. P., Srinivasan, R. & Rose, G. D. (1997) 'Modeling unfolded states of proteins and peptides. II. Backbone solvent accessibility', *Biochemistry*, 36(10), pp. 2832–2835.

Crowe, J.H. *et al.* (1990) 'Are freezing and dehydration similar stress vectors? A comparison of modes of interaction of stabilizing solutes with biomolecules', *Cryobiology*, 27(3), pp. 219-231.

Crowe, J. H., Carpenter, J. F. & Crowe, L. M. (1998) 'The role of vitrification in anhydrobiosis', *Annual Review of Physiology*, 60, pp. 73–103.

Csonka, L. N. & Epstein, W. (1996) 'Osmoregulation. In *Escherichia coli* and *Salmonella typhimurium*', *cellular and molecular biology*, Neidhard, F.C.; Curtiss, R. III, Ingraham, J. L. *et al.* Washington, D. C., USA. ASM Press: pp. 1210-1223.

Culham, D. E. *et al*. (1993) 'Isolation and sequencing of *Escherichia coli* gene *proP* reveals unusual structural features of the osmoregulatory proline/betaine transporter ProP', *Journal of Molecular Biology*, 229(1), pp. 268-276.

Czech, L. *et al.* (2016) 'EctD‐mediated biotransformation of the chemical chaperone ectoine into hydroxyectoine and its mechanosensitive channel‐independent excretion', *Microbial Cell Factories*, 15(1), p. 126.

Czech, L. *et al*. (2018) 'Tinkering with Osmotically Controlled Transcription Allows Enhanced Production and Excretion of Ectoine and Hydroxyectoine from a Microbial Cell Factory', *Applied and Environmental Microbiol*ogy, 84(2), pp.1772-1817.

Czech, L. *et al*. (2019) 'Exploiting Substrate Promiscuity of Ectoine Hydroxylase for Regio- and Stereoselective Modification of Homoectoine', *Frontiers in Microbiology*, 27(10), p. 2745.

De Grooth, N. S. & Ventura, S. (2006) 'Effect of temperature on protein quality in bacterial inclusion bodies', *FEBS Letters*, 580(27), pp. 6471-6476.

Dinnbier, U. E. *et al*. (1988) 'Transient accumulation of potassium glutamate and its replacement by trehalose during adaptation of growing cells of *Escherichia coli* K-12 to elevated sodium chloride concentrations', *Archives of Microbiology*, 150(4), pp. 348-357.

Donovan, R. S., Robinson, C. W. & Glick, B. R. (1996) 'Review: optimizing inducer and culture conditions for expression of foreign proteins under the control of the lac promoter', *Journal of Industrial Microbiology*, 16(3), pp. 145-154.

Doucette, C. D. *et al.* (2011) 'α-ketoglutarate coordinates carbon and nitrogen utilization via Enzyme I inhibition', *Nature Chemical Biology*, 7(12), pp. 894–901.

Edwards, M. D. *et al*. (2012) 'Characterization of three novel mechanosensitive channel activities *in Escherichia coli*', *Channels (Austin)*, 6(4), pp. 272–281.

Borujeni, A. E., Channarasappa, A. S. & Salis, H. M. (2014) 'Translation rate is controlled by coupled trade-offs between site accessibility, selective RNA unfolding and sliding at upstream standby sites. *Nucleic Acids Research*, 42(4), pp. 2646–2659.

Farewell, A. & Neidhardt, F. C. (1998) 'Effect of Temperature on *in vivo* Protein Synthetic Capacity in *Escherichia coli*', *Journal of Bacteriology*, 180(17), pp. 4704–4710.

Friedman, M. (2018) 'Analysis, Nutrition, and Health Benefits of Tryptophan', *International Journal of Tryptophan Research*, 11, pp. 1-12.

Gadgil, M. *et al.* (2008) 'Transcriptional Response of *Escherichia coli* to Temperature Shift', *Biotechnology Progress* 21(3), pp. 689-699.

Galinski, E. A. (1985) '1,4,5,6-Tetrahydro-2-methyl-4-pyrimidinecarboxylic acid. A novel cyclic amino acid from halophilic phototrophic bacteria of the genus', *European Journal of Biochemistry*, 149(1), pp. 135–139.

Galinski, E. A. & Herzog, R. M. (1990) 'The role of trehalose as a substitute for nitrogen containing compatible solutes (*Ectothiorhodospira halochloris*)', *Archives of Microbiology*, 153, pp. 607-613.

Galinski, E. A. (1993) 'Compatible solutes of halophilic eubacteria: molecular principles, water-solute interaction, stress protection', *Experientia*, 49, pp. 487-496.

Galinski, E. A. & Trüper, H. G. (1994) 'Microbial behaviour in salt-stressed ecosystems', *FEMS Microbiology Reviews*, 15(2-3), pp. 95–108.

Galinski, E. A. (1995) 'Osmoadaptation in bacteria.', *Advances in microbial physiology*, 37, pp. 272–328.

Garibyan, L. & Avashia, N. (2013) 'Research Techniques Made Simple: Polymerase Chain Reaction (PCR)', *Journal of Investigative Dermatology*, 133(3), pp. 1-4.

Gekko, K. & Timasheff, S. N. (1981) 'Mechanism of protein stabilization by glycerol: perferential hydration in glycerol-water mixtures', *Biochemistry*, 20(16), pp. 4667–4676.

Giæver, H. M. *et al*. (1988) 'Biochemical and genetic characterization of osmoregulatory trehalose synthesis in *Escherichia coli*', *Journal of Bacteriology*, 170(6), pp. 2841–2849.

Göller, K. & Galinski, E. A. (1999) 'Protection of a model enzyme (lactate dehydrogenase) against heat, urea and freeze-thaw treatment by compatible solute additives', *Journal of Molecular Catalysis B: Enzymatic*, 7(1-4), pp. 37–45.

Golomb, M. & Chamberlin, M. (1974) 'Characterization of T7-specific ribonucleic acid polymerase. IV. Resolution of the major *in vitro* transcripts by gel electrophoresis', Journal of Biological Chemistry, 249, pp. 2858–2863.

Graf, R. *et al*. (2008) 'The multifunctional role of ectoine as a natural cell protectant', *Clinics in Dermatology* 26(4), pp. 326-333.

Grammann, K., Volke, A. & Kunte, H. J. (2002) 'New type of osmoregulated solute transporter identified in halophilic members of the *bacteria* domain: TRAP transporter TeaABC mediates uptake of ectoine and hydroxyectoine in *Halomonas elongata* DSM 2581T', *Journal of Bacteriology*, 184(11), pp. 3078–3085.

Grant, W. D. (2004) 'Life at low water activity', *Philosophical transactions of the Royal Society of London. Series B, Biological* sciences, 359(1448), pp. 1249-1266.

Green, J. L. & Angell, C. A. (1989) 'Phase relations and vitrification in saccharide-water solutions and the trehalose anomaly', *Journal of Physical Chemistry*, 93, pp. 2880–2882.

Guyer, M. S. *et al.* (1981) 'Identification of a sex-factor-affinity site in *E. coli* as gamma delta', *Cold Spring Harbor symposia on quantitative biology*, 45(1), pp. 135–140.

Haardt, M. *et al.* (1995) 'The osmoprotectant proline betaine is a major substrate for the binding-protein-dependent transport system ProU of *Escherichia coli* K-12', *Molecular and General Genetics*, 246(6), pp. 783-796.

Hahn, M. B. *et al*. (2017) 'DNA protection by ectoine from ionizing radiation: molecular mechanisms', *Physical Chemistry Chemical Physics*, 19(37), pp. 25717–25722.

Hanahan, D. (1983) 'Studies on Transformation of *Escherichia coli* with Plasmids', *Journal of Molecular Biology*, 166(4), pp. 557–580.

Harding, T. *et al.* (2016) 'Osmoadaptative strategy and its molecular signature in obligately halophilic heterotrophic protists', *Genome Biology and Evolution*, 8(7), pp. 2241–2258.

Harishchandra, R. K. *et al.* (2010) 'The effect of compatible solute ectoines on the structural organization of lipid monolayer and bilayer membranes', *Biophysical Chemistry*, 150(1-3), pp. 37–46.

Harishchandra, R. K. *et al.* (2011) 'Compatible solutes: Ectoine and hydroxyectoine improve functional nanostructures in artificial lung surfactants', *Biochimica et Biophysica Acta*, 1808(12), pp. 2830-2840.

Harrison, A. P., Jarvis, B. W. & Johnson, J. L. (1980) 'Heterotrophic bacteria from cultures of autotrophic *Thiobacillus ferrooxidans*: Relationships as studied by means of deoxyribonucleic acid homology', *Journal of Bacteriology*, 143(1), pp. 448–454.

Hartinger, D. *et al.* (2010) 'Enhancement of solubility in *Escherichia coli* and purification of an aminotransferase from *Sphingopyxis* sp. MTA144 for deamination of hydrolyzed fumonisin B1', *Microbial Cell Fact*ories, 9(1), p. 62.

Hausinger, R. P. (2004) 'FeII/alpha-ketoglutarate-dependent hydroxylases and related enzymes', *Critical Reviews in Biochemistry and Molecular Biology*, 39(1), pp. 21-68.

Hensel, R. & König, H. (1987) 'Thermoadaptation of methanogenic bacteria by intracellular ion concentration', *FEMS Microbiology Letters*, 49(1), pp. 75-79.

Herr, C. Q. & Hausinger, R. P. (2018) 'Amazing Diversity in Biochemical Roles of Fe(II)/2-Oxoglutarate Oxygenases', *Trends in Biochemical Sciences*, 43(7), pp. 517-532.

Holtmann, G. & Bremer, E. (2004) 'Thermoprotection of *Bacillus subtilis* by exogenously provided glycine betaine and structurally related compatible solutes: Involvement of opu transporters', *Journal of Bacteriology*, pp. 1683–1693.

Hoffmann, T. & Bremer, E. (2011) 'Protection of *Bacillus subtilis* against cold stress via compatible-solute acquisition', *Journal of Bacteriology*, 193(7), pp. 1552–1562.

Hoffmann, F. & Rinas, U. (2004) 'Stress induced by recombinant protein production in *Escherichia coli*', *Advances in Biochemical Engineering and biotechnology*, 89, pp. 73-92.

Hottiger, T. *et al.* (1994) 'The role of trehalose synthesis for the acquisition of thermotolerance in yeast. II. Physiological concentrations of trehalose increase the thermal stability of proteins *in vitro*', *European Journal of Biochemistry*, 219(1-2), pp. 187-193.

Höppner, A. *et al.* (2014) 'Crystal structure of the ectoine hydroxylase, a snapshot of the active site' *Journal of Biological Chemistry*, 289(43), pp. 29570–29583.

Hua, L. *et al.* (2008) 'Urea denaturation by stronger dispersion interactions with proteins than water implies a 2-stage unfolding', *Proceedings of the National Academy of Sciences of the United States of America*, 105 (44), pp. 16928-16933.

Imhoff, J. F. & Trüper, H. G. (1977) '*Ectothiorhodospira halochloris* sp. nov., a new extremely halophilic phototrophic bacterium containing bacteriochlorophyll b', *Archives of Microbiology*, 114(2), pp. 115–121.

Inbar, L. & Lapidot, A. (1988) 'The structure and biosynthesis of new tetrahydropyrimidine derivatives in actinomycin D producer *Streptomyces parvulus*. Use of ^{13}C- and ^{15}N-labeled L-glutamate and ^{13}C and ^{15}N NMR spectroscopy', *Journal of Biological Chem*istry, 263(31), pp. 16014-16022.

Inbar, L., Frolow, F. & Lapidot, A. (1993) 'The conformation of new tetrahydropyrimidine derivatives in solution and in the crystal', *European Journal of Biochem*istry, 214(3), pp. 897-906.

Janssen, K. (2015) 'Nutzung von Ectoin-Hydroxylasen in der Ganzzellbiokatalyse', Project thesis, Rheinische Friedrich-Wilhelms-Universität Bonn.

Jebbar, M. *et al*. (1992) 'Osmoprotection of *Escherichia coli* by ectoine: uptake and accumulation characteristics', *Journal of Bacteriology*, 174(15), pp. 5027-5035.

Jensen, R. A. (1976) 'Enzyme recruitment in evolution of new function', *Annual Review of Microbiol*ogy, 30, pp. 409–425.

Julca, I. *et al*. (2012) 'Xeroprotectants for the stabilization of biomaterials', *Biotechnology Advances*, 30(6), pp. 1641–1654.

Jung, H. W. *et al*. (2019) 'Metabolic perturbations in mutants of glucose transporters and their applications in metabolite production in *Escherichia coli*', *Microbial Cell Factories*, 18(1), p. 170.

Kauzmann, W. (1959) 'Some factors in the interpretation of protein denaturation', *Advances in Protein Chemistry*, 14, pp. 1-63.

Kempf, B. & Bremer, E. (1998) 'Uptake and synthesis of compatible solutes as microbial stress responses to high-osmolality environments', *Archives of Microbiology*, 170(5), pp. 319-330.

Killian, M. S., Taylor, A. J. & Castner, D. G. (2018) 'Stabilization of dry protein coatings with compatible solutes', *Biointerphases*, 13(6), 06E401.

Knapp, S. *et al.* (1999) 'Extrinsic protein stabilization by the naturally occurring osmolytes β-hydroxyectoine and betaine', *Extremophiles*, 3(3), pp. 191–198.

Koichi, M. *et al*. (1991) 'Production of tetrahydropyrimidine derivatives', Patent number JPH0331265A

Korsten, A. (2011) 'Das seltene kompatible Solut N-Acetyl-glutaminylglutamin-1-amid (NAGGN): Heterologe Expression des Genclusters aus *Pseudomonas putida* und Untersuchungen zur Funktion der putativen Biosyntheseenzyme', Dissertation, Rheinische Friedrich-Wilhelms-Universtität Bonn.

Kunte, H. J., Galinski, E. A. & Trüper, H. G. (1993) 'A modified FMOC-method for the detection of amino acid-type osmolytes and tetrahydropyrimidines (ectoines)', *Journal of Microbiological Methods*, 17(2), pp. 129-136.

Kunte, H. J., Lentzen, G. & Galinski, E. A. (2014) 'Industrial production of the cell protectant ectoine: Protection mechanisms, processes, and products', *Current Biotechnology*, 3(1), pp. 10–25.

Kurz, M. (2008) 'Compatible solute influence on nucleic acids: Many questions but few answers', *Saline Systems*, 4:6

Laemmli, U. K. (1970) 'Cleavage of Structural Proteins during the Assembly of the Head of Bacteriophage T4', *Nature*, 227(5259), pp. 680–685.

Lanyi, J. K. (1974) 'Salt-dependent properties of proteins from extremely halophilic bacteria', *Bacteriological Reviews*, 38(3), pp. 272–290.

Larsen, P. I. *et al*. (1987) 'Osmoregulation in *Escherichia coli* by accumulation of organic osmolytes: betaines, glutamic acid, and trehalose', *Archives of Microbiology*, 147(1), pp. 1–7.

Lee, S. Y. (1996) 'High cell-density culture of *Escherichia coli*', *Trends in Biotechnology*, 14(3), pp. 98–105.

Lins, L. & Brasseur, R. (1995) 'The hydrophobic effect in protein folding', *FASEB Journal*, 9(7), pp. 535-540.

Lippert, K. & Galinski, E. (1992) 'Enzyme stabilization be ectoine-type compatible solutes: protection against heating, freezing and drying', *Applied Microbiology and Biotechnology*, 37(1), pp. 61–65.

Liu, Y. & Bolen, D. W. (1995) 'The peptide backbone plays a dominant role in protein stabilization by naturally occuring osmolytes', *Biochemistry*, 34(39), pp. 12884–12891.

Louis, P., Trüper, H. G. & Galinski, E. A. (1994) 'Survival of *Escherichia coli* during drying and storage in the presence of compatible solutes', *Applied Microbiology and Biotechnology*, 41, pp. 684–688.

Luli, G. W. & Strohl, W. (1990) 'Comparison of growth, acetate production, and acetate inhibition of *Escherichia coli* strains in batch and fed-batch fermentations', *Applied and Environmental Microbiology*, 56(4), pp. 1004-1011.

Ma, Y. *et al*. (2010) 'Halophiles 2010: Life in Saline Environments', *Applied and Environ Microbiology*, 76(21), pp. 6971-6981.

MacElroy, R. (1974) 'Some comments on the evolution of extremophiles', *Biosystems*, 6, pp. 74-75.

MacMillan, S. V. *et al*. (1999) 'The ion coupling and organic substrate specificities of osmoregulatory transporter ProP in *Escherichia coli*', *Biochimica et Biophysica Acta*, 1420(1-2), pp. 30-44.

Malin, G. & Lapidot, A. (1996) 'Induction of synthesis of tetrahydropyrimidine derivatives in *Streptomyces* strains and their effect on *Escherichia coli* in response to osmotic and heat stress', *Journal of Bacteriology*, 178(2), pp. 385–395.

Manzanera, M. *et al.* (2002) 'Hydroxyectoine is superior to trehalose for anhydrobiotic engineering of *Pseudomonas putida* KT2440', *Applied and Environmental Microbiology*, 68(9), pp. 4328–4333.

Manzanera, M. *et al*. (2004) 'High survival and stability rates of *Escherichia coli* dried in hydroxyectoine', *FEMS Microbiology Letters*, 233(2), pp. 347–352.

Marisch, K. *et al.* (2013) 'Evaluation of three industrial *Escherichia coli* strains in fed-batch cultivations during high-level SOD protein production', *Microbial Cell Factories*, 12 (58), pp. 1–11.

Marteinsson, V. T. *et al.* (1999) '*Thermococcus barophilus* sp. nov., a new barophilic and hyperthermophilic archaeon isolated under high hydrostatic pressure from a deep-sea hydrothermal vent', *International Journal of Systematic Bacteriology*, 49(2), pp. 351–359.

McLaggan, D. J. *et al.* (1994) 'Interdependence of K+ and glutamate accumulation during osmotic adaptation of *Escherichia coli*', *Journal of Biological Chemistry*, 269(3), pp. 1911-1917.

Meffert, A. (2011) 'Die Hydroxylierung von Ectoin und Derivaten durch die Hydroxylase EctD aus *Halomonas elongata*', Dissertation, Rheinische Friedrich-Wilhelms-Universtität Bonn.

Mevarech, M., Frolow, F. & Gloss, L. M. (2000) 'Halophilic enzymes: proteins with a grain of salt', *Biophysical Chemistry*, 86(2-3), pp. 155-164.

Milner, J. L., Grothe, S. & Wood, J. M. (1988) 'Proline porter II is activated by a hyperosmotic shift in both whole cells and membrane vesicles of *Escherichia coli* K12', *Journal of Biological Chemistry*, 263(29), pp. 14900-14905.

Misra, P. P. & Kishore, N. (2012) 'Glycine betaine: A widely reported osmolyte induces differential and selective conformational stability and enhances aggregation in some proteins in the presence of surfactants', *Biopolymers*, 97(12), pp. 933-949.

Mohammed, A. & Anderson, J. G. (2009) 'Effect of salt concentration on the growth of heat stressed and unstressed *Escherichia coli*', *Journal of Food Agriculture and Environment*, 7(3-4), pp. 51-54.

Molitor, C. (2015) 'Gewinnung hydroxylierter Ectoin-Derivate mittels Ganz-Zell-Biokatalyse', Master thesis, Rheinische Friedrich-Wilhelms-Universität Bonn.

Moritz, K. D. (2018) '*Escherichia coli* und *Synechocystis sp.* als heterologe Produktionssysteme für Ectoin und Hydroxyectoin', Dissertation, Rheinische Friedrich-Wilhelms-Universität Bonn.

Mullis, K. *et al.* (1986) 'Specific enzymatic amplification of DNA *in vitro*: the polymerase chain reaction', *Cold Spring Harbor Symposia on Quantitative Biology*, 51(1), pp. 263–273.

Nagata, S. (2001) 'Growth of *Escherichia coli* ATCC 9637 through the uptake of compatible solutes at high osmolarity', *Journal of Bioscience and Bioengineering*, 92(4), pp. 324-329.

Nedwell, D. B. (1999) 'Effect of low temperature on microbial growth: lowered affinity for substrates limits growth at low temperature', *FEMS Microbiology Ecology*, 30(2), pp. 101–111.

Ono, H. *et al.* (1999) 'Characterization of biosynthetic enzymes for ectoine as a compatiblesolute in a moderately halophilic eubacterium, *Halomonas elongata*', *Journal of Bacteriology*, 181(1), pp. 91–99.

Oren, A. (2008) 'Microbial life at high salt concentrations: phylogenetic and metabolic diversity', *Saline Systems*, 4:2.

Pastor, J. M. *et al*. (2010) 'Ectoines in cell stress protection: Uses and biotechnological production', *Biotechnology Adances*, 28(6), pp. 782–801.

Peng, J. *et al.* (1999) 'Process for producing trehalose', Patent number EP0555540A1

Peters, P., Galinski, E.A. & Trüper, H.G. (1990) 'The biosynthesis of ectoine', *FEMS Microbiology Letters*, 71(1-2), pp. 157-162.

Price, J. C. *et al*. (2003) 'The first direct characterization of a high-valent iron intermediate in the reaction of an alpha-ketoglutaratedependent dioxygenase: a high-spin FeIV complex in taurine/alpha-ketoglutarate dioxygenase (TauD) from *Escherichia coli*', *Biochemistry*, 42(24), pp. 7497-7508.

Rampelotto, P. H. (2013): 'Extremophiles and Extreme Environments', *Life*, 3(3), pp. 482–485.

Reitzer, L. (2003) 'Nitrogen assimilation and global regulation in *Escherichia coli*', *Annual Review of Microbiology*, 57, pp. 155–176.

Reuter, K. *et al.* (2010) 'Synthesis of 5-hydroxyectoine from ectoine: Crystal structure of the non-heme iron(II) and 2-oxoglutarate-dependent dioxygenase EctD.' *Plos one*, 5(5), e10647.

Rieckmann, T. *et al.* (2019) 'The inflammation-reducing compatible solute ectoine does not impair the cytotoxic effect of ionizing radiation on head and neck cancer cells', *Scientific Reports*, 9(1), pp. 1–8.

Rod, M. L. *et al.* (1988) 'Accumulation of trehalose by *Escherichia coli* K-12 at high osmotic pressure depends on the presence of amber suppressors', *Journal of bacteriology*, 170(8), pp. 3601–3610.

Roeβler, M. & Müller, V. (2001) 'Osmoadaptation in bacteria and archaea: common principles and differences', *Environmental Microbiology*, 3(12), pp. 743–754.

Ruprecht, C. (2014) 'Hydroxylation of ectoine derivatives using a whole-cell biotransformation system', Master thesis, Rheinische Friedrich-Wilhelms-Universität Bonn.

Russo, E. (2003) 'The birth of biotechnology', *Nature*, 421(6921), pp. 456–457.

Saiki, R. K. (1988) 'Primer-directed enzymatic amplification of DNA with a thermostable DNA polymerase', *Science*, 239(4839), pp. 487–491.

Sakurai, M. *et al.* (2008) 'Vitrification is essential for anhydrobiosis in an African chironomid, *Polypedilum vanderplanki*', *Proceedings of the National Academy of Sciences*, 105(13), pp. 5093–5098.

Salis, H. M., Mirsky, E. A. & Voigt, C. A. (2009) 'Automated design of synthetic ribosome binding sites to control protein expression' *Nature Biotechnology*, 27(10), pp. 946–950.

Sambrook, J., Russel, D. & Maniatis, T. (1989) 'Molecular Cloning: A Laboratory Manual', *Cold Spring Harbor Protocols*, 4th Edition.

Satyanarayana, T., Raghukumar, C. & Shivaji, S. (2005) 'Extremophilic microbes: Diversity and perspectives', *Current Science*, 89(1), pp. 78–90.

Sauer, T. & Galinski, E. A. (1998) 'Bacterial milking: a novel bioprocess for production of compatible solutes', *Biotechnology and Bioengineering*, 57(3), pp. 306–13.

Schiraldi, C. *et al.* (2006) 'High-yield cultivation of *Marinococcus* M52 for production and recovery of hydroxyectoine', *Research in Microbiology*, 157(7), pp. 693-699.

Schnoor, M. *et al.* (2004) 'Characterization of the synthetic compatible solute homoectoine as a potent PCR enhancer', *Biochemical and Biophysical. Research Communications*, 322(3), pp. 867–872.

Schubert, T. *et al.* (2007) 'Continuous synthesis and excretion of the compatible solute ectoine by a transgenic, nonhalophilic bacterium', *Applied and Environmental Microbiology*, 73(10), pp. 3343-3347.

Schuh, W. *et al.* (1985) 'Die Kristallstruktur des Ectoin, einer neuen osmoregulatorisch wirksamen Aminosäure', *Zeitschrift für Naturforschung*, 40c, pp. 780-784.

Sell, K. (2009) 'Die antimikrobielle Wirkung von zwitterionischen Guanidiniumverbindungen', Diploma thesis, Rheinische Friedrich-Wilhelms-Universität Bonn.

Shabala, L. *et al.* (2009) 'Ion transport and osmotic adjustment in *Escherichia coli* in response to ionic and non-ionic osmotica', *Applied and Environmental Microbiology*, 11(1), pp. 137-148.

Shi, X. & Jarvis, D. L. (2006) 'A new rapid amplification of cDNA ends method for extremely guanine plus cytosine-rich genes', *Analytical Biochemistry*, 356(2), pp. 222–228.

Smith, P. K. *et al.* (1985) 'Measurement of protein using bicinchoninic acid', *Analytical Biochemistry*, 150(1), pp. 76–85.

Sorensen, H. P. & Mortensen, K. K. (2005) 'Soluble expression of recombinant proteins in the cytoplasm of *Escherichia coli*', *Microbial Cell Factories*, 4(1):1

Stelea, S. D. *et al.* (2001) 'Thermal unfolding of ribonuclease A in phosphate at neutral pH: Deviations from the two–state model', Protein Science, 10(5), pp. 970–978.

Stiller, L. M. *et al*. (2018) 'Engineering the Salt-Inducible Ectoine Promoter Region of *Halomonas elongata* for Protein Expression in a Unique Stabilizing Environment', *Genes*, 9(4), p.184.

Street, T. O., Bolen, D. W. & Rose, G. D. (2006) 'A molecular mechanism for osmolyte-induced protein stability', *Proceedings of the National Academy of Sciences of the United States of America*, 103(38), pp. 13997-14002.

Studier, F. W. & Moffatt, B. A. (1986) 'Use of bacteriophage T7 RNA polymerase to direct selective high-level expression of cloned genes', *Journal of Molecular Biology*, 189(1), pp. 113–130.

Sun, W. Q. & Leopold, A. C. (1997) 'Cytoplasmic Vitrification and Survival of Anhydrobiotic Organisms', *Comparative Biochemistry and Physiology Part A: Physiology*, 117(3), pp. 327–333.

Tanne, C. (2013) 'Untersuchung mikrobieller Glasbildner für die Biostabilisierung und biomimetische Applikation in einem Biosensor', Dissertation, Rheinische Friedrich-Wilhelms-Universtität Bonn.

Tanne, C. *et al.* (2014) 'Glass-forming property of hydroxyectoine is the cause of its superior function as a dessication protectant', *Frontiers in Microbiology*, 5, 150.

Tetsch, L. (2001) 'Aufreinigung und Charakterisierung von TeaA, dem Substratbindeprotein des osmoregulierten Ectointransporters TeaABC', Diploma thesis, Rheinische Friedrich-Wilhelms-Universität Bonn.

Timasheff, S. N. (1998) 'Control of protein stability and reactions by weakly interacting cosolvents: the simplicity of the complicated', *Advances in protein chemistry*, 51, pp. 355-432.

Toxopeus, J., Warner, A. H. & MacRae, T. H. (2014) 'Group 1 LEA proteins contribute to the desiccation and freeze tolerance of Artemia franciscana embryos during diapause', *Cell Stress Chaperones*, 19(6), pp. 939–948.

Ures, A. (2006) 'Charakterisierung und Identifizierung des Ectoin-Hydroxylasegens *ectD* aus *Halomonas elongata* DSM 2581T', Diploma thesis, Rheinische Friedrich-Wilhelms-Universität Bonn.

Vancanneyt, M. *et al.* (2001) '*Sphingomonas alaskensis* sp. nov., a dominant bacterium from a marine oligotrophic environment', *International Journal of Systematic and Evolutionary Microbiology*, 51(1), pp. 73-79.

Vasala, A. *et al.* (2006) 'A new wireless system for decentralised measurement of physiological parameters from shake flasks', *Microbial Cell Factories*, 5(8).

Ventosa, A., Nieto, J. J. & Oren A. (1998) 'Biology of moderately halophilic aerobic bacteria', *Microbiology and Molecular Biology Reviews*, 62(2), pp. 504–544.

Vielgraf, S. L. (2008) 'Stereospezifische Hydroxylierung kompatibler Solute über Ganzzellkatalyse in *Escherichia coli*', Diploma thesis, Rheinische Friedrich-Wilhelms-Universität Bonn.

Vogel, U. & Jensen, K.F. (1994) 'The RNA chain elongation rate in *Escherichia coli* depends on the growth rate', *Journal of Bacteriology*, 176(10), pp. 2807-2813.

Voß, P. (2002) 'Synthese von kompatiblen Soluten mit ectoinanaloger Struktur und Charakterisierung des protektiven Effektes auf biochemische Modellsysteme und *Escherichia coli*', Dissertation, Westfälische Wilhelms-Universität Münster.

Vreeland, R. H. *et al*. (1980) '*Halomonas elongata*, a New Genus and Species of Extremely Salt-Tolerant Bacteria', *International Journal of Systematic Bacteriology*, 30(2), pp. 485–495.

Waßmann, K. C. (2013) 'Unravelling the antimicrobial features of the incompatible solutes creatine and guanidino-ectoine', Dissertation, Rheinische Friedrich-Wilhelms-Universität Bonn.

Wedeking, A. *et al.* (2014) 'A Lipid Anchor Improves the Protective Effect of Ectoine in Inflammation', *Current Medicinal Chemistry*, 21(22), pp. 2565-2572.

Welsh, D. T. *et al*. (1991) 'The role of trehalose in the osmoadaptation of *Escherichia coli* NCIB 9484: interaction of trehalose, K^+ and glutamate during osmoadaptation in continuous culture', *Journal of General Microbiology*, 137(4), pp. 745-750.

Widderich, N. *et al.* (2014) 'Biochemical Properties of Ectoine Hydroxylases from Extremophiles and their wider Taxonomic Distribution among Microorganisms', *Plos one*, 9(4), e93809.

Widderich, N. *et al.* (2016) 'Strangers in the archaeal world: osmostress-responsive biosynthesis of ectoine and hydroxyectoine by the marine thaumarchaeon *Nitrosopumilus maritimus*', *Environmenal Microbiology*, 18(4), pp.1227–1248.

Witt, E. (2011) 'Nebenreaktionen der Ectoin-Synthase aus *Halomonas elongata* DSM 2581T und Entwicklung eines salzinduzierten Expressionssystems', Dissertation, Rheinische Friedrich-Wilhelms-Universität Bonn.

Wohlfarth, A., Severin, J. & Galinski, E. A. (1990) 'The spectrum of compatible solutes in heterotrophic halophilic eubacteria of the family *Halomonadaceae*', *Journal of General Microbiology*, 136(4), pp. 705–712.

Yan, Y. *et al*. (2008) 'Nitrogen fixation island and rhizosphere competence traits in the genome of root-associated *Pseudomonas stutzeri* A1501', *Proceedings of the National Academy of Sciences of the United States of America*, 105(21), pp. 7564-7569.

Yan, D., Lenz, P. & Hwa, T. (2011) 'Overcoming fluctuation and leakage problems in the quantification of intracellular 2-oxoglutarate levels in *Escherichia coli*', *Applied and Environmental Microbiology*, 77(19), pp. 6763-6771.

Yancey, P. H., Blake, W. R. & Conley, J. (2002) 'Unusual Organic Osmolytes in Deep-Sea Animals: Adaptations to Hydrostatic Pressure and Other Perturbants', *Comparative Biochemistry and Physiology - Part A: Molecular & Integrative Physiology*, 133(3), pp. 667-76.

Yancey, P. H. (2005) 'Organic osmolytes as compatible, metabolic and counteracting cytoprotectants in high osmolarity and other stresses', *Journal of Experimental Biology*, 208(15), pp. 2819–2830.

Yang, P. H., & Rupley, J. A. (1979) 'Protein-water interactions. Heat capacity of the lysozyme water system', *Biochemistry,* 18(12), pp. 2654-2661.

Zaccai, G. *et al*. (2016) 'Neutrons describe ectoine effects on water H-bonding and hydration around a soluble protein and a cell membrane', *Scientific Reports*, 6:31434.

Zeidler, S. & Müller, V. (2019) 'The role of compatible solutes in desiccation resistance of *Acinetobacter baumannii'*, *Microbiologyopen.* 8(5), e00740.

Zhang, J. (2006) 'Method of producing Betaine compound', Patent number US7005543B2.

Zhou, H. & Pang, X. (2018) 'Electrostatic Interactions in Protein Structure, Folding, Binding, and Condensation', *Chemical Reviews*, 118(4), pp. 1691-1741.

Internet sources

https://www.neubert-glas.de